The effect of liver warm ischaemia reperfusion injury and modulation on bile composition evaluated by magnetic resonance spectroscopy

Submitted by

Dr Tariq Hafez

University Department of Surgery

Royal Free and University College Medical School,

University College London,

University of London

2013

This thesis is submitted to the University of London in fulfilment of the requirements for the degree of Doctor of Philosophy. I was responsible for the majority of the work carried out including acquisition of samples, their spectroscopic processing and analysis after the pilot study, where I was greatly aided by Dr Cox, the statistical analysis of the results in addition to the preparation of all the reagents used in the experiments. All the experiments carried out were in this study were conducted in accordance with the Animals Scientific Procedures Act (1986) and with licence from the Home Office. With the aim of reduction in the use of animals in scientific research, different samples were extracted from the animal experiments to serve several projects simultaneously. I contributed considerably to these operative experiments, and I have acknowledged the valuable work of my colleagues below who also shared in the experimental work. Dr Yang conducted the ICG measurements. I wrote the manuscript and any remaining errors are solely my responsibility.

This thesis is dedicated to my wife Heba,

without whose constant encouragement and support

I would not have been able to finish it.

Acknowledgement

I would like to thank the Royal Free University Department of Surgery past and present: Karen Cheetam, Geoff Punshon, Bernard Cousins, Kevin Sales, and Professor Alexander M. Seifalian for their help during my work in the department. I thank also Duncan Moore from the comparative biology unit and my colleagues Dr Georgios Glantzounis, Mr Hemant Sheth and Mr Giuseppe (Kito) Fusai for their assistance in the animal experimental model and operative work.

I am especially grateful to Dr Harold Parkes, at the Institute of Child Health, and Institute of Neurology, University College London, for his help and advice on bile analysis with NMR spectroscopy. I also thank Dr J. Cox from Imperial College for her help during the pilot study. Dr Mark Cope and Professor David Delpy spent many years developing and modifying the near infrared spectroscopy which was used in this study and I would like to thank them for their time and effort.

I am eternally grateful to Dr Wenxuan Yang for his assistance with the operative and laboratory work and his invaluable guidance throughout the whole period of my work. His sudden and unexpected death in January 2006 left a huge void in the Department of Surgery. I will always remember his kind and warm personality.

Finally, I would like to express my sincere gratitude to my supervisors, Professor Brian R. Davidson and Professor Barry Fuller for their invaluable help, their endless enthusiasm, guidance and continuous encouragement throughout the period of my study.

Table of contents

Acknowledgement *4*
List of Figures *9*
List of Tables *11*
List of abbreviations ..... *xii*
Abstract 1
1 Introduction 5
2 Review of literature 11
2.1 Physiology of Bile secretion and composition 12
2.1.1 Bile acids and bile flow 12
2.1.2 Bile secretion 13
2.1.3 Bile studies 13
2.1.4 Post-transplant biliary obstruction 14
2.1.5 Bile flow and composition studies 15
2.1.6 Apparent choleretic activity studies 16
2.1.7 Other procedures for the assessment of bile flow 17
2.1.8 Bile studies and immunosuppressive drugs 17
2.1.9 Serum bile acid studies 18
2.1.10 Combined serum and biliary bile acid studies 19
2.2 Modulation of ischaemia reperfusion injury 20
2.2.1 N-acetylcysteine 20
2.2.1.1 Reactive oxygen species 20
2.2.1.2 Pharmacology of N-acetylcysteine 23
2.2.1.3 Role of N-acetylcysteine in endothelial function 24
2.2.1.4 The molecular basis of N-acetylcysteine action 25
2.2.1.5 N-acetylcysteine in the liver 28
2.2.1.6 Role of N-acetylcysteine in liver ischaemia-reperfusion injury 29
2.2.1.7 Role of N-acetylcysteine in clinical liver transplantation 30
2.2.2 Glycine 30
2.2.2.1 Kupffer cell activation in I/R 31
2.2.2.2 Anti-inflammatory action of glycine 32
2.2.2.3 Glycine receptors 33
2.2.2.4 Cytoprotective action of glycine 35
2.2.3 Steatosis 36
2.2.3.1 Steatosis in liver transplantation 36
2.2.3.2 Steatosis in liver resection 36
2.2.3.3 Impaired microcirculation 37
2.2.3.4 Steatosis and hepatic energy metabolism 37
2.2.3.5 Other mechanisms of injury in steatotic livers 37
2.2.4 Ischaemic preconditioning 39
2.3 Magnetic resonance 42
2.3.1 Introduction 42
2.3.2 Historical perspective 43
2.3.2.1 Scattered beginnings 44
2.3.2.2 The chemistry revealed 45
2.3.2.3 Radiofrequency pulses and Fourier techniques 46
2.3.2.4 The formation of MR imaging 47

2.3.2.5 The separation of high resolution NMR and medical applications 48
2.3.2.6 The delay in clinical MRS applications 50
2.3.2.7 Technical developments meet the request of new MRI sequences 51
2.3.2.8 Advances in NMR 51
2.3.2.9 Advances in diagnostic MRI 52
2.3.2.10 Advances in biomedical and clinical MRS 54
2.3.2.11 Future developments 55
2.3.3 Application of MRS to the hepatobiliary and liver transplant field 56
2.3.3.1 MRS studies of bile 56
2.3.3.2 MRS in liver failure 57
2.3.3.3 MRS in hepatic steatosis 58
2.3.3.4 MRS in ischemic preconditioning 58
2.3.3.5 MRS in hepatic energetics 58
2.3.3.6 MRS in analysis of organ viability for transplant 59
2.3.3.7 MRS in liver transplantation 59
2.3.3.8 MRS in primary graft non-function and dysfunction 61
3 Materials and Methods 63
3.1 Rabbit model of lobar ischaemia/reperfusion 64
3.1.1 Lobar Clamping 65
3.1.2 Model stability 65
3.1.3 Liver blood flow 66
3.1.3.1 What happens on portal flow reduction or clamping 66
3.1.3.2 Hepatic Compliance 67
3.1.3.3 Hepatic Arterial Buffer Response 67
3.1.3.4 Hepatorenal Reflex 68
3.1.3.5 Hepatic Mass Regulation 68
3.1.4 Models of total hepatic ischaemia 68
3.1.5 Ischaemic or non-ischaemic bile 70
3.1.6 Bile or Urine 71
3.2 Hepatic microcirculation 72
3.2.1 Basic principles 72
3.2.2 LDF application in the rabbit, data collection, analysis 73
3.3 Intracellular oxygenation and mitochondrial activity 76
3.3.1 Basic principles of NIRS 80
3.3.2 Near infrared spectrophotometer 82
3.3.3 NIRS application in the rabbit, data collection, analysis 85
3.4 Ultrasonic transit time flowmetry 86
3.4.1 Principle of ultrasonic transit time flowmetry 86
3.4.2 Ultrasonic flowmetry in the rabbit model 87
3.4.3 Ultrasonic transit time flowmetry data collection and analysis 87
3.5 Indocyanine green (ICG) clearance 89
3.6 Liver transaminases 90
3.7 Histology 90
3.8 Proton Nuclear Magnetic Resonance (^{1}HNMR) Spectroscopy 91
3.8.1 Nuclear moment, excitation, and induction decay 91
3.8.2 Magnetic field variations 93
3.8.3 Experimental ^{1}HNMR protocol 95
3.9 Bile sampling for MRS 98
3.10 Blood sampling for liver function 99
3.11 Data collection and statistical analysis 99
3.12 Metabolomics in MRS analysis 101
3.12.1 The “–omics” sciences 101
3.12.2 Metabolomics 102

3.12.2.1 Principal component analysis 103
3.12.2.2 Multivariate Data Analysis 103
3.12.2.3 Partial least squares discriminant analysis 104
4 Pilot study to determine the effect of hepatic warm ischaemia reperfusion on bile composition 105
4.1 Introduction 106
4.2 Objectives 107
4.3 Materials and methods 107
4.3.1 Model of lobar ischaemia/reperfusion 107
4.3.2 Experimental groups and protocol 108
4.3.3 Blood sampling for liver function 108
4.3.4 Liver Histopathology 108
4.3.5 Measurement of cytochrome oxidase activity 109
4.3.6 Measurement of bile flow and ^{1}HNMR bile spectroscopy 109
4.3.7 Data collection and statistical analysis 110
4.4 Results 111
4.4.1 Liver biochemistry 111
4.4.2 Liver Histopathology 111
4.4.3 Bile Flow 111
4.4.4 Cytochrome oxidase activity 111
4.4.5 ^{1}HNMR spectroscopy of bile 115
4.5 Discussion 122
5 Modulation of warm hepatic ischaemia reperfusion using NAC and its effect on bile composition 125
5.1 Introduction 126
5.2 Objectives 127
5.3 Materials and methods 127
5.3.1 Ischaemia reperfusion procedure 127
5.3.2 Experimental groups and protocol 128
5.3.3 Blood sampling for liver function 128
5.3.4 Measurement of portal flow 129
5.3.5 Measurement of bile flow and ^{1}HNMR bile spectroscopy 129
5.3.6 Assessment of the hepatic microcirculation 129
5.3.7 Measurement of hepatic tissue oxygenation 130
5.3.8 Data collection and statistical analysis 130
5.4 Results 131
5.4.1 Liver function 131
5.4.2 Bile Flow 131
5.4.3 ^{1}HNMR spectroscopy of bile 134
5.5 Discussion 142
6 Modulation of warm hepatic ischaemia reperfusion using glycine and its effect on bile composition 145
6.1 Introduction 146
6.2 Objectives 147
6.3 Materials and Methods 148
6.3.1 Experimental Groups 148
6.3.2 Ischaemia-Reperfusion Injury protocol 148
6.3.3 Bile flow and Proton nuclear magnetic resonance ^{1}HNMR spectroscopy 149
6.3.4 Statistical analysis 149
6.4 Results 150
6.4.1 Bile flow 150
6.4.2 ^{1}HNMR spectroscopy of bile 150
6.5 Discussion 160

7 Modulation of warm hepatic ischaemia reperfusion in steatotic liver using NAC and its effect on bile composition 163
7.1 Introduction 164
7.2 Objectives 165
7.3 Materials and methods 165
7.3.1 Animal model 165
7.3.2 Experimental groups and protocol 166
7.3.3 Bile flow and composition 167
7.3.4 Data collection and statistical analysis 168
7.4 Results 169
7.4.1 Systemic haemodynamics 169
7.4.2 Hepatic haemodynamics 169
7.4.3 Hepatic microcirculation 172
7.4.4 Liver function tests 172
7.4.5 Bile flow and Proton nuclear magnetic resonance (^{1}HNMR) spectroscopy 172
7.5 Discussion 180
8 Modulation of warm hepatic ischaemia reperfusion in steatotic livers using ischaemic preconditioning and its effect on bile composition 183
8.1 Introduction 184
8.2 Objectives 185
8.3 Material and Methods 185
8.3.1 Animal Model, Anaesthesia and Surgical Procedure 185
8.3.2 Experimental Groups & Protocol 187
8.3.3 Measurement of tissue oxygenation 187
8.3.4 Measurement of the hepatic microcirculation 187
8.3.5 Measurement of indocyanine green clearance 188
8.3.6 Measurement of bile flow and composition 188
8.3.7 Assessment of hepatocellular injury 189
8.3.8 Histological examination 189
8.3.9 Data collection and statistical analysis 189
8.4 Results 190
8.4.1 Effect of IPC on aminotransferase levels 190
8.4.2 Effect of IPC on systemic and hepatic haemodynamics 190
8.4.3 Effect of IPC on tissue oxygenation 190
8.4.4 Effect of IPC on ICG clearance 191
8.4.5 Effect of IPC on bile composition 191
8.5 Discussion 202
9 Thesis discussion 208
10 Appendix 217
10.1 Quantification of biliary constituents in micromolar concentrations 218
10.1.1 Introduction 218
10.1.2 Materials and Methods 218
10.1.3 Results 218
10.2 Localization of overlapping peaks acetoacetate and pyruvate 220
10.2.1 Introduction 220
10.2.2 Materials and Methods 220
10.2.3 Results 220
10.3 Presentations and publications arising from this thesis 222
10.3.1 Conference presentations 222
10.3.2 Abstracts 223
10.3.3 Original articles 224
11 References 226

List of Figures

Figure 1: Comparison between liver transplants and patients on waiting list 7
Figure 2: Dual channel surface laser Doppler flowmeter and its probes 75
Figure 3: Cellular respiration.....78
Figure 4: Near infrared spectrometer.....84
Figure 5: Dual ultrasonic transit time flowmeter.....88
Figure 6: The physics of NMR 94
Figure 7: ^{1}HNMR spectrometer.....97
Figure 8: Changes in alanine transaminase during I/R.....112
Figure 9: Changes in aspartate transaminase during I/R 112
Figure 10: Light microscopy of liver changes during I/R.....113
Figure 11: Bile flow following warm liver I/R 114
Figure 12: Cytochrome activity during warm liver I/R 114
Figure 13: ^{1}HNMR spectrum of baseline bile.....116
Figure 14: Biliary lactate levels following warm liver I/R 117
Figure 15: Biliary phosphatidylcholine levels following warm liver I/R 118
Figure 16: Bile Acetate levels following warm liver I/R 119
Figure 17: Correlation of ALT and biliary acetate 120
Figure 18: Correlation of AST with biliary acetate.....120
Figure 19: Correlation between change in liver cytochrome oxidase and biliary acetate.....121
Figure 20: Alanine aminotransferase serum levels following warm liver I/R and I/R+NAC 132
Figure 21: Bile flow following warm liver I/R and I/R+NAC 133
Figure 22: Lactate levels following warm liver I/R.....135
Figure 23: Phosphatidylcholine levels following warm liver I/R.....136
Figure 24: Conjugated bile acid levels following warm liver I/R.....137
Figure 25: Acetate levels following warm liver I/R 139
Figure 26: ^{1}HNMR spectra of acetate levels following warm I/R 139
Figure 27: Correlation of bile acetate and serum ALT 140
Figure 28: Correlation of bile acetate and liver tissue cytochrome oxidase.....141
Figure 29: Bile flow following warm liver I/R and I/R+glycine 151
Figure 30: Bile Acid levels following warm liver I/R and I/R+glycine.....152
Figure 31: Phosphatidylcholine levels following warm liver I/R and I/R+glycine.....154
Figure 32: Lactate levels following warm liver I/R and I/R+glycine.....155
Figure 33: Acetate levels following warm liver I/R and I/R+glycine 156
Figure 34: Pyruvate levels following warm liver I/R and I/R+glycine 157
Figure 35: Glucose levels following warm liver I/R and I/R+glycine 158
Figure 36: Acetoacetate levels following warm liver I/R and I/R+glycine.....159
Figure 37: Histology demonstrating centrilobular steatosis 170
Figure 38: Portal flow in the I/R+NAC and I/R group 171
Figure 39: LDF in the I/R+NAC and I/R group. 173
Figure 40: ALT levels in the I/R+NAC and I/R group 174
Figure 41: Bile flow measurements in the I/R+NAC and I/R group.....175
Figure 42: Baseline bile spectra of steatotic bile.....176
Figure 43: ^{1}HNMR spectra of acetate levels following warm I/R 179
Figure 44: Moderate hepatic steatosis.....192

Figure 45: Effect of I/R and IPC on aminotransferase levels 193
Figure 46: The effect of I/R and IPC on hepatic microcirculation..... 195
Figure 47: Effect of and I/R IPC on COX 196
Figure 48: Hepatic ICG uptake following I/R..... 197
Figure 49: Effect of I/R and IPC+I/R on hepatic ICG clearance..... 198
Figure 50: Bile ^{1}HNMR spectra showing β-hydroxybutyrate and acetoacetate. 199
Figure 51: Bile redox ratios for I/R and IPC+I/R 201
Figure 52: ^{1}HNMR spectra of taurocholic acid 219
Figure 53: Standard curve for quantification 219
Figure 54: ^{1}HNMR spectra of normal and pyruvate-augmented bile 221
Figure 55: ^{1}HNMR spectra of pyruvate- and acetoacetate-augmented bile 221

List of Tables

Table 1: Postulated roles for NAC in ischaemia-reperfusion injury.....24
Table 2: ^{1}HNMR Peak Assignments 98
Table 3: Results of peak integration of ^{1}HNMR bile spectra 177
Table 4: Effect of I/R and IPC on hepatic haemodynamics 194
Table 5: ^{1}HNMR bile composition in I/R and IPC+I/R in steatotic livers 200

List of abbreviations

^{1}HNMR	proton nuclear magnetic resonance spectroscopy
^{13}CNMR	carbon nuclear magnetic resonance spectroscopy
^{31}PNMR	phosphorous nuclear magnetic resonance spectroscopy
a_3/Cu_B	binuclear haem-copper coupled centre (of COX)
ABC	ATP-binding cassette
ACA	apparent choleretic activity
AcAc	acetoacetate
Acetyl-CoA	acetyl coenzyme A
ALT	aminotransferase
AMs	alveolar macrophages
AST	aminotransferase
ATP	adenosine triphosphate
βHb	β-hydroxybutyrate
BL	baseline
BF	bile flow
BSEP	bile salt export pump
CoA	coenzyme A
COX	cytochrome oxidase c
CSI	chemical shift images
CT	computed tomography
Cu_A	copper-copper dimer
CW	continuous wave
DNA	deoxyribonucleic acid
DTNB	5,5'-dithiobis-(2-nitrobenzoic acid) (Ellman's reagent)

EC	endothelial cell
EHC	enterohepatic circulation
eNOS	endothelial nitric oxide synthase
EPI	echo planar imaging
E-selectin	endothelial selectin
ESR	electron spin resonance
ERK	extracellular signal-related kinase
FID	free induction decay
fMRI	functional magnetic resonance imaging
GlyR	glycine receptor
GSH	glutathione
HA	hepatic artery
Hb	deoxyhaemoglobin
HbO_2	oxyhaemoglobin
H&E	haematoxylin and eosin
HM	hepatic microcirculation
HO-1	heme oxygenase
HR	heart rate
hrs	hours
HSCs	hepatic stellate cells
HUVEC	human umbilical vein endothelial cells
ICAM-1	intracellular adhesion molecule-1
ICG	indocyanine green
I-κβ	inhibitor of NF-kβ
IL-1	interleukin-1
IL-4	interleukin-4
iNOS	inducible nitric oxide synthase

IPC	Ischemic preconditioning
I/R	ischaemia reperfusion
IRI	ischaemia reperfusion injury
IV	intravenous
KC	Kupffer cell
LDF	laser doppler flowmeter
LPS	lipopolysaccharide
MAP	mean arterial pressure
MAPK	mitogen-activated protein kinase
MR	magnetic resonance
mRNA	messenger ribonucleic acid
MRI	magnetic resonance imaging
MRS	magnetic resonance spectroscopy
mPTP	mitochondrial permeability transition pore
n	number
NAC	*N*-acetylcysteine
NAD(P)	nicotinamide adenine dinucleotide (phosphate)
NADH	nicotinamide adenine dinucleotide (reduced form)
NIR	near infrared
NIRS	near infrared spectroscopy
NF-kβ	nuclear factor-kβ
NMR	nuclear magnetic resonance
NO	nitric oxide
NS	not significant
OLT	orthotopic liver transplantation
PC	phosphatidylcholine (lecithine)
PDE	phospho-di-esters
PDTC	pyrrolidine dithiocarbamate

PET	positron emission tomography
Pi	inorganic phosphate
PKC	protein kinase C
PME	phospho-mono-esters
PMN	polymorph neutrophils
PNs	peritoneal neutrophils
PNF	primary graft non-function
PV	portal vein
PVF	portal venous flow
RF	radiofrequency
ROS	reactive oxygen species
RNS	reactive nitrogen species
SaO_2	oxygen saturation
-SH	sulfhydryl
SI	spectroscopic imaging
SNR	signal to noise ratio
SO	superoxide
sICAM-1	soluble ICAM-1
SD	standard deviation
SOD	superoxide dismutase
SPECT	single photon emission computer tomography
STBA	serum total bile acid
sVCAM-1	soluble VCAM-1
THBF	total hepatic blood flow
TNF-α	tumour necrosis factor-α
Tris	tris(hydroxymethyl)aminomethane
Triton-X100	$C_{14}H_{22}O(C_2H_4O)_n$

TSP	trimethylsilyl-[$^{2}H_{4}$]propionate
ßHb	ß-hydroxybutyrate
PME	phosphomonoesters
PDE	phosphodiesters
US	ultrasound
VCAM-1	vascular cell adhesion molecule-1
VEGF	vascular endothelial growth factor
XO	xanthine oxidase

Abstract

Orthotopic liver transplantation has become the preferred treatment for a variety of end-stage liver disease. As competency and survival rates increase, so does increasing demand, which puts greater strain on a static donor pool. This increases pressure to accept more marginal grafts, e.g. non-heart-beating and steatotic donors. However, graft dysfunction post-transplantation contributes considerably to postoperative morbidity and mortality.

Proton nuclear magnetic resonance (^{1}HNMR) spectroscopy is a powerful technique to explore the biochemical composition of biological fluids; it is rapid, non-invasive, non-destructive and it can detect metabolites at millimolar concentrations. In this study, ^{1}HNMR assessed the changes in bile composition during liver ischaemia/reperfusion. The primary hypothesis was that bile composition changes during liver ischaemia reperfusion injury (IRI). The aims were to document these changes, identify biliary markers for liver IRI using ^{1}HNMR, validate these markers using known modulators, determine if the same was true for steatotic livers and attempt to understand the mechanisms by which these changes happen in relation to the redox state of the liver.

Materials and methods: A rabbit model of hepatic lobar IRI was used. In most experiments 3 groups were used (n=6): Sham group (laparotomy alone), I/R group (1hr ischaemia and 6hrs reperfusion), and a modulation group similar to I/R with the addition of N-acetylcysteine (I/R+NAC: 150mg/kg of NAC) and glycine (I/R+glycine: 5mg/kg glycine). Steatosis was induced by feeding with a 2% cholesterol diet for 8 weeks. Experiments were repeated on steatotic animals with Sham, I/R, I/R+NAC and IPC+I/R (5min ischaemia followed by 10min of reperfusion before prolonged ischaemia was induced) groups. The following parameters were measured: portal blood flow, bile flow (BF) and bile ^{1}HNMR spectroscopy, hepatic microcirculation, intracellular tissue oxygenation, serum ALT, AST and ICG clearance were measured at 1, 2, 5 and 7 hours following reperfusion.

Results: Bile spectroscopy demonstrated significant changes in bile composition following I/R and alterations with NAC, glycine and IPC. These changes are evident despite a constant post-reperfusion rate of BF. They were also present in steatotic livers, and were modulated by NAC and IPC.

In experiment 1: BF, COX and biliary acetate decreased following I/R while AST, ALT, biliary PC and lactate increased along with PMN accumulation in sinusoids, KC hypertrophy, necrosis and apoptosis in normal livers.

In experiment 2: BF, COX and biliary acetate decreased following I/R while ALT, PC, conjugated bile acids and lactate increased in the I/R group in normal livers. NAC administration attenuated the increase in ALT and lactate following I/R in the NAC+I/R group compared to the I/R group. Changes in conjugated bile acids seem to reflect changes in BF.

In experiment 3: I/R+glycine was associated with increased BF, bile acid, acetate, pyruvate, glucose, acetoacetate, and decreased bile lactate and PC levels in normal livers.

In experiment 4: NAC administration in steatotic livers reduced the extent of IRI, increased portal blood flow and liver parenchymal perfusion. NAC increased BF, biliary acetate and pyruvate and reduced acute liver injury, ALT and biliary PC.

In experiment 5: IPC protected the steatotic liver from IRI and maintained hepatic oxygenation, tissue perfusion and mitochondrial redox state. COX activity was decreased by IRI in the fatty liver, but can was protected by IPC.

Conclusions: This thesis has demonstrated changes in bile composition during warm normal liver I/R and its modulation with NAC and glycine. It has

also demonstrated changes in bile composition during warm steatotic liver I/R and its modulation with NAC and IPC. It has noted several metabolites that are consistently changed, as well as the bile redox ratio of metabolites that provides a clearer indication of liver redox state than individual metabolites.

1 Introduction

In the past two decades, orthotopic liver transplantation (OLT) has become the preferred therapy for a variety of causes of end-stage organ disease and is a routinely applied procedure. As liver transplantation becomes the treatment of choice in an ever-widening spectrum of indications, greater strain is put on a static donor pool in the UK (figure 1), with the result of increasing numbers of patients spending longer on waiting lists and dying on these lists[1]. The availability of organs during that same time period has increased much more slowly and appears to have plateaued at approximately 5,000 liver grafts per year in the US[2].

This has put increasing pressure on surgeons and physicians to accept more marginal grafts including those from non-heart-beating and steatotic donors. However, graft dysfunction after liver transplantation continues to contribute considerably to postoperative morbidity and mortality with a primary graft nonfunction rate of 6-8% and initial poor function in 15-16%[3,4]. Improvements in graft preservation and anti-reperfusion therapeutics are required to cope with the increase in the use of marginal grafts.

This disparity between demand and supply has led to a large expansion in the United Network for Organ Sharing liver transplant waiting list in the US and a 5-fold increase in deaths while still awaiting OLT[2]. During this period, several developments have led to any improvement in the survival rate in transplanted patients: more stringent criteria for the selection of suitable donors and recipients; a better understanding of the rejection process and of the modalities to interfere with rejection (prevention and treatment); improvements in the diagnosis and treatment of infectious complications; and better monitoring of transplanted patients[5].

Figure 1: Comparison between liver transplants and patients on waiting list

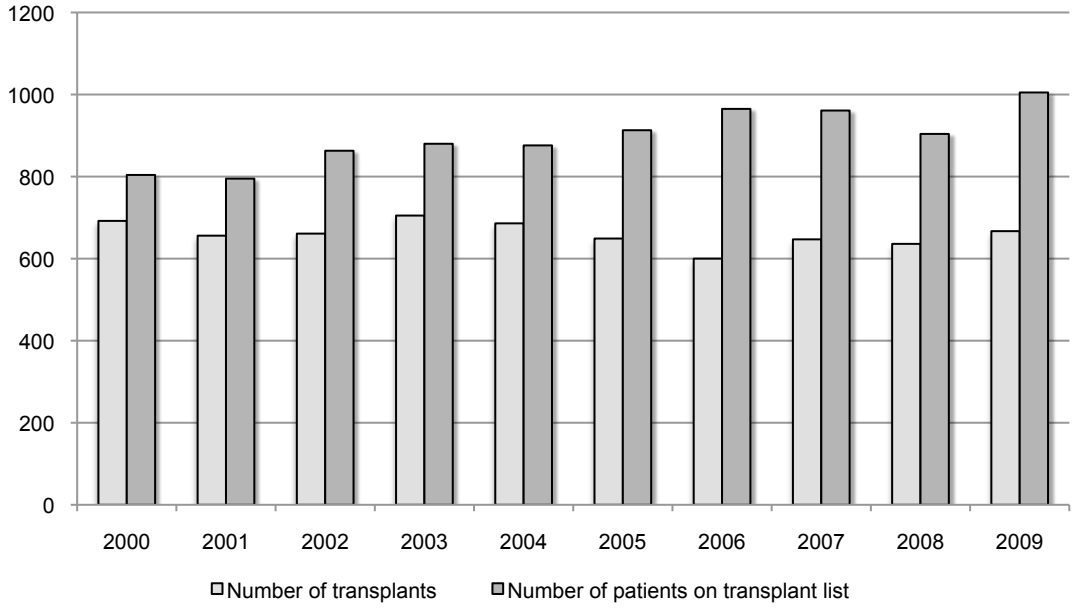

Disparity between number of liver transplants and number of patients on the transplant waiting list in the UK (as of 31st of March for each year cited)

Source: UK Transplant[6]

Certainly, the success rate of solid organ transplantation, in terms of recipient actuarial survival, has dramatically increased since the introduction of cyclosporine and immunosuppressive therapies that can manage acute rejection, however, chronic rejection remains the major complication. This involves both the reaction of the host to the graft (mainly T-cell mediated and B-lymphocyte-driven) and reactions in the graft towards injury (vasculopathy or graft vessel disease). The first reaction requires improved immunosuppressants including tolerance-inducing approaches, the second for interventions to protect the graft (e.g. endothelial cells) from damage like ischaemia/reperfusion injury or for treatment of vessel disease[5,7].

MR spectroscopy has obviously lagged behind the development of MRI for several reasons, one of it being the enormous technical demands, however, clinical MRS is entering the realm of possible, with it becoming almost routine in several fields, particularly the brain and breast. As further technological improvements can be expected in the coming years, spectroscopic applications will increase. It can be expected that MRS will slowly become establish as a tool in individual diagnostics, initially in some niche specialities, and later more generally. The improvements that are needed for this to happen are unspectacular yet necessary such as establishing standards and reference values. The wealth of metabolic data offered by MRS may uncover pathways in ischaemia reperfusion that have not previously been investigated.

In recent years, high resolution proton nuclear magnetic resonance (^{1}HNMR) spectroscopy has been established as a powerful technique to explore the biochemical composition of biological fluids such as plasma, bile, seminal and synovial fluids, in various pathological conditions[8]. This technique is rapid, non-invasive and non-destructive and can detect metabolites present at the millimolar concentrations and can be applied to detect unexpected compounds in biological fluids[9]. In bile, it has been used to confirm the hydrophobic association in micelles of conjugated bile acids

and biliary lipids[10,11]. It has also been used to assess micelle formation[12], the effects of cholesterol on the fluidity of human gallbladder bile[13], the amount of conjugated bile acids in bile[14] and to identify the lipid content of plasma membranes[15]. NMR has also been used to assess hepatic glutamine metabolism[16], hepatic energetic status after warm ischaemia[17], and to study effects of ischaemia reperfusion (I/R) on liver cell membranes[18]. A preliminary study of ^{1}HNMR analysis of bile after liver transplantation has been reported by Powell et al in 1990, suggesting that this technique might help to distinguish ischaemia from rejection post-transplant by detecting large resonance peaks for lactate and acetate[18]. More recently there has been growing interest in attempting to predict graft function by analysing bile production immediately after transplantation[18].

In this study MRS will be used to assess the changes in bile composition during liver ischaemia/reperfusion. The aim is to determine readily recognizable markers for liver IRI using MRS and also attempt to understand the mechanisms by which these changes happen.

The clinical application of this approach would be as a non-invasive assessment modality of graft suitability prior to transplantation, and subsequently, assessment of post-transplantation graft viability. The importance of this study is underlined by the continuing advances taking place in clinical MRI scanners where bile composition may be analysed in vitro non-invasively through MRI voxel analysis[19,20]. MRS is coming of age, but without the research to lend its focus on clinical questions, it will remain a research tool.

The advantages of a non-invasive modality that reveals some of the chemical composition of the object studied is very attractive. Moreover, the documentation of these changes after IRI may allow for the identification of markers of injury. Some may be detectable by MRS techniques, but others may be more easily detected by simpler

techniques once they are identified. Briefly, the aims of this study were:

- To determine if bile composition changed during IRI.
- To determine markers of this change, that may predict IRI in organs.
- To observe the changes in these markers when IRI is suppressed through pharmacological modulation, using agents known to modulate or ameliorate IRI.
- To determine if bile composition is different in IRI of steatotic livers.
- To observe the changes in these markers when I/R injury in steatotic livers is suppressed through pharmacological modulation or the use of ischaemic preconditioning
- To correlate the changes in bile composition to changes in the redox state of the liver.

The hypothesis of this thesis being that since bile requires active, energy dependant, secretion, changes during I/R will affect its composition, and the energy state of the liver may be detected through detecting these changes.

Due to unusual personal circumstances, the experimental work in this thesis was carried out from 2001-2003 but it was examined in 2013. Interestingly, certain advances have been made in both experimental model and MRS analysis and their relevance to this thesis is discussed in sections 3.1, 3.9, 3.11 and 3.12. This is an attempt to do justice to the fact that the thesis is being examined in 2013, and if the experimental work were more contemporary, this is how it would have been investigated.

2 Review of literature

2.1 Physiology of Bile secretion and composition

Bile formation is an osmotic filtration-driven process that depends on the proper function of transport systems in both the basolateral and apical or canalicular membranes of hepatocytes[21,22]. Bile secretion is driven by active excretion of organic solutes into the bile canaliculus, followed by passive inflow of water, electrolytes, and non-electrolytes from hepatocytes and across semi-permeable tight junctions[22].

Liver ischaemia reduces energy dependant transport processes and is therefore associated with reduced Bile flow (BF)[23]. BF recommences on reperfusion, and has thus been considered to be a marker of liver function and used to assess clinical liver transplantation studies[8,9,11]. However the changes in bile composition during ischaemia and reperfusion have not been widely investigated.

2.1.1 Bile acids and bile flow

Bile acids are quantitatively the major component of human bile and their hepatic flux markedly influences BF and the concentrations of other biliary lipids, particularly phospholipids and cholesterol[24]. Hepatic bile formation is an active secretory process involving bile salt-dependent and -independent mechanisms[25], it occurs at two levels, canalicular and ductular. Canalicular BF is mainly dependent on bile acid secretion, bile acid-dependent BF, and accounts for 70% to 85% of the total canalicular flow. Bile acid-independent BF is probably driven by inorganic ion transport[26] and is both canalicular and ductular. Apparent choleretic activity (ACA) is a concept that expresses the relationship between the bile acid secretion rates and the BF and is calculated from the equation of a positive slope of a linear regression, indicating that more bile acid secretion produces more BF (bile acid-dependent BF). Bile acid-independent BF is calculated from the estimated intercept of the slope[27,28]. More than 95% of the bile acids entering the duodenum are absorbed from the intestinal lumen and returned to the liver via the portal vein to be re-secreted at the canalicular level, which is termed the enterohepatic circulation (EHC). Bile acid uptake by the

hepatocytes is very efficient, with a high first-pass extraction rate, but bile acids can still be found in systemic blood bound mainly to albumin[27]. Serum bile acids had been considered a simple but reliable method for assessing hepatic function in liver disease, and it can help to understand the dynamics of bile acid metabolism[29].

2.1.2 Bile secretion

Bile acids are a major component of bile and have a significant influence on BF and the secretion of biliary lipids such as phosphatidylcholine (PC; also known as lecithin) and cholesterol[30]. The hepatocyte is a secretory epithelial cell with a basolateral (sinusoidal and lateral) and apical (canalicular) membrane[31]. Bile is formed by several energy dependant mechanisms, and secretion is relatively independent of perfusion pressure[32]. The passage of bile salts into the biliary canaliculus is the most important factor promoting bile formation. This bile acid-dependent flow accounts for approximately 50% of canalicular BF. Water follows osmotically and there is an excellent correlation between BF and bile salt secretion[33]. Bile salts are transported across the canalicular membrane in a primary active adenosine triphosphate (ATP)-dependent fashion[24,25] which is mediated by the bile salt export pump (BSEP)[26]. BSEP is a genuine ATP-binding cassette (ABC) transporter similar to ABC transporters expressed in many tissues and involved in active outward transport of molecules across the plasma membrane[23].

2.1.3 Bile studies

Developments in liver transplantation over the past 4 decades has fuelled a parallel interest in bile studies[24]. However, *in vivo* analysis of bile secretory function in humans is far from easy, and many measurement techniques have been described, including those of BF and bile acid concentrations of hepatic bile *per se*, bile secretion using duodenal aspirates or markers of water fluxes, and more indirectly, the measurement of bile acid concentrations in serum. Liver ischaemia and reperfusion has been shown to decrease BF *in vivo*[25,34] and *in vitro*[35]. BF has been considered to be a marker of

liver function[25,36-44] and has been used to assess therapeutic and preservation strategies in liver transplantation[45,46].

2.1.4 Post-transplant biliary obstruction

Studies of bile production after liver transplantation were initially plagued with biliary obstruction. Javitt et al., in 1971, were among the first to recognize the potential of bile measurements to monitor liver function after transplantation[47]. A T-tube placed in the common bile duct allowed the collection of bile from one patient during the first 20 days after transplantation found a rapid increase in bile salt synthesis within the first 24 hours which was attributed to the loss of bile salt through the T-tube, such as occurs when the EHC is interrupted by an external biliary drainage, ileal bypass, or administration of cholestyramine. Deoxycholate was still present for several days after transplant, indicating that not all the bile was diverted by the T-tube, despite the authors' suggestion that this represented residual bile salt left within the donor biliary tree at the time of organ retrieval[47].

As the number of liver transplants increased, biliary tract obstruction caused by bile cast formation became recognized as a major postoperative complication. Abnormal bile composition was suggested as a cause—bile supersaturated with cholesterol—possibly potentiated by infection and mucosal damage[48,49]. It was also suggested to be a surgical problem related to bile duct reconstruction[50]. New surgical techniques were developed to try to reduce the incidence of biliary complications, including Roux-en-Y anastomosis to the gallbladder and the gallbladder conduit[51], but these modifications did not resolve the problem. It was discovered that during the first days post-transplantation, bile supersaturated with cholesterol was primarily attributable to low levels of bile acids following interruption of the EHC and depletion of the bile acid pool[52,53]. However, there was poor correlation between the development of supersaturated bile and biliary obstruction[52,53]. The primary mechanism of bile sludge formation was shown to be necrosis of donor bile duct mucosa caused by ischaemic

injury and the presence of bile within the biliary tree during the period of cold preservation[54]. Flushing of the biliary tree during organ retrieval was introduced, with resolution of the problem[54].

2.1.5 Bile flow and composition studies

It was recognised that the composition of bile produced by the transplanted liver was determined not only by the metabolic state of the recipient, but also by that of the donor[55]. Low levels of both cholesterol and bile acids were detected in T-tube bile, which were thought to be due to cholestasis following early severe acute rejection. These findings contradicted earlier reports of supersaturation of bile with cholesterol[48,52,53] and may be explained by the introduction of intrabiliary flushing during organ retrieval. Nevertheless, attention was directed toward the ability of the transplanted liver to secrete bile; in a preliminary report, Shiffman et al. introduced the idea of measurement of BF, bile acid concentration, and bile acid output as potentially useful parameters for assessing graft function and, in particular, acute rejection[56]. Using a Soloway T-tube, which preserves the EHC, BF was found to be initially depressed after orthotopic liver transplantation (OLT) but then increased significantly over the next few days[57]. Furthermore, one patient was noted to have a fall in BF, which signalled the development of hepatic artery thrombosis. Using the same Soloway T-tube, persistent supersaturation of bile with cholesterol in the first week after transplantation was demonstrated when bile acids were depleted[58]. Of their six patients, three developed choledocholithiasis 15 to 42 months later; however, there was no correlation between the degree of cholesterol saturation after surgery and later development of biliary stones. In 1996, Tisone et al. used daily monitoring of biliary bile acids and lipid composition to try to differentiate patients with PNF from those with moderate graft dysfunction or normal function[59]. They showed that patients with primary nonfunction had lower bile acid concentrations and higher biliary lecithin concentrations compared with patients with normal graft function in whom there was a

rapid increase in the bile secretion of primary bile acids. They concluded that it is possible to recognize primary nonfunction; however, the use of T-tube bile and the small number of patients (n=16) studied limit the value of this study.

2.1.6 Apparent choleretic activity studies

Based on earlier studies, Ericzon et al., using T-tube bile samples taken from 10 patients with liver grafts retrieved from nonheartbeating donors, demonstrated a significant correlation between BF and bile acid output, ACA, and applied, for the first time in OLT, the concept of bile acid-independent BF[59]. Total BF, concentration of bile acids, phospholipids, and cholesterol were low during the first week after transplant, reflecting graft recovery from the preservation, ischaemia, and reperfusion. Analysis of bile acid composition was not reliable because of EHC interruption, and although changes in biliary lipid composition occurred rapidly with graft dysfunction, it did not provide more information than standard liver function tests. They did, however, detect improved bile lipid concentrations following successful anti-rejection treatment.

In carefully selected patients considered to have healthy hepatic grafts, with a normal pattern of recovery, and who were considered to provide a baseline of adequate BF, a linear relationship was found between BF and bile salt output[60], which represents the bile salt-dependent flow, and they described two phases of graft recovery over a 10- to 12-day period: an early phase with rapid increase of bile salt concentration and a later phase with more prolonged recovery of bile salt output, suggesting that bile salt-independent flow recovered more slowly than bile salt-dependent flow. They suggested that variations in the ACA may be related to alterations in the hydrophobicity and structure of the bile salt pool and that the presence of increased BF was associated with hypoxia following donor organ retrieval and vagal denervation of the transplanted graft[60]. The ACA in patients with interruption of the EHC was measured and showed a linear correlation between BF and bile acid output with a markedly elevated ACA value and a low concentration of bile acids following

transplantation[28]. This anomalous choleresis may suggest the presence of an increased proportion of other osmotically active solutes in bile probably due to impaired biliary epithelial cell function, and they drew attention to the influence of such factors as the removal of the circulating bile acid pool, graft dysfunction and denervation on BF[28].

2.1.7 Other procedures for the assessment of bile flow

EHC interruption by use of a T-tube for varying periods and at different times after transplant renders interpretation and comparison of the results of the above studies of bile secretion difficult. Measurement of biliary bile acid secretion without interruption of EHC was performed by Theilman et al., in 1991, using duodenal perfusion with a nonabsorbable marker in patients at least 6 weeks after transplant[61]. Biliary secretion was assessed at hourly intervals, and the mean biliary output of bile acids was higher in comparison with their controls. In the bile of the transplant recipients, the majority of bile acids were cholate and chenodeoxycholate with only low percentages of deoxycholate and lithocholate, presumably because of changes in intestinal bacterial flora secondary to perioperative antibiotics[61].

A linear relationship was found between BF and the clearance of the ^{3}H-labeled polyethylene glycol, a marker of water fluxes, 3-6 weeks after OLT[62]. A reduced canalicular flow was noted (including a reduced bile acid-independent BF), despite the patients receiving ursodeoxycholic acid, which has a well-defined choleretic effect. They suggested that these findings were related to immunological, preservation, or reperfusion injury.

2.1.8 Bile studies and immunosuppressive drugs

Cyclosporin A (CsA) was noted to have an apparent cholestatic effect and inhibit bile acid secretion *in vivo* and *in vitro*[63,64], and tacrolimus has been related with hepatotoxicity when administered at higher doses in animals[65]. In humans, McCashland et al. found decreased bile acid secretion and BF in patients receiving

either CsA or tacrolimus and described a reduction in chenodeoxycholic acid biosynthesis related only to patients receiving CsA[28]. However, Ericzon et al. concluded that patients with tacrolimus showed a more rapid recovery of biliary secretion[66,67], and this observation was supported by Sauer et al., using a duodenal perfusion method, 3-6 weeks after transplantation[68]. In patients receiving tacrolimus, there was complete recovery of biliary secretion, despite the presence of elevated serum alkaline phosphatase and γ-glutamyl transferase levels[68]. The effect of CsA on the kinetics of primary bile acids at 6-20 months after transplantation using isotope dilution to measure pool size, synthesis, and turnover rates of cholic and chenodeoxycholic acids showed no change [69].

Recently, Ericzon et al., using T-tube bile samples, showed that bile secretion and composition were not different in patients receiving either CsA or tacrolimus after transplantation[70]. The ACA assessment showed that bile acid-dependent BF was lower in the tacrolimus group than in the CsA group. This was interpreted as evidence of a more rapid recovery of bile secretion capacity in the first group and may due to a lower incidence of acute rejection or a greater hepatotrophic effect of tacrolimus as compared with CsA.

2.1.9 Serum bile acid studies

In 1987, Mora et al., along with Codoceo et al. and Herrera et al. later, investigated the potential value of monitoring serum total bile acids (STBA) as a guide to early graft function[71-73]. They found that STBA levels increased during the anhepatic phase of liver transplantation and were rapidly corrected after revascularization. Kohlhaw et al. noted a prompt drop of STBA levels after reperfusion in 24 of 30 post-transplant patients, which correlated with good early graft function[74]. The other six patients showed either no fall or a rise in STBA and all subsequently lost their graft. Although STBA levels failed to correlate with other parameters of liver function, such as serum transaminases, bilirubin, and coagulation factors, they concluded that STBA

monitoring could be helpful in assessing early graft function[74]. Muraca et al. extended this work and suggested that STBA measurement could be used as a sensitive and specific indicator of hepatic graft dysfunction, particularly during graft rejection when levels increased 3.6-fold and as a marker of successful anti-rejection therapy when levels fell rapidly [75]. Azer et al. also suggested that individual serum bile acids are highly sensitive and specific in assessing graft function, and changes in the added serum concentration of glycocholic and glycodeoxycholic acids and the taurocholic/taurodeoxycholic ratio usually antedated more traditional biochemical indicators of graft rejection[76]. These studies demonstrated the value of STBA levels in liver transplantation; however, their routine use has not been adopted in clinical practice probably because of the lack of reliable and automated measuring techniques.

2.1.10 Combined serum and biliary bile acid studies

STBA levels in liver transplant recipients were found to fall progressively in serum with concomitant increases in bile acids in bile after transplantation[77,78]. The effect of marked depletion of the bile acid pool and the use of T-tube diversion was only reversed by day 15 after transplantation, when normal concentrations of bile acids were achieved. Determination of STBA and biliary bile acid levels could be used simultaneously to detect graft dysfunction 1-3 days earlier than would be indicated by other standard liver function tests[77,78].

2.2 Modulation of ischaemia reperfusion injury

2.2.1 N-acetylcysteine

2.2.1.1 Reactive oxygen species

Reactive oxygen species (ROS) are produced primarily by the mitochondria in cells as a by-product of normal metabolism during conversion of molecular oxygen (O_2) to water (H_2O). These include superoxide radical, $O_2^{\bullet-}$, hydrogen peroxide, H_2O_2, and hydroxyl radical ($^{\bullet}OH$). A “radical” is defined as any atom or biomolecule that contains unpaired electrons[79]. These unpaired electrons influence the chemical reactivity, making the radical more reactive than the corresponding nonradical. Transfer of an electron to oxygen by cytochrome oxidase c (COX) and flavin enzymes results in production of $O_2^{\bullet-}$. The enzyme superoxide dismutase (SOD) converts it into H_2O_2 and O_2. Besides normal cells, phagocytes combat microorganisms with oxidative burst of ROS. Peroxisomes produce H_2O_2 during fatty acid degradation. H_2O_2 is mostly degraded into water by catalase, but some may also escape into the cell[80].

Cells have several antioxiodant defence mechanisms. These include vitamins C and E, and enzymes such as SOD, catalase and glutathione peroxidase[81]. Oxidative stress is generated when there is an imbalance between oxidants and antioxidants. ROS can modify or damage macromolecules in cells including oxidation and peroxidation of DNA, proteins and lipids[82,83]. Trace amounts of metals ions (principally iron or copper) react with H_2O_2 in what is known as the Fenton reaction to produce the toxic radical $^{\bullet}OH$[84]. This radical can cleave covalent bonds in proteins and carbohydrates and destroy cell membranes. ROS at low concentrations can also serve as mediators for a variety of signal transduction pathways and ultimately gene expression[85,86]. Both oxidants and antioxidants have a profound impact on the expression of genes[87-89].

The body has developed major antioxidant defense mechanisms to protect it from damage from free radicals. An antioxidant is any substance that when present at low concentrations, compared with those of an oxidizable substrate, significantly delays or prevents oxidation of the substrate[90]. The endogenous antioxidants mainly are small molecular weight substances that are able to prevent initiation of oxidative damage or to limit its propagation and enzymes that convert and detoxify ROS.[89]

Cellular redox balance is in normal circumstances under tight control. However, when ROS are produced at levels that cannot be counteracted by endogenous antioxidant systems, an imbalance takes place, called oxidative stress[91]. This condition can lead to the damage of lipids, proteins, carbohydrates, and nucleic acids. Hepatocytes tend to be resistant to injury by ROS, since they contain high intracellular concentrations of glutathione (GSH), SOD, catalase, and lipid soluble antioxidants[89].

The antioxidant system is very important for the living species and has allowed them to use O_2 for energy production, without being exposed to the deleterious effects of O_2. The composition of antioxidant defences differs in different cells, tissues, and organs. Different organs contain different concentrations of antioxidants, and for this reason there is variability in organ resistance to I/R. However, there is evidence that the antioxidants operate as a balanced and coordinated system and each relies on the action of the others[92,93].

One of the antioxidant defences in cells is endogenous thiols (sulfhydryl containing compounds) such as GSH and thioredoxin[94].

One of the main systems that can break down H_2O_2 is the glutathione peroxidases. This group includes 4 different isoforms—cellular, gastrointestinal, extracellular, and phospholipids[95]. They have a major role in removing hydrogen peroxide generated by SOD with the oxidation of GSH to its oxidized form, glutathione disulphide (GSSG) (equation 1):

$$2GSH + H_2O_2 \rightarrow GSSG + 2H_2O \quad (1)$$

Glutathione reductase is also an important enzyme in this system. It expresses its action through the regeneration of GSH from glutathione disulphide using nicotinamide adenine dinucleotide phosphate[96].

GSH is a tripeptide present in millimolar concentrations in virtually all cells. It is an important component of the endogenous antioxidant system. GSH's main function is to act as a cosubstrate of glutathione peroxidase to reduce intracellularly generated peroxides. GSH also scavenges directly ROS and RNS. GSH is involved in many other metabolic processes including prevention of oxidation of protein sulfhydryl groups and chelation of copper ions. GSH is also present in the extracellular fluids in very small concentrations[89,97].

Sulphydryl (-SH) groups exert their antioxidant action through the oxidation of the thiol (sulfhydryl) group of cysteine. Furthermore, they have a central role as mediators to the majority of redox-sensitive cell signaling mechanisms[93,98]. The main representative in this group is GSH. It serves as a substrate for glutathione peroxidase and also scavenges ROS directly[99,100]. Glutathione peroxidase is the major defense system of the cell against ROS found in the cytosol and mitochondria and detoxifies H_2O_2 very effectively. The main problem is that its efficacy is dependent on the availability of intracellular GSH and the ability of the cell to re-reduce the oxidized form, glutathione disulphide[101].

N-acetylcysteine (NAC) is a thiol-containing compound used successfully in the management of fulminant liver failure after acetaminophen overdose[102,103]. NAC enters the cell and is hydrolysed to L-cysteine, a reduced-glutathione precursor capable of rapidly replenishing depleted intracellular reduced glutathione concentrations[102]. NAC is a source of sulfhydryl groups in cells and a scavenger of free radicals as it interacts with ROS and reactive nitrogen species directly[104].

The administration of GSH or its precursors could be expected to be effective if the compounds are supplied at the time of declining tissue GSH levels. Although initial experimental studies with GSH administration in liver I/R have not shown a protective effect[105], recent studies in rats have shown that intravenous administration of GSH in doses over 100 μmol/h/kg offers significant protection from both warm and cold liver ischaemia[106,107]. Exogenous GSH administration has limited cellular uptake, due to its large molecular size. This may limit its value in situations associated with severe intracellular oxidative stress[101]. Glutathione precursors such as *N*-acetylcysteine (NAC) can enter cells more easily due to its smaller size.

2.2.1.2 Pharmacology of N-acetylcysteine

The diversity in the pharmacological uses of NAC is due to the multiple chemical properties of the cysteinyl thiol of the molecule. These include its nucleophilicity and redox reactions. The main mechanism of action of NAC is through the metabolism to cysteine in vivo and synthesis of GSH[108]. NAC can also act as a chemical antioxidant. In vitro studies show that the interaction with free radical species results in the intermediate formation of NAC thiyl radicals, with NAC disulphide as the major end product[109].

NAC is a well documented substance in medicine. Its defined volume of distribution is 0.33 L/kg, its renal clearance is 0.21 L/hr/kg, and its elimination half-life is 2.27 hours[110]. Originally, NAC has been used to liquefy mucus in bronchi; NAC is also the antidote for paracetamol poisoning. It should also be mentioned that cysteine derivatives have been intensively investigated in military medicine because of their protective effects against radiation and that NAC has been investigated as a modulator of radiographic contrast agent-induced nephrotoxicity[111-113].

It is important that NAC is readily hydrolyzed to cysteine. Cysteine is a precursor of glutathione. By itself, cysteine has no significant hemodynamic effects; but, when combined with nitrates—the indication being either enhancement of the nitrate

mechanism or elimination of nitrate tolerance through -SH donation—it may cause a decrease in blood pressure and, possibly, headache via intracranial blood bed dilation[114]. These findings were made in a study addressing the management of unstable angina pectoris and comparing the effects of intravenous nitroglycerin versus a combination of intravenous nitroglycerin and NAC[114]. New combinations of NAC action under pathophysiologic conditions, particularly in ischaemia-reperfusion situations, continue to emerge. The effects of NAC in I/R are summarised in table 1.

Table 1: Postulated roles for NAC in ischaemia-reperfusion injury

- Direct protection against effects of ROS
- Redox mechanism cysteine-cystine
- Relation to glutathione
- Indirect protection against ROS, formation of mixed disulfides with –SH groups of membrane peptide/enzymes
- Effect on modulating processes and factors
- Effect on platelet function
- Action under low pH (ischaemic) conditions
- Interaction with neutrophils
- NAC induced ACE inhibition
- Modulation of coagulation
- Effect on adhesion processes (via adhesion molecules)

Modified after Sochman[115]

2.2.1.3 Role of N-acetylcysteine in endothelial function

Since superoxide can react with the vasorelaxant NO to produce peroxynitrite—a strong oxidant—increased production of superoxide can inhibit the vasorelaxation properties of a vessel by decreasing the level of available NO and certain epidemiological studies suggest a beneficial role of antioxidants for cardiovascular diseases[116]. Thus, there is a role for NAC to improve the vasorelaxant properties of a vessel by suppressing the endogenous levels of ROS, including superoxide, and thereby increasing the bioavailability of NO. Cytokines such as TNF-α and IL-1, among others, stimulate the expression of VCAM-1, ICAM-1 and E-selectin in endothelial cells (ECs). Antioxidants, NAC and pyrrolidine dithiocarbamate (PDTC),

suppressed the cytokine-stimulated expression of VCAM-1 (90%) by inhibiting the binding of nuclear factor-κβ (NF-κβ) to the κβ motif of VCAM-1 promoter[117]. Under the same conditions antioxidants did not affect the expression of ICAM-1[117]. Furthermore, PDTC was also shown to inhibit VCAM-1-mediated cellular adhesion, suggesting that the adhesiveness of endothelium can be inhibited by antioxidants[118]. It has also been suggested that several radical-generating systems are involved in the induction of VCAM-1 by TNF-α and that NAC and PDTC can inhibit the adhesion of monocytic cells to TNF-α treated human umbilical vein ECs (HUVECs)[119]. In another report, the IL-1-stimulated expression of both VCAM-1 and E-selectin was shown to be inhibited by NAC. However, NAC inhibited the expression of these genes through different mechanisms.

2.2.1.4 The molecular basis of N-acetylcysteine action

2.2.1.4.1 The effect of N-acetylcysteine on adhesion

NAC inhibited the expression of VCAM-1 by inhibiting the binding of NF-κβ to the VCAM-1 κβ motif as mentioned above. Under the same conditions, NAC did not inhibit the binding of NF-κβ to the E-selectin -κβ motif, suggesting that NAC inhibits E-selectin expression through a different mechanism[120]. Since NF-κβ has been shown to be necessary for the cytokine-stimulation of expression of VCAM-1, ICAM-1 and E-selectin, the differential effect of NAC on the binding of NF-κβ to the -κβ motif of different adhesion molecule genes suggests that multiple NF-κβ complexes may be involved in regulating the expression of these adhesion molecules and that the activity of NF-κβ that regulates the expression of VCAM-1 is redox sensitive. The ability of NAC to inhibit TNF-α -induced ROS production suggests an involvement of ROS in NF-κβ activation and ICAM-1 and E-selectin expression[121,122]. It is possible that adhesion molecule genes in HUVEC and pulmonary artery ECs have differential redox sensitivity. In another study with HUVEC, however, NAC had no impact on cytokine-induced E-selectin expression, while several protein thiol-modifying agents inhibited

it[123]. In a study investigating the mechanisms of diabetes-associated atherosclerosis, advanced glycation end products were found to augment NF-κβ activity and VCAM-1 expression that were inhibited by NAC, affirming the role of ROS in the development of diabetic vasculopathy[124]. NAC specifically prevented TNF-activated inhibitor of NF-κβ (I-κβ) kinase-mediated I-κβα phosphorylation and degradation without affecting β and θ I-κβs [125]. This agent was utilized to demonstrate that preconditioning of ECs against ischaemia via induction of adhesion molecules (ICAM-1, E-selectin), NF-κβ activation and subsequent protection was oxidative stress dependent[126]. NAC and catalase also abolished the endothelial induction of ICAM-1 (70%) and VCAM-1 (100%), respectively, by cyclic strain and by oscillatory shear stress, suggesting redox sensitivity of the signal transduction mechanisms[127,128]. The role of the extracellular signal-related kinase (ERK) pathway and ROS in the signalling of cyclic strain-induced early growth response-1 gene expression was demonstrated by their suppression with NAC[128]. This agent also completely blocked IL-4 -induced oxidative stress and downstream activation of Sp1 transcription factor and VCAM-1 expression[129]. By increasing glutathione levels via NAC treatment, many harmful effects of TNF-α related to endothelial dysfunction could be partially overcome[130]. NAC reduced GTPase Rac-1-induced superoxide production and blocked cytoskeletal reorganization in ECs [131]. Although under TNF-induced proinflammatory conditions NAC blocks ICAM-1 and VCAM-1 expression, under noninflammatory conditions (without TNF-α), this agent increased expression of these genes in HUVEC and human aortic cells in some studies[132]. Pretreatment of HUVEC with NAC decreased heme-induced oxidative stress and ICAM-1 expression by 37%[133,134]. Leptin, which is associated with the human obesity and atherosclerosis, induced oxidative stress mediators such as ROS, INK and NF-κβ activation, and NAC completely inhibited these events, thereby demonstrating redox-sensitive signaling of hyperleptinemia[135]. Induction of the major endothelial mitogen, vascular endothelial growth factor (VEGF) by H_2O_2 (a prominent

ROS and a second messenger) was suppressed by NAC in rat heart ECs[136].

2.2.1.4.2 Effect of N-acetylcysteine on nitric oxide synthase

The decrease in cardiovascular mortality by antioxidants in epidemiological studies may be partly due to the ability of NAC to enhance three-fold the endothelial nitric oxide synthase (eNOS) expression and NO bioactivity, a potent vasodilator, which is reduced in hypertension and atherosclerosis[137]. NAC-mediated increase in glutathione levels resulted in the induction of inducible NOS (iNOS) gene transcription and mRNA expression[138]. By increasing cellular glutathione, NAC was able to attenuate TNF-α-induced p38 mitogen-activated protein kinase (MAPK) activity in human pulmonary vascular ECs, suggesting redox regulation of p38 MAPK pathway and protective role of antioxidants in lung injury[139]. While investigating the mechanisms of hyperglycemia-induced proatherogenic changes in ECs, NAC was shown to block glucose-stimulated ERK5 activity[140].

2.2.1.4.3 Effect of N-acetylcysteine on heme oxygenase

Induction of heme oxygenase (HO-1) by TNF-α and IL-1 in ECs is also partly ROS dependent that can be inhibited by NAC[141]. Peroxynitrite generated by interaction of NO and superoxide anion leads to the formation of hydroxyl radical, induction of HO-1 and EC apoptosis. NAC completely abolished HO-1 increase and activity[142]. This protein may have a protective role against apoptosis. Oscillatory shear- and laminar shear stress-induced HO-1 upregulation could be inhibited by NAC in ECs; however, the former induced a sustained pro-oxidant response while the latter also activated antioxidant defenses[127]. Shear flow-induced c-Fos gene expression was mediated by ROS as this response was inhibited by NAC[143]. NAC inhibited shear-induced tyrosine phosphorylation in bovine ECs, which is mediated by Rac-l-dependent ROS production. Overall, these studies suggest that NAC could improve endothelial function and may attenuate vascular inflammatory disease by antagonizing the effects of intracellular ROS generation, by increasing the bioavailability of nitric oxide and by

reducing leukocyte adhesion to the endothelium. Furthermore, NAC may also be beneficial for treating obesity-related endothelial dysfunction and for attenuating ischaemia-reperfusion injury that remains to be studied in patients with these disorders.

2.2.1.5 N-acetylcysteine in the liver

Oxidative stress generated by various conditions activates hepatic stellate cells (HSCs) and constitutes a possible link between chronic liver damage and hepatic fibrosis ultimately leading to cirrhosis. NAC administration in rats reduced di-methylnitrosamine (a profibrotic agent) -induced fibronectin deposit[144]. At the molecular level, NAC arrested HSCs at the G1 phase of the cell cycle by modifying the redox status of cysteines in Raf-1, MEK and ERK signalling proteins, resulting in sustained activation of ERK-MAPK, induction of the cell cycle inhibitor p21Cip1 and increased Sp1 phosphorylation. These actions of NAC were related to its reducing activity [145]. Co-administration of NAC with toxic cadmium in rats diminished lipid peroxidation and gave protection against hepatic toxicity, suggesting the role of oxidative stress in the toxicity[146]. Administration of NAC within 10-18 hours in patients with acetaminophen overdose and alcoholism prevents liver damage and significantly reduces mortality[147,148]. The possible mechanisms of antitoxicity include improved liver blood flow, glutathione replenishment and free radical scavenging[149]. Cocaine-induced mitochondrial damage in hepatocytes was partially reduced by NAC[150]. Liver injury by oxidative stress during reperfusion of liver transplantation can be significantly reduced by NAC treatment through downregulation of α-glutathione S-transferase and circulating adhesion molecules, sICAM-1 and sVCAM-1 in the donor liver[151]. NAC treatment of ischaemia and reperfusion-injured rat livers blocked NF-$\kappa\beta$ activity and iNOS expression[152]. Hepatocyte apoptosis induced by transplantation related cold storage of rat liver could be diminished by NAC treatment, and its addition before rewarming may be beneficial for successful transplantation[153]. Hepatitis C virus nonstructural protein 5A or hepatitis B virus X protein

generate oxidative stress in the liver and activate NF-κβ and STAT3 transcription factors that can be eliminated by NAC[154]. NAC and related agents such as *S,N*-diacetylcysteine monoethyl ester could improve the status of protective -SH compounds such as glutathione in rat liver[155]. Glutathione levels depleted by acetaminophen overdose in HIV infected patients can be replenished by NAC. Thus, NAC has therapeutic potential for liver against oxidative stress, transplantation-related damage, fibrosis, hepatitis, acetaminophen overdose, chronic alcoholism and heavy metal toxicity.

2.2.1.6 Role of N-acetylcysteine in liver ischaemia-reperfusion injury

NAC has only recently been recognized to protect the liver from warm and cold IRI[156,157] where it was used as a glutathione donor[158] as it increased reduced glutathione levels in the liver after reperfusion[159]. It was also seen to enhance sinusoidal perfusion by intravital microscopy on reperfusion[160] and transplantation[45]. Improvement in microcirculation was observed with NAC increasing acinar and sinusoidal perfusion, on I/R and on transplantation, and reducing neutrophil sequestration, on transplantation[161]. Its use during preservation revealed reduced sinusoidal oxidative stress, and, under a glutathione-depleted conditions, reduced hepatocellular and sinusoidal oxidative stress[162]. The use of NAC-pretreatment in a large animal transplantation model showed that NAC less cytolysis, transaminase elevation, better coagulation, it reduced the incidence of graft dysfunction and primary non-function[163] although this is still controversial[164]. NAC was also observed to reduce remote lung injury following liver I/R[165,166]. Further investigation the mechanisms by which NAC was able to produce these effects revealed that it inhibited TNF-α and IL-10[167], maintained tissue glutathione levels, reduced the rise in malondialdehyde, glutathione peroxidase and superoxide catalase, following I/R, and increased glutathione reductase activities[168,169]. The effect of oxidative stress on NF-κβ and iNOS was elucidated when NAC was seen to inhibit the expression of iNOS mRNA and block upregulated NF-κβ binding activity on reperfusion[152]. NAC was seen to inhibit the

kinase JNK1/SAPK1, a member of MAPK family, which regulates cell adaptation to stressful conditions[170].

2.2.1.7 Role of N-acetylcysteine in clinical liver transplantation

In the first reported trial in clinical liver transplantation, NAC failed to show any beneficial effect of the intraoperative administration of NAC on hemodynamics and graft function in liver transplantation in cirrhotic patients[171]. However it was later reported to produce a distinct reduction in IRI and improved liver function with less elevated peak transaminases, better macrocirculation, improved liver synthetic function and a lower incidence of PNF[172]. NAC was observed to increase selectin shedding following OLT[173]. Furthermore, it was observed to inhibited the increase in circulating ICAM-1 and VCAM-1 24 hr after reperfusion in OLT and reduced the rise in alpha-glutathione S-transferase after reperfusion of the donor liver[151]. Although not all the effects of NAC observed in OLT were beneficial[174].

In summary, NAC can scavenge ROS, increase glutathione levels, undergo auto-oxidation (and produce H_2O_2) and serve as reducing agent. Activation of NF-$\kappa\beta$ in response to a variety of signals (IL-1, TNF, H_2O_2) can be inhibited by NAC, suggesting ROS as common signalling modulators. NAC has been an extensively utilized tool for investigating redox sensitivity of biological or pathological processes. However, due to multiple activities of NAC and the possibility of direct modification of certain signals and signalling proteins, caution is warranted in interpretations. Such putative redox-sensitive mechanisms should be confirmed by additional approaches such as overexpression of antioxidant enzymes and proteins. In liver, NAC diminishes oxidative stress by various agents, and gives some protection against fibrosis, viral infections and toxicity[117].

2.2.2 Glycine

Several process have been implicated in the cascade of events that contribute to IRI, including the generation of ROS[101], generation of pH paradox with mitochondrial

permeability transition[175], generation of inflammatory cytokines[176] and microcirculatory failure, no reflow[177] and the reflow paradox[178]. Complement activation is related to KC and neutrophil activation, with inflammatory and endothelial cell activation further aggravating microcirculatory failure and hepatocytic injury[179].

Since the mechanisms of IRI are diverse, interventions at multiple sites may be necessary to achieve reduction in IRI[180]. Thus, the earlier in the cascade the blockade is achieved, the more effective it may be. In this respect, in addition to microcirculation, blocking activation of KCs and neutrophils provides an important pathway to modulate IRI[179].

2.2.2.1 Kupffer cell activation in I/R

The role of Kupfer cells (KCs) and neutrophils in IRI is pivotal and has been previously reviewed[179-182]. In brief, this involves production of redox stress, inflammatory cytokines, chemokines and proteases. KCs produce a burst of SO during reperfusion[183,184], as well as cytokines such as TNFα and IL-1. KCs are responsible for the initial burst of redox stress and organ injury[185] with neutrophils responsible for injury in the late phase[186]. Blocking KC activation reduces injury in both phases, possibly through blocking the chemotactic effect of KCs on neutrophils[187]. Inflammatory cytokines produced by activated KCs result in local injury through caspase activation and are also implicated in activation and expression of cell adhesion molecules. Neutrophils, once activated, contribute to the injury through ROS production[188] as well as protease secretion[189].

To achieve modulation of hepatic IRI requires targeting of several parts of the inflammatory cascade. Glycine is a particularly good candidate as it is non-toxic at doses that can block KC, neutrophil and possibly lymphocyte activation[190]. In addition glycine provides and broad non-specific cytoprotective effect. Glycine is part of the normal human diet. The body is able to synthesize glycine in the absence of dietary intake, from serine and in the central nervous system from threonine, and it is

therefore classified as a non-essential amino acid. The average daily diet provides up to 2 grams of glycine, as it is the second most common amino acid found in proteins, with fish, meat, beans and dairy products being rich sources[190].

2.2.2.2 Anti-inflammatory action of glycine

Glycine is an inhibitory neurotransmitter in the central nervous system where it hyper-polarizes the post synaptic spinal motor neurons[191] and has been used therapeutically in central nervous disorders. In 1987, Weinberg et al discovered that the cytoprotective effect of glycine on hypoxic cultured renal tubule cells was equivalent to glutathione[192]. In 1991 Marsh et al reported on the cytoprotective effects of glycine on cold stored rat hepatocytes[193], and later that it protected hepatocytes from mitochondrial inhibitors[194]. In 1994, Nichols et al made progress in elucidating the mechanism of this cytoprotection when they demonstrated that glycine inhibited extra cellular Ca^{+2} dependent non-lysosomal proteolysis in anoxic hepatocytes[195].

Intracellular calcium is confined to the endoplasmic reticulum[196] keeping the concentration of free cytoplasmic calcium (Ca_f) low while the extracellular fluid has a relatively higher concentration of calcium. Mammalian cells express two types of Ca^{+2} channels, voltage gated and receptor (agonist/antagonist) gated. Cell injury leads to an increase in intracellular Ca_f by opening voltage gated Ca^{+2} channels[197,198]. Membrane voltage gated channels are activated by membrane depolarization. How this membrane depolarization is triggered in IRI and other inflammatory conditions is not clearly understood[199], but their activation results in cytoplasmic influx of Ca^{+2} along the concentration gradient. Glycine has been shown to reduce this rise in intracellular Ca^{+2}. This is achieved by through glycine receptor (GlyR) activation resulting in increased intracellular Cl^{-1}, which hyperpolarizes the cell membrane, protecting it against IR-induced depolarization thereby preventing voltage gated Ca^{+2} channel activation[200]. Resultant reduced cellular influx of extracellular calcium may be beneficial in preventing calcium mediated cell injury. Voltage gated Ca^{+2} channels are

present in the membranes of a variety of immune and other cells, and may be involved in the pathogenesis of cell injury[201]. Glycine induced movement of radiolabled Cl in alveolar and splenic macrophages as well as hepatocytes and peritoneal neutrophils[202-204] has been used to provide evidence for glycine receptors in these cells, and glycine has been shown to reduce intracellular Ca_f following lipopolysaccharide (LPS) stimulation in a variety of cell types. This reduced influx of Ca^{+2} by glycine has been shown to reduce production of inflammatory mediators and increase production of anti-inflammatory mediators.

KCs are known to contain voltage sensitive Ca^{+2} channels and an increase in the free intracellular Ca^{+2} (Ca_f) concentration is known to be essential for LPS-mediated inflammatory cytokine secretion by activated KCs[190]. In 1997, Ikejima et al demonstrated that KC membranes also expressed glycine sensitive Cl^{-1} channels, and showed that glycine produces hyperpolarisation of the KC membranes and reduces LPS-induced TNF-α production by inhibiting Ca^{+2} influx. In 1999, Wheeler et al provided evidence for the presence of glycine sensitive Cl^{-1} channels on alveolar macrophage cell membranes, and glycine mediated suppression of TNF-α and LPS-induced ROS production[204].

Recently further evidence has accumulated rapidly that glycine has significant cytoprotective and anti-inflammatory activity. These effects depend on special structural characteristics, which glycine shares with other agents such as alanine, taurine and strychnine[205].

2.2.2.3 Glycine receptors

Glycine receptor (GlyR) stimulation produces hyperpolarisation of the cell membrane by Cl^{-1} influx and consequent inhibition of excitation under inflammatory stimuli. GlyR were originally discovered in the CNS, where glycine acts as an inhibitory neurotransmitter, later GlyR were found to be present on peripheral cells[206].

2.2.2.3.1 Central Glycine receptors

Glycine is an inhibitory neurotransmitter in the spinal cord and brainstem[207], and is responsible for the reciprocal inhibition necessary for spinal cord reflexes and muscle tone[208]. This inhibitory effect is mediated by GlyR, which are primarily localized at the post synaptic membrane in the spinal cord, brain stem, caudal brain and retina[209]. The receptor consists of a glycine gated chloride channel.

In the brain, glycine acts as the principal mediator of fast inhibitory neurotransmission[210]. Fast synaptic transmission involves conversion of an electrical signal into a chemical signal at the pre-synaptic terminal. The neurotransmitter so released causes postsynaptic ion channel opening. Opening of cationic channels (Na^+ and Ca^{+2}) by nicotinic acetylcholine, glutamate or serotonin receptors leads to post-synaptic membrane depolarisation and neuronal firing whereas activation of anionic (Cl^{-1} and bicarbonate) channels by glycine and gamma aminobutyric acid, respectively, causes post synaptic membrane hyperpolarisation and suppression of neuronal firing. Activation of the GlyR makes the cells resistant to stimulatory neurotransmitters[190].

2.2.2.3.2 Peripheral Glycine receptors

Peripheral GlyR are present in almost all cell types studied including white cells i.e. Kupffer cells[211], alveolar macrophages (AMs)[211], splenic macrophages[211], monocytes[212], neutrophils[203,211], lymphocytes[213], epithelial cells such as hepatocytes[214] and ECs[215].

Use of Ca^{+2} sensitive dye has shown that glycine inhibits LPS-induced increase in Ca_f in KCs[200], AMs[204], splenic macrophages[202], peritoneal neutrophils (PNs)[203], rat T-cells[213], and VEGF induced increase in Ca_f in ECs[215] and phenylephrine and prostaglandin E_2 mediated Ca_f increase in hepatocytes[214].

Glycine causes a dose dependent influx of radiolabelled Cl^{-1} in AMs[204], splenic macrophages[202] and in PNs[203]. The effect of glycine on Ca_f is dependent on extracellular Cl^{-1} in AMs[204], PNs[203], and ECs[215], while the LPS-induced rise in Ca_f is

independent of extracellular Cl^{-1} in AMs[204] and in PNs[203]. This suggests that under some conditions the effect of glycine is directly related to increased intracellular Cl^{-1} flux, but under other conditions, other mechanisms of action may be involved[190].

Molecular evidence for the presence of GlyR on peripheral cells is based on the demonstration of mRNA and protein expression of GlyR subunits in KCs and AMs[211]. Yamashina et al provided evidence for the presence of GlyR β subunit on ECs using Western Blot analysis[215].

2.2.2.4 Cytoprotective action of glycine

The cytoprotective effect of glycine has been shown to be independent of Ca^{+2} homeostasis and Cl^{-1} conductance in cultured cells[216]. Calcium has been shown as the final common pathway leading to cell death induced by toxic influences[217], and rise in intracellular Ca^{+2} is a common feature between apoptotic and necrotic mechanisms of cell death[218]. Glycine can still provide cytoprotection despite allowing a rise in intracellular Ca^{+2} and can prevent lysis in cells cultured in low Ca^{+2} medium[190]. As opposed to it's anti-inflammatory GlyR-mediated blunting of the intracellular Ca^{+2} rise, the cytoprotective effect is possibly mediated by blocking pre-lytic opening of large cell membrane pores (death channels), which would normally allow large molecules to leak into, or out of the cell and lead to cell lysis. Glycine prevents the cell membrane bleb dilatation in response to increasing membrane permeability[190].

After exposure to toxin or ATP depletion, cell permeability increases[219], eventually leading to cell lysis. Evidence has accumulated suggesting the opening of glycine responsive cell membrane channels, as a terminal mechanism of cell lysis. Although the presence of glycine in the medium does not influence the early changes in molecular permeability, or the morphological changes occurring after toxic injury or ATP depletion, it does prevent the terminal changes and cell lysis[219].

Hepatic IRI leads to cellular ultrastructural changes such as the vesicular

development, alterations of junctional complexes and the development of electron densities[220]. Cell swelling and bleb formation has also been described in hepatocytes after cold and warm IRI[221,222]. Estacion et al have shown that glycine containing medium, added to bovine aortic endothelial cells blocked cell permeability to large molecules, prevented dilatation of blebs and cell lysis, providing evidence of cytoprotection independent of the presence of GlyR[219].

2.2.3 Steatosis

Hepatic steatosis is a common problem in Western countries, with an incidence of 6-11% in autopsies of accidental deaths[223,224] and is as high as 20% in hepatic resection patients [225] and 26% in potential donors for liver transplantation[226,227] (possibly due to population selection, poor nutritional status and prolonged intensive care units)[228,229].

2.2.3.1 Steatosis in liver transplantation

There is an association between severe donor steatosis and primary nonfunction (PNF)[230] or dysfunction[231]. In a multivariate analysis including 227 patients, severe steatosis was identified as an important significant risk factor for primary graft non- or dysfunction[3]. This has been confirmed by others[232-234] and estimated that severe steatosis is associated with a 60% risk of PNF[234]. Moderate steatosis has no impact on graft or patient survival[234,235], but primary graft dysfunction (e.g., elevated serum transaminases) was uniformly more frequent in the steatotic groups which is associated with decreased 1-year survival of patients[4,229,236].

2.2.3.2 Steatosis in liver resection

There is also an increased risk of complications for liver resections in fatty livers[237] with a mortality rate up to 14% in patients undergoing major hepatic resections[238]. There is currently a consensus in the hepatobiliary and transplant community that steatosis increases the risk of postoperative complications and patient death following liver transplantation and major liver resection. Until recently most transplant centres refused

to accept steatotic livers with more than 20% steatosis. With increasing demand for livers and a static donor pool, the interest in steatotic donors has increased[229].

2.2.3.3 Impaired microcirculation

During liver resection, hepatic inflow occlusion (Pringle manoeuvre) is often used to minimize blood loss. In addition, cold preservation, rewarming, and warm ischaemia are inherent in liver transplantation procedures. Impaired microcirculation has been proposed as an important factor in the decreased tolerance of the steatotic liver to ischemic injury. Fat accumulation in the cytoplasm of the hepatocytes is associated with an increase in the cell volume[239,240] which may result in partial or complete obstruction of the hepatic sinusoidal space[239-241]. The impaired microcirculation may amplify the negative effects of additional ischemic insults. Ischaemia and reperfusion injuries also cause cell swelling and adherence of platelets and leukocytes[242,243], which in combination with pre-existing reduced sinusoidal space may lead to a more severe injury. Sinusoidal flow has been shown to decrease by half in rat livers containing 30 to 60% steatosis compared with controls[244,245].

2.2.3.4 Steatosis and hepatic energy metabolism

Steatosis of different aetiologies leads to an accumulation of nonesterified fatty acids which have an inhibitory effect on the β-oxidation system resulting in a decrease of acetyl-coenzyme A (CoA) production. Acetyl-CoA is an important precursor for the Krebs cycle and gluconeogenesis. Thus important energy sources for the liver, β-oxidation and gluconeogenesis, are decreased in steatosis[229,246-249].

2.2.3.5 Other mechanisms of injury in steatotic livers

Steatosis increased neutrophil adhesion following 60 minutes of normothermic ischaemia[37,250]. Others have suggested KC dysfunction as a factor involved in poor outcome in the fatty liver[250].

A feature of ischemic liver injury is apoptosis, an active energy-requiring type of cell death. In apoptosis, unwanted cells are transformed into smaller apoptotic bodies that

are removed with minimal inflammation. The amount of apoptotic hepatocytes after I/R correlates with liver injury and survival[251,252]. Antiapoptotic strategies are highly protective against ischemic injury of the liver[253-256]. Steatotic livers have shown a dysfunction of the apoptotic pathway[256]. Massive hepatocyte necrosis occurred in fatty rats after 60 minutes of ischaemia, whereas only minimal necrosis was present in the lean control group, blocking apoptosis significantly reduced ischemic injury in lean animals but had no effect in steatotic rats[229,256].

Steatosis is associated with decreased hepatic microcirculation, a dysfunction of mitochondrial ATP generation, and impaired apoptosis as the physiologic form of cell death is impaired in fatty hepatocytes, resulting in the necrotic form of cell death with the release of cytoplasmic contents, which further aggravates inflammation and liver injury. Finally, liver regeneration is reduced in steatosis and tissue loss cannot be restored[229,257].

As a period of ischaemia is often necessary in liver surgery, and is inevitable in organ retrieval and transplantation, pharmacological modulation could potentially protect steatotic livers, minimizing the detrimental effects of IRI.

2.2.4 Ischaemic preconditioning

Murry et al. first described IPC on observing that brief periods of ischaemia improves the tolerance to subsequent, prolonged ischaemia in various organ systems[258]. IPC has been shown to decrease liver injury after warm IR[34,259-261] as well as after cold ischemic storage[262-264]. IPC is protective against IRI in normal[261-264] and fatty liver[265]. The benefit of IPC has also been proven in human liver resection surgery[260]. Recent studies show that IPC increases the tolerance of fatty livers to IRI in animal model of steatosis[265,266].

IPC significantly improves blood flow in the microcirculation during the reperfusion phase[267] in a rat IRI model and NIRS showed that preconditioned livers exposed to hypoxia maintained their COX redox state[268]. There is growing evidence that mitochondria are a major target of IRI[269].

The mechanism of ischemic preconditioning is uncertain, but it is considered to be a biphasic event. The early stage of protection lasts about 2 hours after the trigger, while a second phase of protection occurs during the following 24 hours. As the effects can be observed shortly after the stimulus, the mechanisms involved might be related to pre-existing molecules as effectors of natural defense events against subsequent ischemic injury[270].

IPC modulates oxidative stress by limiting the accumulation of xanthine, and through reducing the conversion of xanthine dehydrogenase to xanthine oxidase (XO). XO requires molecular oxygen introduced on tissue reperfusion to convert hypoxanthine to xanthine with SO release. IPC inhibits XO-derived oxidant stress thus limiting this pathway of oxidative injury[271].

IPC reduces oxidative stress by suppression of ROS released by KCs, because IPC has no benefit on Kupffer cell-depleted rat livers[272]. Ischemic pre-conditioning decreases endothelial adhesion molecule expression (P-selectin) in warm IRI of the

rodent liver, thereby diminishing the neutrophil adhesion and resulting in decrease of oxidative neutrophil-mediated damage[243,272].

In case of sustained oxygen deficit, ATP is rapidly consumed to generate energy for cellular metabolism, thereby resulting in adenosine production. At some stage in reperfusion, adenosine is washed out of the tissues, causing adenosine depletion. Moreover, adenosine is transformed to hypoxanthine and xanthine leading to ROS production. Adenosine-related mechanisms during IPC seem to be mediated by A2 receptors, because their blockade results in inhibition of NO production and subsequent cessation of protective effects of IPC[272,273].

Adenosine activates eNOS, resulting in NO synthesis. It is widely accepted that NO is an important mediator of IRI associated with improvement of liver microcirculation and tissue oxygenation by attenuating neutrophil adherence and inhibiting platelet aggregation. NO inhibits the release of endothelins—a member of a family of potent and long-acting vasoconstrictive mediators[274]. Inhibition of NO synthesis blocks the protective effect of IPC[275,276]. IPC stimulates the activity of various intracellular kinases via activation of cell membrane receptors by adenosine and other effectors. Protein kinase C (PKC) and p38 mitogen-activated protein kinase have been shown to reduce hepatocyte injury. This is mainly due to activation of another intracellular kinase (protein kinase B; Akt/PKB), which has antiapoptotic effects and stimulates NO synthesis via eNOS[277,278].

IPC of an organ may protect others organs from IRI. This mechanism is recognized as remote IPC. It was first described in a model of canine of heart ischaemia, and involves the release of effectors into systemic circulation. Liver preconditioning-induced resistance to IRI damage in remote organs is thought to be elicited by decreased hepatic TNF-α release.

Recently, it was shown that remote ischemic preconditioning of the hind limb reduces

warm ischaemia-reperfusion injury in the livers of rabbits and rats. Although the mechanism of remote ischemic preconditioning remains poorly understood—adenosine, bradykinin, and opioids are released in systemic circulation after sublethal ischemic injury seems to be involved in the process[279,280].

Delayed ischemic preconditioning onsets 24 hours after reperfusion and protection may persist for several days. Gene expression and synthesis of proteins have been investigated in delayed ischemic preconditioning. The activation of NF-kβ and other transcription factors can induce the synthesis of iNOS, heat-shock proteins, and antioxidants. Heat-shock proteins contribute to the diminishment of TNF-α synthesis and reduce inflammatory injury in livers subjected to IPC[259,281].

2.3 Magnetic resonance

2.3.1 Introduction

In this chapter I would like to review the history of magnetic resonance (MR) and its applications in medicine. I would like to focus on magnetic resonance spectroscopy (MRS) and its growing importance in medical applications.

It is difficult for those from a medical background to understand MR applications, to follow MR literature, and to interpret the MR specific terminology. Extensive use of mathematical treatment of the MR effect and its applications is thus avoided in this thesis.

Clinicians will most likely encounter MR through looking at a diagnostic MR images (MRI) displaying anatomy with excellent contrast and resolution. When the first human MR images became available, radiologists and clinicians were already familiar with sectional images of the body through the advent of computer tomography (CT). To relate MRI as an extension of CT, ultrasound (US) or other morphological imaging modalities would be a great injustice. CT is modulated through only one major parameter, the energy of X-rays, and displays only one measured parameter, X-ray absorption. In contrast, MR images are determined by multiple parameters and the way an image is acquired can change the appearance of the picture and the information content completely. The physics of image acquisition manipulates the contrast and resolution of the image and is used to render other parameters such as flow, oxygenation, chemical environment, and many other characteristics determined by the molecular structure of tissue[282].

Very briefly MR is produced when nuclei with a nuclear spin (with non-zero spin numbers) are subjected to a strong magnetic field, they are split into a set with the sum of their spin aligned parallel to the magnetic field and a set whose sum spin are anti-parallel. The nuclei spin (precess) around the axial magnetic field. While the proportion is nearly equal, slightly more are oriented at the low energy angle. The

frequency with which the dipole moments precess is called the “Larmor frequency”. The nuclei are then briefly exposed to pulses of electromagnetic radiofrequency energy (RF) in a plane perpendicular to the magnetic field, causing some of the magnetically aligned nuclei to assume a temporary non-aligned high-energy state. The frequency of the pulses is governed by the “Larmor equation”. As the high-energy nuclei relax and realign, they emit energy at rates, which are recorded to provide a wealth of information about their environment.

One of the most informative parameters encoded in the magnetic resonance signal is the “chemical shift”. While this information is only partially used in MRI, it is the very basis of magnetic resonance spectroscopy and of the applications in physics, chemistry, and biology. An MR spectrum represents signals of different metabolites ordered in a plot along a chemical shift axis. MR spectroscopy is a representation of the different metabolites in the tissue or liquid being analysed. The wealth of information recorded in a spectrum makes this method rather difficult and demanding to interpret. Single proteins or other macromolecules can be characterized perfectly in well-defined solutions, even allowing the analysis of their three-dimensional structure. In vivo, MR spectra are generated by a complicated mixture of elements and metabolites in tissue, making the interpretation of the crowded spectra difficult. However, it represents a unique tool to obtain a chemical “snap shot” non-invasively and from living tissue[282].

2.3.2 Historical perspective

While MRI has become established and well known in medicine, only a few specialists really know that the effect of nuclear magnetism has its roots in physics. This would only be of historical interest if the development of MR in medicine had been completed. However, looking at the history of MR and at its applications in different fields reveals the flexibility of this modality and gives an indication to the potential of this method[282-284]. In this respect, looking back at the history of MR may help in

understanding its future.

2.3.2.1 Scattered beginnings

The beginning of MR as we know it today can be traced back to the famous experiment of Stern and Gerlach in 1921. Stern and Gerlach passed a beam of silver atoms through an inhomogeneous magnetic field and observed that two distinct beams were formed instead of a homogeneously spreading one[285]. This observation was repeated in a subsequent experiment in Stern"s laboratory in 1933 using hydrogen molecules[286]. The fact that a discrete number of beams were formed could not at the time be explained by classical physics. It required the theoretical basis of quantum mechanics to reveal that these beams were formed due to the angular momentum, i.e., the "spin" of a nucleus or an electron, and magnetic moment, they are strongly related to each other and exist in a limited number of allowed states only. These first experiments that lead eventually to the discovery of MR were initially designed to understand quantum mechanics and the characteristics of nuclei and electrons. Otto Stern was subsequently awarded the Nobel Prize in Physics in 1943[282].

A series of experiments of several groups followed, still aimed at an exact determination of the magnetic properties of the nuclei. One of these scientists was Isidor Isaac Rabi who published a one page report on "A new method of Measuring Nuclear Magnetic Moment" using oscillating fields to reorient the nuclear spins[287]. Rabi received the 1944 Nobel Prize in Physics for this discovery; however, not all ingenious experiments lead to success and awards. We know of at least two scientists who contributed significantly to the field but failed in one way or the other. It seems that Zavoisky, a scientist in Kazan/Russia, observed an NMR effect in 1941 but was not able to reproduce it, mainly due to the war[284]. Gorter, attempted to measure nuclear paramagnetism, but failed several times[288,289], however he inspired Rabi"s group for their successful experiment[282,287].

Although World War II diverted recourses away from theoretical physics, it promoted

the development of radar and subsequently improved radio-transmitters and amplifiers, which were necessary for the discovery of magnetic resonance. At the end of the war, Purcell, Torrey, and Pound[290] published a report on NMR effects in solids in 1946. At the same time, Bloch, Hansen, and Packard[291,292] made a similar attempt to measure what they called “Nuclear Induction”. It seems that it was not immediately clear that the two independent groups described the same effect. These reports were important as they transferred knowledge about Rabi”s work in molecular beams into an effect that had been observed in bulk matter. The scientific world recognized the importance of this work that led to the discovery of modern NMR and Bloch and Purcell received the 1952 Nobel Prize in Physics[282].

Thus far, NMR contributed almost exclusively to the development of nuclear physics and the aim of the research in this field still was to characterize materials and to measure nuclear parameters. A major step forward from measuring nuclear properties to the more detailed characterization of matter came in 1948 in the form of the landmark paper of Bloembergen, Purcell, and Pound (“B.P.P. theory”) on relaxation effects and the influence of motion[293].

2.3.2.2 The chemistry revealed

The development of NMR has gone hand in hand with the development of related technologies. The next achievement was only made possible by the improvement in the strength and homogeneity of the magnets used in the experiments in the early 1950s. The phenomenon of a chemical shift was observed when stronger and more uniform magnetic fields were used. Up to then, different parts of the sample experienced very different magnetic field strengths, and the observed signal of the sample was a mixture of responses. In homogeneous magnets, all parts of the sample experience the same field strength and, therefore, it was expected that the response would occur at a single frequency. However, instead of observing a single resonance line in a spectrum, various groups separately began to observe multiple resonance

lines when they improved their magnets[283,284].

Arnold et al. observed that the relative position of the left-most resonance in the spectrum was temperature dependent[294]. Liddel and Ramsey explained this effect by hydrogen bonds between the molecules and a chemical exchange of these groups[295]. Proctor and Yu observed an additional effect that was still hidden in Arnold's ethanol spectrum–the spin-spin coupling[296]. Spin-spin coupling is a direct consequence of chemical bonds and the multiplicity of the lines can be used to identify chemical groups. The observation of spin-spin coupling in liquids required a continuation of the improvements in magnet technology since the separation of the coupled lines was much smaller than typical chemical shift differences[282].

With chemical shift, spin-spin coupling, and chemical exchange, three new and exciting molecular aspects of NMR have been discovered in the early 1950s. At this stage in the early 1950s, chemists started to become more interested in NMR to NMR started to used it for the characterization of chemical substances and reactions rather than the physicists who wanted to characterize nuclear properties[282].

2.3.2.3 Radiofrequency pulses and Fourier techniques

In the early years of NMR, a spectrum was measured by a continuous irradiation with radiofrequency (RF) waves. This procedure was called continuous wave detection (CW), meaning that every frequency response had to be detected separately. Torrey showed in 1949 that signals could be observed after excitation with a radiofrequency pulse and subsequent detection without irradiation[297]. In parallel, Erwin Hahn worked on the signal that was called "free induction decay" (FID)[298]. In 1950, he showed that these decaying NMR-signals could be partially refocused by a series of following RF-pulses, in a landmark paper, resulting in so-called "spin echoes"[298]. Modern NMR techniques and in particular magnetic resonance imaging rely heavily on spin-echoes and would not exist without this fundamental paper. These techniques were extended by Carr and Prucell in 1954 and Meiboom and Gill in 1958 and effectively laid the

basis of modern spin echo trains[299,300]. They considered also diffusion of the molecules, another molecular effect that influences NMR signals[282].

The following years interest in NMR increased rapidly. In the mid 1960s, Ernst and Anderson realized that in this FID, the whole information of a spectrum was encoded[301]. They applied a widely used mathematical treatment, developed in the 18th century by Jean Baptiste Fourier, to the FID to improve the signal-to-noise ratio and experimental flexibility, thus introducing the "Fourier technique" into NMR and the analysis of the data acquired in an FID or a spin echo. However, the new method required a considerable computer power, which was not available those early days. Fourier spectroscopy required the advent of computer technology and had to wait two decades before it became practicable. Fourier spectroscopy showed its enormous advantages over conventional CW techniques and founded modern NMR spectroscopy, including multidimensional data acquisition[302]. This was closely followed by the development of two-dimensional NMR spectroscopy[303,304] which is also the basis for modern imaging techniques[305] in medicine[282].

In 1991, Richard Ernst was awarded the Nobel Prize in Chemistry for "his contributions to the development of the methodology of high resolution NMR spectroscopy".

2.3.2.4 The formation of MR imaging

The early 1970s was the start of MR research being integrated to develop an imaging modality. Lauterbur published a landmark paper about the use of magnetic field gradients to form images of protons (^{1}H) in water[306]. This paper gave the most explicit suggestion at the time of how NMR can be used to obtain images. Lauterbur based his concept on the method CT generates images[307]. He suggested the acquisition of a series of projections, similar to the projections obtained by X-rays in CT, followed by a "projection reconstruction"[306]. This concept has been replaced by the Fourier technique suggested by Ernst"s group[305] and refined by Edelstein et al. in the so-called spin-warp technique[308]. Other suggestions were made on how images could be obtained[283,284]

however, all the different pulse sequences developed in the following years were based on the Fourier principles[282].

The possibility to obtain images from an intact body was crying out for medical applications. However, several problems had to be resolved first, primarily the construction of magnets large enough for the human body fuelling the advancement of the technology in the following years. As it entered the clinical arena, a new problem arose when NMR had to be explained to patients, the term “nuclear” led to confusion with methods known from “nuclear medicine” which have the disadvantage of using radioactive isotopes and ionizing radiation. Since NMR does not generate ionizing radiation, a better differentiation was desirable and “NMR” lost the “nuclear” and mutated to “MR”. Thereafter, a convenient yet not strict nomenclature evolved: NMR was used for in vitro experiments, while MR characterized mainly in vivo examinations, separated into MRI and MRS to describe the different sub-specialties[282].

2.3.2.5 The separation of high resolution NMR and medical applications

NMR in chemistry and biophysics became increasingly important as a routine analytical method. Commercial spectrometers became available, providing magnetic fields of about 8T in the middle of 1970s and almost 20T in the late 1990s. The growth of computer power allowed increasingly complex experiments and data analysis. The spectral resolution of analytical NMR systems was extremely high and led to the acronym “High resolution NMR” in contrast to applications in solid state physics that were at a much lower resolution. Early on, NMR laboratories began using conventional electromagnets with horizontal field lines and a gap between two poles, but eventually superconducting technology was required to provide the enormous field strength of modern magnets. “High resolution spectra” were acquired in small bore, vertical magnets from samples within a tube of typically 5mm diameter. The tube with the solution examined rotated at very high speed (“spinning”) to equalize the stabilized (“locked”) magnetic field strength. “High resolution NMR” developed with an increasing

pace and a number of sub-specialties were created. Chemists were able to characterize small yet very complex molecules in detail and followed chemical reactions[309-311]. Biophysicists on the other hand increased the size of the biomolecules observed and began to elucidate the three-dimensional conformation of proteins and nucleic acids[282,312-315].

Lauterbur"s publication on image formation[306] coupled with Damadian"s observation that tumours had different relaxation times compared to healthy tissue[316] generated a demand to develop magnets and systems capable of imaging the human body. This sparked a race to develop an MR imaging system that started in the 1970s and ongoing. The medical field demanded a whole-body magnet with a bore of about 100cm and equipped with gradient coils. At the beginning, these magnets had quite a low field strength of typically 0.05 or 0.1T. Damadian et al were the first to produce an image of the human chest in such a large magnet[317], by moving the focused region of interest through the body. Mansfield et al followed soon after with an image of the abdomen[318] and a group at EMI (Electric and Musical Industries Ltd, Central Research Laboratories in Hayes, Middlesex, UK) using what was then called the "EMI scanner", presented the first image of a human head[319]. A race for higher field strength began and eventually, whole body magnets with field strengths of 1.5T were widely available[282].

A new problem was generated when NMR had to be explained to patients—the term "nuclear'' led to some confusion with methods known from "nuclear medicine". While some of these methods, in particular positron emission tomography (PET) and single photon emission computer tomography (SPECT), are extremely elegant to measure the distribution of much diluted metabolites, they have the disadvantage of using radioactive isotopes and ionizing radiation. Since NMR leaves the nucleus intact and does not generate ionizing radiation, a better differentiation was desirable and "NMR" lost the "nuclear" and mutated to "MR". In the following, a convenient yet not strict

nomenclature evolved: NMR was used for in vitro experiments, while MR characterized mainly *in vivo* examinations, separated into MRI and MRS to describe the different sub-specialties. This nomenclature is convenient, however, it ignores to a certain extent the existence of electron spin resonance (ESR). So far, this did not cause major problems since there are only very few ESR applications *in vivo*–mainly due to the very high RF frequencies that are too strongly absorbed in human tissue[282].

2.3.2.6 The delay in clinical MRS applications

MRS needed field strengths and homogeneity that were not available before the end of the 1980s. In a parallel yet much less noticed development, small-bore magnets at higher field of 2.35 and 4.7T became available. These magnets were typically used for MRS studies in extremities and smaller animals[282].

Another element used in MRI was adopted for the development of "chemical shift images" (CSI) or "spectroscopic imaging" (SI)[320-322]. The almost independent development of diagnostic MRI in whole-body magnets and biomedical MRS in small-bore magnets led to a separation of the two fields. This separation in the development of the two technologies and the differing demands led to the somewhat delayed development of in vivo spectroscopy. Small-bore magnets had only surface coils to locate the signal in the body or had considerable problems with the gradient systems. Whole body systems, although advancing due to the development of MRI, had minor or no capabilities to do spectroscopy. It was to the unintended benefit of MRS that several MRI applications also required very homogeneous fields and stable gradient systems. The quality of current magnet technology has led to a late but noticeable reunion of parts of biomedical MRS and diagnostic MRI. One commercial product (PROBE, proton brain examinations) even allows acquiring ^{1}HNMR spectra from the human brain in an automatic way, comparable to imaging sequences. MRS of other nuclei than ^{1}H, however remains possible in only very few commercial systems and only as a research tool. This fact is one reason that delays a widespread use of

diagnostic MRS[282].

2.3.2.7 Technical developments meet the request of new MRI sequences

The time between 1985 and 1995 has seen an enormous effort of commercial companies in technological development, often based on ideas from academic researchers. Passive and active shielding of magnets enabled them to be housed in radiology departments where previously they had been isolated to avoid problems with stray fields. Earlier acquisition times of MR sequences were typically 10-30min. Much faster sequences were suggested[323,324] and adapted by the industry. Although Mansfield's "echo planar imaging" (EPI) promised to allow image acquisition almost in real time, it was particularly demanding[325] and about a decade ahead of the technological possibilities. In 1985, the same author proposed a solution of this problem in the form of actively shielded gradients[326]. The technical improvement of gradients as a result of this idea and the desire to obtain images in real time is an illustrative example of the driving force of MRI. RF emitting and receiving parts of the MR systems experienced a steady improvement over the decade with better coils being constructed and transmitters and receivers being digitized. The enormous amount of data acquired during EPI acquisitions demanded increasingly faster analogue-digital converters[282].

2.3.2.8 Advances in NMR

NMR in physics, chemistry, and biology is far more successful and widely used than recognized by the medical MR community, e.g. rarely a new drug will become available that has not been characterized extensively by NMR. In solid state physics the aims, the problems, and the methods are so different that there is rarely an overlap between the two fields. One of these uncommon yet theoretically exciting examples has been observed in human muscle[327]. ^{1}HNMR spectra showed orientation-dependent effects in vivo that required theories typically used in solid state NMR to be explained[282].

High resolution NMR in liquids is nowadays an indispensable method in chemistry and is used to characterize reactions, products, molecular conformations, etc.[309-311,328]. An extension of classical high resolution NMR as used in chemistry can be found in biological research[314,315,329-331]. While chemistry uses NMR to analyze relatively small molecules extensively, biological NMR benefits from the fact that the molecules can be studied in solution. Other powerful methods such as X-ray diffraction have proven their value for decades, however, crystals are not a biological environment, and the study of (large) biological molecules in solution is desirable. Modern NMR uses a combination of chemical methods (labelling) and sophisticated pulse sequences (two-, three-, and four-dimensional spectroscopy) resulting in a tremendous wealth of information contained in such spectra. This helps in particular to study conformation changes and plasticity of molecules that can be hidden in crystals. Strong magnetic field strengths together with sophisticated pulse sequences promoted examinations of larger and biologically important molecules such as proteins and nucleic acids. Wuthrich's group investigated conformation of biological molecules in solution and has pushed the boundaries of the field in the last decades with the increasing help of the whole arsenal of NMR methods to increase the size of the investigated molecules from fragments of hormones[332] to much larger proteins[314] and DNA[282].

2.3.2.9 Advances in diagnostic MRI

Diagnostic MRI became an essential tool in radiology in 1980s and 1990s. This success of diagnostic MRI was supported by the excellent soft tissue contrast, the variable orientation of the scan planes, the possibility to acquire three-dimensional data sets, the high information content of contrast agent application, the combination of morphological imaging with flow sensitive methods, MR sequences that display functions of different organs, and others. More advanced types of MR examinations are known, successfully presented in scientific meetings, and used in some advanced departments. However, these methods still need methodological or technical

improvements and the majority of the radiologists do not use them frequently. A few examples of these techniques include interventional MRI, functional MRI of the brain for pre-surgical examinations, quantitative analysis of MR images, MR-angiography of the coronary arteries[282].

The demonstration of the feasibility by academic institutions is often followed by an enormous effort of the commercial MRI suppliers to meet the required specifications. An impressive example has been given by the group at Harvard who initiated the construction of a totally new type of an open magnet used for interventional MRI[333-335]. The revolutionary design of the magnet allows surgeons to step into the magnet and to observe the imaged volume from outside as well as from inside on the MRI screen. Another method with an enormous potential is functional MRI (fMRI) of brain activity. It began with the observation of blood flow in the brain using contrast agents[336,337]. Another breakthrough was achieved when blood deoxygenation was recognized as a natural contrast agent[338]. fMRI is now able to follow brain activity at a spatial resolution that is far better than the closest rival, PET. Diffusion weighted MRI is based on the Brownian motion of the water molecules[339,340]. The mobility of the water molecules is limited in one or more spatial directions in intact tissue. Diffusion weighted MRI is used for the detection of stroke in an early phase and the differentiation of stroke ad penumbra. Magnetization transfer MRI measures an exchange of magnetization between bound pools of tissue (e.g., tissue water bound to membranes etc) and free pools[341,342]. The amount of interaction can either be used to increase contrast (as it is done in low field MR systems), or it can be used to evaluate spatial neighbourhood on the nanometer scale[282].

MRI methods are still developing and surprising applications are being developed in scientific laboratories. Some are taken up by commercial research and development departments and get a chance to be used by the larger MR community–others do not. It is a characteristic of scientific MR meetings that totally new ideas are presented, not

only improvements of already known applications. This is a consequence of the tremendous versatility of MR, which is also the reason for the parallel development of different applications in chemistry, physics, and biology. An example of an MRI method that has not been considered by a larger group before was the use of hyperpolarized gases to image the lung cavity[343,344]. Another very sophisticated application uses multiquantum filters that have been developed in high-resolution NMR and which allow the observation of order in biological tissue, e.g., in tendons[345] or to measure shearing stress on vessel walls[282,346].

2.3.2.10 Advances in biomedical and clinical MRS

Most of the current *in vivo* applications of MRS are research studies in animals or cohorts of volunteers and patients. The motivations for such studies are often pathophysiological or biochemical questions. The majority of these studies aim at a better understanding of biomedical mechanisms and may not have an immediate therapeutic bearing on patients. The topics of these studies cover a wide range, including sophisticated experiments with enriched isotopes for the observation of biochemical fluxes, studies of blood-brain barrier, liver metabolism, glucose uptake in muscle of diabetes patients, muscle force production, tumour viability, and many other basic medical problems[282,347-357].

With the appearance of whole body MR systems and the success of MRI in clinical routine, MRS has also been forced into individual diagnosis–with little success until recently. The reasons for the delayed introduction of MRS into clinical routine are multiple: the complexity of MRS, the biochemical background that is needed to perform adequate MRS examinations, lack of standardized protocols and normal values, variability of the experimental circumstances, different philosophy of spectroscopists and clinicians, large volumes that are required for signal generation, etc. With the advent of ^{1}H-MRS in standard 1.5T MR systems, clinical MRS examinations became much more feasible. An automated and partially standardized

procedure and sequence for the acquisition of brain spectra became available for one commercial MR system (PROBE from General Electric), integrating to a certain extent the push-button philosophy of MRI into MRS applications. Another recent development since 2005 that has resulted in more widespread use of clinical MRS, particularly brain MRS, is that it became reimbursable by some health management organizations in some countries, particularly the USA in the states of California and Ohio. More MRS users may help to acquire a sufficient number of pathologies such that a set of brain pathologies will be well documented[282]. Brain MRS is one of the few fields where MRS has entered the realm of a diagnostic modality, particularly in seizure lateralization[358], differentiation of neoplasms[359-361], ischaemia[362,363] and others[348]. ^{1}H-MRS of the prostate seems to be another application that is able to generate clinically relevant data[282,364,365].

2.3.2.11 Future developments

The number of MR systems, the technical evolution, and the number of relevant applications has always increased much faster than anyone could imagine. When the first images were taken, several serious authors claimed that MRI would never surpass CT in image quality and would never replace CT in some applications. When images of reasonable quality were made in about 20min, everyone believed that time would be the crucial problem of MRI forever. When diagnostic imaging was established, many radiologists concluded that the main development was over and were surprised when, e.g., fMRI became feasible. The only conclusion that is possible from looking back at the last decade is that the development of MR is far from over[282].

It seems to be one characteristic of MR that often not specific inventions pushed the development but a series of “small” improvements. Major improvements in MR (and NMR) are often a consequence of a series of small steps that lead to better signal to noise ratio (SNR), improved image quality, etc. Currently, the human body is the inherent limit for some “brute-force” developments such as stronger and faster gradients. It can be expected that the future will not so much see faster and stronger

gradients but improved quality. Magnetic field strength on the other hand will increase dramatically for some applications. The typical 0.5 or 1.5T system will still be used for routine clinical imaging. Research systems, however, are available at much higher field strength, i.e., up to 4.7T[366,367] or even 8T[368]. These strong fields are particularly suited to MRS and fMRI. RF parts such as coils, transmitters, and receivers have already a very high quality, however, it can be expected that new developments and techniques will lead to higher SNR and, consequently, to better spatial resolution[282].

It may happen that MRI will reach a plateau. Some applications, however, are still in a development phase and need further consolidation and verification. This includes popular fields like fMRI, interventional MRI, hyperpolarized gases, imaging of coronary arteries, etc. Among the most promising aspects for the future of MRI are molecular effects such as diffusion, magnetization transfer, multiquantum filters, etc. Observation of processes and structures on the molecular level can be assessed by MR if appropriate methods are chosen[282].

2.3.3 Application of MRS to the hepatobiliary and liver transplant field

2.3.3.1 MRS studies of bile

In recent years, high resolution ^{1}HNMR spectroscopy has been established as a powerful technique to explore the biochemical composition of biological fluids such as plasma, bile, seminal and synovial fluids, in various pathological conditions[23]. This technique is rapid, non-invasive and non-destructive and can detect metabolites present at the millimolar without preparation of the sample; another application of this technique is to detect unexpected compounds in biological fluids[369]. It has been used to confirm the hydrophobic association in micelles of conjugated bile acids and biliary lipids[8]. It has also been used to assess micelle formation[9], the effects of cholesterol on the fluidity of human gallbladder bile[10,370], the amount of conjugated bile acids in bile[371] and to identify the lipid content of plasma membranes[13,372]. A preliminary study of ^{1}HNMR analysis of bile after liver transplantation has been reported by Powell et al in

1990, suggesting that this technique might help to distinguish ischaemia from rejection post-transplant by detecting large resonance peaks for lactate and acetate[17]. More recently, attempts to predict graft function by analysing bile production immediately after transplantation showed that bile from steatotic grafts collected before transplantation had more PC than bile from normal grafts. It also showed slower clearance of University of Wisconsin solution in grafts with subsequent primary graft dysfunction, suggesting a slower recovery of bile secretion[18].

2.3.3.2 MRS in liver failure

In a recent study, Dabos et al used ^{1}HNMR of plasma to develop a prognostic model of outcome for patients with paracetamol induced acute liver injury[373]. They identified plasma phenylalanine, pyruvate, alanine, acetate, calcium, haemoglobin and lactate as independent variables of poor prognosis (i.e. death or the need for a liver transplant). A prognostic model was then constructed by stepwise forward logistic regression analysis: [(400 X pyruvate (mmols/L)+(50 X phenylalanine (mmols/L)]-[4 X hemoglobin (g/dL)]. They were able to identify patients who died from paracetamol overdose fulminant hepatic failure as accurately as King's College criteria, but at a much earlier stage in their condition[373]. This followed on from previous similar work on non-paracetamol induced fulminant hepatic failure, where Dabos et al identified significantly lower levels of lactate, alanine, valine, and bilirubin and significantly higher levels of pyruvate and albumin in patients who survived spontaneously compared with those that died or needed or received transplants[374]. By use of multiple logistic regression analysis, an equation was devised that best predicted clinical outcome: 0.5x(albumin [g/L])-2x(lactate [mmol/L])-36x(valine [mmol/L])-38x(pyruvate [mmol/L]). This algorithm was applied on admission, thus expediting decision-making[374].

Liver failure may cause low-grade reversible brain oedema through an increase in brain glutamine. Cordoba et al used ^{1}HNMR to demonstrated cerebral oedema in non-encephalopathic non-alcoholic cirrhosis, which was not evident by standard

neuroimaging techniques[375]. They assessed magnetization transfer ratio and ^{1}HNMR before and after liver transplantation to determine changes in brain water content in cirrhosis. Cirrhotic patients showed a decrease in magnetization transfer ratio and an increase in glutamine/glutamate signal, which correlated to the decrease in magnetization transfer ratio and to neuropsychological function. Following liver transplantation, there was a progressive normalization of magnetization transfer ratio, glutamine/glutamate signal and neuropsychological function. Accordingly, correlations between these variables were lost after liver transplantation[375].

2.3.3.3 MRS in hepatic steatosis

The presence of non-alcoholic fatty liver disease often precludes potential organs from being used for transplantation. Alwayn et al investigated the effect of omega-3 polyunsaturated fatty acid supplementation on the treatment of hepatic steatosis in mice fed a high-carbohydrate, fat-free diet and in obese mice[376]. The percentage of fat content relative to water was determined by MRS using numeric integration of areas under lipid and water peaks. Omega-3 fatty acid supplementation reversed hepatic steatosis in mice fed a high-carbohydrate, fat-free diet and converted macrovesicular to microvesicular steatosis in obese mice as determined by histology, magnetic resonance spectroscopy, and liver biochemistry[376].

2.3.3.4 MRS in ischemic preconditioning

Livers from obese donors often have fatty infiltrates and are more susceptible to ischaemia-reperfusion injury and subsequent graft dysfunction. Niemann et al investigated IPC as a protective modality in obese Zucker rats during cold ischaemia. Liver samples were analyzed by ^{1}H- and ^{31}PNMR to assess whether IPC improves hepatic cellular metabolism. IPC significantly improved high energy phosphate metabolism and graft survival in obese rat livers[377].

2.3.3.5 MRS in hepatic energetics

^{31}PNMR was already in the focus in the late 70s and early 80s to optimize organ

preservation techniques. The energy status of solid organs had been recorded as a function of the duration of cold ischaemia for various buffer solutions[378]. ^{31}PNMR has been applied to monitor the hepatic energetics of intact cold preserved pig liver using standard clinical harvesting and storage techniques[5,379].

This principle has been applied clinically in a recent study from Hong Kong in paediatric liver transplants where ^{31}PNMR was used to determine hepatic functional status. Chu et al compared ^{31}PNMR with blood biochemistry and liver biopsy results in paediatric patients after liver transplantation[380]. Patients with good graft function displayed spectral profiles similar to those of the healthy subjects. Patients with abnormal liver function and biopsy-proven hepatic complications showed elevated phosphomonoesters to total phosphorus ratios when compared with those of both the control subjects and the group with good graft function[380].

2.3.3.6 MRS in analysis of organ viability for transplant

The continuing shortage of donor organs is seriously limiting transplant programs. Organs from marginal and non-heart-beating donors are increasingly being used, but their viability may be compromised. There is currently no rapid yet accurate method for assessing donor organ viability that can be applied within the window of opportunity between harvesting and implantation. MRS techniques might be useful in the noninvasive assessment of isolated donor organ viability. In particular ^{31}PNMR has been extensively applied to assess organ viability probing endogenous tissue metabolites such as energy phosphates, phospho- mono- and di-esters (PME and PDE) and inorganic phosphate levels[5].

2.3.3.7 MRS in liver transplantation

The use of MRS in liver transplantation has been reviewed by Davidson et al[381].

A recent report of ^{1}HNMR of serum and urine samples from one paediatric living related OLT recipient revealed an increase in serum and urinary glutamine post-

transplantation associated with reduced urea levels in urine were found to be evidence of impairment in urea cycle and compatible with persistently abnormal graft function[382]. Toxic ammonia is converted into urea through the urea cycle in the liver. A small proportion also gets metabolized into glutamine[383]. In acute and chronic liver cell failure, there is impairment in the urea cycle, resulting in abnormally high levels of blood ammonia and decreased urea levels. Increased ammonia level triggers glutamine synthesis[384,385]. Ischaemia-induced acute liver failure treated with a bioartificial liver has been studied by two-dimensional NMR of plasma from pigs[386]. The concentrations of choline and trimethylamine-N-oxide were found to increase in pigs after treating with the bioartificial liver, from the beginning to the end[386]. Metabolites such as glutamine, N-acetylglucosamine and pyruvate were also detected. Usually blood ammonia levels are measured biochemically, but the accuracy of ammonia measurement is constrained by time, temperature and haemolysis of the sample drawn[383].

One interesting aspect of the report by Singh et al, 2003 is that ^{1}HNMR actually demonstrated graft failure before the infarct could be detected by histology[382]. On day 3 post-transplantation, the patient developed both portal vein (PV) and hepatic artery (HA) thromboses. Abrupt increase of glutamine levels both in serum and urine and abrupt decrease of urea to undetectable level in urine on day 3 were observed. An immediate re-exploration thrombectomy with revision of both PV and HA anastomoses were carried out. The liver still looked viable, and biopsy did not reveal major infarct. Increased levels of glutamine in serum and urine as observed by ^{1}HNMR spectroscopy were compatible with persistent abnormal graft function in terms of INR, ALT, AST and serum lactate levels[382].

Patients with liver cirrhosis are transplantation candidates. Adipose tissue fatty acid composition in malnourished cirrhotics and in healthy volunteers was investigate by *in vivo* ^{13}C MRS to assess it as a predictor for transplant survival[387]. *In vivo* ^{13}CNMR

spectra from the subcutaneous adipose tissue before and 8 weeks after orthotopic liver transplantation revealed significant differences in levels of individual fatty acids, particularly n-3 fatty acids which were lower in cirrhotics. Eight weeks following transplantation, recipients showed a considerable increase in body mass. ^{13}CNMR revealed a significant increase in saturated fatty acids and a decrease in unsaturated fatty acids[387]. This may be useful in optimizing the dietary management of severely malnourished cirrhotics before liver transplantation[387].

2.3.3.8 MRS in primary graft non-function and dysfunction

The current shortage of donor organs in liver transplantation has led experienced transplant centres to use more marginal grafts. Melendez et al proposed that the development of a reliable technique of bile collection[388] could allow the characterization of hepatic grafts from both donors and recipients[18]. He collected bile from eight liver donors (four with normal and four with steatotic grafts) during organ retrieval and four transplant recipients (two with good early graft function and two with primary dysfunction) immediately after graft reperfusion. Bile analysed using ^{1}HNMR showed that the hepatic bile from steatotic grafts collected before transplantation had more intense phosphatidylcholine head group resonance than bile from normal grafts. It also showed slower clearance of University of Wisconsin (UW) solution in grafts with subsequent primary graft dysfunction, suggesting a slower recovery of bile secretion. He suggested a role for the monitoring of the resonance signal of UW solution washout, bile acid, and biliary lipid secretion may help to predict the development of primary graft dysfunction and avoid the need for retransplantation[18].

Metabolic assessment of viability indicators in UW solution of isolated human donor liver of prognostic value for transplantation outcome using ^{31}PNMR revealed that the individual PME, inorganic phosphate (Pi), PDE, and nicotine adenine dinucleotide peaks did not correlate with post-operative hepatocellular damage or liver metabolic capacity[389]. It did not result in a reliable noninvasive test to predict primary graft

dysfunction[389].

^{31}PNMR has been applied to characterise human liver allografts postoperatively. Patients with chronic ductopenic rejection were shown to have significantly elevated PME/NTP and PDE/NTP ratios, whereas patients with good graft function displayed no spectral abnormalities *in vivo*[390]. *In vitro* spectra from chronic ductopenic rejection patients displayed elevated phosphoethanolamine and phosphocholine, mirroring the *in vivo* changes in PME, but reduced glycerophosphorylethanolamine and glycerophosphorylcholine concentrations, in contrast to the *in vivo* PDE findings. The increase in PME/NTP reflects altered phospholipid metabolism in patients with chronic ductopenic rejection, while the increase in PDE/NTP may represent a significant contribution from bile phospholipid[390].

This review chapter had two aims: firstly, to describe the main pathways by which the different agents modulating IRI in the liver. Secondly, to highlight the history and new developments that are ongoing in ^{1}HNMR spectroscopy and to present the experimental and clinical evidence about its role in the study of hepatic IRI to date.

3 Materials and Methods

3.1 Rabbit model of lobar ischaemia/reperfusion

The study was conducted under a project license granted by the Home Office in accordance with the Animals (Scientific Procedures) Act 1986. New Zealand white rabbits were used for the experiments. All animals were kept in temperature controlled environment with 12 hour light-dark cycle. Animals were kept without food overnight prior to the experiments. Experimental research protocols were approved by the hospital ethics committee.

New Zealand white rabbits (3.8±0.5kg) were used in a validated model of lobar ischaemia[391-400]. Anaesthesia was induced by an intramuscular injection of 0.5ml/kg fentanyl citrate and fluanisone (Hypnorm; Janssen Animal Health Ltd., Buckinghamshire, UK). Following tracheostomy anaesthesia was maintained with 1.5-3% isoflurane (Forane; Abbott Laboratories, Chicago, IL, USA), through an anaesthetic circuit. Body temperature was maintained at 37-38.5^{o}C by a warming blanket (Homoeothermic blanket control unit; Harvard Apparatus, Southmatick, Massachusetts, USA). Haemoglobin saturation and heart rate were continuously recorded by a pulse oxymeter (Ohmeda Biox 3740 pulse oxymeter; Ohmeda, Louisville, Colorado, USA). A radio-opaque catheter 20 gauge (G) was inserted into the right femoral artery, in the pilot study, but changed to the right ear marginal artery for all other studies, and connected to a pressure transducer for monitoring of mean arterial blood pressure[401]. Ear marginal veins were cannulated with radio-opaque catheters (22G) for the administration of anaesthetics, fluids and medication.

After induction of anaesthesia a midline laparotomy was performed. The ligamentous attachments of the liver were divided and the liver was exposed. The bile duct was cannulated with a polyethylene catheter (PE-50, 0.58mm inner diameter, Portex, Kent, UK) for continuous measurement of BF and collection of samples for ^{1}HNMR.

Laparotomy was performed through a midline or transverse subcostal incision. The ligamentous attachments from the liver to the diaphragm were divided and the liver

was exposed.

3.1.1 Lobar Clamping

Lobar ischaemia was induced by clamping the vascular pedicles of the median and left lobes of the liver, using an atraumatic microvascular clip. This method produces a severe ischaemic insult without mesenteric venous hypertension[400,402], which can confound observations, and hemodynamic instability[396,402].

Moreover, lobar clamping avoids the cessation of biliary drainage, a characteristic of the total hepatic ischaemia model[403], permitting the effects of I/R on biliary composition to be evaluated. As common bile duct cannulation results in the collection of bile from both the ischemic and non-ischemic lobes we compared the findings from the I/R group with a sham control (non-ischemic) group to ensure that these changes in bile composition were the result of the I/R procedure (ischemic lobe) although previous studies have shown no difference in bile salt secretion or any other measured parameters, besides a decrease in BF, between ischemic and non-ischemic lobes in a similar lobar ischaemia rat model[404].

3.1.2 Model stability

Tracheostomy and ventilation stabilized the model hemodynamically and permitted bile constituents to be analyzed into the late phase of I/R. An inhaled anaesthetic agent isoflurane, which is mainly metabolized in the lungs rather than in the liver, was also used for maintenance of anaesthesia, in order to avoid cumulative effects or hepatotoxicity.

After 60 min of ischaemia, the vascular clip was removed and reperfusion was allowed for up to 7 hours. At the end of the experiment the animals were killed by exsanguination.

A rabbit model was used instead of a rat model since the size of rabbits is more convenient for the placement of probes, BF measurement and blood uptake at

different time points. The period of hepatic inflow ischaemia (1 hr) is also similar to the warm ischaemia time during human liver resection and transplantation.

There are certain limitations to the experimental model, a) partial lobar ischaemia and not total hepatic ischaemia b) biliary drainage from both lobes and not the ischaemic lobe and c) the availability of another body fluid suitable to MRS.

3.1.3 Liver blood flow

The liver gets a dual blood supply from the portal vein and hepatic arteries. The hepatic portal vein supplies 75% of the liver's blood supply. It drains venous blood from the splanchnic circulation. It divides into two branches, the right and the left portal veins, which divide into sectoral and segmental branches interhepatically[405]. The hepatic arteries supply the remaining 25% of the liver's blood supply, and is one of three terminal branches of the coeliac trunk of the aorta. It divides, into lobar, sectoral and segmental branches interhepatically[405]. The liver's oxygen is supplied 50% through the hepatic artery, and 50% through the portal vein[406]. Blood flows through the liver sinusoids and empties into the central vein of each lobule. The central veins coalesce into hepatic veins, which leave the liver into the inferior vena cava.

3.1.3.1 What happens on portal flow reduction or clamping

There is a reciprocal relationship between arterial and portal volume flow; it is effectuated by the state of constriction or dilation of the mesenteric and hepatic arterioles, both under myogenic control. Portal blood delivers directly to the hepatocyte all water-soluble substances absorbed from the intestines or produced in the intestinal walls. The hepatic artery maintains an appropriate PO_2 gradient between the acinar zones and flow of blood against increased tissue resistance; it assures a steady clearance of blood-borne substances, e.g., hormones and endogenous products[407].

Hepatic parenchymal cell metabolic status does not control the hepatic arterial blood flow[408]. Regulation of arterial flow is less neural than neurohumoral, through an arterial

adenosine-dependant humoral paracrine pathway. In order to maintain a relatively stable overall hepatic inflow, arterial vasodilation occurs in cases of decreased portal flow and vasoconstriction in cases of increased portal flow[407,409]. Portal blood flow is a major intrinsic regulator of hepatic arterial tone. Hepatic arterial blood flow changes so as to buffer the impact of portal flow alterations on total hepatic blood flow, thus tending to regulate total hepatic flow at a constant level. This response is called the "hepatic arterial buffer response" (HABR).[408] The mechanism of the arterial buffer response seems to depend on portal blood flow washing away local concentrations of adenosine from the area of the arterial resistance site. If portal flow decreases, less adenosine is washed away and the local concentration rises resulting in arterial dilation[408].

3.1.3.2 Hepatic Compliance

One mechanism is a simple physical consequence of the very high vascular blood volume and compliance (change in hepatic blood volume per unit change in intrahepatic pressure). A decrease in portal blood flow leads to a passive decrease in intrahepatic pressure and a passive expulsion of blood from the large hepatic reservoir into the central venous system. This increase in venous return leads to increased cardiac output that, in turn, leads to elevated blood flow in the splanchnic arteries that feed the portal venous bed, thus at least partially correcting the initial flow deficit[410].

3.1.3.3 Hepatic Arterial Buffer Response

Reduced portal flow activates the HABR secondary to reduced washout of adenosine from the space of Mall, which surrounds the terminal branches of the portal vein and hepatic artery before they drain into the hepatic sinusoids. Adenosine appears to be secreted at a constant rate into the space of Mall, with the local concentration of the potent vasodilator being regulated by the rate of washout into the portal blood. By this mechanism, reduced portal flow leads to accumulation of adenosine and hepatic

arterial dilation, thereby serving to buffer the impact that changes in portal flow have on total hepatic blood flow[410].

3.1.3.4 Hepatorenal Reflex

The accumulated adenosine also activates sensory nerves in the liver, which results in activation of a hepatorenal reflex (HRR). This reflex leads to reduced renal output and fluid retention, thereby elevating blood volume, venous return, cardiac output, and splanchnic blood flow. The elevated adenosine level that occurs in response to reduced portal flow leads to rapid responses. The hepatic artery is dilated within seconds and the response is well maintained. Although the HRR is also activated immediately, but the renal fluid retention only has cardiovascular impact after fluid retention becomes significant, which is over a longer timescale[410].

3.1.3.5 Hepatic Mass Regulation

A third mechanism is modulated through high or low vascular shear stress regulates NO and prostaglandin release to trigger a cascade leading to hepatocyte proliferation or apoptosis. By this mechanism, hepatic cell mass is adjusted to maintain a constant ratio to the average hepatic blood supply over a long time period[410].

3.1.4 Models of total hepatic ischaemia

Ideally, experimental design should not include too many compromises, however, the principle of reduction in animal experimentation, an important principle in modern life-sciences, necessitates thinking very carefully how best to use every experiment to benefit a maximum number of experiments. Model standardisation, also allows sharing of data across several sets of experiments, as the model is the same. So a sham group can be shared, or a control I/R group can be shared, across several modulating/interventional agents, or different investigative approaches.

Most experimental animal models for studying hepatic IRI involve partial or segmental ischaemia of the liver with the disadvantage of triggering the above mechanisms or a

portocaval shunt procedure to avoid mesenteric congestion, which is technically difficult the smaller the animal model. From a technical aspect, vascular anastomosis required in portal shunting is very labour intensive, over several experimental groups, and if this were going to be attempted, then the investment in time and effort would best be directed at transplantation. Transplantation in the rat has a stable model, but one which needs months of technical training to achieve, and consequently defies the principle of reduction in animal experiments.

In these experiments, there was a requirement for several samples, of both blood and liver, which would not have been achievable in a smaller rat model, due to liver size. Interestingly, a rat model of total hepatic ischaemia (arterial and portal clamping) is more tolerant, even without portal shunting, and can achieve an hour of total hepatic ischaemia. Although without portal shunting, gut I/R would have been a confounding variable. Essentially, this model does not reflect the global ischemia that occurs during liver transplantation. Survival of a rabbit model of total hepatic ischemia without a portocaval shunt was questionable for the 60 mins of ischaemia required. As the group of experiments that formed this thesis were coming to an end, Towards the end of the period when these experiments were conducted—they spanned a period between 2001 and 2004—a total hepatic ischemia without a portocaval shunt model in the rabbit was attempted in the department[400]. Four groups were prepared, sham-operated, 20-minute total hepatic ischemia, 25-minute total hepatic ischemia and 30-minute total hepatic ischemia. Total hepatic ischemia was induced by occluding the portal inflow vessels—portal vein and artery—with an atraumatic vascular loop and were measurements taken for 2 hours during reperfusion. A total hepatic ischemia of 30 minutes caused severe liver injury resulting in cardiac arrest at 2 hours of reperfusion in all five animals due to metabolic acidosis. Twenty minutes of total ischemia was tolerated and did not produce significant liver injury. Twenty-five minutes

of total ischemia was tolerated but at 2 hours of reperfusion. In addition, the model needed to be stable for a significant reperfusion period to assist in observing a timeline of reperfusion changes.

These experiments aimed to simulate ischaemic operative challenges in liver surgery, and 60 min of ischaemia was selected as a time-frame that would be representative of the amount of warm ischaemia experienced during liver surgery, and one where significant damage would be guaranteed. Sixty minutes of total hepatic ischaemia was initially thought to be unachievable in the rabbit model, and was later proven to be so, with only 25 mins being achievable, and shorter timeframes not resulting in liver injury at all. However, if this model had been available at the time of conducting these experiments, it may have offered a closer representation of liver ischaemia without the reliance on sham and control group comparison. There is an argument that such a model should have been developed for these studies, but as suspected, and since proven, the tendency to follow a 60 min ischaemia model prevented its consideration, this may appear in hindsight a limitation of these studies.

3.1.5 Ischaemic or non-ischaemic bile

The second issue is the bile retrieval from the common hepatic duct not originating from the ischaemic or partially ischaemic lobe. Direct cannulation of the ischaemic lobe is possible, but in doing so the cannula would have to pass through the common bile duct, and then into the ischemic lobe bile duct to ensure tight fixation. Such a technique would naturally block the non-ischaemic lobe, which would lead to increased bile flow[411], rise in plasma bilirubin[412] and changes in canalicular permeability[413] that may affect the interpretation of bile volumes and composition, an integral part of this thesis.

These studies relied on the established technique of utilizing sham and control groups to prove a causal link. In experimental procedures, many factors are standardized,

while one of two are varied to study their effect, and the resulting observations are attributed to the varied factors. In these studies, the variable interventions were the lobar clamping, and drug modulation. If sham and controls are compared, the only variable is lobar clamping. There is an argument as to which lobe produces the bile compositional changes observed, and the comparison of sham and control suggests that the change in bile composition is due to lobar clamping and ischaemia, as in both cases the CBD is cannulated and mixed lobar bile is collected. Although this does not fully answer the question of which lobe, it does strongly suggest that the variation is due to ischaemia. It would be a very interesting subject of further study, the effect of ischaemia on a non-ischaemic lobe.

3.1.6 Bile or Urine

Clinical MRS more recently has been moving over to urine MRS in its search for biomarkers. The reason is that urine samples are more accessible in more quantity, with non- or minimally invasive techniques, and while bile can be reasonably resolved at 11 Tesla strengths, it is not as easily resolved at lower clinical MRS strengths. Clinical MRS is increasing in strengths with 3 Tesla becoming more prevalent, however using urine to look for biomarkers resolves the need for high strength clinical MRI scanners, once a biomarker is identified, and due to its high accessibility, can even be extracted and measured in a high strength magnet without much inconvenience to the subject being studied, so not only does it resolve more at lesser strengths, but can be moved to higher strengths if required easily. The initial hypothesis was that bile would directly reflect the changes taking place in the liver, however, urine is an excellent surrogate for changes in serum concentrations[414], In the true metabolomic sense, it can mirror the changes in patients with or without HIV and can identify if they are taking treatment with more resolution than that evident in the blood[414,415]. Where blood constituents are masked with large protein peaks, and bile by

lipid peaks, urine does not contain these difficulties, with a much sharper resolution with twice as many metabolites identified as blood[415]. It has been used to delineate pathology in chronic obstructive pulmonary disese[416], lung cancer[417], atherosclerosis development[418], inflammatory bowel disease[419], metabolic syndrome[420], hyperlipidaemia[421], hepatoxicity[422], alcoholic liver injury[423], ischaemic heart failure[424] and hepatic encephalopathy[425].

Hepatic microcirculation was continuously measured via a probe placed on a fixed site on the median lobe of the liver and held in place by a retort holder during ischaemia and reperfusion period. Hepatic tissue oxygenation was continuously measured via optodes placed on the surface of the left liver lobe during ischaemia and reperfusion period.

Blood samples (1ml each) were collected from the arterial line at different time points during the experiment for serum transminases.

Liver tissue at baseline and at the end of the experiment was taken from the ischaemic liver lobe fixed in 10% formalin for histological study.

Steatosis was induced by feeding the animals with a high-cholesterol (2%) diet for 8 weeks. Unlike the commonly used low-choline methionine diet, which produces periportal fatty infiltration[240,426], with this model a central lobular deposition of fat is observed, similar to that found in the majority of human fatty livers, such as in diabetes, obesity and alcoholism[427].

3.2 Hepatic microcirculation

3.2.1 Basic principles

Hepatic microcirculation (HM) was measured by a surface laser Doppler flowmeter (LDF) (DRT4, Moor Instruments Limited, Axminster, UK) in flux units. Measurement is

easy to perform and provides a continuous signal without interference with tissue blood flow[428-430].

Briefly, a monochromatic laser light from a 2mV-helium neon laser operating at 632nm is guided to the tissue via optical fibres. The back-scattered light from the tissue is transmitted through optical fibres to photodetectors. Only the photons which are scattered by moving red blood cells will have a Doppler frequency shift, whereas those from the static tissue matrix will not be Doppler shifted. Mixing of these components at the photo detector surface produces an electrical signal containing all of the Doppler frequency shift information. Further processing of the signal produces an output voltage that varies linearly with the product of total number of moving red blood cells in the measured volume of a few cubic millimetres multiplied by the mean velocity of these cells.

Linearity of the LDF signal from the liver with total organ perfusion has been demonstrated and the technique has been shown to be sensitive to rapid changes in organ blood flow[428,429,431]. The LDF measurements are expressed in arbitrary perfusion units (flux). Due to the problems associated with variation in signal across the surface of the liver, it is not possible to apply a conversion factor so that the LDF signal can be expressed in absolute flow units[428,431].

The application and reproducibility of LDF measurement for assessment of liver microcirculation has been validated in both experimental animals[431] and human liver transplantation[432].

3.2.2 LDF application in the rabbit, data collection, analysis

The hepatic microcirculation in this study was assessed using a commercially available dual channel surface LDF (DRT4, Moor Instruments Ltd., Devon, UK) as shown in figure 2. The LDF was calibrated before each study against a standard reference (Brownian motion of polystyrene micro spheres in water) provided by the

manufacturer. The LDF probe was placed on a fixed site on the median lobe of the liver in order to avoid any error due to anatomical variation in the microcirculation. It was held in place by a probe holder in order to minimise any disturbance to blood flow by the LDF probe pressure on the tissue. Data were collected continuously. Data from the continuous measurement by LDF was collected via the near infrared spectroscopy (NIRS) software that can accept the input of 4 different clinical monitors. After conversion of the NIRS data to excel sheets, the LDF data at the relevant points in each experiment was calculated as a mean of 2-min data.

Figure 2: Dual channel surface laser Doppler flowmeter and its probes

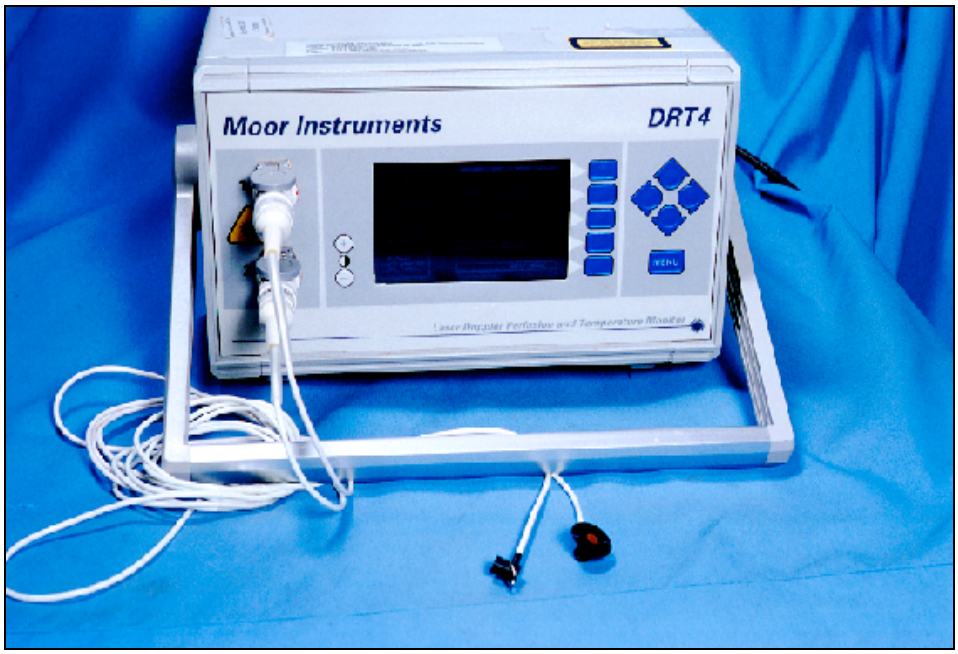

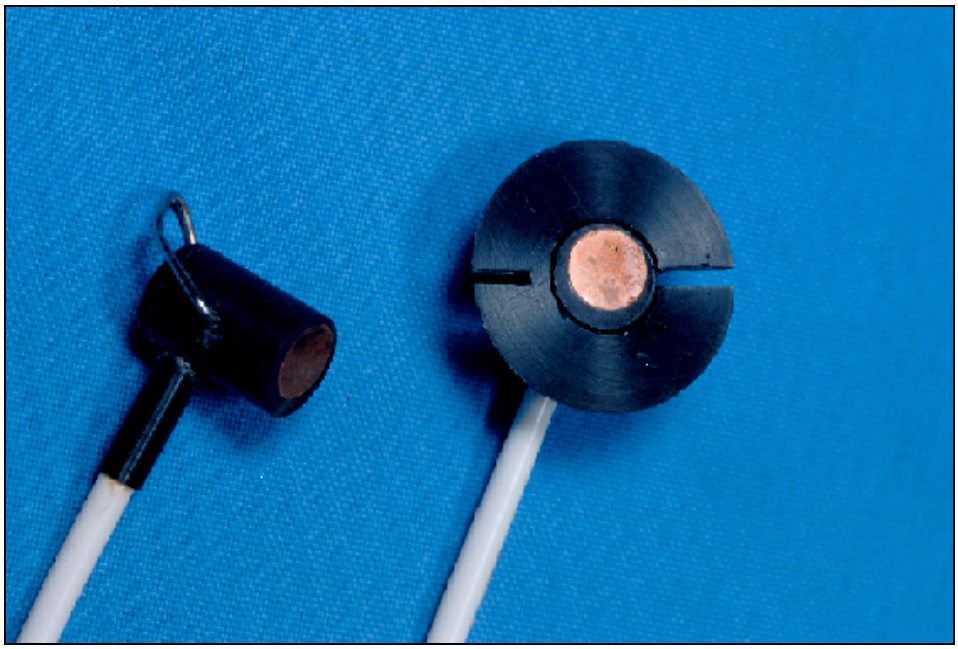

Laser Doppler flowmeter (LDF) and its probes (DRT4, Moor Instruments Ltd., Devon, UK)

3.3 Intracellular oxygenation and mitochondrial activity

Under aerobic conditions, the mitochondrial membrane functions as an energy production system through the coupling of the electron transport system and ATP synthase. The mitochondrial respiratory chain is a multi-enzyme complex forming an integral part of the mitochondrial inner membrane[433,434] (figure 3). The respiratory chain includes five complexes, each with several subunits.

The reducing equivalents nicotine adenine dinucleotide (NADH) and flavin adenine dinucleotide ($FADH_2$), that are generated by the tricarboxylic acid cycle, are transferred to the respiratory chain as a substrate, where electrons are then transferred from NADH or $FADH_2$ to oxygen[433,434]. The electrons that are donated by NADH and $FADH_2$ enter the respiratory chain at complex I (NADH dehydrogenase) and complex II (succinate dehydrogenase). Electrons are then transferred to complex III (cytochrome c), complex IV (cytochrome oxidase: COX), and finally, to molecular oxygen, which then combines with protons to produce water. The passage of electrons through the respiratory chain is associated with the translocation of protons from the mitochondrial matrix into the intermembrane compartment. This generates an electrical membrane potential and proton concentration gradient[433,434]. The energy which is released during re-entry of protons into the matrix is then utilised by ATP synthase (complex V) to generate ATP from adenosine diphosphate (ADP) and inorganic phosphate (P_i)[433,434] (figure 3). About 95% of the total cellular ATP is produced via this mitochondrial oxidative phosphorylation[433,434]. The rate of oxidative phosphorylation is governed by the interplay of four factors: the concentration of the respiratory chain enzyme; the concentration of oxygen; the relative concentrations of the substrates including glucose, ADP, adenosine monophosphate (AMP), and P_i; and the rate of ATP utilisation[433,434].

COX activity as a reflection of hepatic intracellular oxygenation was continuously measured using NIRS. In all tissues a number of colour-bearing compounds

(chromophores), namely oxyhaemoglobin (HbO_2), deoxyhaemoglobin (Hb) and COX are present in variable concentrations. They have different absorption spectra (figure 4c) in the near infrared (NIR) light and their absorption characteristics are oxygen dependent[435].

COX is the terminal complex of the mitochondrial respiratory chain (figure 3). It takes electrons from cytochrome c and catalyses the reduction of oxygen to water with the concomitant synthesis of ATP through the oxidative phosphorylation process[436,437]. In hepatocytes, approximately 90% of the oxygen is consumed by mitochondrial COX. COX contains four redox-active metal sites: two haem iron (haem a and haem a_3) centres, the copper-copper dimer (Cu_A), and the binuclear haem-copper coupled centre (haem a_3/Cu_B). These four metal centres accept or donate electrons during the electron transfer through the respiratory chain, changing their redox state. The oxygen-binding site of the enzyme is the binuclear unit formed of the Cu_B and haem a_3. The donation of electrons from this unit to oxygen accounts for the majority of oxygen consumption in the tissues. The Cu_A and haem a centres donate electrons to the binuclear unit and therefore are not directly involved in oxygen reduction[436,438]. In the absence of oxygen, electron transfer to oxygen cannot take place. Electrons accumulate on the haem and copper atoms and COX becomes reduced. With oxygen availability the electrons are transferred rapidly from the metal centres to oxygen and COX becomes oxidised. Many factors can affect the COX redox state *in vivo*, but the most significant factors are the oxygen concentration[436,439], NO in physiological circumstances[440,441] and oxidants such as ROS and RNS during oxidative stress[442,443].

Figure 3: Cellular respiration

(a) Components of mitochondrial electron transport chain

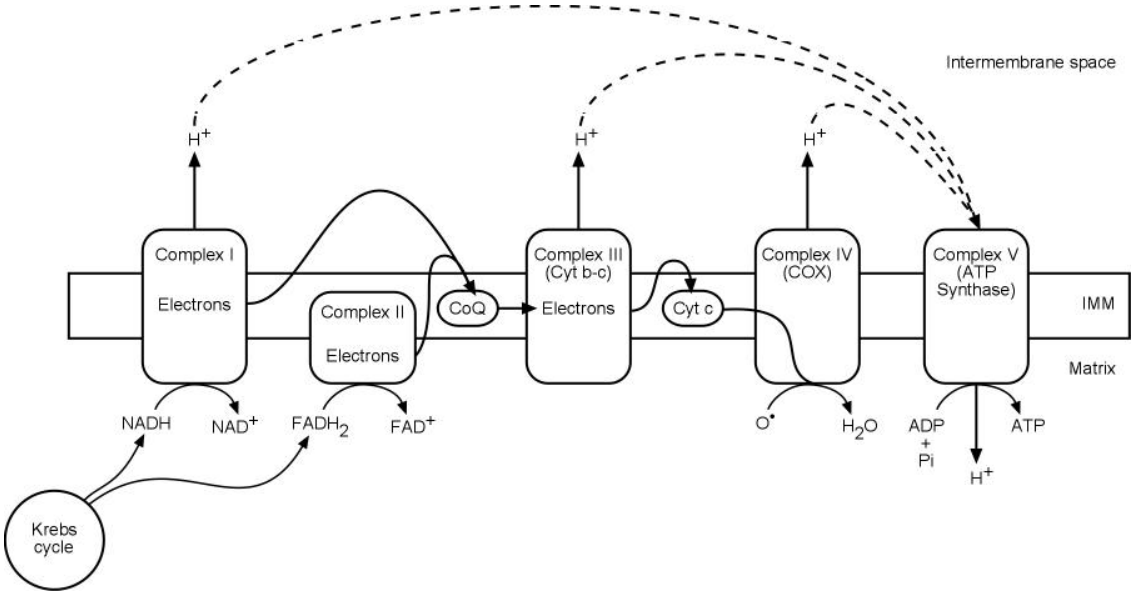

The process of ATP production through the c, also known as the respiratory chain, is called oxidative phosphorylation: NAD+=nicotinamide adenine dinucleotide; NADH=reduced form of NAD+; FAD+=flavin adenine dinucleotide; FADH=reduced form of FAD+; CoQ=coenzyme Q; Cyt c=cytochrome c; $O^{\bullet}$=oxygen radical; H_2O=water; ADP=adenosine 5'-diphosphate; Pi=inorganic phosphate; IMM=inner mitochondrial membrane[444].

(b) Glycolysis, Krebs cycle and ketone body formation

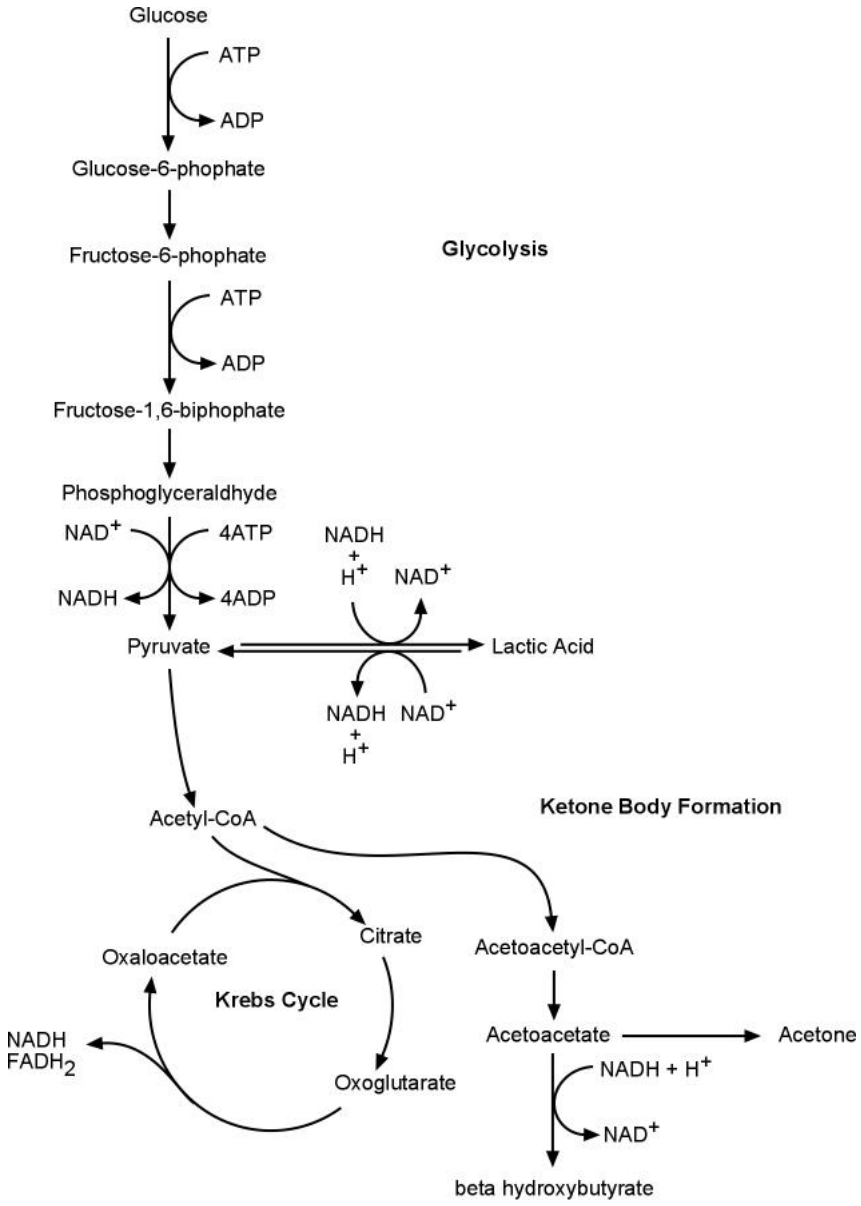

Glucose-6-phosphate produced from glucose can be converted to glycogen or is metabolized through the pentose-phosphate pathway. Acetyl-CoA is oxidized through the Krebs cycle or utilised to produce ketone bodies.

All 4 centres exhibit different absorption characteristics depending on their redox state. The copper centres are optically sensitive in the NIR region in contrast with the haem centres that absorb visible light[436,437,441,445]. Absorption of the NIR light by COX occurs primarily at the Cu_A centre within COX. The oxidised Cu_A centre has a characteristic shape spectrum with a broad peak centred around 845nm[435,439]. The signal intensity decreases on reduction of this centre. The contribution of haem iron centres to absorption of NIR is less than 10% of the total signal in the reduced–oxidised spectrum[439,446].

The redox state of COX Cu_A is dependent on cellular oxygen availability[436,437,441,447]. In the presence of oxygen electron transfer occurs and the enzyme becomes oxidised whereas lack of oxygen results in a decreased flow of electrons and COX becomes reduced. The increase in the reduction state of COX reflects severe cellular hypoxia.

Another synthetic chromophore that can be measured by NIRS is indocyanine green (ICG). ICG is an anionic dye that has been used for many years to measure hepatic blood flow and as a test of liver function[448]. It has a characteristic maximum absorption peak at 805nm in the NIR light region allowing its absorption coefficient to be incorporated in the NIRS algorithm to measure directly its concentration in the hepatic tissue[449].

3.3.1 Basic principles of NIRS

Light interactions with the tissue involve the combination of reflectance, scattering and absorption which depends upon many factors including the light wavelength and the illuminated tissue type[435]. In the visible region of the spectrum (450-650nm) light is strongly attenuated due to the intense absorption by haemoglobin and light scattering in tissues, which increases with decreasing the wavelength. Therefore, light fails to penetrate more than 1cm of tissue[435,450,451]. However, the NIR region of the electromagnetic spectrum (700-1000nm) represents an optical window of relative transparency and a significant amount of radiation can be effectively transmitted

through biological materials over distances of up to 8cm[435,452].

The technique of NIRS relies upon two main physical properties: (1) the relative transparency of biological tissue to light in the NIR region of the spectrum and (2) the existence of different tissue chromophores with characteristic absorption spectra in the NIR light spectrum[453-456]. In tissue with homogeneous scattering the calculation of light attenuation and the relationship between the optical absorption and chromophore concentration may be described by a modified Beer-Lambert's law. The law modifications include (a) an additive term, G, due to scattering losses and (b) a multiplier, to account for the increased optical pathlength due to scattering. This law can be used to convert the obtained optical densities to concentration changes of Hb, HbO_2, and COX in μmole/L per optical pathlength[454]:

$$A = \alpha . c . d . B + G$$

A is the attenuation of light (optical density), α is the absorption coefficient of the chromophore ($\mu mole^{-1}.cm^{-1}$), c is the concentration of the absorbing compound (μmole/L) and d is the geometrical distance between the points where light enters and leaves the tissue (cm). B the differential pathlength factor (DPF) which accounts for the increase in optical pathlength due to light scattering (which causes the optical pathlength to be greater than d) and G is a constant geometrical factor which accounts for loss of photons by scattering. As G cannot be quantified in vivo and is dependent upon the scattering coefficient of the tissue interrogated, it is not possible to measure the absolute concentration of the chromophore in the tissue from measurement of the absolute attenuation. If α, B, and d are known and G assumed to remain constant during measurement, we can measure the change in the chromophore concentration (Δc) from measuring the change in attenuation (ΔA) from the following formula:

$$\Delta c = \Delta A / \alpha . d . B .$$

Since the absolute concentration of tissue chromophores are unknown and cannot be calculated due to the effect of light scattering within the tissue, all NIRS measurements are expressed as absolute concentration changes (μmole/L) from an arbitrary zero at the start of the measurement. The absorption coefficient of COX was obtained in vivo from the brains of experimental animals whose blood had been replaced by a blood substitute (fluorocarbon) with exposure to 100% O_2 or N_2 to obtain the oxidised and reduced COX spectra[454-457].

For simultaneous computation of the changes in concentration of a number of chromophores from changes in attenuation at a number of wavelength, an algorithm can be used which incorporates the relevant absorption coefficient for each chromophore at each[454-456,458].

3.3.2 Near infrared spectrophotometer

The NIR spectrometer used in this study is the NIRO 500 (Hamamatsu Photonics K.K., Hamamatsu, Japan) (Figure 4). This spectrometer is the commercial version of an instrument developed by colleagues in the Department of Medical Physics and Bioengineering, University College London[458]. In the NIRO 500, the light source is monochromatic light generated from semiconductor laser diodes. The light is produced at four wavelengths (774, 826, 849, and 906nm). The choice of the wavelengths is based on 765nm, the absorption maximum for Hb; 810nm, the isobestic wavelength at which the extinction coefficients of HbO_2 and Hb are equal which can be used to calculate haemoglobin concentration independent of oxygen saturation; 845nm, the absorption maximum for oxidised COX; and 900nm, a reference wavelength[435,454,455].

The light is produced by laser diodes and carried to the liver via a bundle of optical fibres in sequential pulses. The optical fibres are covered by a light proof protective sheath and its distal end terminated in a very small glass prism which reflects the light through 90^o to direct it into the tissue[453]. Photons emerging from the liver are collected by the second bundle of optical fibres and detected by a photomultiplier tube light

detector[453]. The incident and transmitted light intensities are recorded and from these the changes in the concentration of tissue chromophores (μmol/L) are calculated using an algorithm incorporating the known chromophores absorption coefficients and an experimentally measured optical pathlength.

Figure 4: Near infrared spectrometer

(a)

(b)

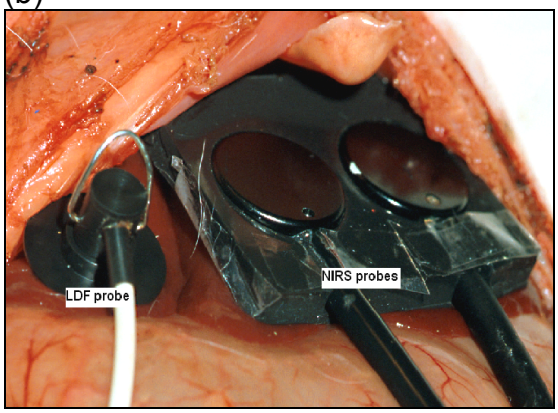

(a) The NIRO 500 dual channel surface laser Doppler flowmeter (Hamamatsu Photonics KK, Hamamatsu, Japan). (b) The NIRS and LDF probe placement on the liver lobes.

(c)

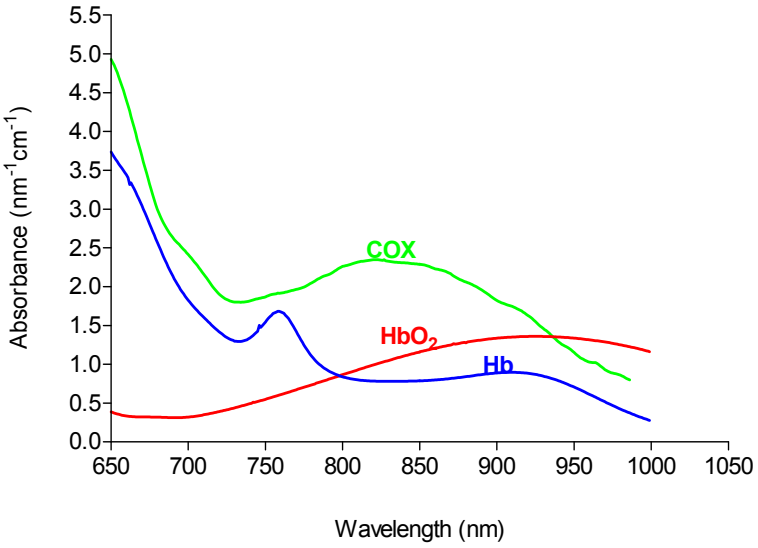

(c) Absorption spectra of HbO_2,Hb, & COX in the NIR light region[435]

The standard NIRO 500 algorithm was developed using the wavelength dependant-pathlength for the brain tissue[459]. As a part of this study, modification of the NIRO 500 algorithm has been carried out in the Department of Medical Physics and Bioengineering, University College London for its hepatic application[458]**.** The absorption coefficient of a freshly dissected and viable blood free pig liver was measured. The absorption coefficient was found to be 0.04mm^{-1} at 800nm which is some four times larger than that of normally perfused brain tissue although the transport scattering coefficient was similar near 1.0mm^{-1}. When the absorption coefficient of blood in a normally perfused liver was added to the blood free absorption coefficient the overall absorption coefficient was near 0.1mm^{-1} with the scattering coefficient essentially unchanged. The optical pathlength as a function of wavelength for normally perfused liver was then calculated incorporating the measured absorption coefficient and the scattering coefficient mathematically corrected for the contribution of haemoglobin absorption. The average blood content of the liver was assumed to be 12% by volume[460] at an average haemoglobin saturation of 60%.

3.3.3 NIRS application in the rabbit, data collection, analysis

NIRS probes were mounted inside a probe holder and placed on the liver surface at a fixed site of the left lobe of the liver in all the animals in each experiment to avoid any anatomical variation, which could influence in tissue oxygenation and blood volume. As a part of the modification of this instrument for use on the liver, a flexible rubber holder was made to hold the NIRS probes at a fixed spacing over the liver surface (Figure 4). This probe holder ensured that the sites of light entry and exit are maintained at a constant and known spacing distance which minimises the possibility of artefact due to changes in the distance between the probe ends. Also, it allows a satisfactory contact between the liver surface and the probe ends.

The NIRS includes the facility to set the attenuation and therefore chromophore

concentration changes to zero with the NIRS initial setting. Since all the measurements are changes from an arbitrary initial zero, this function is important to ensure that artefacts such as system drift, optode movement, and excessive light having a minimal effect on the data. The NIRS data were continuously collected in a laptop computer connected to the NIRS. These data are the changes in light attenuation (optical densities: OD) at four wavelengths due to absorption by the tissue chromophores. A software program called ONMAIN® (Hamamatsu Photonics K.K., Hamamatsu, Japan) was used to convert these data into changes in concentration changes of COX (μmol/L) using the previously defined algorithm in the NIRO 500. This was then transferred to excel® data sheets (Microsoft Company, Seattle, USA) for analysis. The data at the relevant time points were collected as the mean of 2-minute data and calculated in regard to the baseline value at the start of the experiment.

3.4 Ultrasonic transit time flowmetry

In this study blood flow through the PV was measured using ultrasonic transit time flowmetry.

3.4.1 Principle of ultrasonic transit time flowmetry

Using wide-beam illumination, two transducers pass ultrasonic signals back and forth, alternately intersecting the flowing liquid in the upstream and downstream directions. The transit time of such beam is a function of the volume flow intersecting this beam, regardless of vessel dimensions or cross-sectional area. In the same way that a swimmer will move quicker in the downstream direction than in the upstream direction, the speed of the ultrasound is affected by the flow of liquid passing the 'acoustic window' of the flow probe. The flowmeter derives an accurate measure of the transit time it took the wave of ultrasound to travel from one transducer to the other. The difference between the upstream and downstream-integrated transit times is a measure of volume flow rather than velocity[461]. The ultrasonic transit time flowmetry has been demonstrated to provide an accurate method for hepatic blood flow

measurement[462-464].

3.4.2 Ultrasonic flowmetry in the rabbit model

Portal vein blood flow was measured continuously using a dual ultrasonic transit time flowmeter (HT207, Transonic Systems Inc, NY, USA) as shown in figure 5. The flowmeter perivascular probes were placed around the portal vein (figure 5). The accuracy of this technique is dependent on careful positioning and alignment of the probe with respect to the vessel. The vessel should be positioned within the central area of uniform ultrasonic intensity of the probe window i.e. away from the probe window edges, which have lower ultrasonic beam intensity[461]. Also, it requires accurate selection of the probe size, which was determined by the outer diameter of the blood vessel.

3.4.3 Ultrasonic transit time flowmetry data collection and analysis

Data from continuous measurement by the ultrasonic flowmeter was collected via the NIRS software. After conversion of the NIRS data to Microsoft Excel sheets, the ultrasonic flowmeter data at the relevant points in each experiment was calculated as a mean of 1-minute data.

Figure 5: Dual ultrasonic transit time flowmeter

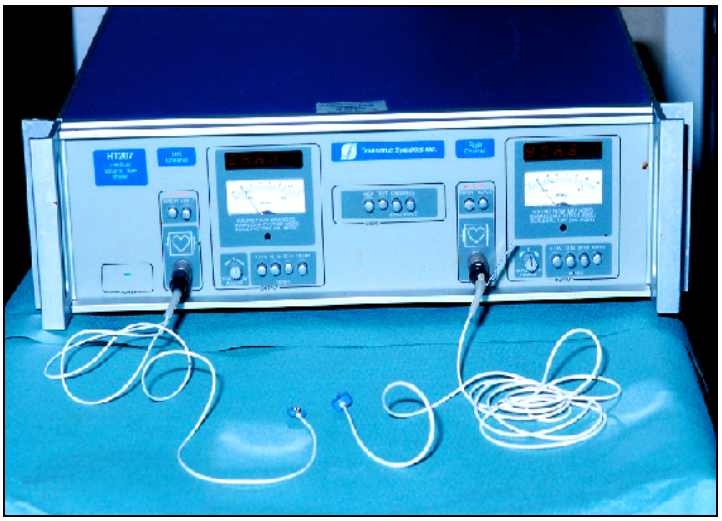

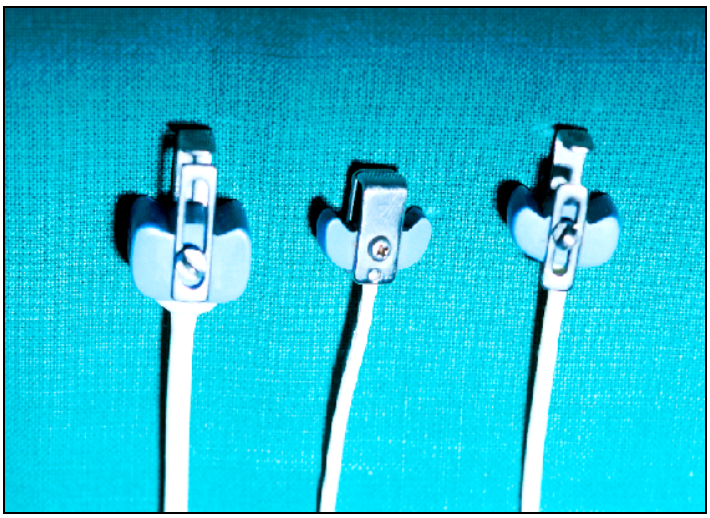

Dual ultrasonic transit time flowmeter (HT207, Transonic Systems Inc., NY, USA) and the perivascular probes.

3.5 Indocyanine green (ICG) clearance

Measurement of ICG blood clearance 24hrs following liver transplantation proved to be more accurate than the conventional liver function tests as a predictor of liver-related graft outcome[465]. Its clearance also showed significant correlation with the severity of preservation injury, the duration of intensive care unit and hospital stay, prolonged liver dysfunction, and septic complications[465]. ICG clearance was also found to correlate significantly with free oxygen radicals and neutrophil elastase, as mediators for I/R injury, after liver transplantation[466]. Also, ICG clearance correlated with parameters of liver injury such as AST and prothrombin time at 24hrs post-transplantation[466]. Measurement of blood ICG clearance requires frequent blood sampling and gives a global idea about both hepatic circulation and function.

For measurement of hepatic ICG clearance, a bolus of ICG (Cardiogreen, 90% dye content, Sigma, Dorset, UK) 0.5 mg/kg was given. ICG was dissolved in sterile water (1mg/ml) and given via the ear vein over 20 seconds. ICG was prepared immediately before administration to avoid its degradation by light, which results in slower hepatic uptake and excretion that could cause inter-animal variation[467]. An ICG of 0.5 mg/kg was used to ensure that ICG clearance is controlled by both the blood flow and hepatic function[468]. For continuous measurement of hepatic tissue ICG concentration, the NIRO 500 probes were placed, with a 10 mm separation, on the left lobe of the liver for 30 minutes after ICG injection (figure 4b).

Continuous measurement of hepatic ICG by NIRS produces a concentration-time curve. This curve was analysed to produce two exponential rate constants, representing hepatic ICG uptake from the plasma to the hepatocytes (α) and hepatic ICG excretion from the liver by cytoplasmic transport and biliary excretion (β). These rate constants were calculated by fitting the ICG concentration-time curve to a two-compartment mathematical model as defined

by the sum of two exponential equations as previously reported by Shinohara and colleagues[449]:

$$ICG(t) = -A \exp(-\alpha t) + B \exp(-\beta t)$$

Where ICG (t) is the hepatic concentration of ICG at any time (t), α and β (min^{-1}) are the rate constants for the hepatic ICG uptake and excretion, respectively. A and B are the zero time intercepts, both theoretically equal to the initial hepatic concentration. The assumption is that $\alpha > \beta$ and $A \approx B$.

The fitting to this model was done using a commercial computer package based on the non-linear least square regression (Graph Pad Prism, Graph Pad Software Inc., San Diego, USA). The iterative procedure of the program minimises the reduced sum of squares. The goodness of the fit was evaluated by the R^2 value.

3.6 Liver transaminases

Alanine aminotransferase (ALT), aspartate aminotransferase (AST) and creatinine kinase (CK) activity were measured in serum. Blood samples were centrifuged at 2,000G for 10min at room temperature. Serum was separated from the samples and stored at –20°C until assayed. Measurements were made using an automated clinical chemistry analyser (Hitachi 747, Roche Diagnostics, Lewes, UK).

3.7 Histology

Small wedge biopsies were taken in baseline and at the end of the procedure from the ischaemic liver lobes. The liver tissue was fixed in neutral buffered formalin (10%), embedded in paraffin and stained with haematoxylin and eosin (H&E). Sections were examined under microscope (digital light microscope CLF 60 optical system, Nikon UK Ltd, Surrey, UK). For assessment of the degree of injury a semi quantitative method was used in which a blinded liver pathologist estimated the number of neutrophils

(PMN) in sinusoids, the aggregation of PMN, structural changes in KC and the presence of necrosis and apoptosis in 5 high power fields per slide.

For steatotic livers formalin fixed but not paraffin embedded tissue was stained for fat using the Swank & Davenport modification of the Marchi method[469]. The grade of steatosis was analysed in a semi-quantitative manner: mild (<30 %), moderate (30-60 %) and severe (>60 %) using a clinically applied grading system[235].

3.8 Proton Nuclear Magnetic Resonance (^{1}HNMR) Spectroscopy

High resolution proton nuclear magnetic resonance (^{1}HNMR) spectroscopy has been established as a powerful technique to explore the biochemical composition of biological fluids such as plasma, bile, seminal and synovial fluids, in various pathological conditions[8]. This technique is rapid, non-invasive and non-destructive and can detect metabolites present at the millimolar concentrations and can be applied to detect unexpected compounds in biological fluids[9]. It has been used to study bile composition[10-15]. ^{1}HNMR analysis of bile after liver transplantation suggested that this technique might help to distinguish ischaemia from rejection post-transplant[17] and there has been growing interest in attempting to predict graft function by analysing bile production immediately after transplantation[18].

3.8.1 Nuclear moment, excitation, and induction decay

Many nuclides possess permanent magnetic moments (spin) and, when placed into an external magnetic field, align (the axis of their spin) along the magnetic field. The orientation is never complete due to thermal fluctuations, and some nuclides orient parallel to the field while others prefer the anti-parallel arrangement. At equilibrium, the magnetic moments of all nuclides present in a sample produce a net macroscopic magnetization called nuclear magnetization, which can be represented by a magnetization vector (Figure 6a)[470,471].

In equilibrium, nuclear magnetization is aligned along the magnetic field and is almost

impossible to detect against the main field background. By applying a suitable radiofrequency pulse, nuclear magnetization can be rotated by any desired angle and thus brought into a non-equilibrium state in which it is no longer aligned with the field. This is called excitation (Figure 6b)[471]. The excitation pulse is typically very powerful (0.1-10 kW) but short (of the order of 1-100 microseconds)[470,471].

Once excited, the nuclear magnetization vector is not longer aligned with the magnetic field. Those vectors that are transversal to the magnetic field precesses (rotates) around the field direction with a frequency f proportional to the field strength B, $f = \gamma B$, where the proportionality constant γ is characteristic of the particular nuclide. This "Larmor frequency" is usually in the radiofrequency range[470,471].

The excitation pulse, in order to be effective, must have a carrier frequency very close to the Larmor frequency (the resonance condition). Consequently, it can only excite, for example, ^{1}H nuclides or ^{13}C nuclides, but not both at the same time.

The precessing component of nuclear magnetization, though tiny, is easy to detect because it rotates and thus can induce RF signals in a nearby receiver coil (hence the term nuclear induction) as shown in figure 6c[470,471].

After excitation, nuclear magnetization returns back to its equilibrium state. This process is called relaxation and the return paths (relaxation curves) can be quite complex. In the simplest and somewhat idealized case, it is characterized by two times:

- T_1, the exponential rate with which the longitudinal component of the magnetization returns to its equilibrium value, and
- T_2, the exponential rate with which the transversal component, while precessing around the field direction, decreases in magnitude towards zero.

The two relaxation times are subject to the condition $T_2 \leq T_1$. Their numeric values are characteristics of the measured substance and of its thermodynamic state and can assume values ranging from a few microseconds to several days. This means that, after excitation, there is often a relatively long period during which the receiver coil picks up a decaying (transient) response signal, called “free induction decay”[470,471].

3.8.2 Magnetic field variations

What makes magnetic resonance interesting, is that there are differences between the magnetic fields perceived by individual nuclides due to local variations induced by the electronic shells of molecules (chemical shifts), variations at a nuclide's location due to interactions with close-by nuclides, field variations between different areas of a heterogeneous sample, variations produced on purpose by precisely controlled magnetic field gradients which vary the field perceived in each voxel of the sample according to its location in space[470,471]. This is the technical basis of MRI.

Chemical shifts are the basis of NMR spectroscopy and its many applications to chemistry. Being very small, they are measured in parts per million (ppm) with respect to the external field[470,471].

All local field variations translate into corresponding variations of the Larmor frequency of the nuclides. The observed signal is therefore a sum of superposed signals with many different frequencies. Fortunately, there are various ways of mathematically decomposing such a composite signal (interferogram) into its harmonic components[470,471]. The best known and most widely used of these methods is the Fourier transform (figure 6d)[471]. Frequency measurements can be made with incredible precision.

MRS equipment can be tuned, like a radio receiver, to pick up signals from different chemical nuclei within the sample or body[470,471]. The most common nuclei to be studied are protons (hydrogen), phosphorus, carbon, sodium and fluorine.

Figure 6: The physics of NMR

(a) Alignment of nuclear moment at equilibrium in a magnetic field to produce a "magnetization vector."

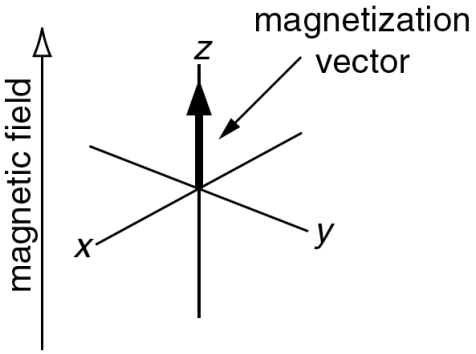

(b) Excitation and precession following a radio frequency pulse

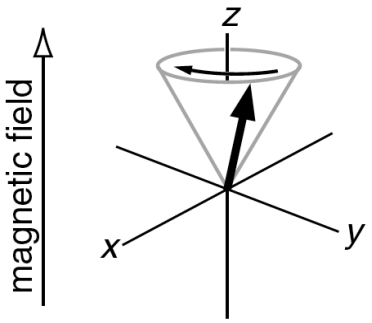

If the magnetization vector is tilted away from the z axis it executes a precessional motion in which the vector sweeps out a cone of constant angle to the magnetic field direction.

(c) Nuclear precession following excitation produces a radio frequency signal in receiver coil

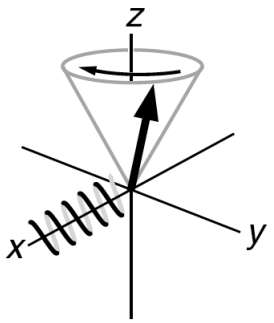

The precessing magnetization will cut a coil wound round the x axis, thereby inducing a current in the coil. This current can be amplified and detected; it is this that forms the free induction signal. For clarity, the coil has only been shown on one side of the x axis.

(d) Fourier transforming the free induction decay signal

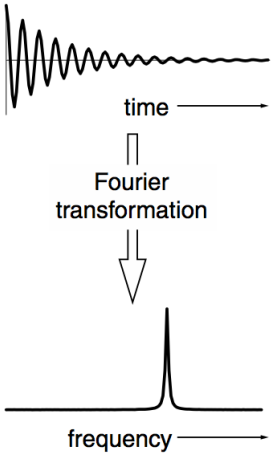

3.8.3 Experimental ^{1}HNMR protocol

In chapter four and five, ^{1}HNMR spectra of hepatic bile samples was obtained using spectrometer (Eclipse+ 500; JEOL Ltd., Tokyo, Japan) operating at 11.7 Tesla (500 MHz for ^{1}H) as shown in figure 7. All Spectra were recorded at 25°C. 600μL of bile was placed in a 5mm tube with a 2mm coaxial insert containing 100μL of 1mg/ml of sodium trimethylsilyl-[$^{2}H_4$]propionate (TSP) dissolved in deuterium oxide ($^{2}H_2O$, Fluorochem Ltd., Old Glossop, Derbyshire, UK) and set at 0.0 parts per million (ppm). To reduce the large water resonance signal a gated secondary irradiation at the water frequency was applied. Published peak assignments[10,18,370,472] were used. Integration of the ^{1}HNMR spectra areas was measured relative to the TSP area and obtained using MestRe-C software (version 2.3a, Departmento de Química Orgánica, Universidade de Santiago de Compostela).

In chapter six, seven and eight, ^{1}HNMR analysis was performed on an 11.7T (500 MHz for protons) spectrometer (Varian Unity +; Varian, Palo Alto, CA, USA) at 25^{o}C. Bile was thawed at room temperature and placed in 5mm NMR tube. For a field/frequency lock a coaxial capillary insert was used (Wilmad, Buena, NJ, USA). This capillary insert was filled with a deuterium oxide solution of sodium TSP that acted both as a chemical shift reference and quantification standard. This capillary

was calibrated by using a series of known concentration solutions of deoxycholate and a calibration curve was obtained (appendix section 10.1). This was then used for quantification of bile components, which enabled an accurate comparison bile levels between the groups. One dimensional NMR spectra were obtained at 500MHz with a sweep width of 6kHz and 32k data points in 64 scans were collected in both normal and spin echo mode. Presaturation of bile was carried out to attenuate the intensity of water signal. The spectra were analysed using software from MestRe-C version 3.1.1 (Universidade de Santiage de Compostela, Spain).

Figure 7: ^{1}HNMR spectrometer

The ^{1}HNMR spectrometer: Eclipse+ 500 (11.7 Tesla) with automatic sample-loader (JEOL Ltd., Tokyo, Japan)

Table 2: ^{1}HNMR Peak Assignments

Peak Assignments	ppm	Range of Integration
TSP	0.0	-0.02-0.02
C-18 bile acids	0.7	0.61-0.73
ß-hydroxybutyrate	1.2	1.18-1.22
Lactate methyl group (CH_3)	1.3	1.25-1.38
Acetate methyl group (CH_3)	1.9	1.89-1.95
Acetoacetate	2.2	2.29-2.25
Pyruvate methyl group (CH_3)	2.3	2.34-2.38
PC head group –N+(CH_3)$_3$	3.2	3.20-3.27
Acetoacetate	3.4	3.42-3.45
Water	4.7	4.61-4.66
C-25 Glycine (CH_2)	3.8	3.76-3.92
β-glucose anameric proton peak	5.2	5.20-5.25

3.9 Bile sampling for MRS

The bile duct was cannulated with a polyethylene catheter (PE-50; Portex, Kent, UK) for measurement of BF and collection of samples for ^{1}HNMR spectroscopy. Bile was stored in liquid nitrogen for days at -80°C in clear polypropylene Eppendorf safe lock microcentrifuge tube 1.5mL. It has been known for several years that chemicals (e.g., BPA and phlalates) can leach out of the plastic, such as toys and baby bottles[473,474]. The impact of these chemicals on human health is well known. Recent scientific reports have now noted that chemicals used in the manufacturing of disposable plastic labware, such as slip agents or plasticizers, can leach out of the plastic and affect laboratory experiments leading to erroneous results[475-477]. If these experiments wwere

to be repeated today, the use of reagent free tubes, or glassware would be encouraged.

3.10 Blood sampling for liver function

Arterial blood samples (1ml each) were taken before the induction of liver ischaemia (baseline), at the end of ischaemia (60 min) and 2, 5 and 7 hours after reperfusion for measurement of ALT activity. An equal volume of normal saline was used to replace the volume of the blood taken. Serum was separated from the samples and stored at -20^{o}C until assayed. The measurements were done using an automated clinical chemistry analyzer (Hitachi 747, Roche Diagnostics Ltd., Sussex, UK).

3.11 Data collection and statistical analysis

Data from the pulse oximeter, blood pressure, LDF and NIRS were collected continuously on a laptop computer. The data were averaged for two minutes before the induction of ischaemia (baseline), at the end of ischaemia and at the end of each hour of the reperfusion period. Changes in hepatic tissue oxygenation at the end of each period were calculated relative to baseline. Values are expressed as mean, standard deviation (SD). ANOVA with Bonferroni adjustment for multiple comparisons, unless otherwise stated. $P<0.050$ was considered statistically significant.

The “Student” t test was developed by W. S. Gossett [1876-1937] to solve problems stemming from his employment in a brewery. Student's *t*-test deals with the problems associated with inference based on “small” samples: the calculated mean (X_{avg}) and standard deviation (σ) may by chance deviate from the “real” mean and standard deviation (i.e., what you'd measure if you had many more data items: a “large” sample).

For example, it is likely that the true mean size of maple leaves is “close” to the mean calculated from a sample of *N* randomly collected leaves.

If N=5, 95% of the time the actual mean would be in the range: X_{avg}± 2.776 /$N^{1/2}$;

if N=10: X_{avg}± 2.262 /$N^{1/2}$;

if N=20: X_{avg}± 2.093 /$N^{1/2}$;

if N=40; X_{avg}± 2.023 /$N^{1/2}$;

and for "large" N: X_{avg}± 1.960 /$N^{1/2}$.

While the t-test is limited to comparing means of two groups, one-way ANOVA (Analysis of Variance) can compare more than two groups. Therefore, the t-test is considered a special case of one-way ANOVA. These analyses do not, however, necessarily imply any causality (i.e., a causal relationship between the left-hand and right-hand side variables). The t-test assumes that samples are randomly drawn from normally distributed populations with unknown population means. Otherwise, their means are no longer the best measures of central tendency and the t-test will not be valid. In a t-test you are able to test one sample mean vs. a single value or two sample means against each other. ANOVA allows you to test if multiple means are equal to each other.

In other words, the null hypothesis of the t-test is: $\mu_1 = \mu_2$

the null hypothesis for ANOVA is: $\mu_1 = \mu_2 = \mu_3 = ... = \mu_n$

The reason we have the different tests is because of the errors in multiple testing.

For example you have four means to look at, μ_1, μ_2, μ_3, μ_4.

If you use t-tests to test if each mean is equal to each other at say the 0.05 significance level then you have a 4C2=6 tests to conduct and a probability of not committing a Type I error decreasing from 0.95 to 0.95^6=0.7350919.

This means that using 6 independent t-tests for the four equality of four means you have a probability of committing a Type I error—reject the null hypothesis when it is true—from 0.05 to over 26%.

This is not desirable, you can correct this by using the Bonferroni correct or Fisher's

LSD or any other multiple testing correction method. In ANOVA, the test is designed to test for multiple mean equalities and the significance of the test is preserved.

3.12 Metabolomics in MRS analysis

A more contemporary technique of analysis of MRS spectra would include metabolomic analysis FIDs themselves, not the outcome of integrations, taking into account every variation in the area under the curve.

The main strengths of NMR spectroscopy are reproducibility[478], with little variance[479], the ability to quantify compounds in mixtures and the ability to identify unknown metabolites. Given that peak area in the NMR spectrum relates directly to the concentration of specific nuclei, quantification of compounds in a complex mixture is very precise[480].

Over the last decade there has been an advance in 'big data' and data-mining techniques, focusing no extracting information and patterns from large data sets. The emerging "-omics" subspecialties are its application in biomedical sciences, such as proteomics, transcriptomics, and—as the probably closest to the "bedside" metabolomics. Metabolomics can learn from the issues that have plagued "-omics" researchers over the last years, namely standardization[480], data processing[481] and data interpretation[482].

3.12.1 The "–omics" sciences

Proteomics is the large-scale study of proteins, particularly their structures and functions[483,484]. The word *proteome* is a blend of *protein* and *genome.* The proteome is the entire complement of proteins[485], including the modifications made to a particular set of proteins, produced by an organism or system

The study of transcriptomics, also referred to as expression profiling, examines the expression level of mRNAs in a given cell population, often using high-throughput techniques based on DNA microarray technology or next generation sequencing

technology called RNA-Seq.

Metabolomics is the study of the unique chemical fingerprints that specific cellular processes leave behind, i.e. the study of their metabolite profiles. “Clinical metabolomics” aims at evaluating and predicting health and disease risk in an individual by investigating metabolic signatures in body fluids or tissues, which are influenced by genetics, epigenetics, environmental exposures, diet, and behavior[486].

3.12.2 Metabolomics

The idea, that biological fluids mirror the health of the whole entity, has existed for a long time. Ancient Chinese doctors used ants to detect glucose in the urine of diabetics[487]. In the Middle Ages, “urine charts” were used to link the colours, tastes and smells of urine to various medical conditions, which are metabolic in origin[488].

Seeley et al. demonstrated the usefulness of using MRS to detect metabolites in unmodified biological samples[489]. As sensitivity of MRS has improved with the evolution of higher magnetic field strengths and magic angle spinning, it continues to be a leading analytical tool to investigate metabolism[487,488]. Professor Jeremy Nicholson has pioneered efforts to use MRS for metabolomics at Birkbeck College, and later at Imperial College London, University of London. In 1984, Nicholson showed ^{1}HNMR spectroscopy could potentially be useful in the diagnosis and treatment of diabetes mellitus. He later pioneered the application of pattern recognition methods to NMR spectroscopic data[490,491] and the quantitative measurement of the dynamic multiparametric metabolic response of biological systems to pathophysiological stimuli. Jeremy Nicholson pioneered this approach at Imperial College London and has been used in toxicology, disease diagnosis and a number of other fields. Historically, the metabonomics approach was one of the first methods to apply the scope of systems biology to studies of metabolism[492-494].

The data generated in metabolomics usually consist of measurements performed on subjects under various conditions. These measurements may be digitized spectra, or a

list of metabolite levels. In its simplest form this generates a matrix with rows corresponding to subjects and columns corresponding to metabolite levels[487]. Several statistical programs are currently available for analysis of both NMR and mass spectrometry data. Metabolomics data may also be analyzed by statistical projection (chemometrics) methods such as principal components analysis and partial least squares regression[495]. The large spectral datasets generated by MRS are often analyzed using data reduction techniques like Principal Component Analysis (PCA). Although rapid, these methods are susceptible to solvent and matrix effects, high rates of false positives, lack of reproducibility and limited data transferability from one platform to the next[496].

3.12.2.1 Principal component analysis

NMR spectra of biological samples are extremely complex and an optimized method to explore the information from the NMR spectral data is needed: this is made possible using multivariate data analysis which, in this context, is called chemometrics[497]. Principal component analysis (PCA) is a commonly used chemometric tool as it simplifies the multivariate data into a few dimensions that can be readily understood and evaluated. In this manner, each sample (spectrum) can be represented by relatively few numbers (PC scores) instead of thousands of variables (spectral data points). PC scores can then be plotted, making it possible to visually assess similarities and differences between samples and to determine whether samples can be grouped into meaningful patterns. As an exploratory method, PCA is most commonly used to identify how one sample is different from another, and which variables contribute the most to this difference.

3.12.2.2 Multivariate Data Analysis

Multivariate Data Analysis (MVA) extracts the information from large data sets and presents the results as interpretable plots based on the mathematical principle of projection. Even data characterized by thousands of variables can be reduced to just a

few information rich plots.

3.12.2.3 Partial least squares discriminant analysis

Partial least squares discriminant analysis (PLS-DA) determines the relationship between the response vector Y (i.e. sham control group versus ichaemia/reperfusion) and the matrix X (concentration of particular metabolites) by simultaneous projections of both Y and X spaces to a plane. PLS-DA generates a prediction score (0–1) for each animal based on the value of the metabolites (i.e., scores <0.5 would be predicted to be sham control animals versus I/R animal >0.5). This process identifies the metabolites whose concentrations differed significantly between groups of animals. As might be expected, most metabolites measured do not differ greatly between groups. In contrast, the greater the consistent difference in metabolite concentration between groups, the more important a metabolite becomes.

Due to the large discrepancy between when these experiments were conducted, and when the thesis was examined, these new techniques which have emerged in the interim should have been utilized in the analysis but have not been.

4 Pilot study to determine the effect of hepatic warm ischaemia reperfusion on bile composition

4.1 Introduction

Bile formation is an active secretory process involving bile salt dependent and independent mechanisms[25]. Bile excretion is used as an indicator of liver function and recovery following ischaemia in experimental studies[25,34,39-41,43,44,498-500] and clinical liver transplantation[501]. However, little is known about changes in bile composition during liver ischaemia and following reperfusion.

In recent years, high resolution ^{1}HNMR has been established as a powerful technique to explore the biochemical composition of biological fluids such as plasma, bile, seminal and synovial fluids, in various pathological conditions[371]. This technique is rapid, non-invasive and non-destructive and can detect metabolites present at the millimolar concentration. In bile, it has been used to investigate biliary lipids[14] and conjugated bile acids[15]. In the liver, NMR has also been used to assess glutamine metabolism[16], energy status after warm ischaemia[17], and to study effects of I/R on liver cell membranes[18,502]. A preliminary study of ^{1}HNMR analysis of bile after liver transplantation suggested that this technique might help to distinguish ischaemia from rejection post-transplant by detecting large resonance peaks for the ischemic metabolites lactate and acetate[18]. More recently there has been growing interest in attempting to predict graft function by analyzing bile production immediately after transplantation[503].

Melendez et al in 2001 published a small pilot study consisting of only four liver transplants in which they analyzed donor organ bile before and after transplant. One recipient had primary graft non-function, another had early graft dysfunction and two had good early graft function. ^{1}HNMR analysis of bile demonstrated that good graft function was associated with rapid clearance of sugar peaks derived from University of Wisconsin solution, lower lactate and an increase in PC head group and bile acid levels[19].

With advances in MRI technology, spectroscopy is an increasingly available option utilising voxel analysis[19,504-510]. In vivo MRS assay of the gall bladder has recently been reported[19] with direct MRS assay of the degree of liver steatosis[506-510]. The obvious implication is for the use of in vivo bile spectroscopy to assess liver function in a non-invasive manner. The aim of this study is to examine bile composition during liver ischaemia and reperfusion in an established model of warm lobar liver IRI[396] to determine any compositional changes during I/R.

4.2 Objectives

1. To determine if there is any change in bile composition with I/R
2. To identify the differences in chemical composition between sham and I/R
3. To ascertain if these changes fit with established understanding of the mechanisms involved in liver IRI
4. To compare these changes with some established markers of IRI

4.3 Materials and methods

4.3.1 Model of lobar ischaemia/reperfusion

The study was conducted under a license granted by the Home Office in accordance with the Animals (Scientific Procedures) Act 1986. New Zealand white rabbits (3.8 ± 0.5 kg) were used in a validated model of lobar ischaemia[391-400]. Anaesthesia was induced by an intramuscular injection of 0.5ml/kg fentanyl citrate and fluanisone (Hypnorm; Janssen Animal Health Ltd., Buckinghamshire, UK). Following tracheostomy anaesthesia was maintained with isoflurane (Forane; Abbott Laboratories, Chicago, IL, USA), (0.5-3%) through an anaesthetic circuit. Body temperature was maintained at 37-38.5^{o}C by a warming blanket (Homoeothermic blanket control unit; Harvard Apparatus, Southmatick, Massachusetts, USA). Haemoglobin saturation and heart rate were continuously recorded by a pulse oxymeter (Ohmeda Biox 3740 pulse oxymeter; Ohmeda, Louisville, Colorado, USA). One catheter (20G) was inserted into the right femoral artery for arterial blood

pressure monitoring and collection of blood samples. The femoral vein was cannulated with another catheter (22G) for the administration of anaesthetics and fluids.

Laparotomy was performed through a midline incision. The ligamentous attachments from the liver to the diaphragm were divided and the liver was exposed. The bile duct was cannulated with a polyethylene catheter (PE-50; Portex, Kent, UK) for measurement of BF and collection of samples for ^{1}HNMR spectroscopy.

4.3.2 Experimental groups and protocol

Two groups of animals were used; the I/R group (n=6) had lobar liver ischaemia induced by clamping the vascular pedicles of the median and left lobes of the liver, using an atraumatic microvascular clip. This method produces a severe ischemic insult without inducing mesenteric venous hypertension[398,400]. After 60 min of ischaemia the vascular clip was removed and reperfusion was allowed for 7 hours. During the ischaemia and reperfusion period, the abdomen was covered with a plastic wrap to prevent fluid evaporation. At the end of the experiment the animals were killed by exsanguination. The sham group (n=6) underwent laparotomy for 8 hours, without hepatic inflow occlusion. In both groups 10ml/kg/h of 0.9% NaCl was administered IV to compensate for intraoperative fluid loss.

4.3.3 Blood sampling for liver function

Arterial blood samples (1ml each) were taken before the induction of liver ischaemia (baseline), at the end of ischaemia (60min) and 2, 5 and 7 hours after reperfusion for measurement of ALT activity. An equal volume of normal saline was used to replace the volume of the blood taken. Serum was separated from the samples and stored at -20^{o}C until assayed. The measurements were done using an automated clinical chemistry analyzer (Hitachi 747, Roche Diagnostics Ltd., Sussex, UK).

4.3.4 Liver Histopathology

Small wedge biopsies were taken at the end of the procedure from the ischemic and non-ischemic lobes. Formalin-fixed liver tissue samples were embedded in paraffin

and stained with hematoxylin and eosin for subsequent microscopy (digital light microscope CLF60 optical system, Nikon UK Ltd, Surrey, UK). For assessment of the degree of injury a semi quantitative method was used in which a blinded liver pathologist estimated the number of PMN in sinusoids, the aggregation of PMN, the hypertrophy of KC and the presence of necrosis and apoptosis in 5 high power fields per slide.

4.3.5 Measurement of cytochrome oxidase activity

The effect of I/R on intracellular liver tissue oxygenation was measured by NIRS. Light at visible wavelength (450-700nm) is strongly attenuated and as a result can only penetrate a maximum distance of a few millimetres. However, the absorption of light by tissue chromophores is significantly lower at near infrared wavelengths (700-1000nm), which allows photons at this wavelength to penetrate deeply into the tissue[511]. There are three main components in liver tissue whose NIR absorption characteristics vary with their oxygenation status, namely HbO_2, Hb and redox state of COX[268,396]. The change in the concentration of these chromophores can be quantified by using a modified Beer-Lambert Law[18]. NIRS instrument (NIRO-5000; Hamamatsu Photonics K.K., Hamamatsu, Japan) has been used to measure liver tissue oxygenation changes following warm liver IRI[512]. The optical-fibre bundles (probes) were positioned on the left lobe of the liver, with a 10mm separation. A flexible probe holder was used to ensure that probes have a satisfactory contact with the liver surface and a fixed inter-probe spacing. A NIRS algorithm was developed to measure continuously changes in redox state of Cu_A centre of COX in μmol/L. The pre-ischemic baseline was taken as baseline against which changes recorded.

4.3.6 Measurement of bile flow and ^{1}HNMR bile spectroscopy

The common bile duct was cannulated with a polyethylene catheter (PE-50, Portex, Kent, UK) for continuous collection of bile. Bile samples were collected continuously and aliquoted in separate containers at the end of baseline (before the I/R procedure),

following 60 min ischaemia and hourly during reperfusion. The total bile volume collected was expressed as μL/min/100g of liver wet weight and then each aliquot was analyzed by ^{1}HNMR spectroscopy. Spectra of hepatic bile samples were obtained using a ^{1}HNMR spectrometer (Eclipse+ 500; JEOL Ltd., Tokyo, Japan) operating at 11.7T (500 MHz for ^{1}H). All Spectra were recorded at 25°C. 600μL of bile was placed in a 5mm tube with a 2mm coaxial insert containing a reference standard of 100μL of 1mg/ml of sodium trimethylsilyl-[$^{2}H_4$]propionate (TSP) dissolved in deuterium oxide ($^{2}H_2O$, Fluorochem Ltd., Old Glossop, Derbyshire, UK) and set at 0.0 parts per million (ppm). To reduce the large water resonance signal a gated secondary irradiation at the water frequency was applied. Published peak assignments[10,18,370,472] were used. In brief, these were lactate methyl group peaks (1.33 ppm), acetate peaks (1.91 ppm), PC head group –N+$(CH_3)_3$ (3.20 ppm) and C-25 glycine methylene proton peak (3.80 ppm), as shown in figure 13. Integration of the ^{1}HNMR spectra areas was measured relative to the reference standard TSP area and obtained using MestRe-C software (Departmento de Química Orgánica, Universidade de Santiago de Compostela, Santiago de Compostela, Spain).

4.3.7 Data collection and statistical analysis

Values are expressed as mean ± standard deviation. Spectroscopy values are shown as a percentage change of baseline values. For statistical analysis ANOVA with Bonferroni/Dunn post hoc analysis was performed as well as simple and polynomial regression analysis with $P<0.05$ considered statistically significant. Statistics were calculated using commercially available software (SatView 5.0.1; SAS Institute Inc., Cary, NC, USA).

4.4 Results

4.4.1 Liver biochemistry

In the sham group, levels of ALT rose throughout the experiment from 54.0±5.65 IU/L at baseline to 91.5±36.06 IU/L after 7hrs reperfusion. A similar effect was seen in AST levels. In the I/R group there was a marked significant increase in ALT and AST at 2, 5 and 7hrs reperfusion as shown in figure 8 and 9 respectively.

4.4.2 Liver Histopathology

Examination of liver histology revealed PMN accumulation in sinusoids, PMN aggregation, KC hypertrophy, necrosis and apoptosis in the I/R group compared to the sham group as shown figure 10.

4.4.3 Bile Flow

BF gradually decreased in the sham group over the period of the experiment from 208.5±5.65 μL/min/100g at baseline to 155.0±8.49 μL/min/100g liver wet weight at 7hrs reperfusion (P=0.0051). BF in the I/R group was similar to sham group at baseline, 227.5±29.01 μL/min/100g liver wet weight, but reduced significantly to 60.5±19.16, (26.6% of baseline) during ischaemia (P=0.0008 compared to sham). BF increased on reperfusion to but remained significantly less than sham as shown in figure 11.

4.4.4 Cytochrome oxidase activity

In the I/R group COX reduced significantly during ischaemia (-24.23±5.52 μmol/L vs. 12.75±11.66 μmol/L, P=0.0007) and 7hr (-26.00±10.49 μmol/L vs. 7.00±7.07 μmol/L, P=0.0054) reperfusion as compared to sham as shown in figure 12.

Figure 8: Changes in alanine transaminase during I/R

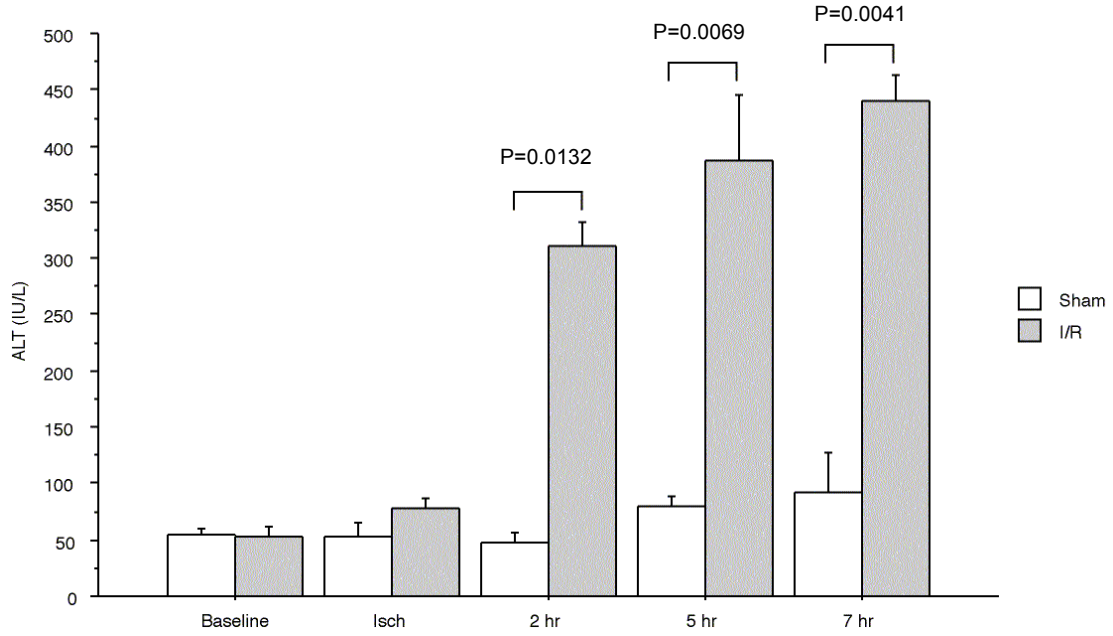

Figure 9: Changes in aspartate transaminase during I/R

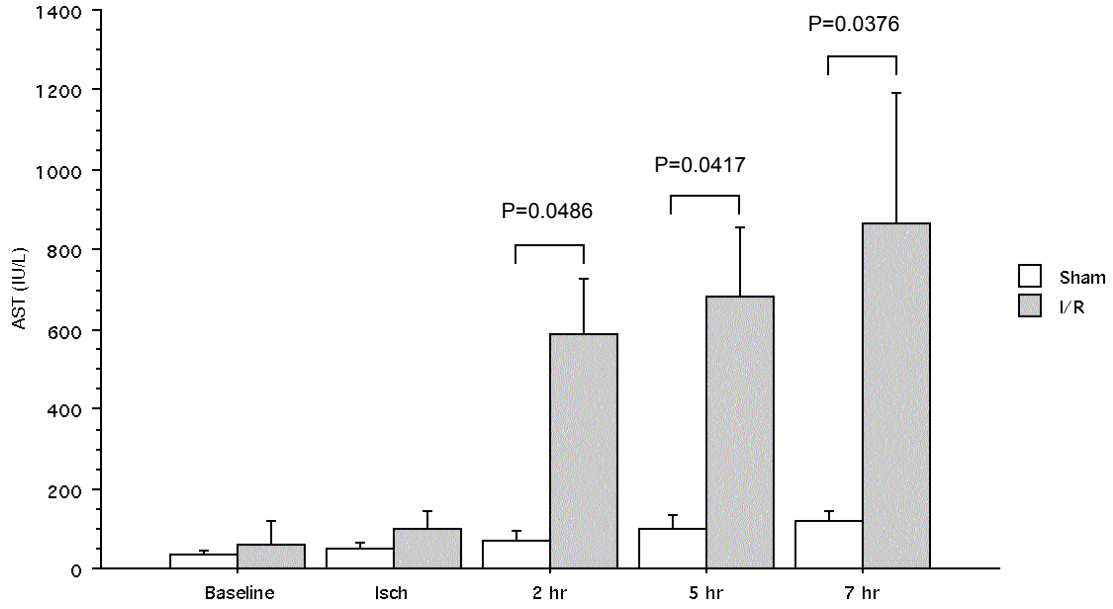

Figure 10: Light microscopy of liver changes during I/R

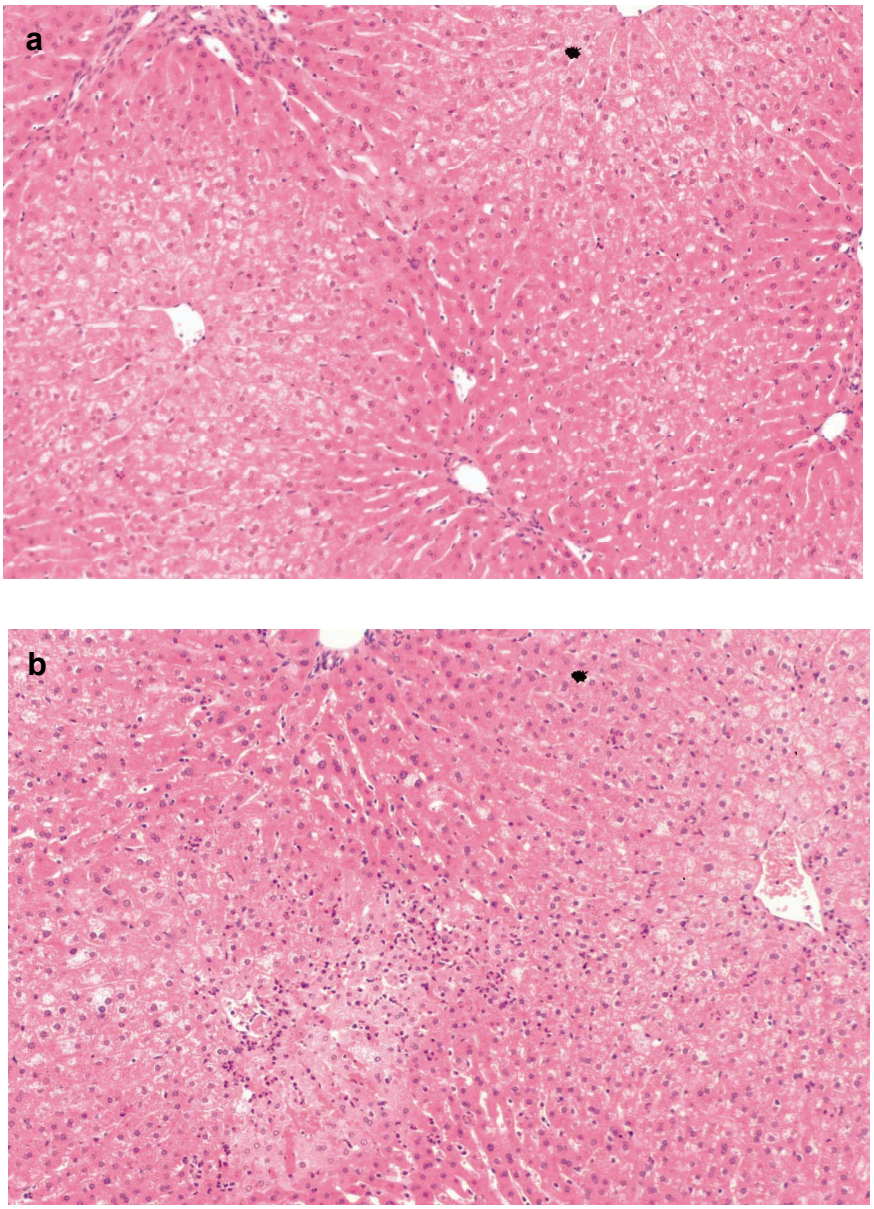

Light microscopy (x100) stained with hematoxylin and eosin showing more I/R associated liver damage in the I/R group (b) than in the sham group (a).

Figure 11: Bile flow following warm liver I/R

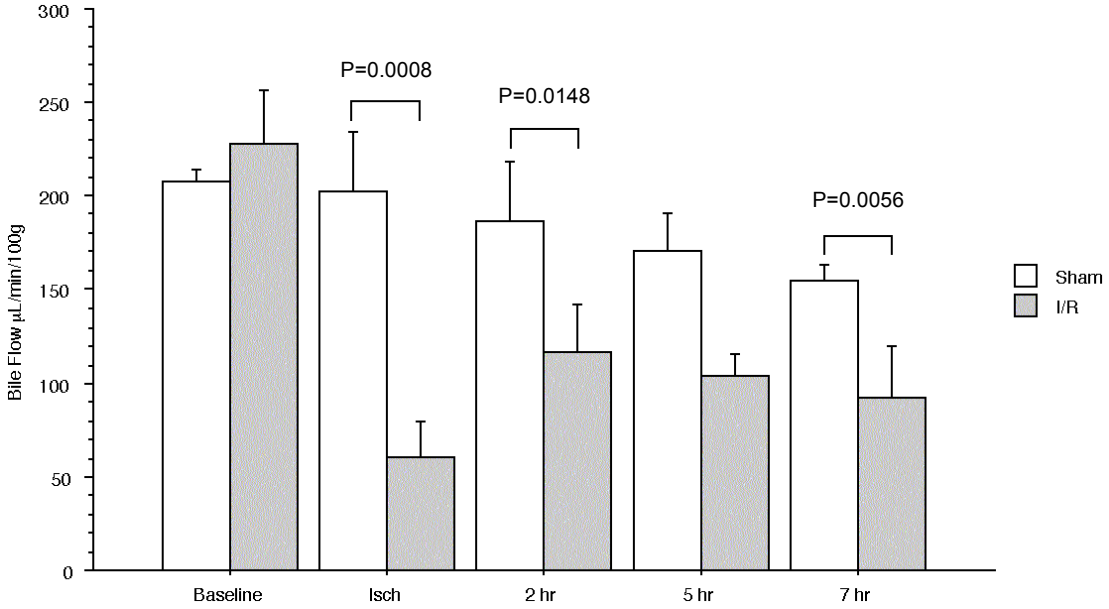

Figure 12: Cytochrome activity during warm liver I/R

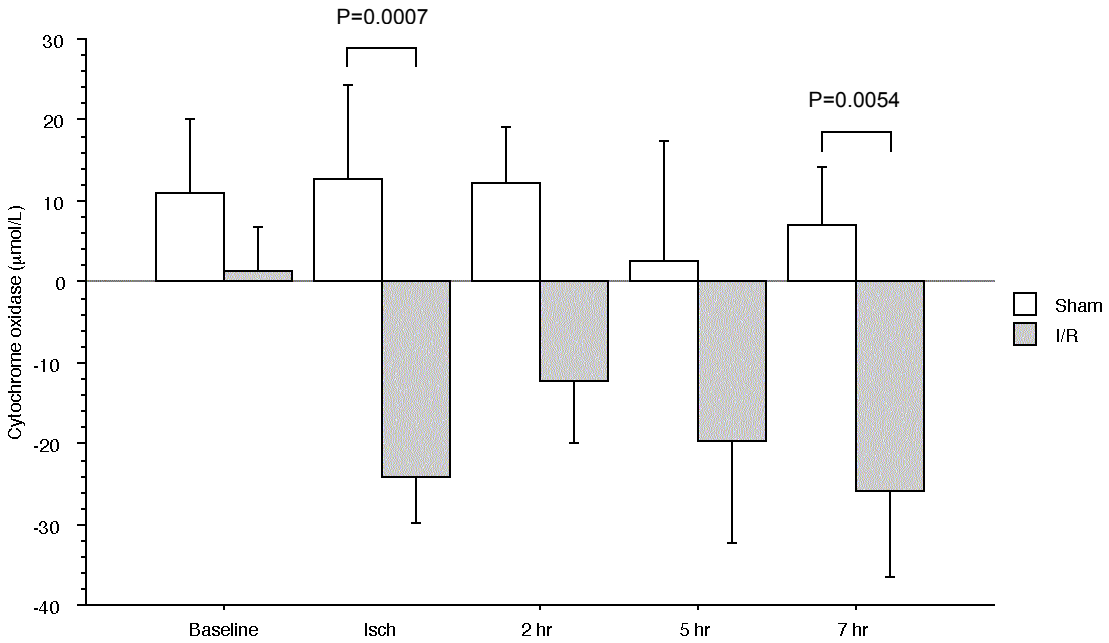

4.4.5 ^{1}HNMR spectroscopy of bile

A baseline spectrum of bile is shown in figure 13. There was no difference in biliary lactate concentration between the sham and I/R groups at baseline. Biliary lactate levels were significantly elevated in the I/R group at 5hrs post-reperfusion to 165.44±22.97% of initial baseline values (P=0.0036 vs. sham), followed by a decline at 7hrs to 89.13±29.91% of baseline values (figure 14).

Analysis and integration of peaks corresponding to phosphatidylcholine (PC) head group (figure 15) revealed that I/R produced a significant two-fold increase during the ischemic phase (213.04±64.06% of baseline vs. 82.13±31.91% of baseline in sham, P=0.0106). Mean values for PC over all time points tended to be higher in the I/R group than sham group (P<0.0001 as assessed by ANOVA).

Acetate levels were reduced compared to baseline throughout the period of the experiment in both the I/R and sham groups (figure 16). The reduction was significantly greater in the I/R group by 5hrs post-reperfusion (50.75±13.24% vs. 70.35±6.86%, P=0.0490) and 7hrs post-reperfusion (37.47±7.49% vs. 69.36±13.29%, P=0.0058) than in the sham group.

Correlation of ^{1}HNMR bile spectroscopy data with other parameters revealed that acetate decreased with increases in ALT (R=0.762, P<0.0001) (figure 17), AST (R=0.679, P=0.0006) (figure 18) and increased with increases in BF (R=0.458, P=0.0109) and ΔCOX (R=0.650, P=0.0001) as shown in figure 19. Phosphatidylcholine increased with increases in ALT (R=0.428, P=0.0295) and decreased with increases in BF (R=0.699, P<0.0001) and ΔCOX (R=0.644, P<0.0001). Lactate increased with increases in AST (R=0.445, P=0.0200) and tended to decrease with increases in ΔCOX (R=0.319, P=0.0857), however these results did not reach statistical significance.

Figure 13: ^{1}HNMR spectrum of baseline bile

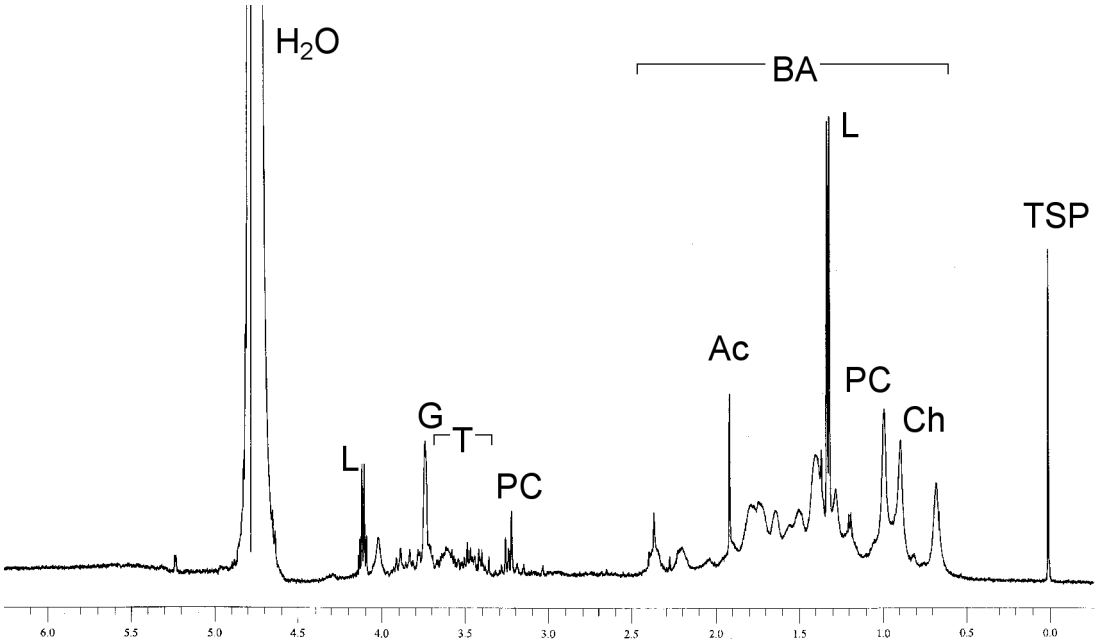

L=lactate, G=glycine, T=taurine, PC=phosphatidylcholine, BA=bile acid, Ch=cholesterol, TSP=sodium trimethylsilyl-[$^{2}H_4$]propionate standard, Ac=acetate

Figure 14: Biliary lactate levels following warm liver I/R

(a)

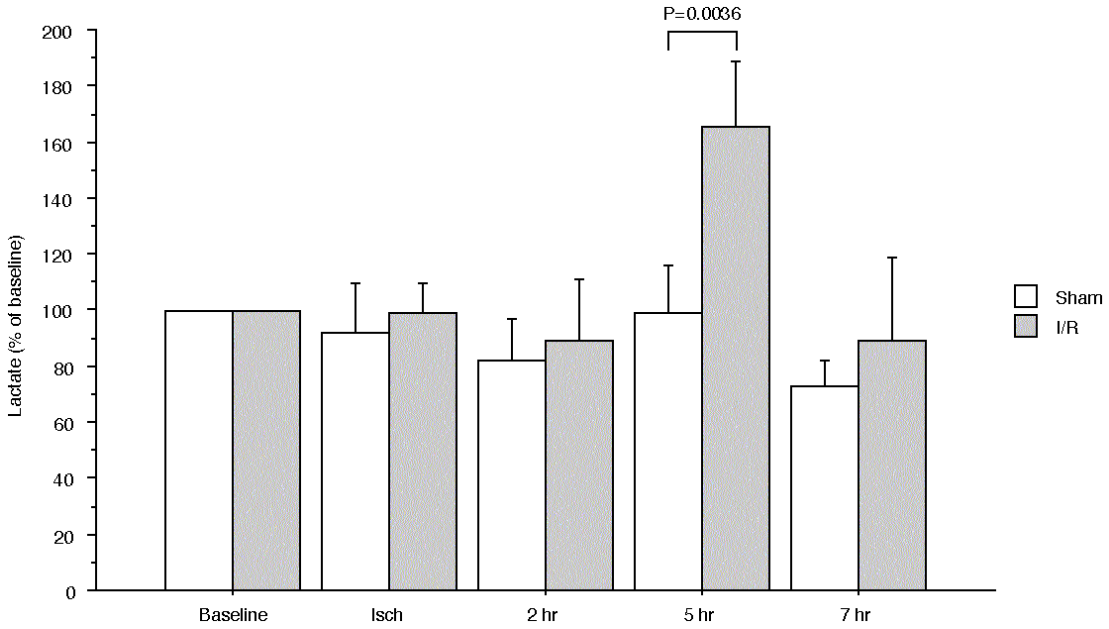

(a) Lactate levels were calculated by integration of peaks at 1.3 ppm and expressed as a percentage of baseline values

(b) (c)

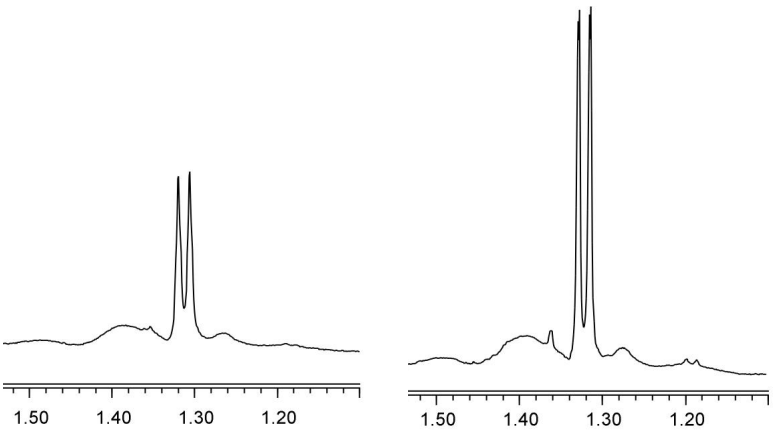

Bile lactate spectra (1.25-1.38 ppm) scaled to TSP from (b) baseline and (c) five hours of reperfusion in the I/R group (scale in ppm).

Figure 15: Biliary phosphatidylcholine levels following warm liver I/R

(a)

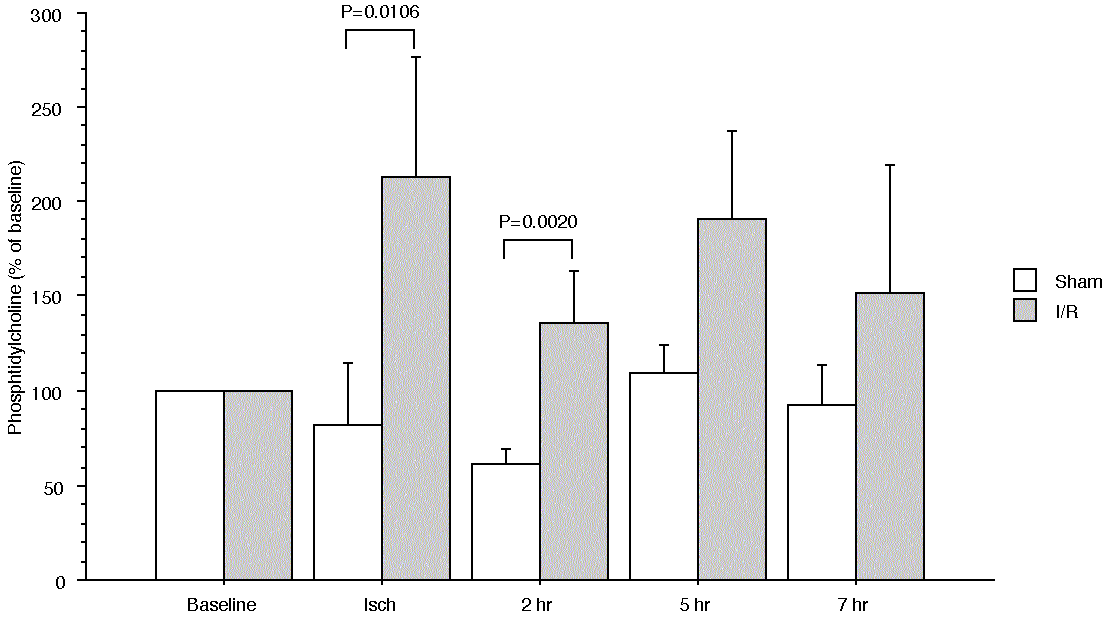

(a) PC levels were calculated by Integration of peaks at 3.2 ppm and expressed as a percentage of baseline values.

(b) (c)

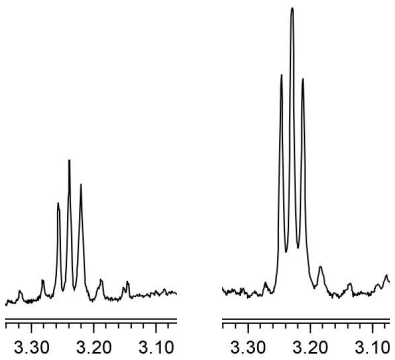

Bile PC spectra (3.20-3.27 ppm) scaled to TSP from (b) baseline and (c) ischaemia in the I/R group (scale in ppm).

Figure 16: Bile Acetate levels following warm liver I/R

(a)

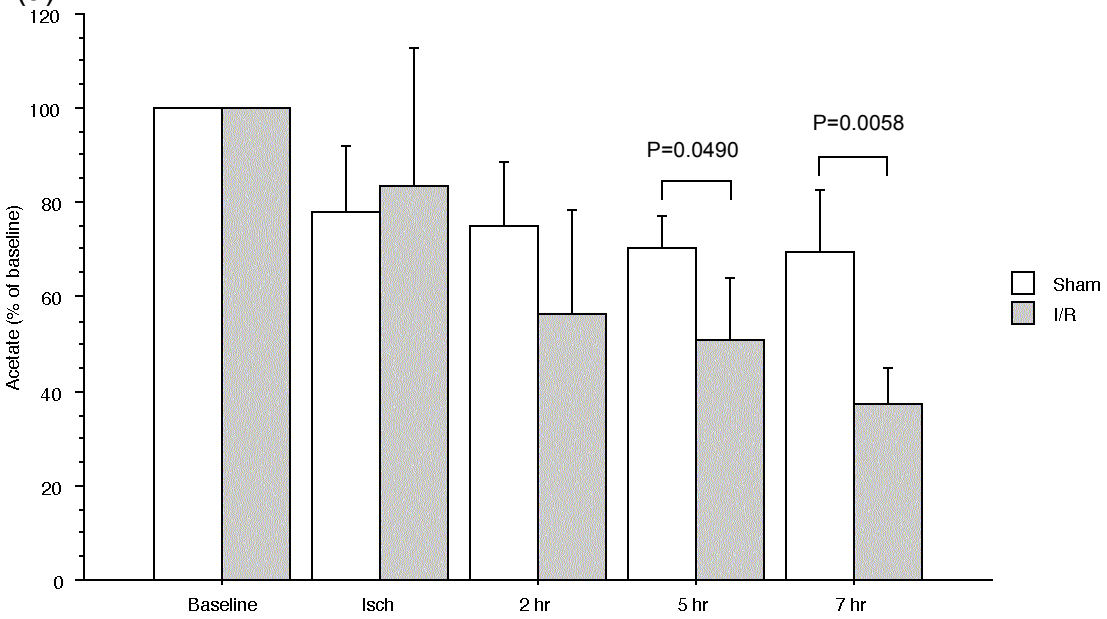

(a) Acetate levels were calculated by integration of acetate peaks at 1.91 ppm and expressed as a percentage of baseline values.

(b) (c)

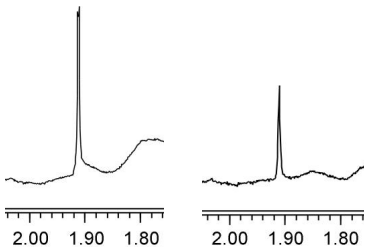

^{1}HNMR bile spectra of acetate peaks (2.0-1.84 ppm) scaled to TSP at (b) baseline and (c) after 7 hours of reperfusion showing significant reduction (scale in ppm).

Figure 17: Correlation of ALT and biliary acetate

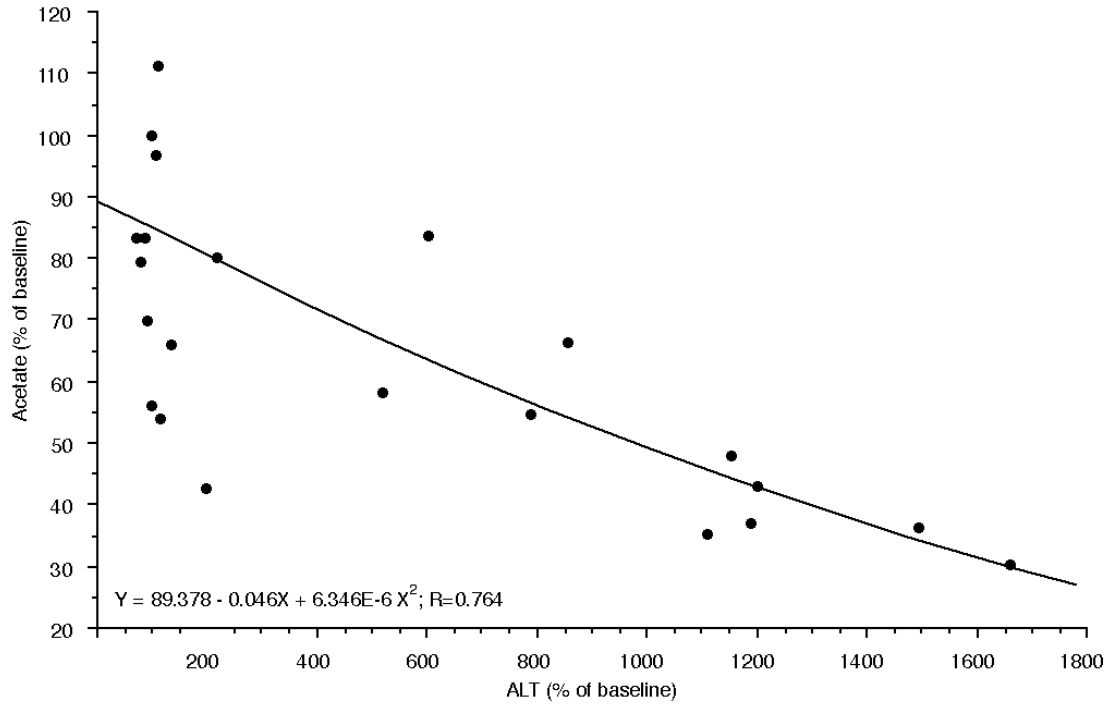

Figure 18: Correlation of AST with biliary acetate

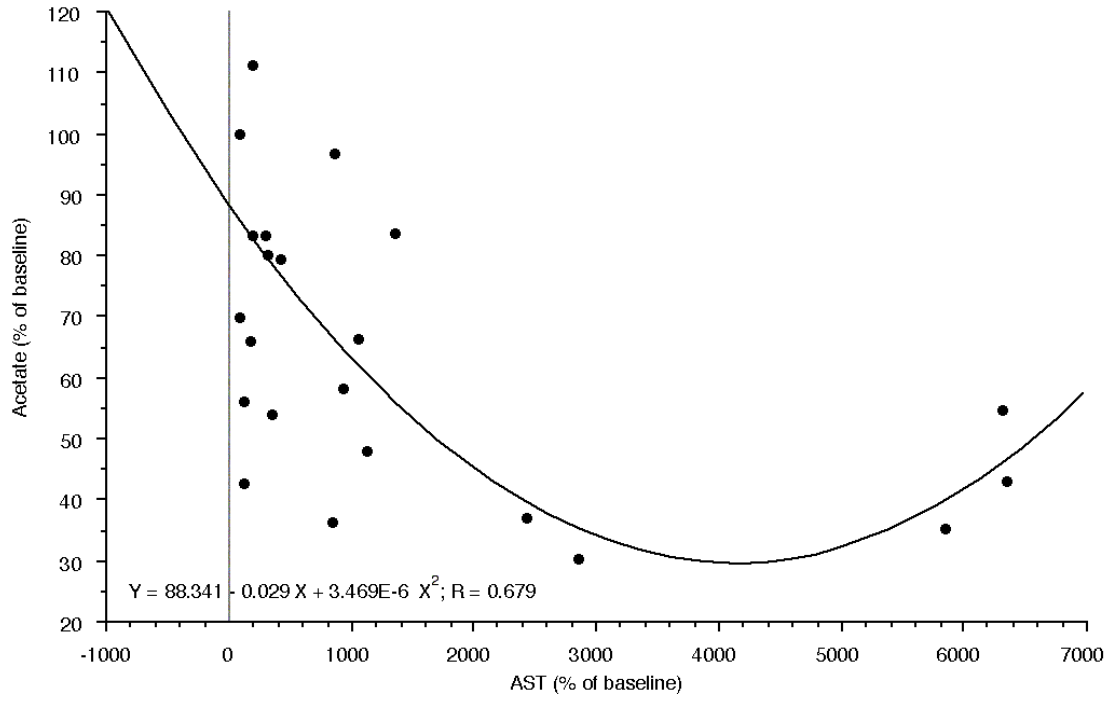

Figure 19: Correlation between change in liver cytochrome oxidase and biliary acetate

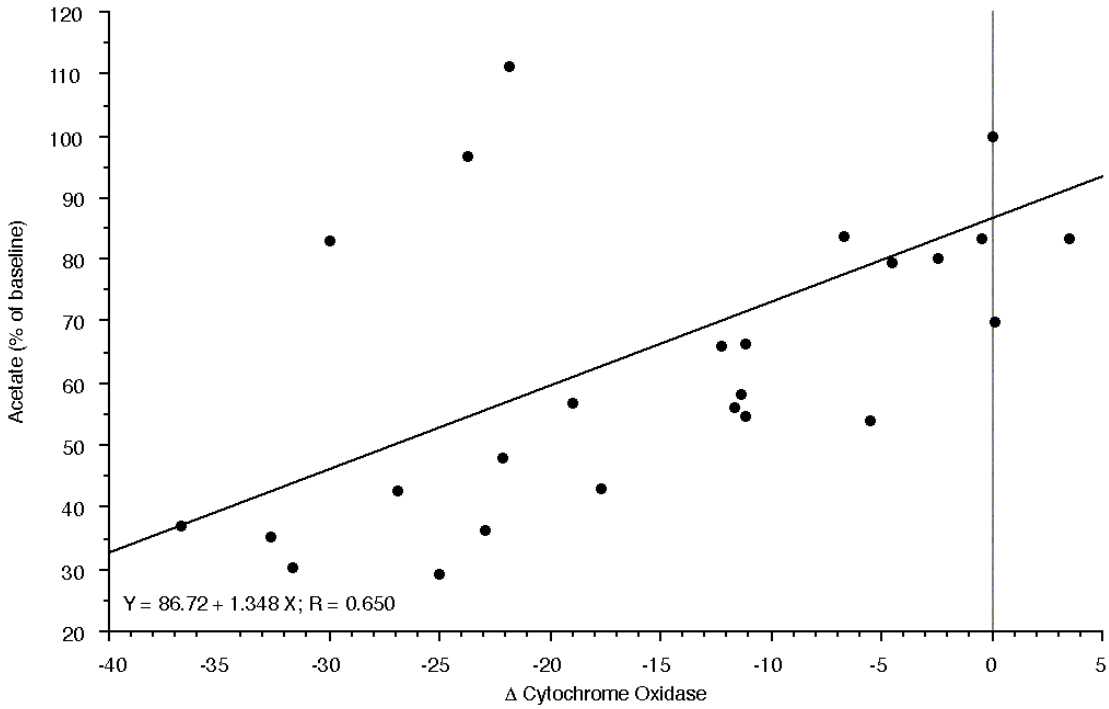

4.5 Discussion

This is the first time that ^{1}HNMR analysis of bile has been applied to a controlled experimental model of warm liver I/R. Liver warm IRI can be divided into an early phase which is associated with KC activation and a cytokine surge[513] and a late phase (>4hrs) which is mainly due to the accumulation of PMN and is associated with more extensive injury[514].

A rabbit lobar I/R model was used with reperfusion period of seven hours[396], The benefits of employing this model have been discussed above (section 3.1), briefly it permitted the analysis of bile constituents in both the early phase and the beginning of the late phase of IRI, avoiding the production of acute portal hypertension and intestinal ischaemia, maintained hemodynamic stability throughout the duration of the experiment, and avoiding the complete occlusion of biliary drainage in the total hepatic ischaemia model permitting the effects of I/R on biliary composition to be evaluated.

BF in the sham-operated group decreased due some to bile acid depletion from bile duct cannulation. ALT activity increased mildly over the duration of the experiment in the sham-operated group suggesting minimal operative and anaesthetic trauma to liver function over this lengthy surgical procedure[436,437]. However, the 6-10 fold rise following reperfusion in the study group suggests significant IRI[436,437,441,447].

COX is the terminal complex of the mitochondrial respiratory chain. It takes electrons from cytochrome c and catalyses the reduction of oxygen to water with the concomitant synthesis of ATP through the oxidative phosphorylation process[396,515]. In hepatocytes, approximately 90% of the oxygen is consumed by mitochondrial COX. Absorption of the NIR light by COX occurs primarily at the Cu_A centre within COX. There is a decrease in signal intensity on reduction of this centre. The redox state of COX Cu_A is dependent on cellular oxygen availability[25,34]. In the presence of oxygen, electron transfer occurs and the enzyme becomes oxidised, whereas lack of oxygen,

results in a decreased flow of electrons and COX becomes reduced. The increase in the reduction state of COX reflects severe cellular hypoxia. NIRS has been used to measure liver tissue oxygenation changes following warm liver IRI[25,39,498,499]. There was a significant chemical reduction in COX following ischaemia that was still persistent at 5 and 7hrs following reperfusion in the I/R group.

The drop in BF during ischaemia corresponds to the exclusion of liver mass in the I/R group during this phase. A post-reperfusion reduction in BF has been reported previously[41,43,44] and bile excretion has been used as an indicator of liver function and recovery following ischaemia in experimental studies[512] and clinical liver transplantation[512,516]. ^{1}HNMR spectroscopy of bile revealed changes in the concentration of some bile constituents. Bile lactate were elevated towards the beginning of the late phase of I/R, at a period when it is known there is significant neutrophil activation[517]. It has been observed that the injury produced during the beginning of the late phase is a more severe hepatocellular injury in comparison to the early phase[517-519]. PMN sequestration, sinusoidal narrowing and vasoconstriction combine to form a “no-reflow paradox” whereby hepatocytes are subjected to a further perfusion deficit and persistent ischaemia[404,520]. This may explain the observed peak in lactate at this late time point[521,522] especially since lactate levels have been shown to become elevated in bile even when they are not elevated in serum[523]. This may explain the observed peak in lactate at this late time-point. Lactate levels have been shown to become elevated in bile even when they are not elevated in serum[524]. ATP degradation after ischaemia leads to the activation of glycolysis, resulting in the net formation of lactate. Serum lactate concentration has been shown to increase progressively following liver ischaemia, primarily from glycolytic/gluconeogenic pathway. This was verified by measuring glucose-6-phosphate and fructose-6-phosphate which were shown to increase with IRI[525].

PC was raised following ischaemia and reperfusion at 2hrs and 5hrs. The main source

of PC in cells is in the plasma membrane, which suggests that the increase during ischaemia and again at 5hr post-reperfusion may be associated with an increase in cellular breakdown and membrane lipid peroxidation[18]. Increased PC has also been observed in other experimental studies[526] and in association with poor graft function[18,524].

Acetate was observed to decrease continuously from baseline throughout the experiment in the I/R group. Hepatocytes are one of the few cells that can utilize fatty acids in the production of energy through the β-oxidation helix[527,528]. This reaction requires ATP at its initiation. Post-reperfusion ATP is consumed to clear excess lactate and pyruvate and may not be readily available for fatty acid oxidation. The ATP reduction as a result of I/R may result in decreased β-oxidation and acetate production is reduced. Biliary acetate decreased with increases in ALT and AST, established markers of hepatocyte damage, and increased with increases in BF and changes in COX, accepted indicators of liver function and viability.

In conclusion, bile spectroscopy has demonstrated significant changes in bile composition during I/R. These changes are evident despite a constant, albeit reduced, post-reperfusion rate of BF.

5 Modulation of warm hepatic ischaemia reperfusion using NAC and its effect on bile composition

5.1 Introduction

As liver transplantation becomes the treatment of choice in an ever-widening spectrum of indications, greater strain is put on a static donor pool, with the result of increasing numbers of patients spending longer on waiting lists and dying on these lists[179]. This has put increasing pressure on surgeons and physicians to accept more marginal grafts including those from non-heart-beating (cardiac death) donors, which have been subjected to periods of warm ischaemia. It increases the need for a greater understanding of warm IRI, its effects and its therapeutic modulation.

Liver IRI occurs during major liver surgery, transplantation and following hypotensive shock/resuscitation[529]. Liver I/R is a complex triggering of a cascade of metabolic pathways and multiple mediators capable of inducing liver injury[102,103]. One of the main contributors to liver damage is the release of ROS and RNS. A complex intracellular antioxidant system protects against oxidative stress, of which glutathione an important component. Glutathione is a powerful active radical scavenger that is depleted during liver IRI[102]. NAC is a thiol-containing compound that is hydrolysed to cysteine—a glutathione precursor, capable of rapidly replenishing depleted concentrations[89], that has been used to reduce liver injury[89].

Bile formation is an active secretory process[25] that is used as an indicator of liver function and recovery following ischaemia[25,34,44]. IRI has been shown to result in poor BF, that recovers in reversibly damaged organs, while persistent low bile output is a sign of PNF[530]. Although BF has been considered a marker of liver function[8] and has been used to assess therapeutic and preservation strategies in liver transplantation[9], little is known, about changes in bile composition during liver I/R. In addition, little is also known about the effect of therapeutic strategies to ameliorate IRI on bile composition.

5.2 Objectives

1. To determine if the changes in bile composition during I/R can be reversed using NAC, an agent known to ameliorate IRI in liver
2. To identify the differences in chemical composition between sham, I/R and NAC+I/R, including further differences not previously identified in the pilot study e.g. conjugated bile acids
3. To ascertain if these changes fit with established understanding of the mechanisms involved in liver IRI and the actions of NAC
4. To compare these changes with some established markers of IRI

5.3 Materials and methods

The study was conducted under a license granted by the Home Office in accordance with the Animals (Scientific Procedures) Act 1986. New Zealand white rabbits (3.7±0.6kg, n=18) were used. Anaesthesia was induced by an intramuscular injection of 0.5ml/kg fentanyl citrate and fluanisone (Hypnorm; Janssen Animal Health Ltd., Buckinghamshire, UK). Following tracheostomy anaesthesia was maintained with Isoflurane (0.5-3%) through an anaesthetic circuit. Body temperature was maintained at 37-38.5^{o}C by a warming blanket (Homoeothermic blanket control unit; Harvard Apparatus, Southmatick, Massachusetts, USA). Haemoglobin saturation and heart rate were continuously recorded by a pulse oxymeter (Ohmeda Biox 3740 pulse oxymeter; Ohmeda, Louisville, Colorado, USA). A catheter (20G) was inserted into the median ear artery for arterial blood pressure monitoring and collection of blood samples. Ear marginal veins were cannulated with radio-opaque catheters (22G) for the administration of anaesthetics, fluids and medications[400].

5.3.1 Ischaemia reperfusion procedure

Laparotomy was performed through a midline incision. The ligamentous attachments from the liver to the diaphragm were divided and the liver was exposed. The bile duct was cannulated with a polyethylene catheter (PE-50, 0.58mm inner diameter, Portex, Kent, UK) for measurement of BF. The portal vein was dissected and a transonic

Doppler flow probe was placed around the vein for measurement of the portal flow.

5.3.2 Experimental groups and protocol

Three groups of animals were used; the control group in which lobar ischaemia was induced by clamping the vascular pedicles of the median and left lobes of the liver, using an atraumatic microvascular clip. This method produces a severe ischemic insult without inducing mesenteric venous hypertension[432]. After 60 min of ischaemia the vascular clip was removed and reperfusion was allowed for 7 hours. During the ischaemia and reperfusion period, the abdomen was covered with a plastic wrap to prevent fluid evaporation. At the end of the experiment the animals were killed by exsanguination. 20 ml of 5% dextrose was infused through the ear vein, over the 15 min before reperfusion and maintained at a dose of 10ml/kg/h during the reperfusion period. In group the 'NAC' group animals underwent a similar procedure and 150 mg/kg of N-acetylcysteine (Parvolex, Medeva Pharma Limited, Lancashire, UK) in 20 ml of 5% dextrose was infused I.V. through the ear vein, over the 15 min before reperfusion and maintained at 10 mg/kg/h in 5% dextrose during the 7 hours reperfusion period. In the 'sham operation' group, animals underwent laparotomy for 8 hours, without hepatic inflow occlusion. In all groups 10 ml/kg/h of 0.9 % NaCl was administered I.V. to compensate for intraoperative fluid loss.

5.3.3 Blood sampling for liver function

Arterial blood samples (1 ml each) were taken before the induction of liver ischaemia (baseline), at the end of ischaemia (60 min) and 2, 5 and 7 hours after reperfusion for measurement of alanine aminotransferase (ALT) activity. An equal volume of normal saline was used to replace the volume of the blood taken. Serum was separated from the samples and stored at -20^{o}C until assayed. The measurements were done using an automated clinical chemistry analyzer (Hitachi 747, Roche Diagnostics Ltd., Sussex, UK).

5.3.4 Measurement of portal flow

Portal flow was monitored continuously, using a perivascular transonic flow probe of 3 mm in diameter (Transonic Medical Flowmeter system, HT207; Transonic Medical System, Ithaca, New York, USA).

5.3.5 Measurement of bile flow and ^{1}HNMR bile spectroscopy

The common bile duct was cannulated with a polyethylene catheter (PE-50, 0.58 mm inner diameter, Portex, Kent, UK) for continuous collection of bile. Bile samples were taken at baseline, following 60 min ischaemia and hourly during reperfusion. Bile volume was expressed as μL/min/100g of liver wet weight. ^{1}HNMR spectra of hepatic bile samples was obtained using spectrometer (Eclipse+ 500; JEOL Ltd., Tokyo, Japan) operating at 11.7T (500 MHz for ^{1}H). All Spectra were recorded at 25°C. 600μL of bile was placed in a 5mm tube with a 2mm coaxial insert containing 100 μL of 1mg/ml of sodium TSP dissolved in deuterium oxide ($^{2}H_2O$, Fluorochem Ltd., Old Glossop, Derbyshire, UK) and set at 0.0 parts per million (ppm). A basic single pulse sequence was used to acquire the one-dimensional spectra using a 45° pulse (8.25μs) with an acquisition duration of 4.36s and a relaxation delay of 5s. To reduce the large water resonance signal a gated secondary irradiation at the water frequency was applied. Published peak assignments[10,18,370,472] used are shown in table 2. Integration of the ^{1}HNMR spectra areas was measured relative to the TSP area and obtained using MestRe-C software (version 2.3a, Departmento de Química Orgánica, Universidade de Santiago de Compostela).

5.3.6 Assessment of the hepatic microcirculation

Hepatic microcirculation was measured by a surface LDF, (DTR4, Moor Instruments Limited, Axminster, UK) in flux units[396]. The LDF probe was placed on a fixed site on the median lobe of the liver. LDF measurements were calculated as a mean of 2-min recording data before clamping (baseline), at the end of ischaemia and at the end of each hour of reperfusion for each animal. The alterations during I/R period were calculated relative to the baseline values.

5.3.7 Measurement of hepatic tissue oxygenation

Hepatic tissue oxygenation was measured by NIRS. NIRS can be used to measure concentration changes of HbO_2, Hb and COX[512]. NIRS has been used to measure liver tissue oxygenation changes following warm liver IRI[516]. For continuous monitoring of hepatic tissue oxygenation NIRS probes were positioned flat on the surface of the left lobe of the liver, with a 10mm separation. NIRS measurements during ischaemia and reperfusion were expressed relative to baseline values before vascular occlusion. For comparison between the different groups, NIRS measurements (at baseline, ischaemia and each hour of reperfusion) were calculated as the mean of 2min measurements at the end of each period.

5.3.8 Data collection and statistical analysis

Data from the transonic flowmeter, LDF and NIRS were collected continuously on a laptop computer. The data were averaged for two minutes before the induction of ischaemia (Baseline), at the end of ischaemia, and each hour of a 7hrs reperfusion period. The hepatic tissue oxygenation changes at the end of each period were calculated relative to baseline. Values are expressed as mean±SD. Spectroscopy values are expressed as a percentage of baseline values. One-way analysis of variance (ANOVA) with Bonferroni adjustment for multiple comparisons were used. Statistics were calculated using commercially available software (SatView 5.0.1; SAS Institute Inc., Cary, NC, USA). $P<0.05$ was considered statistically significant.

5.4 Results

5.4.1 Liver function

In the sham group, levels of ALT rose throughout the experiment from 56.0±2.8 IU/L to 91.5±36.0 IU/L after 8hrs of laparotomy. In the I/R group there was a marked significant increase in ALT levels. The I/R+NAC group did not start to rise till the 2nd hour of reperfusion and increased to 8 fold at 7hrs reperfusion (figure 20).

5.4.2 Bile Flow

BF gradually decreased in the sham group over the period of the experiment from 202±32 to 155.0±8.4 μL/min/100g liver wet weight (baseline vs 8hrs, P=0.045). BF in the I/R group was similar to sham at baseline (227±29 μL/min/100g liver wet weight) but reduced significantly to 60.5±19.0 (26.0±5.6%) during ischaemia (P=0.0001). BF in the I/R group then increased on reperfusion (116.5±33.1 at 2 hrs) but did not return to baseline values and was significantly lower than sham group values (P=0.0003 as per group comparison in ANOVA). Similarly, BF in the I/R+NAC infused group dropped significantly during ischaemia (P=0.001) and recovered to 123±0.4 (58.9±0.2%) at 7hrs reperfusion, which was less than sham (P=0.0158, group comparison in ANOVA) as shown in figure 21.

Figure 20: Alanine aminotransferase serum levels following warm liver I/R and I/R+NAC

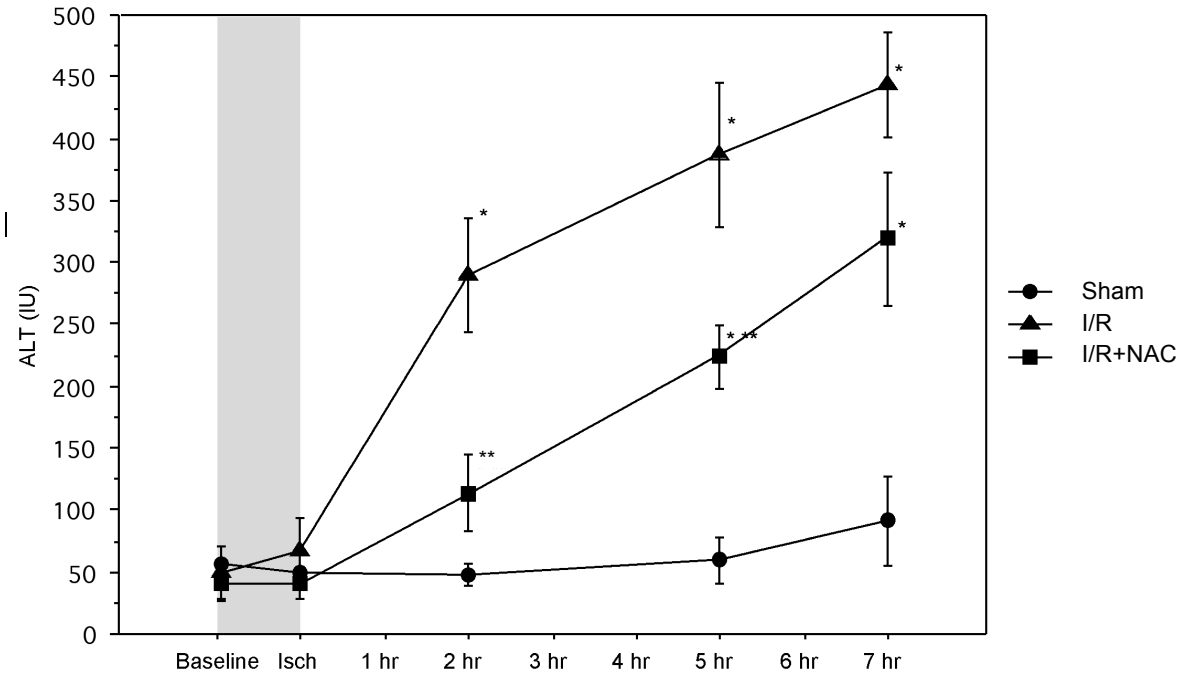

Shaded area ■ denotes 60 minutes of ischaemia in I/R and I/R+NAC, *=*P*<0.05 compared to shams, **=*P*<0.05 compared to controls

Figure 21: Bile flow following warm liver I/R and I/R+NAC

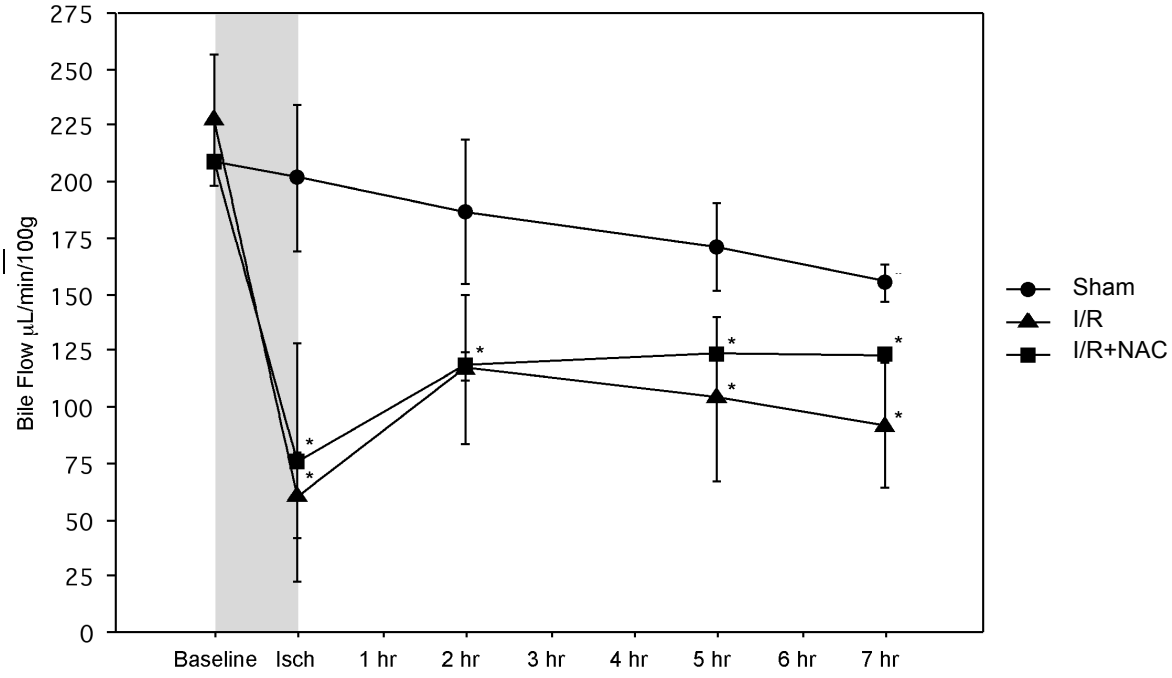

Shaded area ■ denotes 60 minutes of ischaemia in I/R and I/R+NAC, bile flow measured in μL/min/100g liver wet weight, *=*P*<0.05

5.4.3 ^{1}HNMR spectroscopy of bile

A baseline spectrum of bile has been shown in figure 13. Bile lactate levels decreased in I/R group during the ischemic period. Post-reperfusion levels were initially below baseline (88.7±22.4% of baseline values), but were significantly elevated at 5hrs (165.4±22.9% of baseline values, P=0.0061 vs. I/R) followed by a decline at 7hrs (89.1±29.1% of baseline values). In shams bile lactate decreased during the period of anaesthesia but these changes were not statistically significant. In the I/R+NAC group, biliary lactate decreased steadily after reperfusion to reach 63.2±25.1% of baseline values at 7hrs reperfusion (figure 22). Integration of peaks corresponding to PC head group (figure 23) revealed that I/R produced a significant 2 fold rise in controls during the ischemic phase (213±64% vs. 82.1±31.9% in shams, P=0.0023). Mean values for PC over all time points were higher in the control group than in the sham group (156.0±60.4% vs. 89±23.57%, P<0.0001). Addition of NAC significantly depressed the rise of PC during ischaemia (120.3±26.9% vs. 213±64% in controls, P=0.0372) and in total PC was higher than shams (P=0.0280), and lower than controls (P=0.0246).

Integration of the C-25 glycine methylene proton peak associated with conjugated bile acids showed a significant increase after 1hr ischaemia in I/R group (141.2±31.2% vs 64.1±19.9% in shams, P=0.0029), but declined to become similar with shams by 7hrs reperfusion (figure 24). Conjugated bile acids showed a significant increase in the I/R+NAC group after 1hr of ischaemia (117.1±23.1% vs. 64.1±19.9% in shams, P=0.0283) to drop to a similar value as shams at 7hrs reperfusion.

Figure 22: Lactate levels following warm liver I/R

(a)

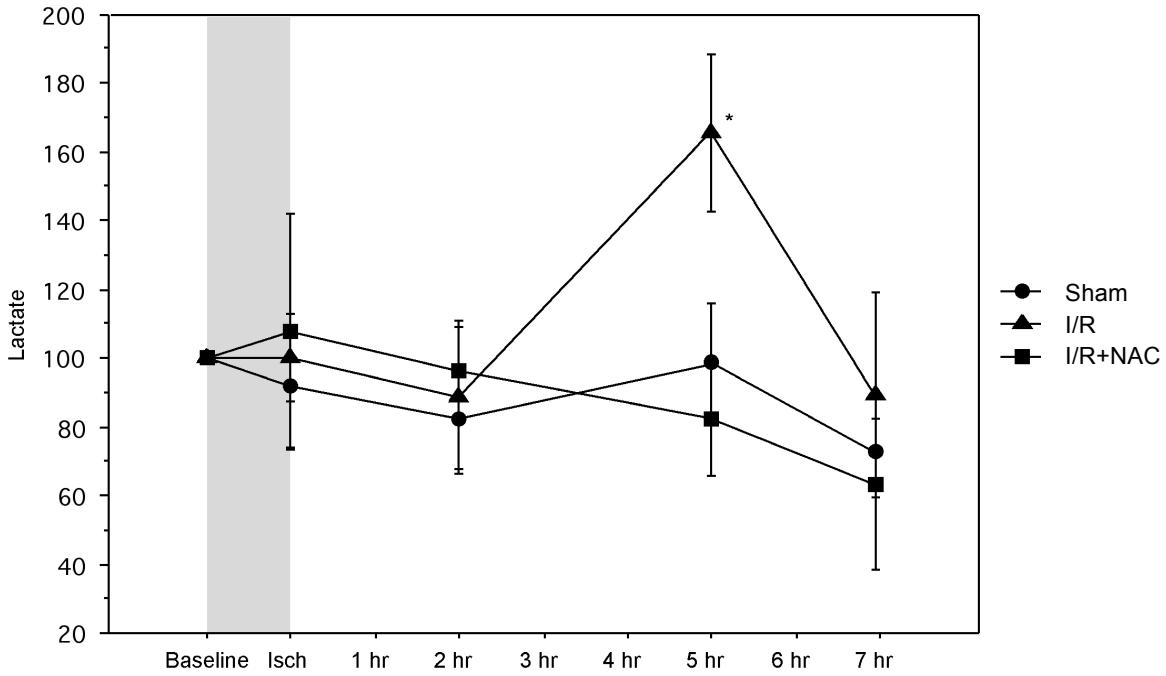

(a) Lactate levels were calculated by Integration of peaks at 1.33 ppm and expressed as a percentage of baseline values, shaded area ■ denotes 60 minutes of ischaemia in I/R and I/R+NAC, * P<0.05

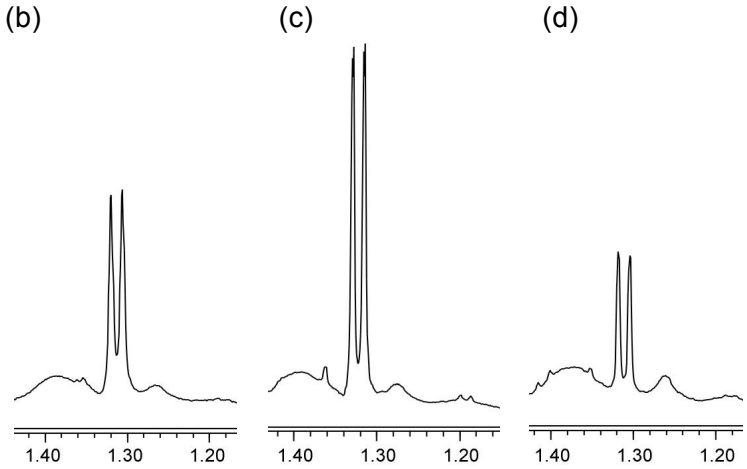

Bile lactate spectra (1.25-1.38 ppm) scaled to TSP from five hours of reperfusion in the (b) sham, (c) I/R group and (d) the I/R+NAC group (scale in ppm).

Figure 23: Phosphatidylcholine levels following warm liver I/R

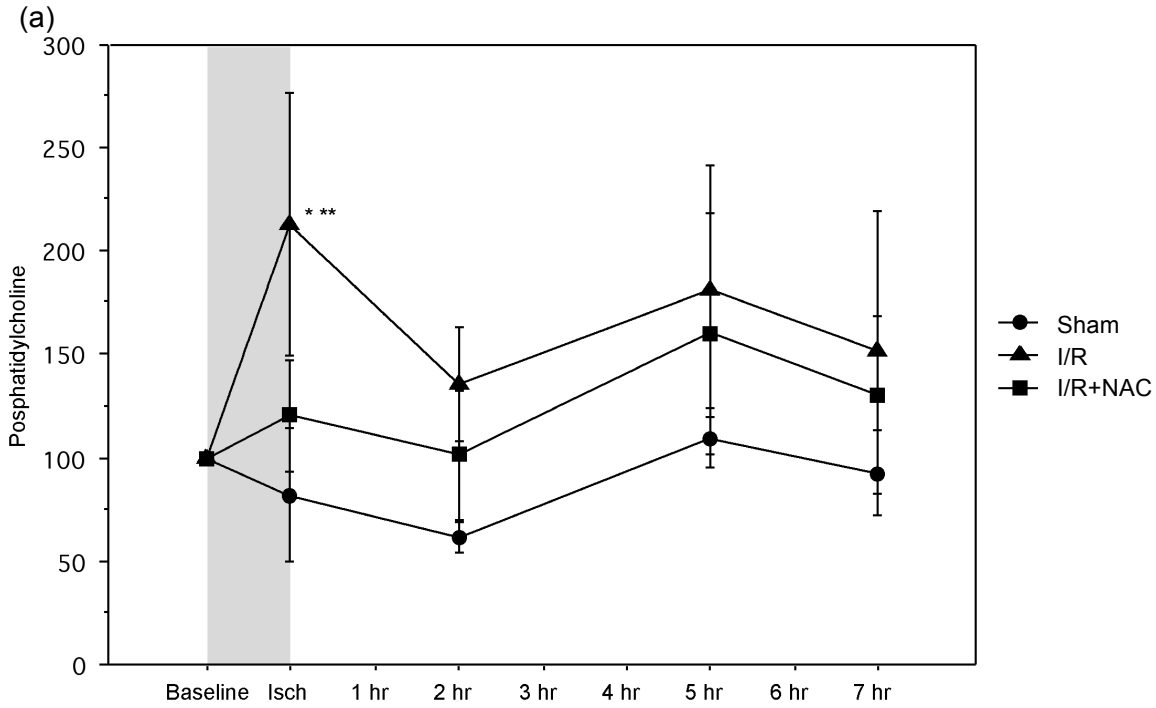

(a) PC levels were calculated by Integration of peaks at 3.2 ppm and expressed as a percentage of baseline values, shaded area ■ denotes 60 minutes of ischaemia in I/R and I/R+NAC, * P<0.05 compared to shams, ** P<0.05 compared to I/R+NAC

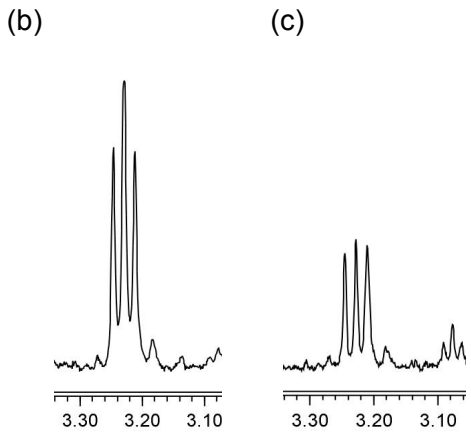

Bile PC spectra (3.20-3.27 ppm) scaled to TSP from ischaemia in the (b) I/R group and (c) I/R+NAC group (scale in ppm).

Figure 24: Conjugated bile acid levels following warm liver I/R

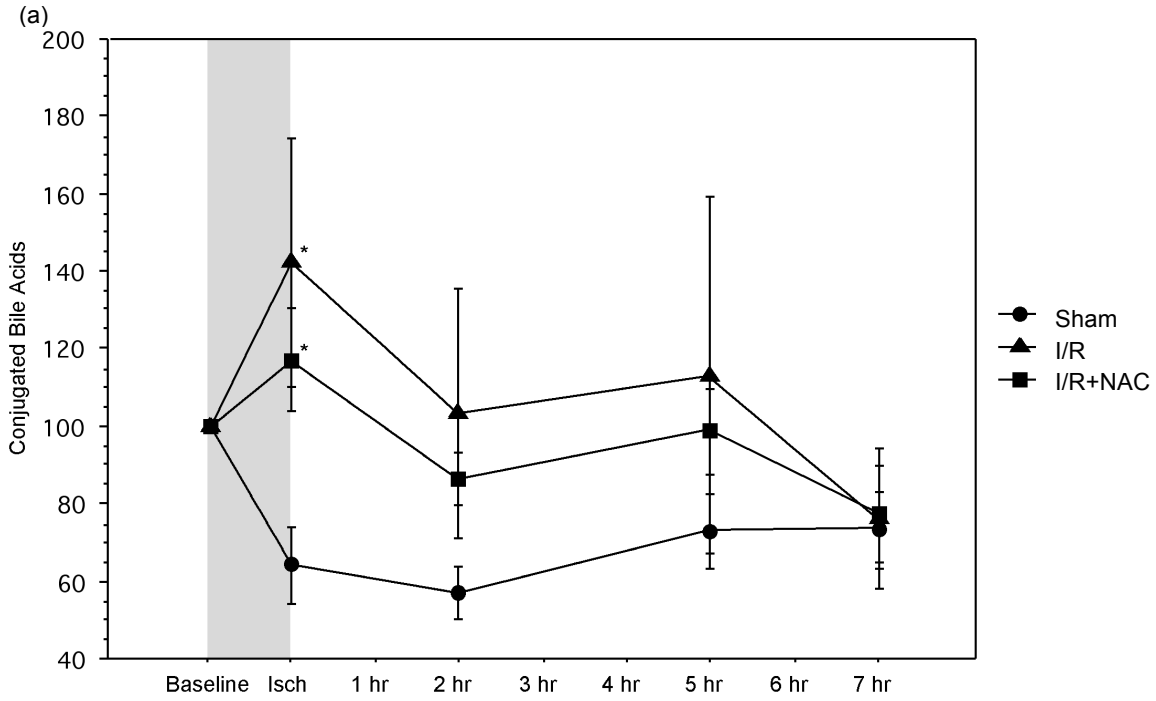

(a) Conjugated bile acid levels were calculated by Integration of peaks at 3.8 ppm and expressed as a percentage of baseline values, shaded area ■ denotes 60 minutes of ischaemia in I/R and I/R+NAC, * P<0.05

(b) (c)

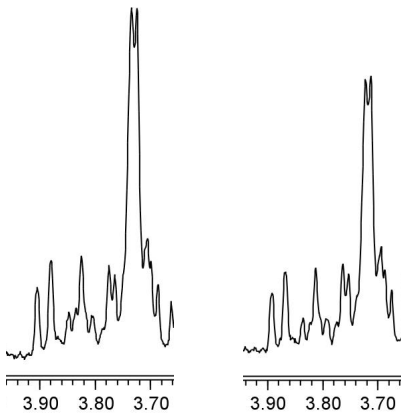

[1]HNMR bile spectra of C25 glycine peak associated with conjugated bile acids (3.76-3.92 ppm) scaled to TSP from ischaemia in the (b) I/R group and (c) I/R+NAC group (scale in ppm).

Acetate levels were reduced during the period of the experiment in both the I/R, I/R+NAC and sham groups (figure 25 & 26). However they were significantly lower in the I/R group by 7hrs reperfusion (37.5±56.0% vs. 69.4±13.3% in shams, P=0.0065).

Correlation of ^{1}HNMR bile spectroscopy data with other parameters revealed that acetate decreased with increases in ALT (R=0.769, P<0.0001) (figure 27), AST (R=0.550, P=0.0003) and portal flow (R=0.412, P=0.0139) and increased with increases in BF (R=0.432, P=0.0054) and ΔCOX (R=0.512, P=0.0006) as shown in figure 28. PC increased with increases in ALT (R=0.401, P=0.0113) and decreased with increases in BF (R=0.616, P<0.0001), ΔLDF (R=0.567, P<0.0001) and ΔCOX (R=0.570, P<0.0001). Bile acids decreased with increased ALT (R=0.435, P=0.0057) portal flow (R=0.482, P=0.0033) and ΔHbO_2 (R=0.369, P=0.0175). Lactate tended to increase with increases in AST (R=0.294, P=0.0657) and decrease with increases in ΔCOX (R=0.290, P=0.0657), however these results did not reach statistical significance.

Figure 25: Acetate levels following warm liver I/R

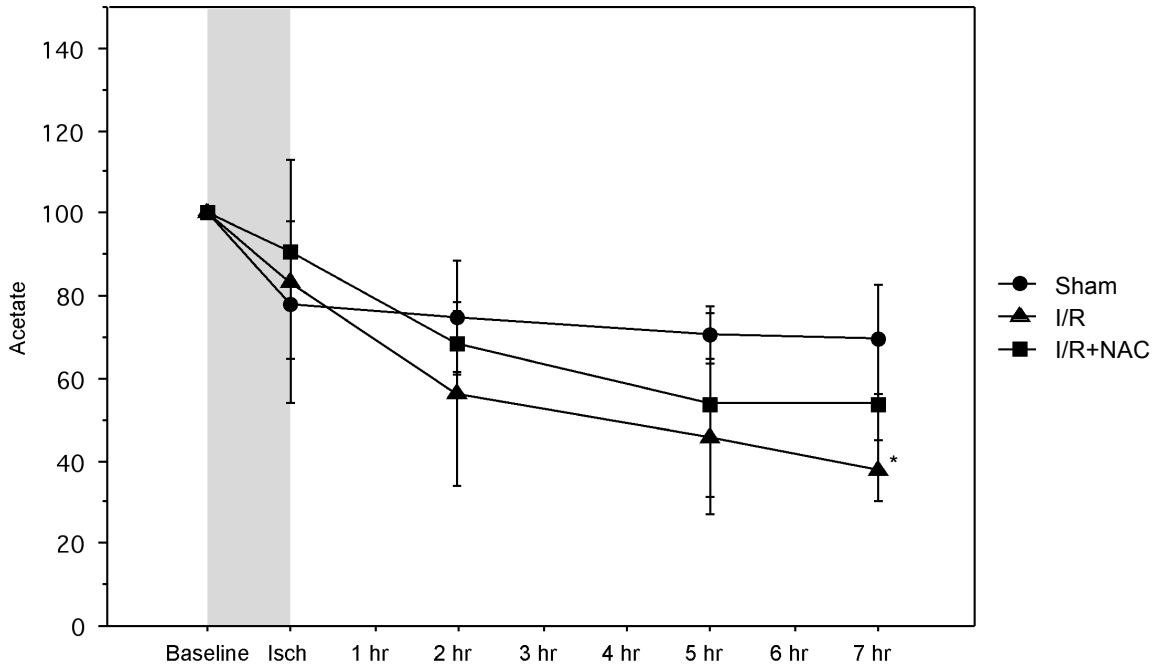

Acetate levels were calculated by Integration of acetate peaks at 1.91 ppm and expressed as a percentage of baseline values, shaded area ■ denotes 60 minutes of ischaemia in I/R and I/R+NAC, * P<0.05

Figure 26: ^{1}HNMR spectra of acetate levels following warm I/R

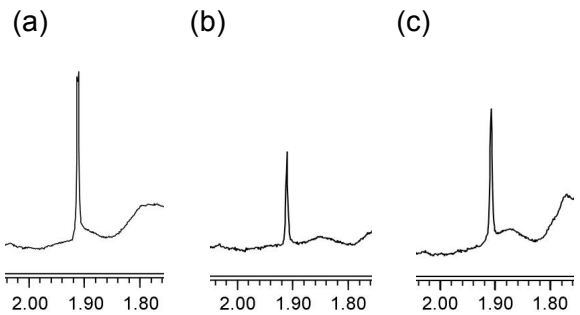

^{1}HNMR bile spectra of acetate peaks (2.0-1.84 ppm) scaled to TSP at (a) baseline in the I/R group and after 7 hours of reperfusion in (b) the I/R and (c) I/R+NAC groups showing significant reduction (scale in ppm).

Figure 27: Correlation of bile acetate and serum ALT

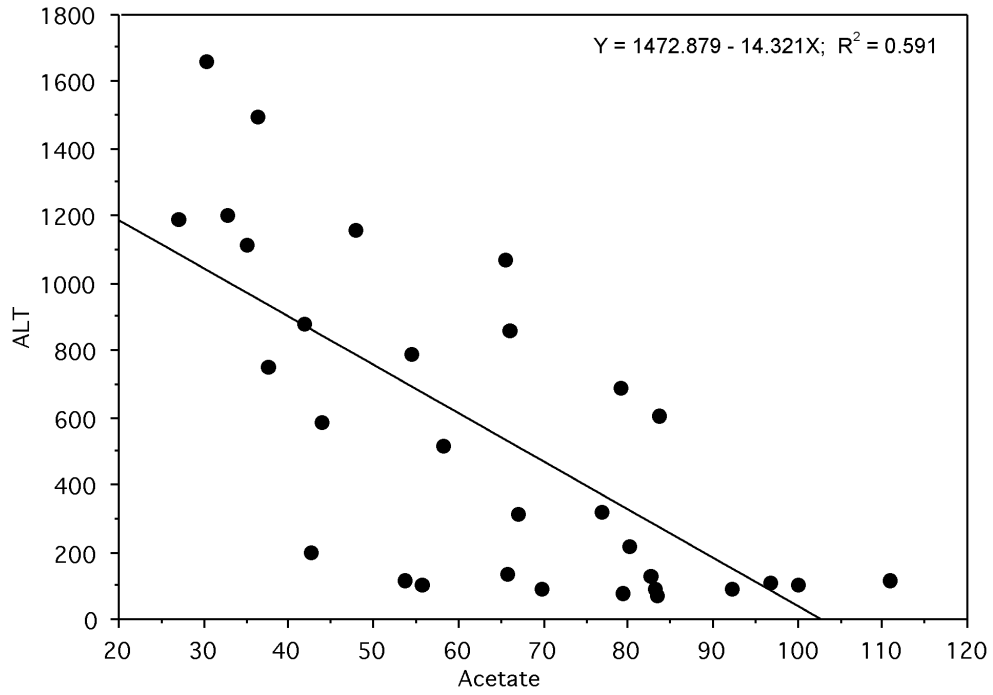

Acetate levels were calculated by Integration of acetate peaks at 1.91 ppm and expressed as a percentage of baseline values while ALT is expressed as a percentage of baseline values

Figure 28: Correlation of bile acetate and liver tissue cytochrome oxidase

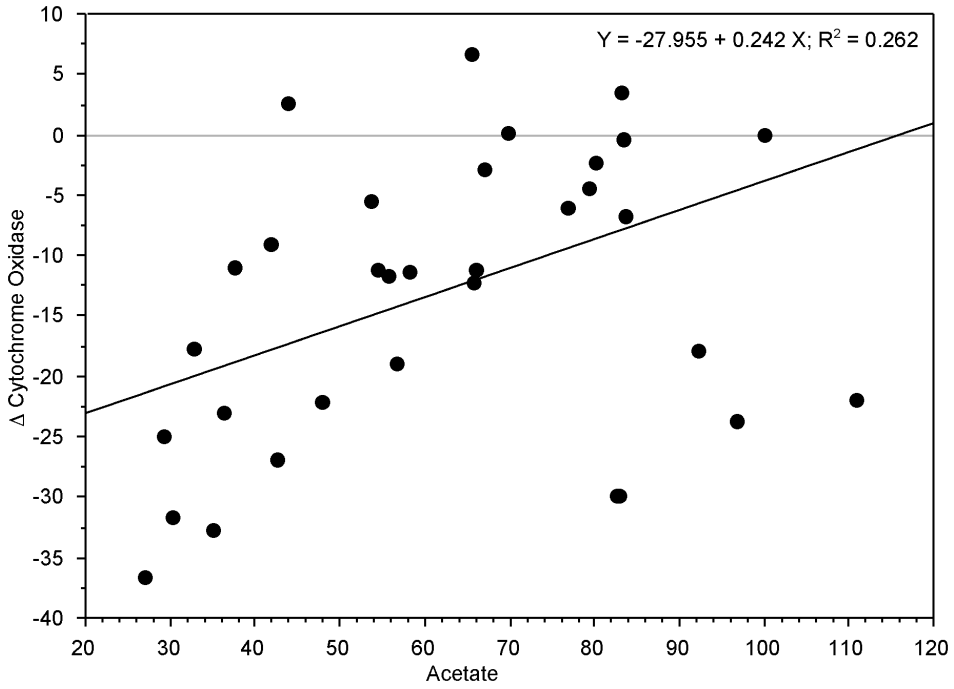

Acetate levels were calculated by Integration of acetate peaks at 1.91 ppm and expressed as a percentage of baseline values while cytochrome oxidase is expressed as change in μmolar units

5.5 Discussion

Liver warm IRI can be divided into two phases, an early phase (<2hrs) which is associated with KC activation and a subsequent cytokine surge[513] and a late phase (>4hrs), which is mainly due to the accumulation of PMN and is associated with more extensive injury[514].

In this experiment, a rabbit lobar I/R model was used with reperfusion period of seven hours[396]. The benefits of employing this model have been discussed above (section 3.1), briefly it permitted the analysis of bile constituents in both the early phase and the beginning of the late phase of IRI, avoiding the production of acute portal hypertension and intestinal ischaemia, maintained hemodynamic stability throughout the duration of the experiment, and avoiding the complete occlusion of biliary drainage in the total hepatic ischaemia model permitting the effects of I/R on biliary composition to be evaluated.

BF in the sham operated I/R group decreased, ALT activity increased and hepatic intracellular oxygenation significantly decreased during the period of anaesthesia compared to baseline. These findings suggest that the operative trauma and the anaesthetic agent could have an effect on liver function during lengthy surgical procedures (>8hrs)[512]. The prolonged anaesthesia did not affect the flow in the hepatic microcirculation. The changes in flow in the hepatic microcirculation and intracellular tissue oxygenation during the early phase of reperfusion were similar with the results of previous studies[512,516,531].

BF fell sharply in response to ischaemia, and recovered after reperfusion, and although it did not regain pre-ischemic baseline values, it was fairly consistent at 31.1–50.1%. Despite this consistent pattern of BF in I/R and I/R+NAC groups, ^{1}HNMR spectroscopy of bile revealed fluctuations in the concentration of some bile constituents.

Lactate in particular shows a large peak at 5hr postreperfusion, this corresponds to a large burst of PMN activity that constitutes the beginning of the late phase of IRI[532]. It has been observed that the injury produced during the beginning of the late phase is a more severe hepatocellular injury in comparison to the early phase[517-519]. PMN sequestration, sinusoidal narrowing and vasoconstriction combine to form a "no-reflow paradox" whereby hepatocytes are subjected to a further perfusion deficit and persistent ischaemia[404,520]. This may explain the observed peak in lactate at this late time point[521,522] especially since lactate levels have been shown to become elevated in bile even when they are not elevated in serum[523]. ATP degradation after ischaemia leads to the activation of glycolysis, resulting in the net formation of lactate[524]. Serum lactate concentration has been shown to increase progressively in ischemic livers, achieving a maximum level at 30min and remaining stable for 90mins. It has also been shown that glycogen concentration decreased as a function of the length of the ischemic period. This suggests that serum lactate may be a product of the glycolytic/gluconeogenic pathway, this was verified by measuring glucose-6-phosphate and fructose-6-phosphate which were shown to increase with ischaemia-reperfusion injury[18]. Interestingly, NAC administration abolished this peak in lactate, as it lowered the levels of ALT.

PC exhibited a biphasic pattern where ischaemia precipitated a 2 fold rise in the I/R group which subsided on reperfusion to be followed by a smaller peak at 5hrs. The main source of PC in cells is in the plasma membrane, this suggests that the increase during ischaemia and again at 5hr post-reperfusion may be associated with an increase in cellular breakdown and membrane lipid peroxidation[533]. This would coincide with a period of hepatocellular injury during ischaemia and the "no-reflow period"[534]. Increased PC has also been observed by other authors in association with poor graft function but not hepatocellular injury[535].

Interestingly, a similar biphasic pattern was apparent in bile acids, which might

suggest that more bile acids are released during periods of hepatocellular damage. This is in concordance with observations by other authors who found total serum bile acids found to be early markers of liver function in porcine[526] and canine[536] liver transplants. Moreover the depression of bile acid synthesis is in accordance with both early and late reperfusion injury when hepatocyte injury is in process. The significant rise in conjugated bile acid during the ischaemia may be a result of the drop in BF. Bile acids fall with increased BF on reperfusion. Furthermore, the depressed rate of BF on reperfusion may contribute to the higher levels of bile acids seen post-reperfusion in the I/R and I/R+NAC groups but not in the sham group. The I/R group is interestingly associated with the lowest BF and the highest bile acid levels while shams have the highest BF and the lowest bile acid levels with the I/R+NAC group residing in between.

Acetate was observed to drop continuously from baseline throughout the experiment, however, it correlated strongly to COX activity. Hepatocytes are one of the few cells that can utilize fatty acids in the production of energy through the β-oxidation helix[537]. However, this reaction requires ATP at its initiation. Post-reperfusion ATP is consumed to clear excess lactate and pyruvate and may not be readily available for fatty acid oxidation. The I/R-induced reduction in ATP may result in decreased β-oxidation causing acetate production to falter; this might also explain its strong association with the change in COX.

In conclusion, bile spectroscopy has demonstrated significant changes in bile composition during I/R and NAC administrations. These changes are evident despite a constant, albeit reduced, post-reperfusion rate of BF. Having identified significant changes in lactate, PC and acetate with I/R and NAC, further studies are required to evaluate the changes with other modifiers of IRI and continue to look for other MRS markers of IRI, to further strengthen the validity of these findings.

6 Modulation of warm hepatic ischaemia reperfusion using glycine and its effect on bile composition

6.1 Introduction

Liver ischaemia-reperfusion (I/R) injury is a common sequel following liver resection[538] and liver transplantation[185]. One of the principle initiating steps of the I/R inflammatory cascade is KC activation[194,539]. KC blockade has been shown to protect against warm IRI[540,541]. Glycine, a nonessential amino acid and an inhibitory neurotransmitter, has recently been shown to be protective against hypoxia and ischaemia[542]. It has been shown to modulate KC activity in animal models[195]. Several mechanisms have been suggested to explain glycine-induced KC inhibition. Increasing chloride conductance which hyperpolarizes the cell membrane, thereby decreasing the rise in intracellular calcium by making voltage dependant calcium channels more difficult to open, is one theory[543]. The inhibition of proteolysis, a pH dependant hydrolytic activity, which is activated following the recovery of intracellular pH post-reperfusion, is another theory[544]. Glycine has also been shown to have a membrane stabilizing action, by suppressing the rearrangement of plasma membrane proteins which form water filled pores large enough to leak macromolecules[25], and it has even been suggested that glycine may inhibit an organic anion channel conducting low molecular weight species which opens prior to cell death[25,34].

Bile formation is an active secretory process mechanisms[44,530] that is used as an indicator of liver function and recovery following ischaemia in experimental studies[25,34] and clinical liver transplantation[35]. IRI has been shown to manifest by poor BF *in vivo*[530] and *in vitro*[30] and reduced bile acid secretion, however gradual recovery occurs in reversibly damaged organs while persistent low bile output is considered a sign of primary graft non function[32]. Little is known, however, about changes in bile composition during liver ischaemia and following reperfusion and less is known about the effect of therapeutic strategies to ameliorate IRI on bile composition.

Bile salts are a major component of bile and have a significant influence on BF and the secretion of biliary lipids such as PC and cholesterol[545]. Bile salts are transported

across the canalicular membrane in a primary active ATP-dependent fashion[24,25] which is mediated by the BSEP[26]. BSEP is a genuine ATP-binding cassette other transporters expressed in many tissues and involved in active outward transport of molecules across the plasma membrane[23].

In recent years, high resolution ^{1}HNMR spectroscopy has been established as a powerful technique to explore the biochemical composition of biological fluids such as plasma, bile, seminal and synovial fluids, in various pathological conditions[8]. This technique is rapid, non-invasive and non-destructive and can detect metabolites present at the millimolar concentrations and can be applied to detect unexpected compounds in biological fluids[9]. NMR has also been used to assess hepatic glutamine metabolism[16], hepatic energetic status after warm ischaemia[17], and to study effects of I/R on liver cell membranes[18]. A preliminary study of ^{1}HNMR analysis of bile after liver transplantation suggested that this technique might help to distinguish ischaemia from rejection post-transplant by detecting large resonance peaks for lactate and acetate[18]. More recently there has been growing interest in attempting to predict graft function by analysing bile production immediately after transplantation[396].

6.2 Objectives

1. To determine if the changes in bile composition during I/R can be reversed using glycine, an agent known to ameliorate IRI in liver
2. To identify the differences in chemical composition between sham, I/R and glycine+I/R, particularly further differences not explored in the previous experiments, e.g. β-glucose and acetoacetate
3. To ascertain if these changes fit with established understanding of the mechanisms involved in liver IRI and the actions of glycine
4. To utilise ^{1}HNMR to quantify the qualitative changes in bile composition previously observed in micromolar concentrations after running a calibration exercise (appendix section 10.1)

6.3 Materials and Methods

This study was conducted under a license granted by the home office in accordance with the Animals (Scientific Procedures) Act 1986. New Zealand white rabbits (3.2±0.4 Kg, n=18) were used. Anaesthesia was induced by an intramuscular injection of 0.5ml/kg of fentanyl citrate and fluanisone (Hypnorm; Janssen Animal Health, Buckinghamshire, UK). Following tracheostomy, anaesthesia was maintained with isoflurane (1.5-3%) through an anaesthetic circuit. Body temperature was maintained at 37-38^{o}C by a warming blanket (Homeothermic blanket control unit; Harvard Apparatus, Southmatick, Massachussets, USA). Arterial haemoglobin oxygen saturation and heart rate were continuously monitored and recorded by a pulse oximeter (Ohmeda Biox 3740 pulse oximeter; Ohmeda Louisville, Colorado, USA). Ear marginal vein and artery were cannulated for administration of fluids, anaesthetics, and blood sampling.

After induction of anaesthesia a midline laparotomy was performed. The ligamentous attachments of the liver were divided and the liver was exposed. The bile duct was cannulated with a polyethylene catheter (PE-50, 0.58mm inner diameter, Portex, Kent , UK) for continuous measurement of BF.

6.3.1 Experimental Groups

Three groups of animals were used (n=6) in each group. Sham group of animals underwent anaesthesia and laparotomy but no ischaemia or reperfusion was induced. The I/R group had 1 hour of ischaemia and 6 hours of reperfusion. The I/R+glycine group received 300mosm of glycine given intravenously at a dose of 5ml/kg body weight prior to induction of ischaemia by slow intravenous infusion over 15min, then treated as I/R group.

6.3.2 Ischaemia-Reperfusion Injury protocol

Lobar ischaemia was induced in the I/R and I/R+glycine group by clamping the left

portal vein, hepatic arteries and biliary radicals using an atraumatic vascular clip. This produces severe ischaemia to the left and median lobes of the liver without significant portal venous congestion. At the end of one hour of ischaemia the vascular clip was removed and reperfusion allowed for 6hrs in the I/R and I/R+glycine groups. At the end of the experiment the animal was killed by exsanguination.

6.3.3 Bile flow and Proton nuclear magnetic resonance ^{1}HNMR spectroscopy

Bile samples were taken at baseline and each hour thereafter and stored at -80°C. Bile volume was expressed as µL/min/100g of liver weight. ^{1}HNMR analysis was performed on an 11.7T (500 MHz for protons) spectrometer (Varian Unity +; Varian, Palo Alto, CA, USA) at 25^{o}C. Bile was thawed at room temperature and placed in 5mm NMR tube. For a field/frequency lock a coaxial capillary insert was used (Wilmad, Buena, NJ, USA). This capillary insert was filled with a deuterium oxide solution of sodium TSP that acted both as a chemical shift reference and quantification standard. This capillary was calibrated by using a series of known concentration solutions of deoxycholate and a calibration curve was obtained (appendix section 10.1). This was then used for quantification of bile components, which enabled an accurate comparison bile levels between the groups. One dimensional NMR spectra were obtained at 500MHz with a sweep width of 6kHz and 32k data points in 64 scans were collected in both normal and spin echo mode. Presaturation of bile was carried out to attenuate the intensity of water signal. The spectra were analysed using software from MestRe-C version 3.1.1 (Universidade de Santiage de Compostela, Spain). All spectra were integrated using a fixed range for each peak and published peak assignments[10,18,370,472] shown in table 2.

6.3.4 Statistical analysis

Results are presented as mean±SD. Statistical analysis was performed using a one-way ANOVA with multiple comparisons adjusted for by the Bonferroni test. Statistics were calculated using commercially available software (SPSS release 11.0.0; SPSS

Inc., Chicago, IL, USA). *P*<0.05 was considered statistically significant.

6.4 Results

6.4.1 Bile flow

There was not significant difference in BF in the sham group throughout the whole experiment (154.02±7.73 μL/min/100 gm wet liver wt) as shown in figure 29. However, in the I/R group, there was 79.71±7.10% drop in BF during the ischemic phase, which was significant (P<0.001) which recovered by the second hour of reperfusion and was maintained at 108.44±25.9 μL/min/100 gm wet liver wt till the end of the experiment. In the I/R+glycine group, there was a similar significant fall during ischaemia but BF was significantly greater than I/R alone during the reperfusion period (figure 29) and the second hour of reperfusion was similar to shams.

6.4.2 ^{1}HNMR spectroscopy of bile

The results of the integration of the area under curve for the peaks assigned to conjugated bile acids in the sham group bile were relatively unchanged throughout the experiment at 4.91±0.95 μmol/L (figure 30). I/R group bile acid levels tended to be higher than shams throughout the experiment (P=0.002 when total group means were compared), however, they did not reach statistical significance when compared at individual time points. I/R+glycine group bile acid levels rose significantly following ischaemia to peak during the 1st hr of reperfusion, where they were significantly higher than both sham (P<0.001) and I/R group (P=0.001).

Figure 29: Bile flow following warm liver I/R and I/R+glycine

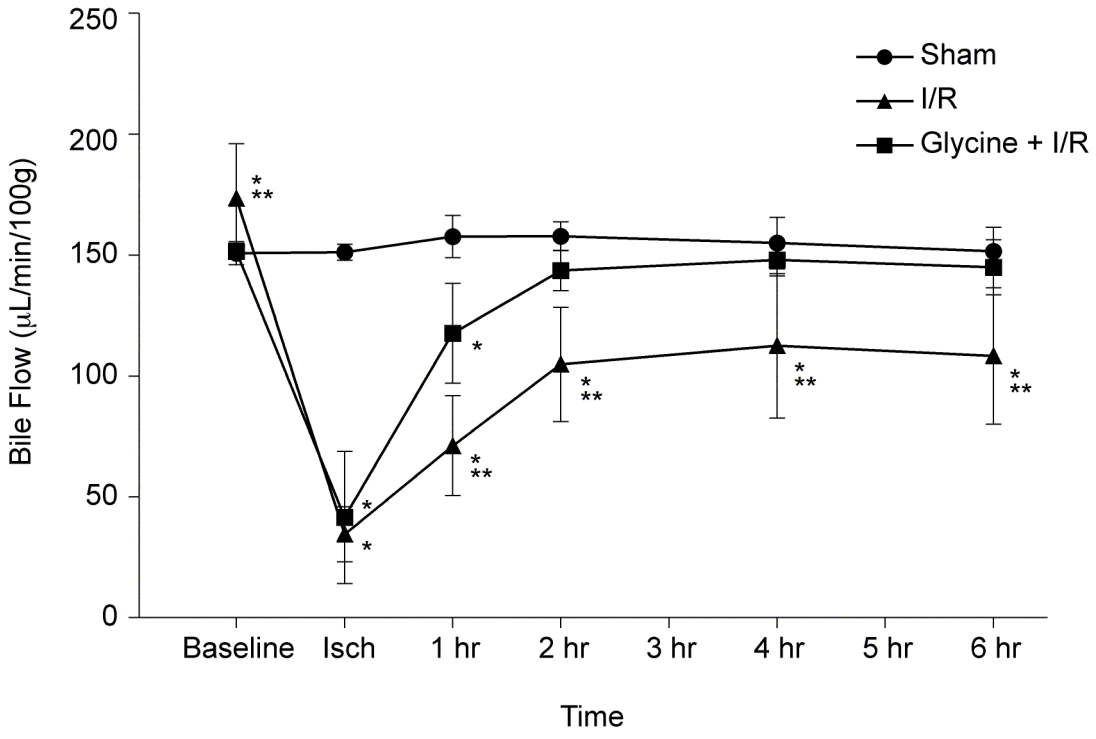

Bile flow measured in μL/min/100g liver wet weight, * P<0.05 compared to sham group, while ** P<0.05 between I/R+glycine and I/R group.

Figure 30: Bile Acid levels following warm liver I/R and I/R+glycine

(a)

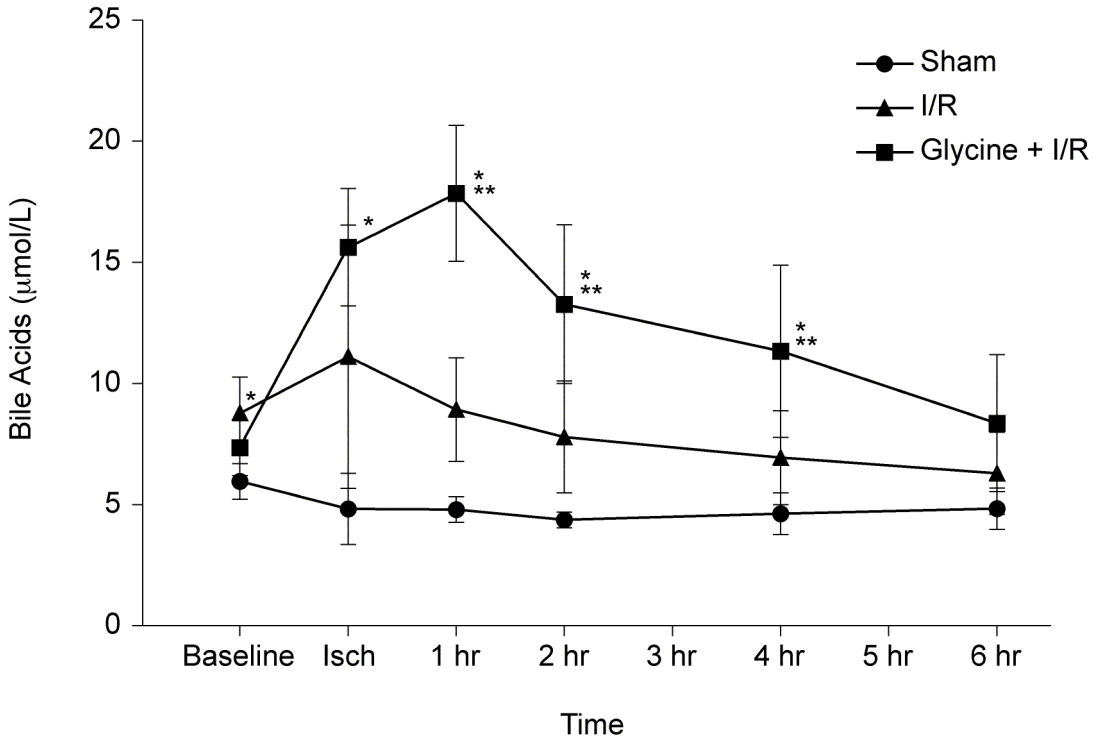

(a) Bile acid levels were calculated by integration of peaks at 0.61-0.73 ppm and expressed as μmol/L, *=*P*<0.05 compared to sham group, while **=*P*<0.05 between I/R+glycine and I/R group.

(b) (c)

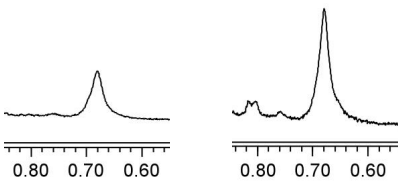

Bile acid spectra (0.61-0.73 ppm) scaled to TSP from one hour of reperfusion in the (b) I/R group and (c) the I/R+glycine group (scale in ppm).

They remained significantly elevated, compared to both sham and I/R groups, during the 2nd and 4th hr of reperfusion (P<0.05).

Integration of peaks corresponding to PC in the I/R group rose gradually till the 2nd and 4th hr of reperfusion where they were significantly higher than I/R+glycine and sham groups (P<0.05). There was no significant difference between I/R+glycine and sham groups throughout the experiment (figure 31). Bile lactate levels in the I/R group rose following reperfusion, to peak significantly at 4 hrs (P<0.001 vs. sham and I/R+glycine). There was no statistical difference in bile lactate levels between I/R+glycine and sham groups during the procedure (figure 32).

There was a wide range of bile acetate levels in each group (figure 33). Levels fell dramatically at 1 hr of reperfusion. Levels then rose during reperfusion and were not statistically different. The I/R group had lower acetate levels than shams (P<0.01)

I/R did not affect pyruvate levels (sham vs I/R, NS) as shown in figure 34. In the I/R+glycine group, however, pyruvate levels were significantly elevated during the 2nd and 4th hr of reperfusion compared to both shams and I/R alone (P<0.05). I/R did not influence bile β-glucose levels (sham vs I/R, NS) as shown in figure 35. However, there was a significant rise in β-glucose levels in the I/R+glycine group from the 1st hr of reperfusion till the 4th hr of reperfusion (P<0.05).

Acetoacetate levels were not statistically different for sham and I/R groups during the experiment (figure 36). The glycine+I/R group, however, showed significantly elevated acetoacetate levels during the ischemic phase, 1st, 4th and 6th hr of reperfusion when compared to both shams and I/R (P<0.05).

Figure 31: Phosphatidylcholine levels following warm liver I/R and I/R+glycine

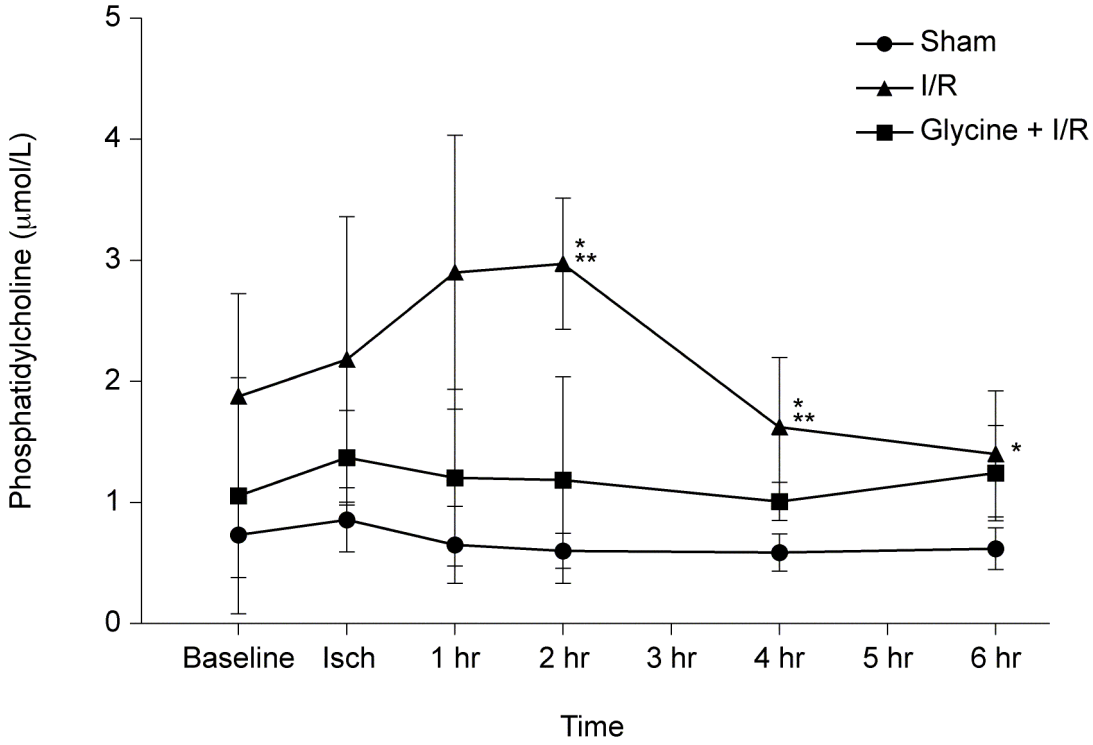

Phosphatidylcholine levels were calculated by integration of peaks at 3.2 ppm and expressed as μmol/L, *=*P*<0.05 compared to sham group, while **=*P*<0.05 between I/R+glycine and I/R group.

Figure 32: Lactate levels following warm liver I/R and I/R+glycine

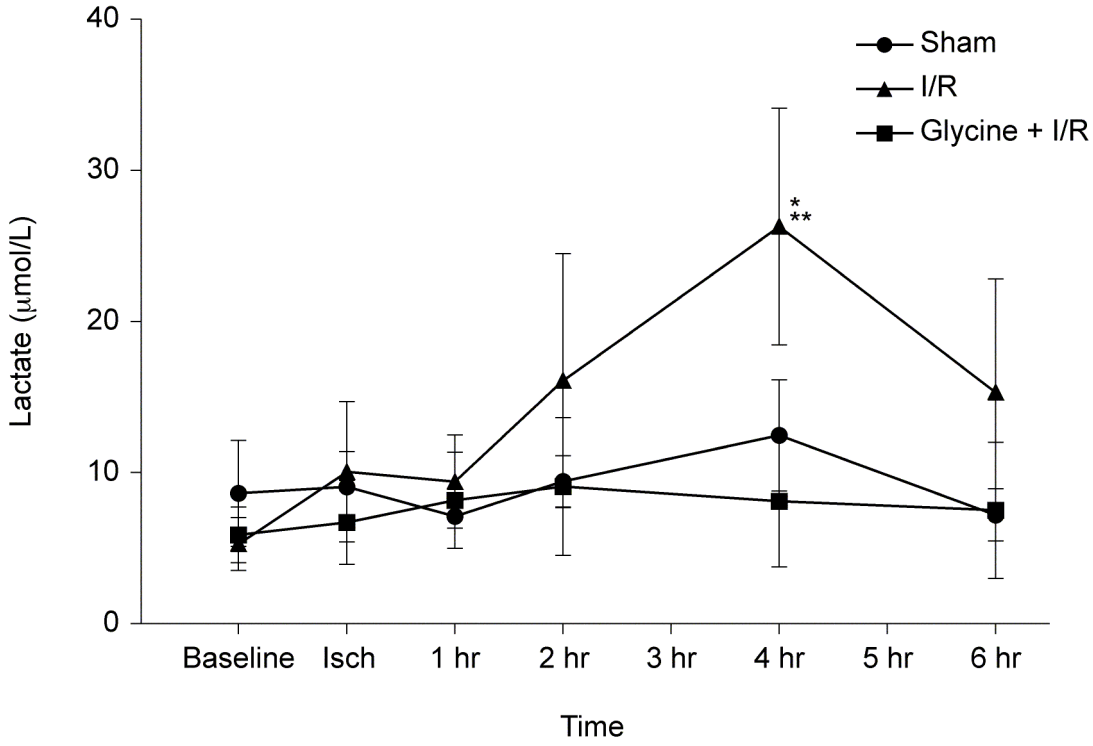

Lactate levels were calculated by integration of peaks at 1.33 ppm and expressed as μmol/L, *=P<0.05 compared to sham group, while **=P<0.05 between I/R+glycine and I/R group.

Figure 33: Acetate levels following warm liver I/R and I/R+glycine

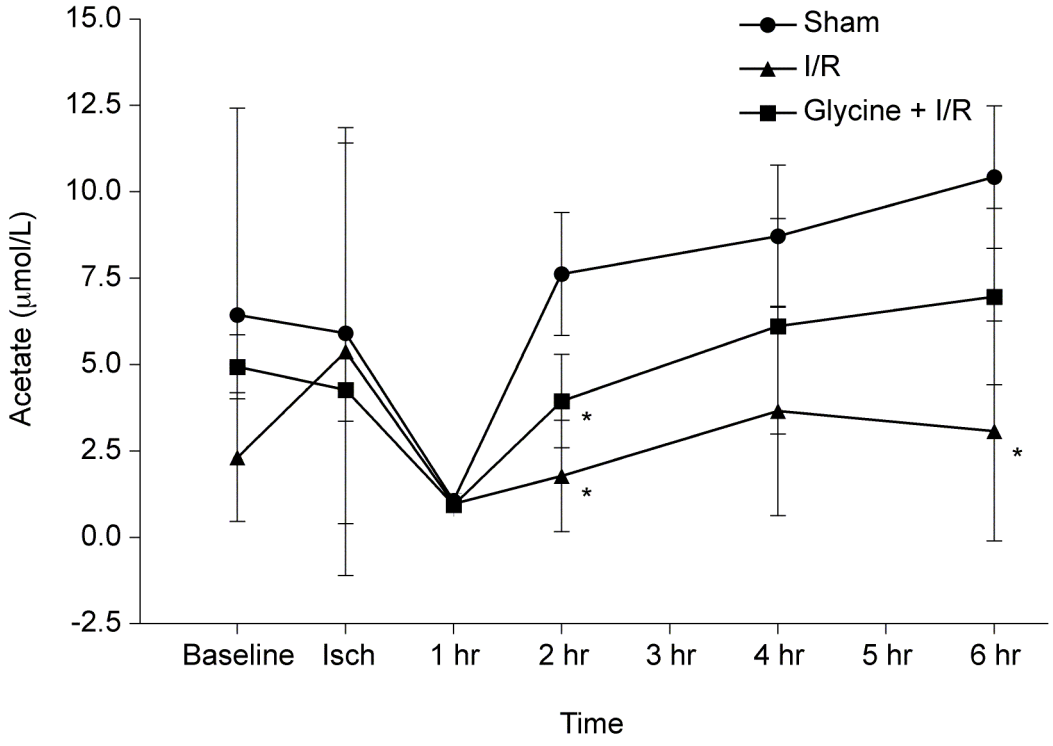

Acetate levels were calculated by integration of peaks at 1.9 ppm and expressed as μmol/L, *=*P*<0.05 compared to sham group.

Figure 34: Pyruvate levels following warm liver I/R and I/R+glycine

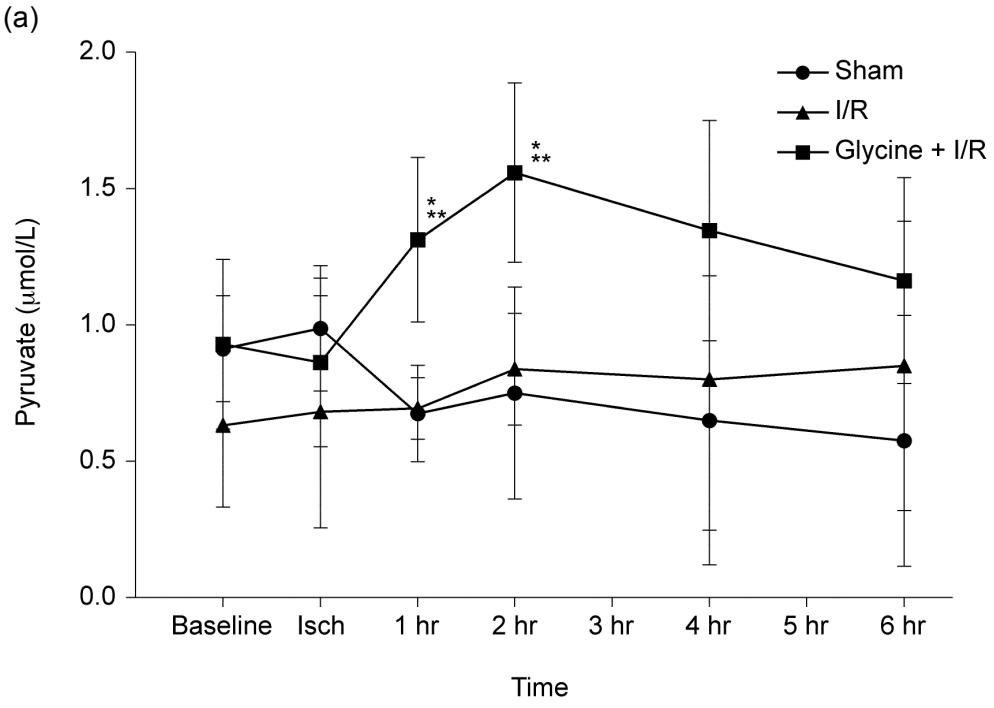

(a) Pyruvate levels were calculated by integration of peaks at 2.3 ppm and expressed as μmol/L, *=*P*<0.05 compared to sham group, while **=*P*<0.05 between I/R+glycine and I/R group.

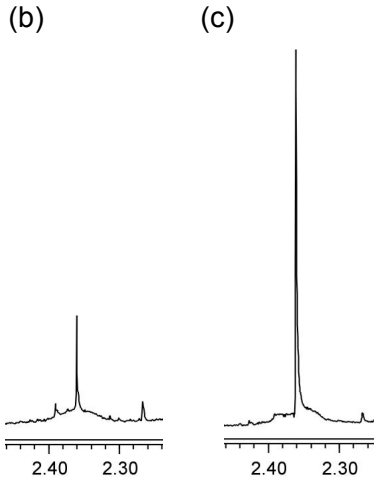

Bile pyruvate spectra (2.34-2.38 ppm) scaled to TSP from two hours of reperfusion in the (b) I/R group and (c) the I/R+glycine group (scale in ppm).

Figure 35: Glucose levels following warm liver I/R and I/R+glycine

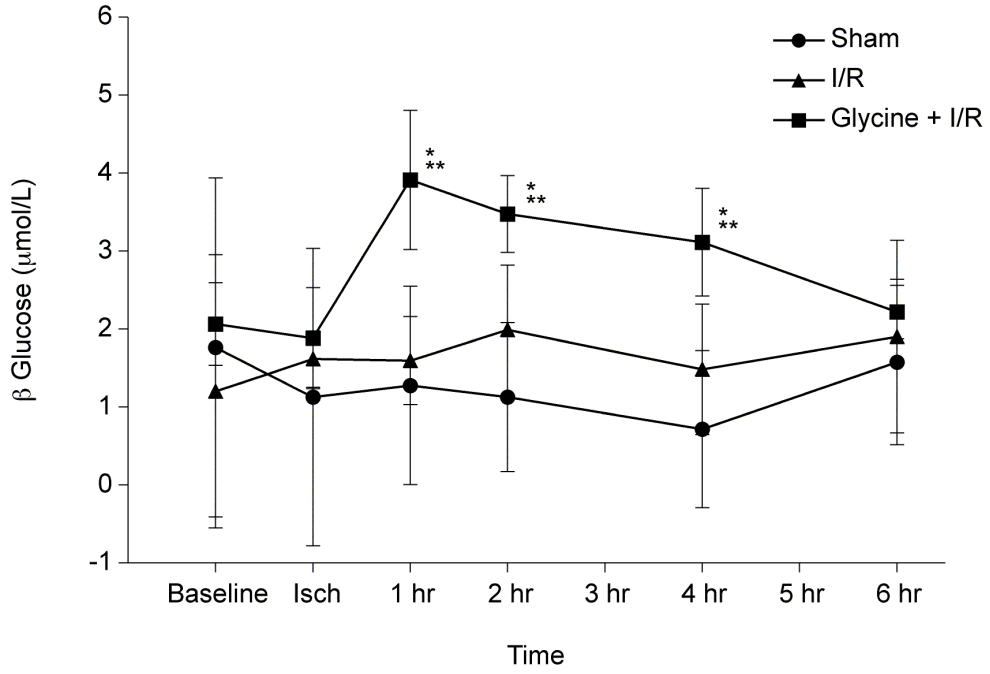

Glucose levels were calculated by integration of peaks at 5.2 ppm and expressed as μmol/L, *=*P*<0.05 compared to sham group, while **=*P*<0.05 between I/R+glycine and I/R group.

Figure 36: Acetoacetate levels following warm liver I/R and I/R+glycine

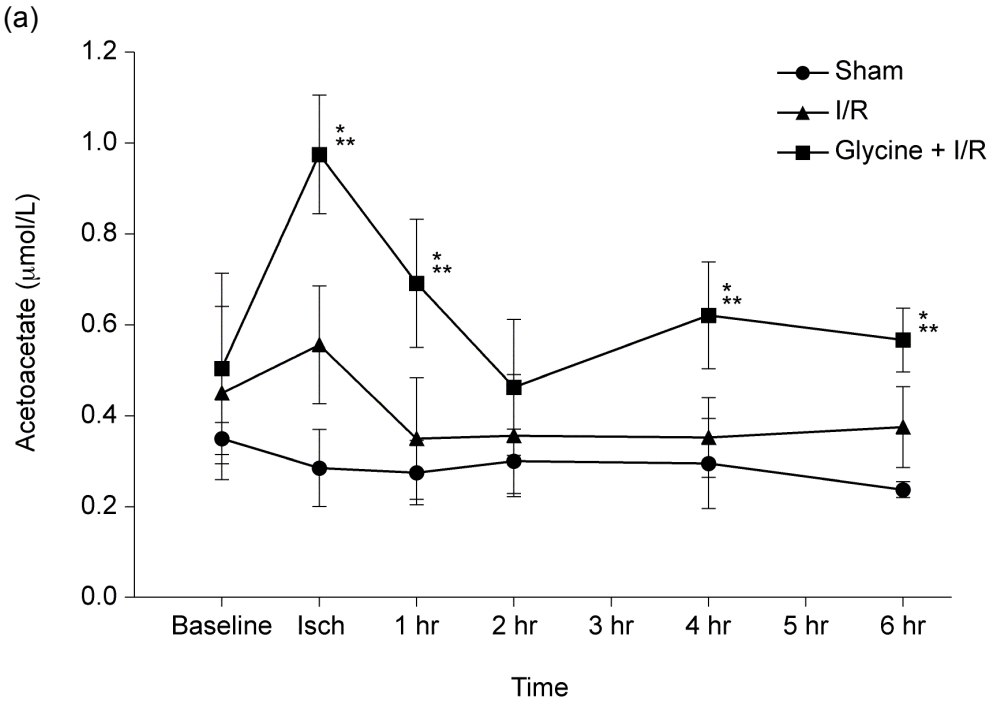

(a) Acetoacetate levels were calculated by integration of peaks at 2.2 ppm and expressed as μmol/L, *=*P*<0.05 compared to sham group, while **=*P*<0.05 between I/R+glycine and I/R group.

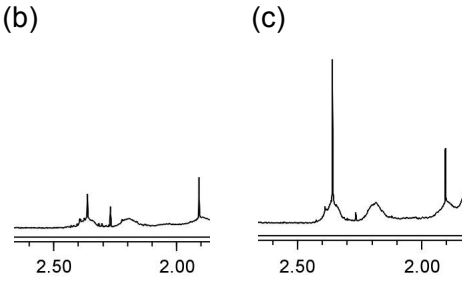

Bile acetoacetate spectra (2.29-2.25 ppm) scaled to TSP from the ischaemia phase in the (b) I/R group and (c) the I/R+glycine group (scale in ppm).

6.5 Discussion

The use of spin echo spectra, in this experiment, allowed us to reduce the interference from broad lipid signals and improved the quantification of biliary constituents. Calibration using known concentrations of deoxycholate, enabled us display the results in micromolar concentrations instead of as a percentage of baseline concentrations.

In this experiment, a rabbit lobar I/R model was used with reperfusion period of six hours[396]. The benefits of employing this model have been discussed above (section 3.1), briefly it permitted the analysis of bile constituents in both the early phase and the beginning of the late phase of IRI, avoiding the production of acute portal hypertension and intestinal ischaemia, maintained hemodynamic stability throughout the duration of the experiment, and avoiding the complete occlusion of biliary drainage in the total hepatic ischaemia model permitting the effects of I/R on biliary composition to be evaluated.

BF was maintained throughout the procedure in the sham group, while it fell following I/R and in the I/R+glycine group. This response to acute liver ischaemia has been noted in previous studies[535]. In the I/R+glycine group, BF on reperfusion recovered to become similar to sham within 2hrs of reperfusion, while in the I/R group remained depressed until the end of the experiment. Moreover, a rise in bile acid secretion was also noted on reperfusion, in the I/R+glycine group, compared to the I/R group. This suggests an early recovery of metabolic activity in the glycine-treated livers, which is supported by observations that total serum bile acids were found to be early markers of liver function in porcine[521,522] and canine[523] liver transplants. The rise in bile acid observed during ischaemia may be a result of the drop in BF.

In this experiment, lactate levels were elevated with I/R and were higher than the sham and I/R+glycine groups. ATP degradation during ischaemia leads to the

activation of glycolysis, resulting in the net formation of lactate[523]. It has also been shown that glycogen concentration decreased as a function of the length of the ischemic period[526]. This suggests that serum lactate may be a product of the glycolytic/gluconeogenic pathway, which was supported by the finding of glucose-6-phosphate and fructose-6-phosphate increasing with IRI[512]. However, the end product of this pathway is normally pyruvate, and lactate is not produced except during anaerobic situations[512,516]. It is interesting that this rise in lactate is observed at 4hrs reperfusion, this corresponds to a large burst of PMN activity that constitutes the beginning of the late phase of IRI[512,516]. It has been observed that the injury produced during the initial part of the late phase involves a more extensive hepatocellular injury in comparison to the early phase[546,547]. Moreover, elements of neutrophil sequestration, sinusoidal narrowing and vasoconstriction combine to form a "no-reflow paradox" whereby hepatocytes are subjected to a further perfusion deficit and persistent ischaemia[178,520]. This may explain the observed peak in lactate at this late time point, especially since lactate levels have been shown to become elevated in bile even when they are not elevated in serum[18].

PC was observed to be similar in sham and I/R+glycine groups, while it was raised in the I/R group during the 2nd and 4th hr of reperfusion. The main source of PC in cells is the plasma membrane, which suggests that the post-reperfusion increase may be associated with an increase in cellular breakdown and membrane lipid peroxidation[526]. Increased bile PC levels has also been observed in association with poor graft function in liver transplants[369].

An increase in post-reperfusion levels of biliary glucose and pyruvate were found on reperfusion in the I/R+glycine group compared to I/R, this suggesting an increased metabolic activity in the glycolytic/gluconeogenic pathway which may be due to conserved cellular energetics. Hepatocytes are one of the few cells that can utilize fatty acids in the production of energy through the β-oxidation helix, a reaction

requiring ATP at its initiation[548]. Ischaemia–induced reduction of ATP may result in a decreased ability to utilize β-oxidation inhibiting acetate production and increasing pyruvate. Glycine-treated livers possessed a greater ability to produce acetate than I/R group, suggesting less injury to their metabolic energetics.

After reduction of hepatic blood flow, the mitochondrial redox potential is reduced. Consequently, there is accelerated production of ketone bodies to compensate for inhibited glucose utilization. Ketone body production is an alternative pathway to supply ATP when there is inhibition of glucose oxidation and the Krebs cycle. Recently, higher acetoacetate perfusate levels have been demonstrated in isolated-perfused rat livers preserved in University of Wisconsin versus Euro-Collins solution[549] which has been shown to correlate with NAD^+/NADH ratio in the hepatocyte mitochondria[550]. The elevated levels of acetoacetate observed in this study, during ischaemia and reperfusion, suggest that glycine-treated livers can utilize this alternative source of ATP, again suggesting conserved cellular energetics in this group.

In this study bile spectroscopy has demonstrated significant changes in bile composition following I/R and alterations with glycine administration. These changes are evident despite a constant post-reperfusion rate of BF. Glycine was associated with increased synthetic functional markers (BF and bile acid synthesis), decreased injury markers (lactate and PC levels) and enhanced metabolic indicators (acetate, pyruvate, glucose and acetoacetate).

7 Modulation of warm hepatic ischaemia reperfusion in steatotic liver using NAC and its effect on bile composition

7.1 Introduction

Hepatic IRI always occurs following liver resection, trauma and transplantation, due to temporary complete or partial cessation of hepatic blood flow[549]. It is widely accepted that the key feature of IRI is the formation of ROS and RNS[551].

There are two distinct phases of liver IRI, the early phase (up to 2hrs post-reperfusion) and the late phase (4-24 hrs)[516,552]. The early phase is characterized mainly by activation of complement and KC and the production of ROS. The main event during the late phase is the accumulation of activated PMN and the production of ROS and proteases. Most liver injury occurs during the late phase[553] and can lead to increased morbidity and mortality and remote organ injury leading to multiorgan failure[554].

Hepatic steatosis occurs with obesity, alcohol abuse and metabolic disorders[427], and an incidence up to 11% has been reported in autopsy studies on accidental deaths[224]. It is now well recognised that steatotic livers are more susceptible to IRI than normal livers[229]. The mechanisms involved are still poorly understood but, as fat accumulates within the hepatocytes, cell volume increases resulting in a decreased sinusoidal space[239,244] and impaired microcirculatory blood flow[229,238]. Sinusoidal blood flow can be reduced by 50% in fatty livers[244,555]. Steatosis represents a risk factor in liver surgery, with a mortality rate up to 14% in patients undergoing major hepatic resection[238]. Similarly, the use of steatotic grafts for transplantation is associated with a much higher risk of primary graft non-function or dysfunction[231]. As a period of ischaemia is often necessary in liver surgery, and is inevitable in organ retrieval and transplantation, pharmacological modulation could potentially protect steatotic livers, minimizing the detrimental effects of IRI.

NAC is a thiol-containing compound that interacts and detoxifies free radicals by non-enzymatic reactions, and is deacetylated to form cysteine, which supports biosynthesis of glutathione, one of the most important components of the intracellular antioxidant

system[556]. Nakano et al. demonstrated that perfusion with NAC prior to organ retrieval reduced the extent of IRI after 24 hours of cold storage in an isolated perfused rat steatotic liver[37]. A previous experiment demonstrated that NAC reduced IRI in normal livers[499] and modified biliary composition.

7.2 Objectives

1. To determine if the changes in bile composition during I/R can be recorded in steatotic livers.
2. To determine if these changes (if they occur) can be reversed using NAC, similar to its action on normal livers.
3. To identify the differences in chemical composition between I/R and I/R+NAC
4. To ascertain if these changes fit with established understanding of the mechanisms involved in liver IRI and the actions of NAC

7.3 Materials and methods

7.3.1 Animal model

The study was conducted under a license granted by the Home Office in accordance with the Animals (Scientific Procedures) Act 1986. A rabbit liver lobar I/R model was used where both the early and late phases of reperfusion injury could be studied. 12 New Zealand white rabbits with a mean body weight of 3.8±0.5kg were used. Steatosis was induced by feeding the animals with a high cholesterol (2%) diet for 8 weeks. Anaesthesia was induced by intramuscular injection of fentanyl-fluanisone 0.5ml/kg (Janssen Animal Health Ltd., Buckinghamshire, UK).

Tracheostomy was performed and anaesthesia was maintained with Isoflurane (0.5-2%) via an anaesthetic circuit. Temperature was measured by a rectal thermometer and maintained at 37-38.5°C with a warming blanket (Homeothermic blanket control unit; Harvard Apparatus, Southmatick, Massachusetts, USA). Arterial oxygen saturation and heart rate were continuously recorded by a pulse oximeter (Ohmeda Biox 3740 pulse oxymeter; Ohmeda, Louisville, Colorado, USA), applied to the tail.

One radiopaque catheter (20G) was inserted into the ear artery to collect blood samples and connected to a pressure transducer to monitor mean arterial blood pressure and heart rate. Ear marginal veins were cannulated in both ears with radiopaque catheters (22G) for the administration of fluids and drugs. Normal saline was infused at a rate of 15 ml/kg/h to replace the intraoperative fluid losses.

Laparotomy was performed through a bilateral subcostal (roof-top) incision. The ligaments from the diaphragm to the liver were divided and the liver was fully exposed. The bile duct was cannulated with a polyethylene catheter (PE-50, 0.58 mm inner diameter, Portex, Kent, UK). BF was measured and calculated as μL/min/100g of liver wet weight. Following dissection of the portal vein, a perivascular Doppler probe (HT207; Transonic Medical System Inc, Ithaca, NY) was positioned around it to monitor the portal blood flow. Lobar ischaemia was induced by clamping the vascular pedicles of the median and left lobes of the liver, using an atraumatic microvascular clip. The microvascular clip was removed after 60 minutes of ischaemia and reperfusion was allowed for 6 hours. At the end of this period the animals were killed by exsanguination.

7.3.2 Experimental groups and protocol

Two animals groups (n=6 each) were used. In the I/R+NAC group 150 mg/kg of N-acetylcysteine (Parvolex, Medeva Pharma Limited, Lancashire, UK) in 20ml of 5% Dextrose was infused intravenously through the ear vein over the 15min immediately before reperfusion and maintained at 10mg/kg/h in 5% Dextrose during the 6hrs reperfusion period. In the I/R group 20ml of 5% Dextrose was infused intravenously 15min before reperfusion and continued at a rate of 10ml/kg/h during the reperfusion period.

In both groups, after laparotomy and a 10min period of stabilization, systemic and hepatic haemodynamics, oxygen saturation, body temperature and BF were recorded continuously. Arterial blood samples were taken before the induction of liver ischaemia

(baseline) and at 2, 5 and 6hrs after reperfusion for measurement of ALT activity. An equal volume of normal saline was used to replace the volume of the blood taken. Serum was separated from the samples and stored at -20°C until assayed. The measurements were done using an automated clinical chemistry analyser (Hitachi 747, Roche Diagnostics Ltd, Sussex, UK). A biopsy was taken from the ischemic left liver at baseline and 6 hours after reperfusion. Formalin-fixed liver tissue samples were embedded in paraffin and stained with haematoxylin and eosin for subsequent microscopy (digital light microscope CLF60 optical system, Nikon UK Ltd, Surrey, UK). Formalin fixed and not paraffin embedded tissue was stained for fat using the Swank & Davenport modification of the Marchi method[469].

7.3.3 Bile flow and composition

To determine the effect of NAC therapy on bile production and excretion, BF was measured and bile composition analysed with proton nuclear magnetic resonance spectroscopy (^{1}HNMR).

Bile samples were taken at baseline and each hour thereafter and stored at -80°C. Bile volume was expressed as µL/min/100g of liver weight.

^{1}HNMR analysis was performed on an 11.7T (500MHz for protons) spectrometer (Varian Unity+; Varian, Palo Alto, CA, USA) at 25°C. Bile was thawed at room temperature and placed in 5mm NMR tube. For a field/frequency lock a coaxial capillary insert was used (Wilmad, Buena, NJ, USA). This capillary insert was filled with a deuterium oxide solution of sodium TSP that acted both as a chemical shift reference and quantification standard. This capillary was calibrated by using a series of known concentration solutions of deoxycholate and a calibration curve was obtained. This was then used for quantification of bile components (lactate, acetate, pyruvate and phosphatidylcholine) which enabled an accurate comparison of bile levels between the groups. One dimensional NMR spectra were obtained at 500 MHz with a sweep width of 6kHz. Presaturation of bile was carried out to attenuate the

intensity of water signal. The spectra were analysed using software from MestRe-C version 3.1.1 (Universidade de Santiage de Compostela, Spain). All spectra were integrated using a fixed range for each peak and published peak assignments[10,18,370,472] shown in table 2.

7.3.4 Data collection and statistical analysis

Data from the pulse oxymeter, blood pressure monitor, transonic flowmeter, LDF and NIRS were continuously recorded on a laptop computer. The data were averaged for two minutes before the induction of ischaemia (baseline), at the end of ischaemia, and each hour of a 6hrs reperfusion period. The hepatic tissue oxygenation changes at the end of each period were calculated relative to the baseline.

Values are expressed as mean±SD. For statistical analysis, ANOVA with Bonferroni post hoc analysis was performed. Statistical analysis was performed using commercially available software (Staview 5.0.1, SAS Institute Inc., Cary, NC, USA). $P<0.05$ was considered statistically significant.

7.4 Results

All animals fed with a high-cholesterol (2%) diet for 8 weeks developed moderate hepatic steatosis. Histology revealed centrilobular steatosis (figure 37). Mild to moderate PMN infiltrate was evident in the liver tissue at the end of reperfusion.

7.4.1 Systemic haemodynamics

In both groups MAP and heart rate fell in the reperfusion period compared to baseline. There was no significant difference in MAP, heart rate and oxygen saturation values between the two groups through out the experiment.

7.4.2 Hepatic haemodynamics

Portal flow values are demonstrated in figure 38. There was no significant difference in baseline values between the two groups.

Portal flow was higher in I/R+NAC group after the third hour of reperfusion and this difference reached significance at the 6^{th}hr (67.2±8.3ml/min vs 52.5±11.2ml/min, I/R+NAC vs I/R, P=0.031).

Figure 37: Histology demonstrating centrilobular steatosis

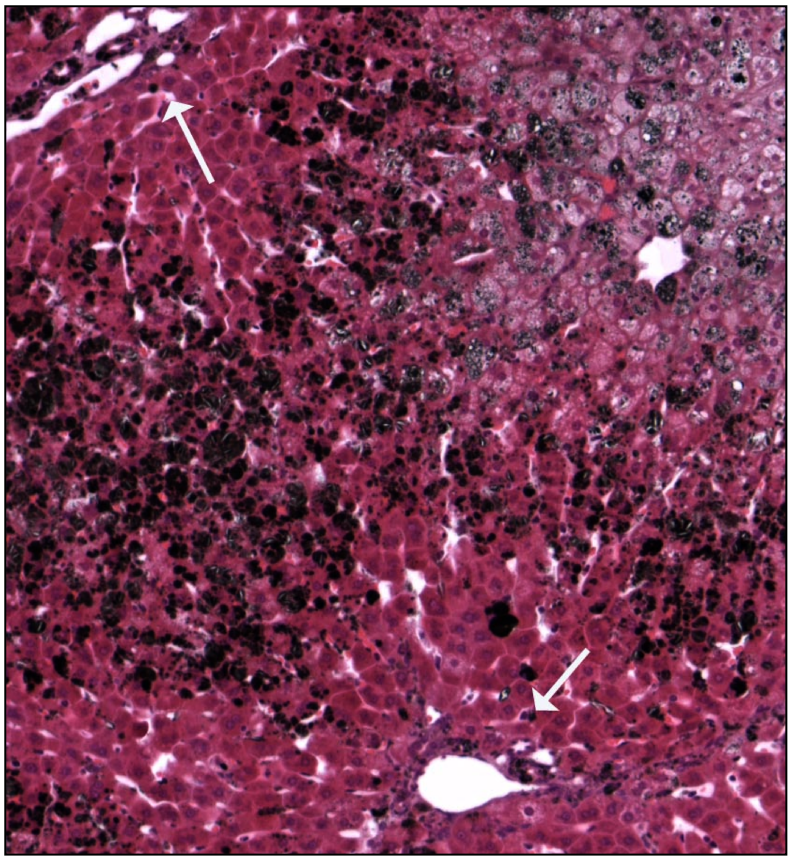

Section of liver stained with the Marchi method showing a moderate amount of centrilobular fat (stained black), as seen generally in the study population. The arrows indicate two portal tracts (magnification 100x).

Figure 38: Portal flow in the I/R+NAC and I/R group

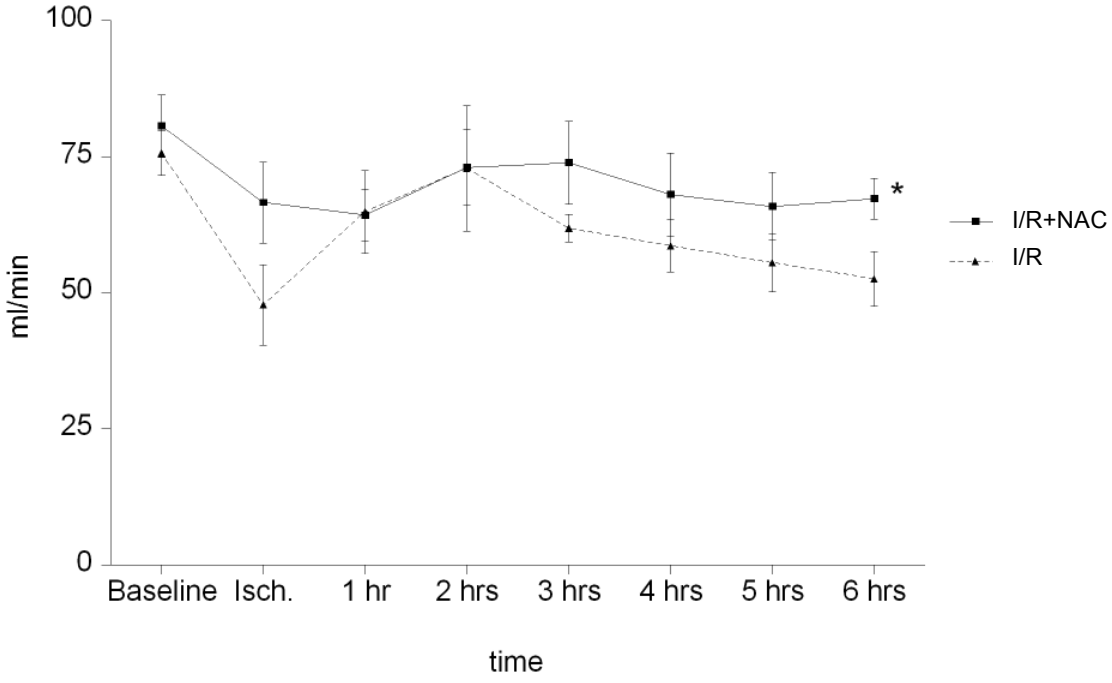

* A significant difference was recorded at 6th hour (P=0.031).

7.4.3 Hepatic microcirculation

During ischaemia LDF values were significantly reduced in both groups and became almost nil (figure 39). In the I/R group, flow in the hepatic microcirculation was significantly reduced from baseline by 5th hr (86±9.5 vs 60±10 flux/min, P=0.032) and 6thhr (86±9.5 vs 64±10 flux/min, P=0.048) post-reperfusion. In the I/R+NAC group no significant difference was recorded in LDF values between baseline and reperfusion.

Flow in hepatic microcirculation was better in the I/R+NAC group in comparison to I/R group after the 3rdhr of reperfusion and this difference became significant at the 5thhr (86.4±21.1 vs. 60±10 flux/min respectively, P=0.034) and at 6thhr (89.6±23 vs. 64.7±10.9 flux/min respectively, P=0.049).

7.4.4 Liver function tests

No significant difference between baseline ALT values in the two groups was recorded (40±12.7 in the I/R group vs. 44.7±11.8 IU/mL in the I/R+NAC group). ALT values were significantly greater in the I/R group at 5thhr (249±8.7 vs. 195±15 IU/mL, P=0.019) and 6th hr of reperfusion (288±24 vs. 216±13.7 IU/mL, P=0.019) as shown in figure 40.

7.4.5 Bile flow and Proton nuclear magnetic resonance (^{1}HNMR) spectroscopy

Baseline BF was similar in the two groups (175 μL/min/100gm in the I/R+NAC group vs. 189 μL/min/100g in the I/R group). BF was significantly greater in the NAC treated animals at 5thhr (123±35 vs. 85±10 μL/min/100g, P=0.016) and 6thhr of reperfusion (122±32 vs. 80±15 μL/min/100g, P=0.008) as shown in figure 41.

Baseline I/R group bile spectra are shown in figure 42. The results of the integration of the area under curve for the assigned peaks are shown in table 3. Bile lactate levels rose slightly in both groups during ischaemia and gradually fell at 5thhr of

Figure 39: LDF in the I/R+NAC and I/R group.

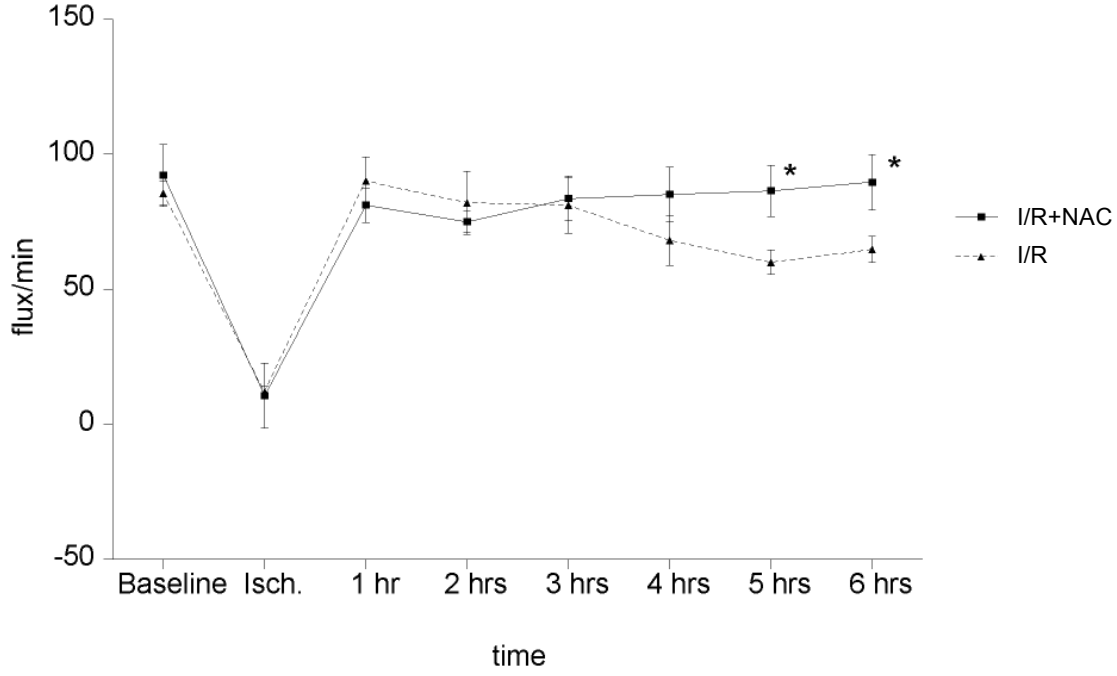

A significant difference was recorded at 5th and 6thhr (*P*=0.032 and *P*=0.048 respectively)

Figure 40: ALT levels in the I/R+NAC and I/R group

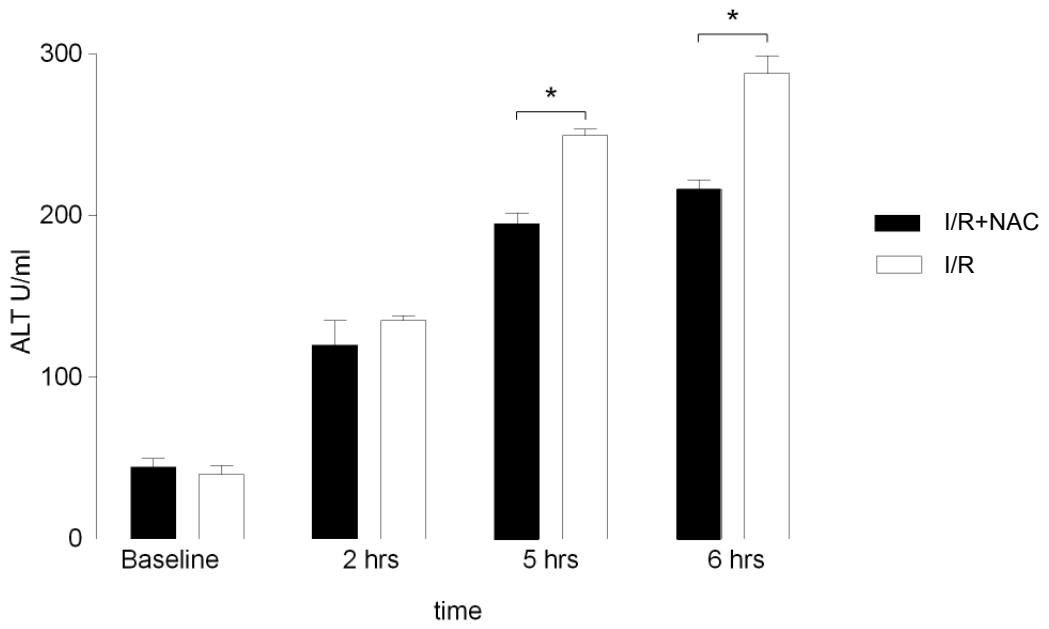

Changes in ALT values were statistically different at 5th and 6th hr in the two groups (P=0.019 at 5th and 6th hr respectively)

Figure 41: Bile flow measurements in the I/R+NAC and I/R group

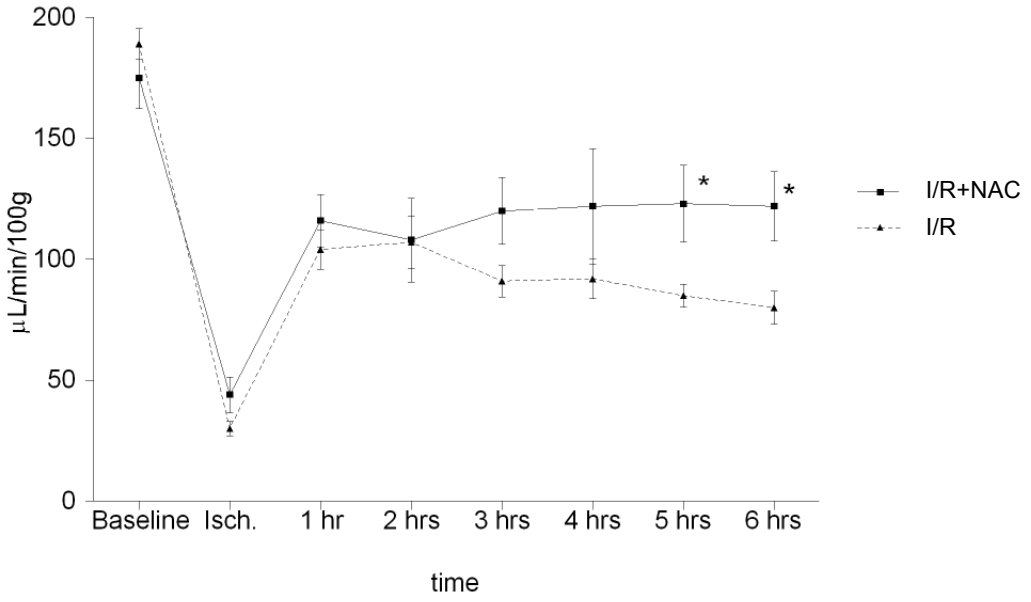

Bile flow was significantly greater in the I/R+NAC group at 5th and 6th hr (P=0.016 at 5th hr and P=0.008 at 6th hr respectively)

Figure 42: Baseline bile spectra of steatotic bile

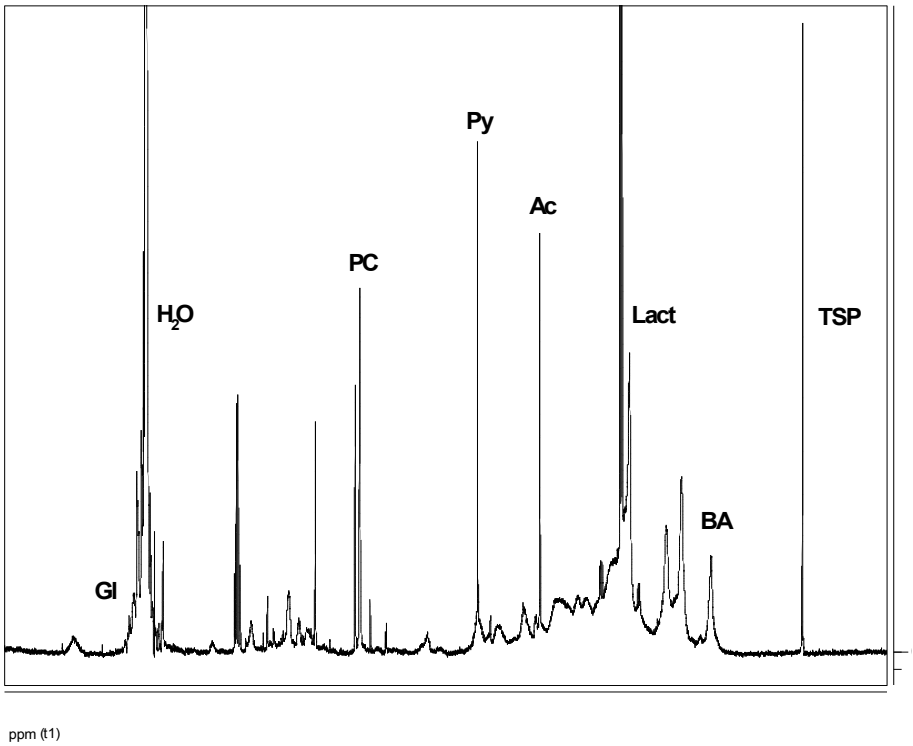

^{1}HNMR spectrum of baseline I/R bile. TSP=sodium trimethylsilyl-[$^{2}H_4$]propionate standard, BA=bile acid, Lact=lactate, Ac=acetate, Py=pyruvate, PC=phosphatidylcholine head group, H_2O=water, Gl=glucose

Table 3: Results of peak integration of ^{1}HNMR bile spectra

	Group	Baseline	Ischaemia	2hr Reperfusion	5hrs Reperfusion	6hrs Reperfusion
Lactate 1.3 ppm	**I/R**	11.73±6.14	12.98±9.01	11.29±6.24	11.32±7.21	12.88±9.73
	I/R+NAC	13.84±3.93	17.22±0.75	17.46±3.02	14.34±4.88	15.16±3.55
	P	0.5365	0.5733	0.0822	0.5137	0.6749
Acetate 1.9 ppm	**I/R**	1.20±0.40	1.24±0.34	0.77±0.25	0.51±0.21	0.74±0.32
	I/R+NAC	1.07±0.19	0.70±0.01	1.04±0.26	1.24±0.37	1.99±0.36
	P	0.5249	0.1211	0.1326	**0.0137**	**0.0022**
Pyruvate	**I/R**	0.98±0.39	0.86±0.38	0.84±0.32	0.56±0.40	0.89±0.43
	I/R+NAC	1.37±0.19	1.75±0.08	1.86±0.31	1.39±0.36	1.57±0.82
	P	0.0749	0.0538	**0.0009**	**0.0224**	0.1911
PC head group	**I/R**	3.75±1.62	8.37±1.9	5.68±2.22	6.26±5.24	4.11±2.88
	I/R+NAC	2.42±0.95	2.58±0.29	4.66±2.62	2.75±0.71	2.62±0.63
	P	0.1510	**0.0339**	0.5237	0.2330	0.3499

Peak integration of area under the curve of ^{1}HNMR bile spectra as per table 2 peak assignments, shown as mean±SD in μmol/L concentrations (quantification as per appendix section 10.1). Numbers in bold are P<0.5 (I/R compared to I/R+NAC group).

reperfusion. They were higher in the I/R+NAC than in I/R group but this difference was not significant. During reperfusion bile acetate levels rose in the I/R+NAC group to almost two fold the baseline level at 5hrs post-reperfusion while in the I/R group they dropped to almost half their baseline levels. Acetate levels were significantly higher in the I/R+NAC group compared to I/R at 5hrs (P=0.0137) and 6hrs reperfusion (P=0.0022) as shown in figure 43.

Bile pyruvate levels fell during ischaemia in the I/R group while they rose in the I/R+NAC group (p=0.0538). Following reperfusion bile pyruvate levels continued to fall in the I/R group while they continued to rise in the I/R+NAC group. I/R+NAC group pyruvate levels were significantly higher compared to I/R group at 2 and 5hrs post-reperfusion (p=0.0009 and p=0.0224 respectively).

During ischaemia there was a two-fold rise in PC levels in the I/R group (P=0.0339) while in the I/R+NAC group, there was only a slight rise. On reperfusion PC levels fell in I/R group after 2hrs reperfusion to rise again at 5hrs post-reperfusion. In the I/R+NAC group PC levels rose to peak after 1hr reperfusion then fell to close to baseline values at 6hrs reperfusion. PC levels were consistently lower in the I/R+NAC group than in I/R group.

Figure 43: ^{1}HNMR spectra of acetate levels following warm I/R

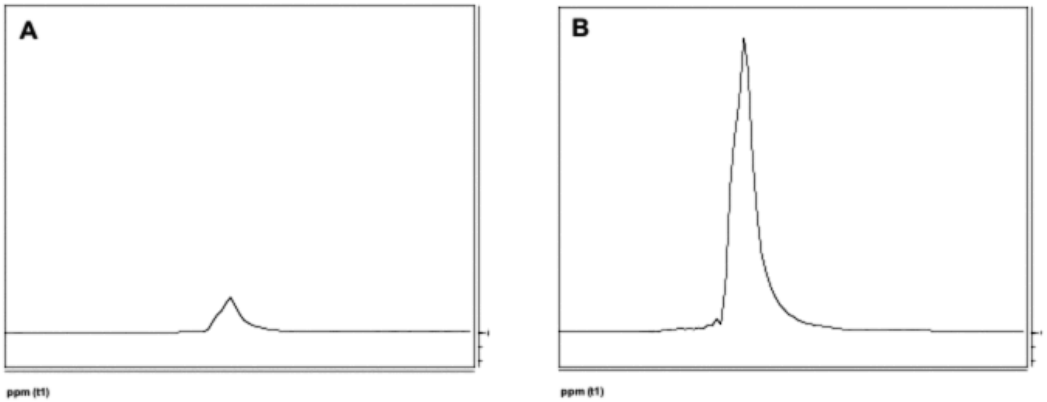

^{1}HNMR spectra of acetate peaks (at 1.9 ppm) in representative samples from (a) the I/R and (b) I/R+NAC group at 6hrs post-reperfusion showing significant increase

7.5 Discussion

This study has shown that NAC administration reduces IRI in the steatotic liver following a 1 hr period of partial inflow occlusion, and the benefit is mainly apparent in the late phase IRI.

Rabbits were fed with high-cholesterol diet (2%) for 8 consecutive weeks in order to induce moderate steatosis[398]. Unlike the commonly used low-choline methionine diet, which produces periportal fatty infiltration[240,426], with this model a central lobular deposition of fat is observed, similar to that found in the majority of human fatty livers, such as in diabetes, obesity and alcoholism[427]. Liver steatosis reduces flow in the hepatic microcirculation and mitochondrial ATP generation[229]. Fat accumulation in the cytoplasm of the hepatocytes causes compression or even complete occlusion of the sinusoidal spaces with shunting of a proportion of total hepatic blood flow (THBF)[240]. Our group previously demonstrated in an experimental model, that in moderate steatosis, the THBF was reduced by 30% and flow in hepatic microcirculation was 50% of normal I/R group[244].

The benefits of employing this model have been discussed above (section 3.1), briefly it permitted the analysis of bile constituents in both the early phase and the beginning of the late phase of IRI, avoiding the production of acute portal hypertension and intestinal ischaemia, maintained hemodynamic stability throughout the duration of the experiment, and avoiding the complete occlusion of biliary drainage in the total hepatic ischaemia model permitting the effects of I/R on biliary composition to be evaluated.

Several studies on liver IRI have focused on the initial reperfusion phase[159,266,399], which is characterised by oxidative stress induced by KC and occurs in the first two hours[185]. In the present study the observation time was extended to 6 hrs as a distinct late phase of warm IRI develops 4 hrs after reperfusion, and is primarily caused by activated PMN with release of ROS and proteases[516,531].

NAC was chosen as an antioxidant to modulate hepatic IRI as it is routinely administered to patients with acute liver failure secondary to acetaminophen (paracetamol) overdose[557], and has been used in other clinical conditions where oxidant damage was the putative or known mechanism of injury, such as acute respiratory distress syndrome[558] and IRI following cardiac surgery[559]. Recent work has also shown beneficial effects of NAC in normal liver following one hour of lobar ischaemia[499]. The dose of NAC administered is that used in clinical practice to treat patients with acute liver failure[557]. The beneficial effect of NAC was demonstrated by improvement in liver microcirculation, bile production, associated with reduced hepatocellular injury.

Several studies have validated the use of LDF to measure changes in hepatic microcirculation[396,560,561]. During partial inflow occlusion, parenchymal perfusion was greatly reduced but was still recordable. This low level of perfusion has also been reported in other studies and can be caused by a random wandering motion of red cells and breathing movements[532]. In the NAC group hepatic microcirculation returned to baseline values at the end of reperfusion suggesting that NAC has reversed the perfusion failure of the late phase of IRI. This correlates well with the return of portal blood flow rates towards baseline at the end of the reperfusion period in the NAC group.

In order to adequately investigate hepatic injury and function, changes in serum ALT activity, BF and composition were studied. ALT is relatively liver specific and reflects the loss of membrane integrity and release of cytoplasmic content into the circulation[221]. Bile production is a reliable marker of liver function[25]. The NAC group had reduced hepatocellular injury as indicated by lower ALT values following reperfusion, and improved biliary excretion, an energy dependent process, resulting in increased bile drainage volumes. A comparable rise in ALT values has been observed during reperfusion in steatotic animals subject to a similar ischaemic insult[37].

The use of spin echo spectra allowed the interference from broad lipid signals to be reduced and more clearly identify and comparatively quantify bile constituents. Continuous BF was recorded in both the I/R and I/R+NAC groups, and ^{1}HNMR spectroscopy revealed fluctuations in the concentration of several bile constituents. More specifically NAC administration enhanced the biliary excretion of acetate and pyruvate and reduced the excretion of PC.

Acetate is produced as a result of fatty acid β-oxidation in the liver[526]. This reaction requires ATP at its initiation. Following IRI ATP is consumed to clear excess lactate and pyruvate and may not be readily available for fatty acid oxidation. The I/R–induced reduction or depletion of ATP may result in a decreased ability to utilize β-oxidation causing acetate production to falter. The higher bile acetate levels in the NAC treated livers would suggest improved ATP production and energetics. The increased excretion of pyruvate in the bile of NAC treated livers is difficult to interpret. Steatotic livers have lower ATP levels after stress compared to normal livers and mitochondrial injury has been proposed as one of the causes of reduced hepatocellular ATP stores in steatosis[427]. The main source of PC in the hepatocytes is the cell membrane. The increase following ischaemia and again at 5hr post-reperfusion correlates well with the theory of cellular breakdown and membrane lipid peroxidation[524]. Increased PC has also been observed by other authors in association with poor graft function[394].

In conclusion, the administration of NAC, prior to and during reperfusion, reduced the extent of IRI in the steatotic liver. This was apparent during the late phase of reperfusion and was demonstrated by increased portal blood flow and liver parenchymal perfusion. Bile excretion, biliary acetate and pyruvate were increased and acute liver injury was reduced.

8 Modulation of warm hepatic ischaemia reperfusion in steatotic livers using ischaemic preconditioning and its effect on bile composition

8.1 Introduction

Fatty liver or hepatic steatosis is a common histological finding in human liver biopsies, which is the result of the abnormal accumulation of triacylglycerol within the cytoplasm of hepatocytes, attributed to the effects of alcohol excess, obesity, diabetes, or drugs[245]. Estimates based on imaging and autopsy studies suggest that about 20% to 30% of adults in the United State and other western countries have excess fat accumulation in the liver[562]. Hepatic steatosis can be graded as mild, moderate or severe, depending on the percentage of fat present[563].

With the increasing numbers of orthotopic liver transplantations and the concomitant lack of suitable donors, many liver transplant programs increasingly use donor livers of "marginal" quality such as fatty livers[229,564,565]. Fatty livers pose an increased risk of initial poor function and primary non-function of the graft after transplantation as they are particularly susceptible to IRI[229,566]. There is therefore, an urgent need for strategies that improve the outcome after transplantation of fatty livers.

Murry et al. first described IPC on observing that brief periods of ischaemia improves the tolerance to subsequent, prolonged ischaemia in various organ systems[258]. IPC has been shown to decrease liver injury after warm IR[34,259-261] as well as after cold ischemic storage[262-264]. Recent studies show that IPC increases the tolerance of fatty livers to IRI in an animal model of steatosis[265,266].

In a recent study, IPC significantly improved blood flow in the microcirculation during the reperfusion phase[267] in a rat IRI model and near infrared spectroscopy showed that preconditioned livers exposed to hypoxia maintained their COX redox state[268]. There is growing evidence that mitochondria are a major target of IRI[269]. For a metabolically active, mitochondria rich, organ such as liver an investigation into the changes in mitochondria function is of particular importance in the understanding of the sub-cellular mechanisms underlying hepatic I/R injury. Consequently, the aim of this study

was to investigate whether IPC protects fatty livers form IRI through a mechanism of improved intracellular tissue oxygenation and maintaining mitochondrial stability and function.

It is not known whether COX activity is a target for IRI in fatty liver and whether maintaining COX activity reduces IRI. This chapter investigated the effects of I/R and IPC on hepatic intracellular tissue oxygenation and COX activity associated with mitochondrial function to establish whether mitochondrial damage is a key mechanism of IRI in fatty liver.

8.2 Objectives

1. To determine if IPC, a process known to ameliorate IRI in normal livers, produces the changes in bile composition during I/R in steatotic livers.
2. To identify and possibly quantify the differences in chemical composition between sham, I/R and IPC+I/R, particularly further differences not explored in the previous experiments, e.g. βHb and acetoacetate
3. To determine if the use of lactate/pyruvate and βHb/AcAc ratios provides a better indicator for IRI
4. To ascertain if these changes fit with established understanding of the mechanisms involved in liver IRI and the actions of IPC

8.3 Material and Methods

8.3.1 Animal Model, Anaesthesia and Surgical Procedure

This study was conducted under a project license in accordance with the Animals (Scientific Procedures) Act 1986. New Zealand white rabbits weighing between 3.0-3.5kg were fed with a cholesterol rich (2%) diet for a period of 8 weeks to induce moderate steatosis.

A rabbit lobar ischaemia model developed for the study of the later phase of IRI was used[499]. Anaesthesia was induced by intramuscular injection of 0.5ml/kg fetanyl citrate

and fluanisone (Hypnorm; Janssen Animal Health Ltd., Buckinghamshire, UK). Following tracheostomy, anaesthesia was maintained by 1.5-2% isoflurane through an anaesthetic circuit. A Homoeothermic blanket control unit was used to maintain body temperature between 37-38.5°C (Harvard Apparatus, Southmatick, Massachusetts, USA). A radiopaque catheter (20G) was inserted into ear artery to monitor arterial blood pressure and collect blood samples. To administer anaesthetics, fluids and medication ear marginal veins were cannulated with radiopaque catheters (22G)[401]. Laparotomy was performed through a midline incision. Exposure of the liver was accomplished by severing the ligaments that attach it to the diaphragm. Lobar ischaemia is induced by clamping the vascular pedicles of the median and left lobes of the liver, using an atraumatic microvascular clip. Blood supply to the caudate and right lobes were unaffected by this method. Removing the vascular clamp allowed reperfusion at the end of ischaemia. This method induces severe ischaemia without inducing mesenteric venous hypertension. The bile duct was cannulated with a polyethylene catheter (PE-50, 0.58 mm inner diameter, Portex, Kent, UK). Bile was collected and frozen at -80° for proton magnetic resonance spectroscopy. Hepatic tissue oxygenation was continuously monitored in the left and median lobes throughout the experiment. Liver tissue biopsies were taken at baseline, 2, 5 and 7hrs of reperfusion.

Haemoglobin saturation and heart rate were continuously recorded by a pulse oxymeter. Laparotomy was performed through a midline incision. Portal flow was monitored continuously, using a perivascular transonic flow probe (Medical Flowmeter system HT207; Transonic Medical System, Ithaca, New York, USA). IPC was induced by 5min of ischaemia followed by 10min of reperfusion. After 60min of ischaemia the vascular clip was removed and reperfusion was allowed for 7hrs. At the end of the experiment the animals were killed by exsanguination.

8.3.2 Experimental Groups & Protocol

Under anaesthesia of isoflurane (1-2%), animals were subjected to 60 min liver lobar ischaemia followed by 7 hours of reperfusion. MAP, SaO_2 and HR were continuously monitored. HM was assessed by LDF. At the end of the reperfusion period, ICG (0.5mg/kg) was administered intravenously and the clearance rate in the liver was measured directly by NIRS.

The animals were divided into following three groups:

Sham Group: Sham laparotomy (n=6): The animals were anaesthetized and laparotomy performed for 8hrs without induction of ischaemia

I/R Group: Ischaemia-Reperfusion (n=6): Animals were subjected to 60min of ischaemia and 7hrs of reperfusion.

IPC+I/R Group: Ischemic Preconditioning (n=8): IPC was induced with 5min ischaemia followed by 10min of reperfusion before prolonged ischaemia was induced for 60mins followed by 7hrs of reperfusion.

8.3.3 Measurement of tissue oxygenation

Hepatic tissue oxygenation was measured *in vivo* by NIRS. NIRS (NIRO-500; Hamamatsu Photonics K.K, Hamamatsu, Japan) measured the concentration changes of Hb and HbO_2 and the reduction oxidation (redox) changes of the copper centre of COX. NIRS probes were positioned flat on the surface of the left lobe of the liver 10mm apart to continuously measure hepatic tissue oxygenation. A flexible probe holder is used to ensure probes are touching liver. This technique has been validated in previous studies[266,268,394,396,499,567].

8.3.4 Measurement of the hepatic microcirculation

HM was measured by a surface LDF, (DTR4, Moor Instruments Limited, Axminster, UK) in flux units[432]. The LDF probe was placed on a fixed site on the median lobe of the liver. LDF measurements were calculated as a mean of 2-min recording data

before clamping (baseline), at the end of ischaemia and at the end of each hour of reperfusion for each animal. The alterations during I/R period were calculated relative to the baseline values

8.3.5 Measurement of indocyanine green clearance

At the end of reperfusion, a bolus of ICG clearance (0.5mg/kg) was administered intravenously. The clearance of ICG in the liver was directly monitored by NIRS for 60min. Bile excretion of ICG during was also measured by spectrophotometry during this period.

Continuous measurement of hepatic ICG by NIRS produces a concentration-time curve. This curve was analysed to produce two exponential rate constants, representing hepatic ICG uptake from the plasma to the hepatocytes (α) and hepatic ICG excretion from the liver by cytoplasmic transport and biliary excretion (β) as shown in figure 48.

8.3.6 Measurement of bile flow and composition

To determine the effect of IPC on bile production and excretion, BF was measured and bile composition analyzed with ^{1}HNMR.

Bile samples were taken at baseline and 2, 5 and 7hrs after reperfusion and stored at -80°C. Bile volume was expressed as µL/min/100g of liver weight.

^{1}HNMR analysis was performed on an 11.7 Tesla (500MHz for protons) spectrometer (Varian Unity+; Varian, Palo Alto, CA, USA) at 25^{o}C. Bile was thawed at room temperature and placed in 5mm NMR tube. For a field/frequency lock a coaxial capillary insert was used (Wilmad, Buena, NJ, USA). This capillary insert was filled with a deuterium oxide solution of sodium TSP that acted both as a chemical shift reference and quantification standard. This capillary was calibrated by using a series of known concentration solutions of deoxycholate and a calibration curve was obtained. This was then used for quantification of bile components (lactate, acetate,

pyruvate and phosphatidylcholine), which enabled an accurate comparison of bile levels between the groups. One dimensional NMR spectra were obtained at 500MHz with a sweep width of 6kHz. Presaturation of bile was carried out to attenuate the intensity of water signal. The spectra were analysed using software from MestRe-C (Mestrelab Research, Santiage de Compostela, A Coruña, Spain). All spectra were integrated using a fixed range for each peak and published peak assignments[10,18,370,472] shown in Table 2.

8.3.7 Assessment of hepatocellular injury

Hepatocellular injury was accessed by measuring serum levels of AST and ALT using an automatic biochemical analyser (Hitachi 747; Roche Diagnostics Ltd., Sussex, UK).

8.3.8 Histological examination

Liver tissue samples were taken at the end of reperfusion and fixed in buffered 10% formalin and embedded in paraffin. 4μm thick sections were cut using a microtome and mounted on slides for H&E staining. Fat infiltration in the liver was detected by staining using Marchi method modified by Swank and Davenport[469].

8.3.9 Data collection and statistical analysis

Data from the pulse oxymeter, blood pressure and portal flow monitor, LDF were collected continuously on a computer. The data were averaged for two minutes before the induction of ischaemia (baseline), at the end of ischaemia, and 2, 5, and 7hrs reperfusion period. Values are expressed as mean±SEM. For statistical analysis ANOVA with Bonferroni adjustment for multiple comparisons were used. $P<0.05$ was considered statistically significant. Statistical analysis was performed using commercially available software (Staview 5.0.1, SAS Institute Inc., Cary, NC, USA).

8.4 Results

All animals developed moderate centrilobular steatosis (figure 44) after 8 weeks on a cholesterol rich diet. There was no mortality in our model to this stage of the induction of steatosis.

8.4.1 Effect of IPC on aminotransferase levels

AST levels are shown in figure 45A where IPC+I/R levels were significantly less at 2hrs (125±18 vs. 273±47; P=0.0049) and 7hrs (199±33 vs. 406±86; P=0.0287) after reperfusion than I/R and not significantly different from sham. ALT levels of IPC+I/R were significantly lower than I/R at 2hrs (40±8 vs. 111±16; P=0.0016), 5hrs (65±9 vs. 159±28; P=0.005) and 7hrs (54±14 vs. 178±34; P=0.0149) after reperfusion (figure 45B).

8.4.2 Effect of IPC on systemic and hepatic haemodynamics

Systemic and hepatic haemodynamics data are summarized in table 4. Heart rate, oxygen saturation and mean arterial pressure remained stable during 7hrs of reperfusion in all three groups. Portal flow was generally low in all three groups. At the end of reperfusion, the flow was better in IPC+I/R group as compared with I/R but the differences were not statistically significant. HM was reduced with induction of ischaemia. However, there were significant differences in HM between I/R and IPC+I/R groups at end of reperfusion (73.3±3.3 vs. 118.3±16.2 flux; P=0.0482) as shown in figure 46.

8.4.3 Effect of IPC on tissue oxygenation

IPC+I/R and I/R groups begin with similar baseline values of COX activity. After the initial 5mins ischaemia the IPC+I/R group displays a clear increase in COX activity which remains constant for the next 10mins. At the beginning of 60 minutes ischaemia the COX activity of both IPC+I/R and I/R drop to similar levels, however IPC+I/R is slightly higher than I/R and remains higher during the course of ischaemia. On reperfusion the I/R and IPC+I/R groups shows an almost identical increase in COX activity; however, this is lower than the baseline values for both groups. In the I/R

group there is a decrease from 120mins, which reaches its lowest point at 240mins, around 2.5hrs reperfusion. IPC+I/R gradually increases until 240mins then levels off with a dip seen at 360mins. During reperfusion the IPC+I/R group maintains the highest level of COX as shown in figure 47.

8.4.4 Effect of IPC on ICG clearance

Hepatic ICG uptake following I/R is shown in figure 48, representing the uptake from plasma to the hepatocytes (α-curve) in figure 48A and the hepatic ICG excretion from the liver by cytoplasmic transport and biliary excretion (β-curve) in figure 48B. The rates of ICG clearance were 57.8±13.5% and 44.4±4.0% in the sham and IPC groups respectively. Comparison bile ICG excretion between the groups is shown in figure 49.

8.4.5 Effect of IPC on bile composition

The result of integration of area under the curve for the assigned peaks is shown in Table 5. A baseline bile I/R bile spectrum is shown in figure 50a showing β-hydroxybutyrate (βHb) and acetoacetate (AcAc). Bile lactate levels were higher in the I/R group than the IPC+I/R group during 5 and 7hrs postreperfusion (P=0.0092 and P=0.0036 respectively). Bile pyruvate levels were higher in the IPC+I/R group compared to the I/R during 2, 5 and 7hrs postreperfusion (P=0.0157, P=0.0018, and P=0.0059 respectively). The redox lactate/pyruvate ratio is shown in figure 51a. PC bile levels were higher in the I/R group than the IPC+I/R group at 2 and 5hrs postreperfusion (P=0.0004 and P=0.0143 respectively). Bile acetate levels were significantly higher in the IPC+I/R group than in the I/R alone group at 5 and 7hrs reperfusion (P=0.0044 and P=0.0027 respectively) as shown in figures 50 b & c. Bile acetoacetate levels were significantly reduced in the I/R group compared to the IPC+I/R group at 2, 5 and 7hrs postreperfusion (P=0.0163, P=0.0002 and P=0.0007 respectively). Bile βHb levels significantly increased at 2hrs reperfusion in both I/R and IPC+I/R groups compared to sham. βHb levels were higher in the I/R group than the IPC+I/R group at 2, 5 and 7hrs reperfusion but they did not reach statistical significance. The redox ratio of βHb/acetoacetate is shown in figure 51b.

Figure 44: Moderate hepatic steatosis

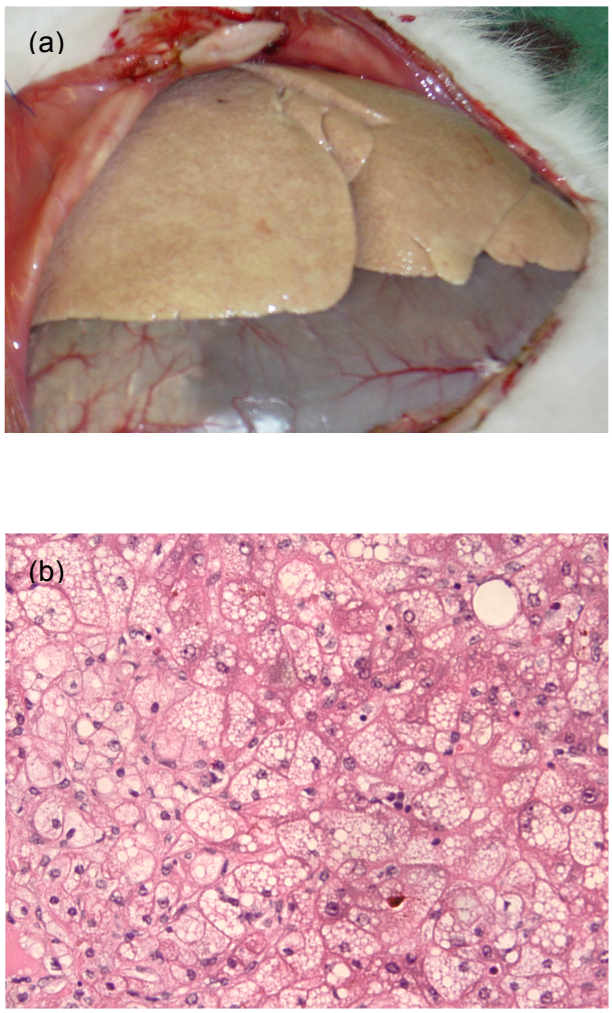

Moderate hepatic steatosis was induced in New Zealand white rabbits by feeding with a cholesterol rich (2%) diet for a period of 8 weeks shown (a) macroscopically and (b) microscopically with haematoxylin and eosin stain. The vaculated appearance of the hepatocytes is due to the dissolution of fat deposits by alcohol during the fixation process.

Figure 45: Effect of I/R and IPC on aminotransferase levels

(a)

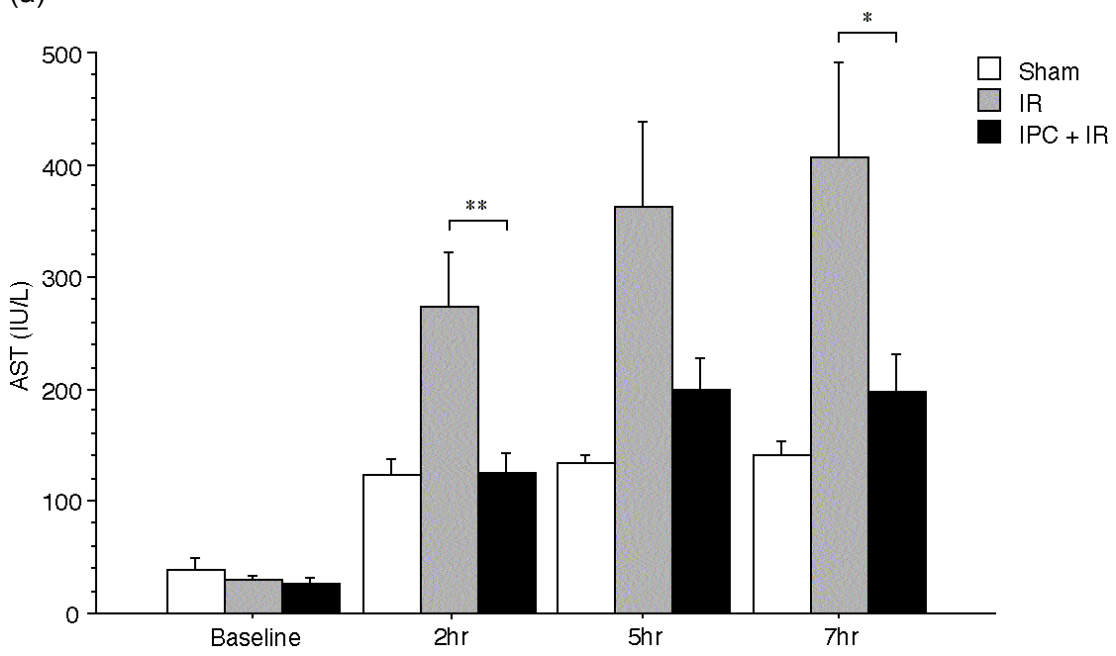

** = P<0.01 and * = P<0.05

(b)

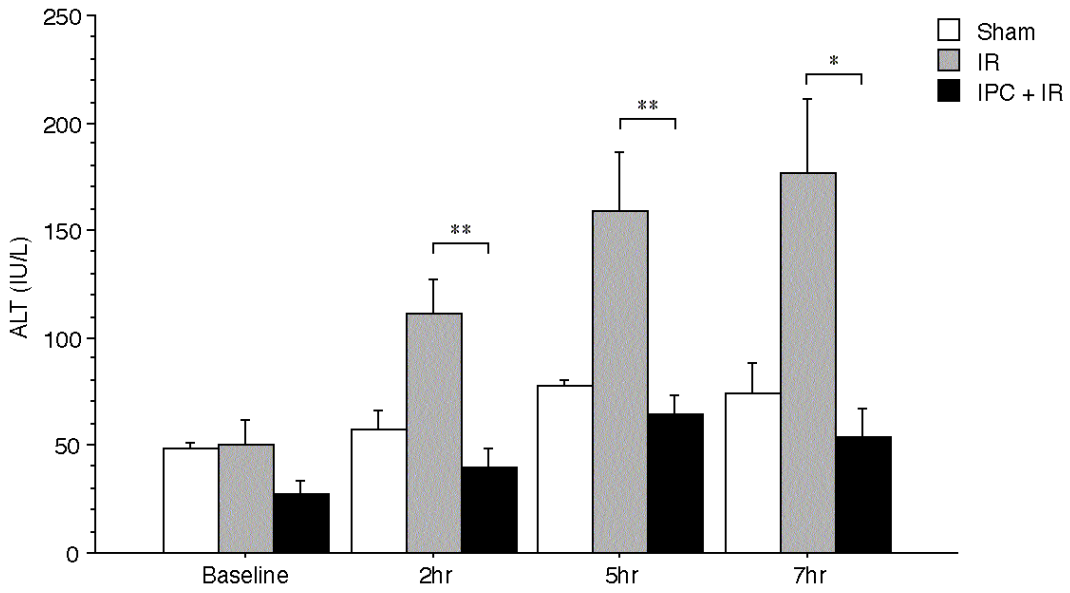

** = P<0.01 and * = P<0.05

Hepatocellular injury shown by aminotransferase levels with of (a) aspartate transaminase in IU/L and (b) alanine transaminase in IU/L.

Table 4: Effect of I/R and IPC on hepatic haemodynamics

	Sham			IR			IPC+IR		
	BL	2hrs	7hrs	BL	2hrs	7hrs	BL	2hrs	7hrs
MAP (mmHg)	73±5.7	62±4.6	66±6.8	75±3.0	63±2	65±5	72±4	68±3	67±6
HR (beat/min)	252±6	246±8	234±5	243±5	207±8	217±7	252±3	253±4	249±4
SaO_2 (%)	97.4±1.0	96.6±0.7	97.8±7.3	96.9±0.3	97.1±0.8	97.6±0.6	97.9±0.4	97.2±0.6	97.0±0.7
PVF (ml/min)	81.0±5.8	86.3±7.8	84.4±8.2	78.1±9.5	69.8±6.9	72.5±8.0	76.5±10.3	73.3±10.0	83.9±8.1

BL, baseline; MAP, mean arterial pressure; HR, heart rate; SaO_2, oxygen saturation; PVF, portal venous flow. Values are presented as mean±SEM of 6 animals from each group.

Figure 46: The effect of I/R and IPC on hepatic microcirculation

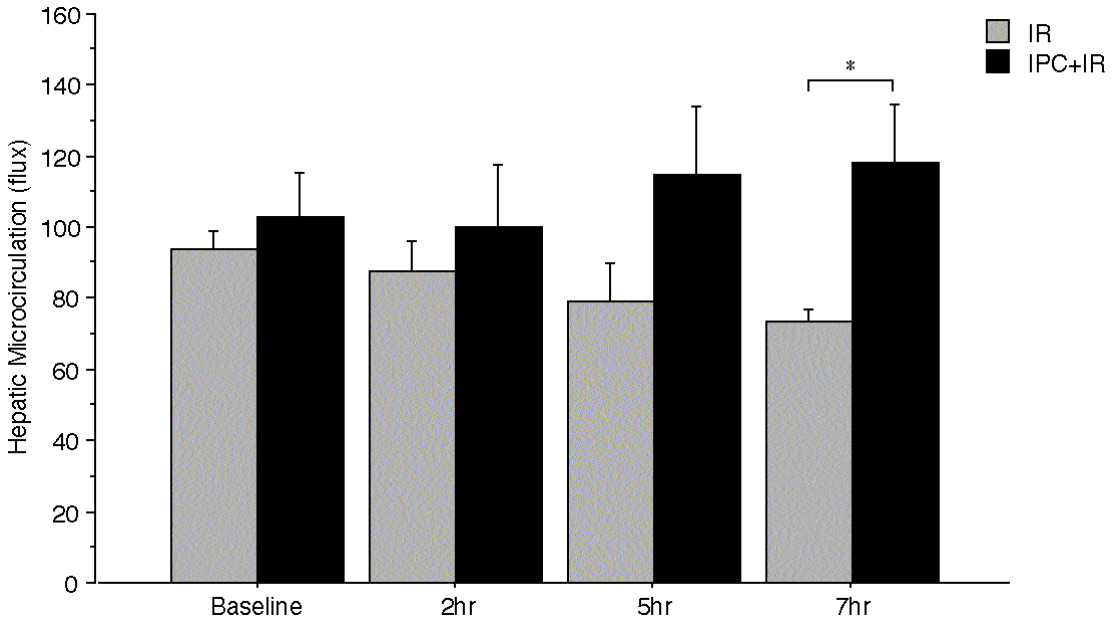

Hepatic microcirculation as measured by Laser Doppler Flowmetry in flux units.

Figure 47: Effect of and I/R IPC on COX

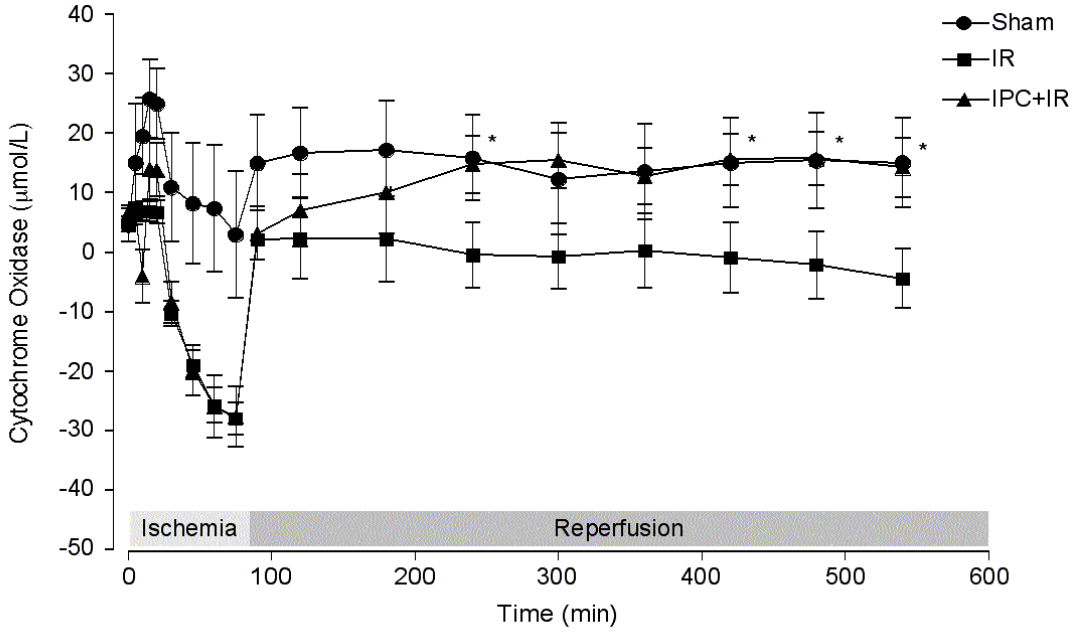

*=*P*<0.05 I/R vs. IPC+IR

The Effect of and I/R IPC on on the copper centre of cytochrome oxidase c (COX) as measured by NIRS.

Figure 48: Hepatic ICG uptake following I/R

(A)

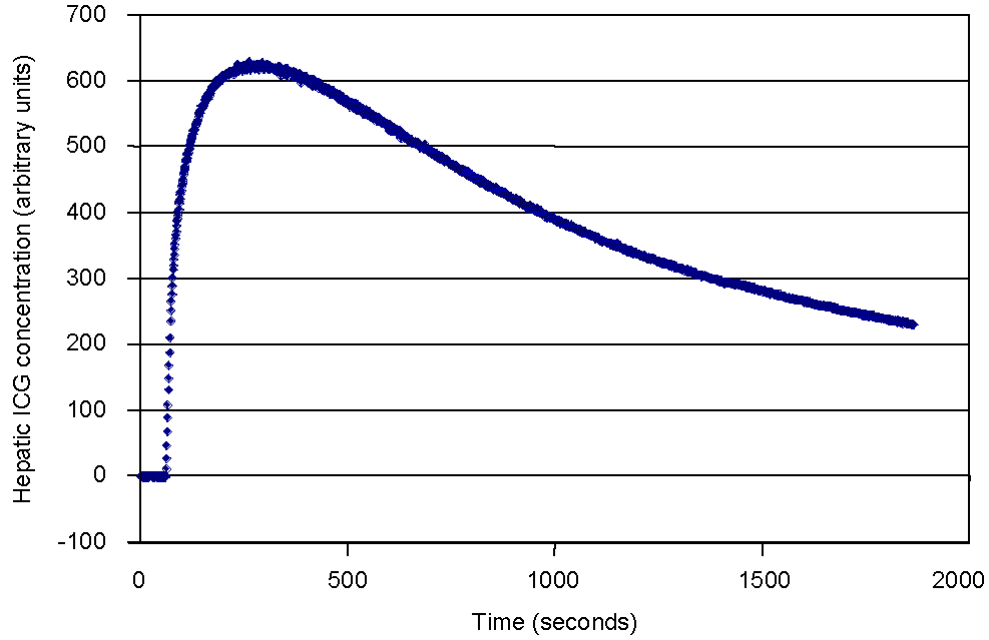

(B)

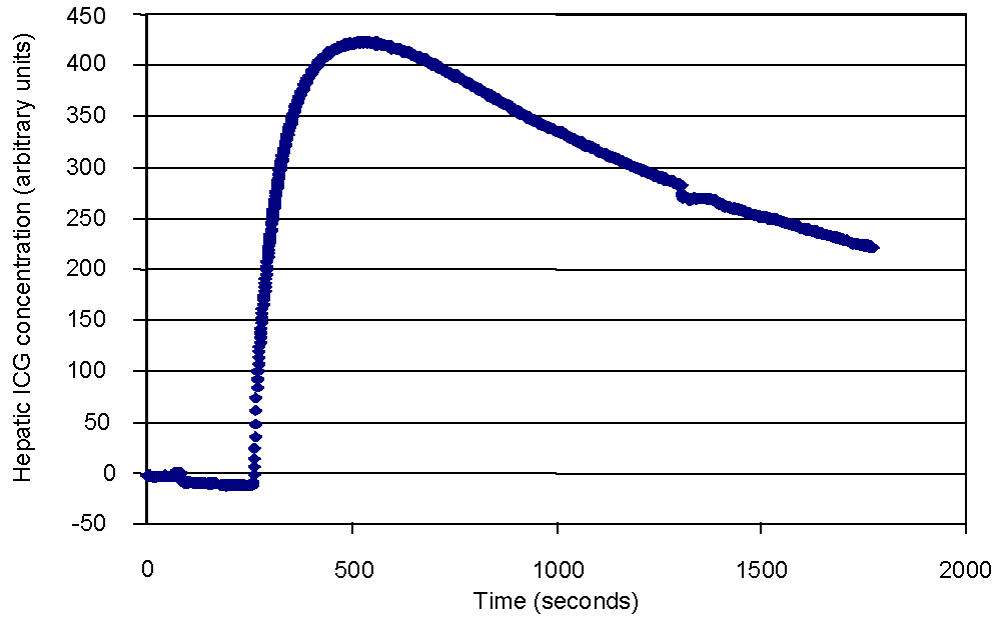

Hepatic ICG uptake following I/R (a) from the plasma to the hepatocytes (α-curve) and (b) hepatic ICG excretion from the liver by cytoplasmic transport and biliary excretion (β-curve).

Figure 49: Effect of I/R and IPC+I/R on hepatic ICG clearance

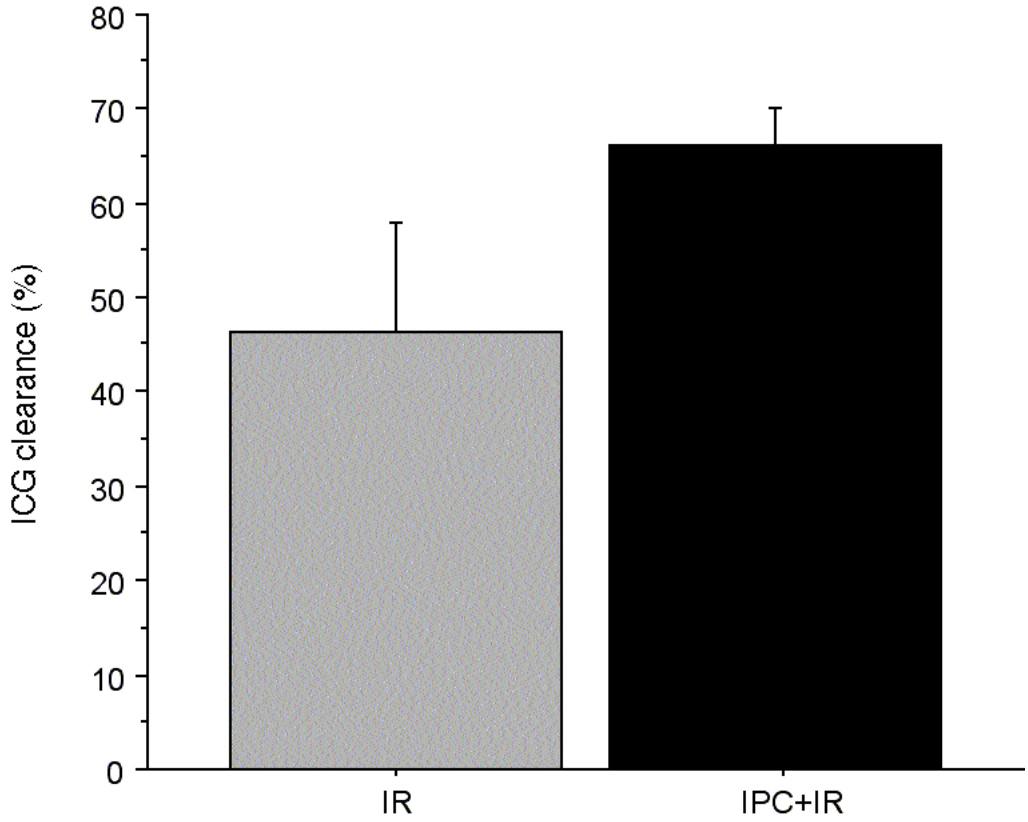

Effect of I/R and IPC+I/R on hepatic ICG clearance through excretion from the liver by cytoplasmic transport and biliary excretion (b).

Figure 50: Bile ^{1}HNMR spectra showing β-hydroxybutyrate and acetoacetate.

(a)

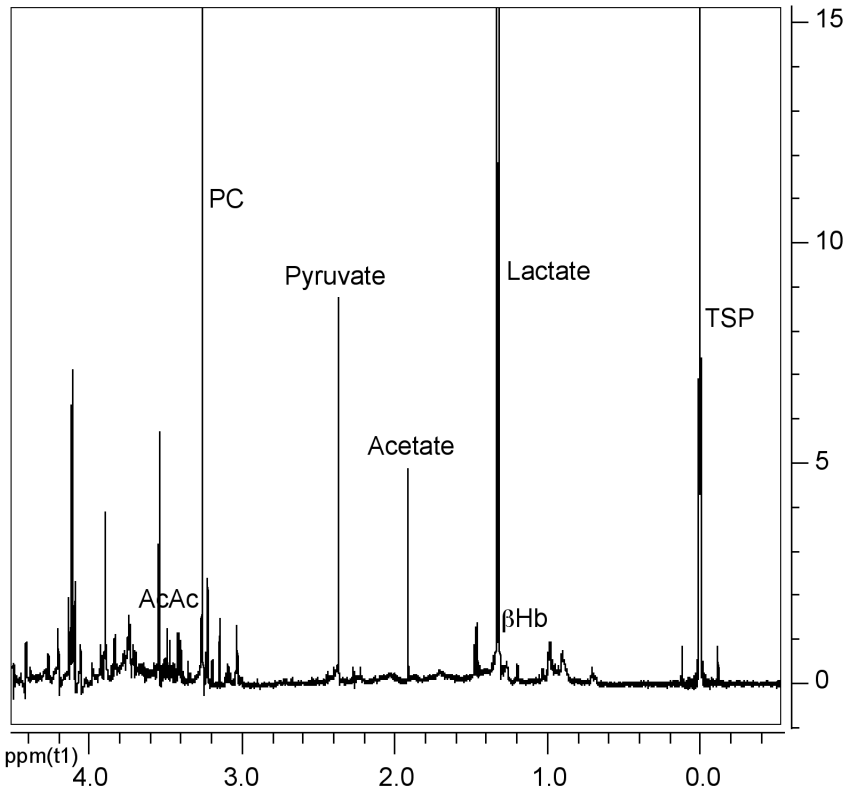

(a) Baseline spin echo spectra of bile. PC, phosphatidylcholine; AcAc, acetoacetate; ßHb, ß-hydroxybutyrate; ppm, parts per million; TSP, sodium [$^{2}d_{4}$]-trimethysilylpropionate

(b) (c)

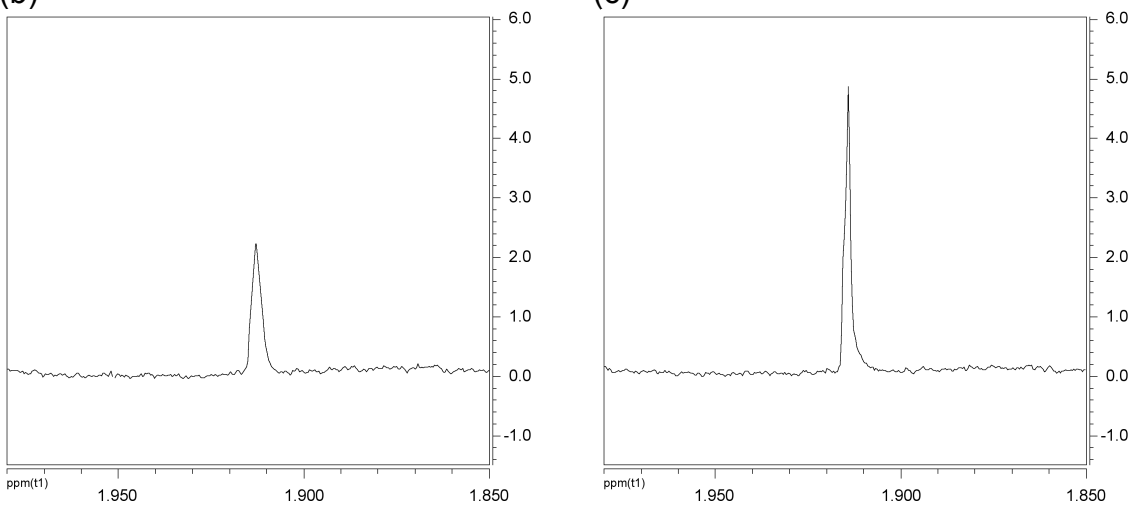

Details of acetate peak at 1.9 ppm (scaled to TSP) in (b) the I/R group at 7hrs reperfusion compared to the same peak in (c) the IPC+I/R group (scale in ppm).

Table 5: ^{1}HNMR bile composition in I/R and IPC+I/R in steatotic livers

	Sham				I/R				IPC+I/R			
	Baseline	**2hr**	**5hr**	**7hr**	**Baseline**	**2hr**	**5hr**	**7hr**	**Baseline**	**2hr**	**5hr**	**7hr**
Lactate	10.68±0.58	11.14±0.95	11.18±1.27	11.25±1.38	11.19±0.97	12.17±1.11	**16.50±1.06**§	17.23±1.88	11.13±0.81	9.05±1.76	**8.74±1.43***	**7.80±1.28***
Pyruvate	0.86±0.12	1.09±0.08	1.13±0.06	1.02±0.09	0.95±0.14	**0.50±0.05**§	**0.49±0.09**§	**0.68±0.09**§	0.73±0.14	**1.51±0.28***	**1.55±0.14***	**1.72±0.23***
Acetate	1.01±0.23	1.16±0.15	1.11±0.13	0.93±0.07	0.88±0.16	**0.38±0.05**§	**0.43±0.04**§	**0.34±0.05**§	0.95±0.23	0.58±0.17	**0.79±0.06§***	**0.85±0.90***
PC	4.11±0.22	4.22±0.32	4.28±0.49	4.40±0.33	4.51±0.35	**8.07±0.32**§	5.54±0.54	4.20±0.52	4.04±0.33	**5.59±0.25§***	**3.55±0.32***	3.91±0.14
Acetoacetate	2.15±0.12	2.13±0.05	2.08±0.12	1.92±0.23	2.07±0.28	**1.04±0.13**§	**0.41±0.05**§	**0.35±0.10**§	2.26±0.18	**1.73±0.17***	**1.48±0.16§***	**1.36±0.16***
βHb	0.46±0.06	0.46±0.05	0.57±0.06	0.61±0.05	0.51±0.03	**1.36±0.29**§	**0.99±0.11**§	0.82±0.17	0.56±0.06	**0.83±0.05**§	0.72±0.04	0.62±0.04

Values represent integration of area under the curve for peak assignments as per table 2, represented as mean±SD of concentrations μmol/L as per appendix section 10.1. Values in bold represent *P*<0.05; *=*P*<0.05 compared to I/R; §=*P*<0.05 compared to sham. PC=phosphatidylcholine; and βHb=β-hydroxybutyrate.

Figure 51: Bile redox ratios for I/R and IPC+I/R

(A)

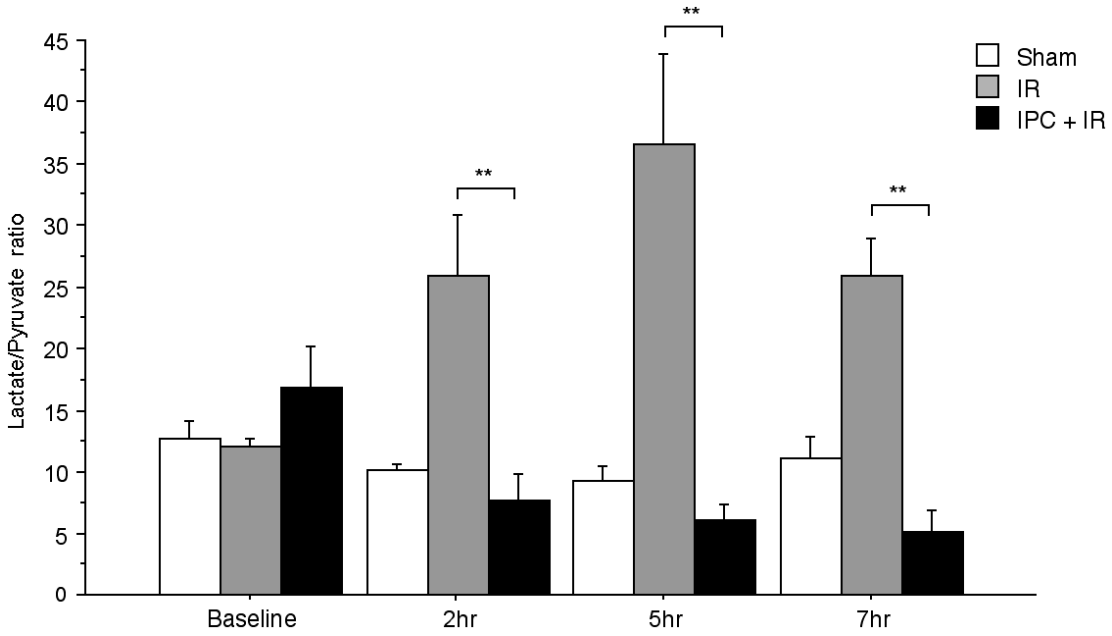

(B)

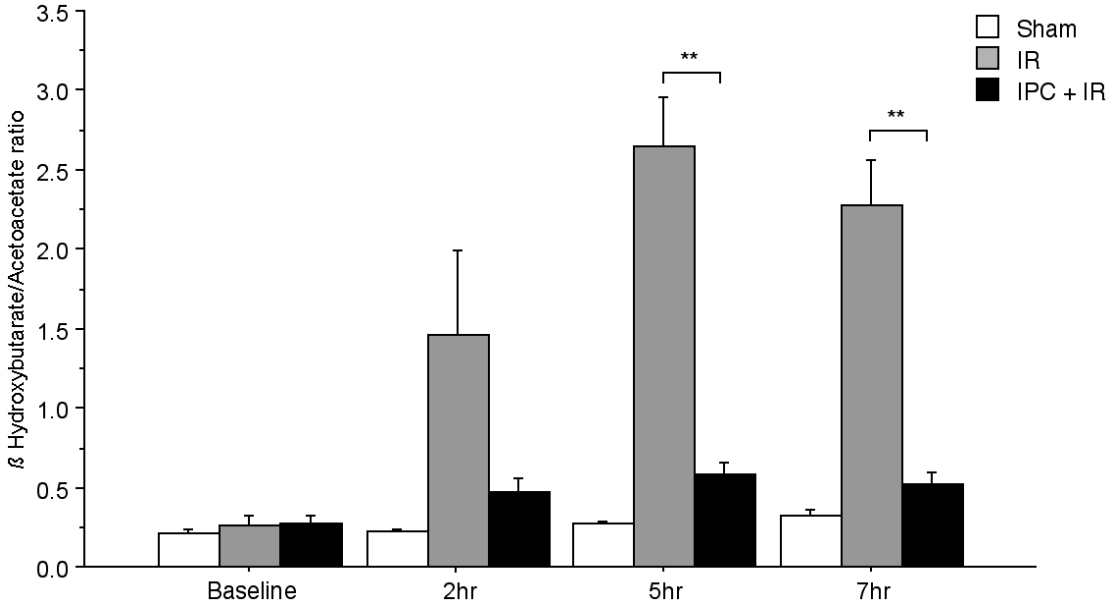

** = P<0.01 and * = P<0.05

Bile redox ratios for I/R and IPC+I/R showing (a) Lactate/Pyruvate and (b) β-hydroxybutyrate/Acetoacetate ratios as measured by ^{1}HNMR spectroscopy.

8.5 Discussion

IPC is protective against IRI in normal[261-264] and fatty liver[265]. The benefit of IPC has also been proven in human liver resection surgery[260].

NIRS *in vivo* measurements show extracellular tissue oxygenation was improved in the IPC+I/R group compared with the I/R group during reperfusion, supporting previous studies in normal liver that have shown that IPC protects hepatic microcirculation[34,267,268]. However, this experiment suggests that IPC also protects fatty liver against microcirculatory dysfunction. This is of importance to fatty liver as it has diminished sinusoidal spaces due to fatty infiltration[239].

This experiment shows that there is a decrease in intracellular hepatic oxygenation and mitochondrial function as represented by COX/CS activity between baseline and 2hrs reperfusion; noted in all three groups studied. The I/R group was worst affected followed by sham and the IPC+I/R group showed the least change in activity of COX enzyme suggesting that IPC plays a protective role in maintaining COX activity. Previous studies have shown that ATP production is closely correlated with HbO_2, Hb and change in COX redox state[398,568], suggesting that ATP generation and overall mitochondrial function in fatty liver is maintained. The results also suggest that most of the mitochondrial damage occurs within the first two hours of reperfusion, because there is less change in activity between 2hrs and 7hrs reperfusion.

The *in vivo* NIRS monitored the change in parameters continuously, indicating redox state of mitochondria and intracellular hepatic oxygenation. Thus showing how much the organ is perfused. The *in vivo* method focuses solely on isolated mitochondria function. There is wide variation in the data. Assays were done using liver tissue stored at –80˚C, mitochondrial function may have been affected according to the duration of storage. Trends seen in IPC+I/R and I/R groups are not statistically significant due to the small number of animals tested. A larger number of animals should be used in future work to prove these findings as statistically significant.

Selzner et al found the mechanism of cell death in fatty liver was significantly different to cell death in normal liver[257]. In fatty liver cell death occurs predominantly by necrosis, whilst apoptosis was dominant in normal liver after IRI. Necrosis is more damaging because it is accompanied by the breakdown of organelles, membranes and the release of cytotoxic cell contents, which induce inflammation, whereas, apoptosis does not. This may contribute to making fatty liver less tolerant to IRI injury[256]. Fatty liver has diminished sinusoidal spaces due to fatty infiltration[239] and inflammatory mediators such as TNF-α and leukocytes cause a further decrease in sinusoidal space and impairs microcirculation which reduces blood flow to certain areas resulting in prolonged periods of ischaemia to certain areas of the liver. This causing activation of KC and other mechanisms of IRI[569].

Glanemann et al have shown that IPC protects normal liver from IRI by maintaining hepatic microcirculation and reducing inflammatory response by preventing activation of KC and maintaining mitochondrial redox state which is dependent upon oxygen availability[34].

The use of spin echo spectra allowed the interference from broad lipid signals to be reduced and more clearly identify and comparatively quantify bile constituents.

The energetic balance and redox status of hepatic tissue are intimately connected by substrate oxidation/reduction reactions *via* oxidized nicotinamide adenine dinucleotide (phosphate) (NAD(P)) at several key points, such as pyruvate/lactate interconversion in the cytosol or βHb/AcAc interconversion in the mitochondria also known as the ketone body ratio. βHb and AcAc are a redox pair coupled by interconversion from AcAc (with oxidation of NADH) to βHb and the βHb/AcAc ratio is an indicator of mitochondrial redox status[570]. βHb/AcAc equilibrates with hepatic mitochondrial NADH/NAD^+ because the enzyme, β-hydroxybutyrate dehydrogenase, resides in mitochondrial cristae[571]. In the IPC+I/R group more of the “oxidized” half of the couplet

(AcAc) could be detected in bile, this suggests a shift toward more aerobic conditions in the mitochondria. This could lead to more aerobic conditions within the cytosol and, thus, the reconversion of lactate to pyruvate during reperfusion, lactate and pyruvate being a redox pair that is an indicator of the cytosolic redox state. This is supported by our findings of decreased lactate/pyruvate ratio in the IPC+I/R group during reperfusion.

Acetate is produced as a result of fatty acid β-oxidation in the liver[572]. This reaction requires ATP at its initiation[573]. ATP is consumed immediately following IRI to clear excess lactate and pyruvate and may not be readily available for fatty acid β-oxidation. IR-induced depletion of ATP may result in a decreased ability to utilize β-oxidation causing acetate production to falter. The higher bile acetate levels in the IPC+I/R treated livers would suggest improved ATP production. The main source of PC in the hepatocytes is the cell membrane. The increase at 2 and 5hrs post-reperfusion correlates well with cellular breakdown and membrane lipid peroxidation[524]. The first peak coincides with hepatocellular injury during ischaemia and the second peak with the 'no-reflow period'[404,520]. PC levels at both peak periods were reduced in the IPC+I/R group, this may suggest less cellular breakdown in the IPC+I/R group.

Hirakawa et al have shown in normal rat liver cytochrome *c* is released into the cytosol by mitochondria during IRI[574]. It is a mediator of apoptosis inducing caspase 3 and 9 activation, which mediate apoptosis. The release of cytochrome *c* and caspases occurred during ischaemia, yet, apoptosis occurred during reperfusion in normal liver[575]. The release of cytochrome *c* is mediated by a membrane pore, known as the mitochondrial permeability transition pore (mPTP). The pore can be defined as a voltage-dependent high-conductance channel of the inner mitochondrial membrane[576]. The pore is normally closed, but is opened at the onset of reperfusion. When cytochrome *c* is released there is no substrate for COX resulting in a decrease in ATP synthesis and mitochondrial function. COX directly binds to oxygen and its activity

results in ATP synthesis. The rate of ATP synthesis is directly dependent on redox state of mitochondria. There is only a shortage in cytochrome *c* if the mPTP in the membrane remains open. The mPTP may remain open in the fatty liver leading to necrosis. IPC of the heart prevents the mPTP opening; it is possible that a similar situation occurs in fatty liver[577].

The presence of non-esterified fatty acids in fatty liver is associated with the decrease in ATP as compared to a normal liver under normal conditions. It has been proposed that the reason fatty liver chooses to undergo necrosis rather than apoptosis is due to a decrease in ATP[256,265]. ATP is essential for apoptosis. Selzner et al have proved that IPC protects fatty liver against necrosis[265]. This may be because IPC maintains ATP levels in fatty liver. This is supported by the results of this experiment that suggest that the IPC+I/R group was in a more “oxidized” state than the I/R group.

During ischaemia there is very little HbO_2 and total Hb, this is associated with a decrease in COX activity. Chandel et al studied whether hypoxia leads to suppression of electron transport chain and whether COX was involved in this process[578]. They showed that oxygen availability determines COX activity. Chandel et al support the reversible two transition state COX model proposed by Wilson et al[579]. Wilson et al proposed that COX switches reversibly between two states of activity, suggesting that COX may possess two different binding sites for oxygen[579]. One binding site decreased whereas the other increased ATP production. The switch between the two states of activity is said to be faster from low activity, in low oxygen states, to high activity when oxygen levels return to normal. This phenomenon is seen during the transition from baseline to end of ischaemia in the results, it takes time for activity to drop along with a decrease in oxygen. The faster change is seen in figure 47 because on reperfusion after extended ischaemia the IPC+I/R group shows a surge in COX activity, which is higher than the initial baseline value. This is also seen in the IPC+I/R group after a brief period of 5 minutes of ischaemia, on reperfusion there is a much

higher COX activity than baseline. Suggesting oxygen supply is sufficient for Complex IV of the electron transport chain, ATP generation and COX function is normal. Improved extracellular oxygenation in IPC+I/R compared to I/R may be the main way in which IPC works to preserve mitochondrial function and blood flow preventing inflammation.

This experiment shows there is *in vivo* and *in vitro* preservation of COX activity in fatty livers, which are preconditioned in comparison to those that are not. This suggests that the mPTP may close after opening briefly on reperfusion and cytochrome *c* and oxygen are available as substrates for COX, as in normal liver. It is likely that ATP synthesis continues and if cell death were to occur, apoptosis may be more likely to be triggered than necrosis, i.e. there is a switch to the apoptotic pathway.

A switch away from necrosis in fatty liver means there is less necrosis-induced inflammation, release of inflammatory mediators, activation of KCs and leukocytes and leukocyte and platelet adhesion to sinusoidal epithelial cells. The hepatic microcirculation and tissue perfusion would be maintained. This would lead to sustained oxygen delivery to mitochondria and would therefore maintain COX activity. Continued oxygen supply means that COX would probably be in a high active transition state with high ATP turnover, whereas a low active state may be related to necrotic pathway. A high active COX state may induce the mPTP to close[580]. A higher COX activity state is less likely to follow the necrotic pathway due to increased ATP production.

During ischaemia COX activity decreased in I/R and IPC+I/R groups, on reperfusion COX activity in both groups increased suggesting that COX activity is affected by lack of oxygen and may be in a low activity state during ischaemia. COX activity in the I/R group on reperfusion was not as high as IPC+I/R group suggesting that COX activity may be used as a marker for IRI damage and can be attenuated by IPC in fatty liver.

In summary, this experiment shows that IPC protects fatty liver from IRI and maintains hepatic oxygenation, tissue perfusion and mitochondrial redox state. Most importantly it has proved that COX activity is compromised by IRI in the fatty liver, but can be protected by IPC. Damage is mostly confined to the period between baseline and 2hrs reperfusion (i.e. the early phase of reperfusion). The data suggests that IRI may be reversible in fatty liver if IPC is employed during liver transplantation, however this would need to be the subject of further research. The data from this experiment also suggests that IPC improves hepatic intracellular tissue oxygenation during beginning of the late phase of IRI.

9 Thesis discussion

Chapter four was intended as a pilot study. It provided a proof of principle, that there was a detectable change in bile acid composition using ^{1}HNMR. It was repeated with the addition of an intervention group to form the basis of chapter five. In chapter five NAC administration resulted in decreased levels of bile lactate and PC and increased levels of acetate following I/R. In chapter five the changes in bile constituents became more apparent. There were several differences in bile composition between the experiments in this chapter five and four. In chapter five the monitoring of the haemodynamic data was through the ear artery and vein, rather than the femoral artery and vein, which lead to a more stable experimental model[401].

There were clear differences in both I/R and I/R+NAC groups when compared to shams. There were no significant differences between the groups in conjugated bile acids, this was both disappointing and interesting. Due to active nature of conjugation of bile acids, this was initially thought to be an area where a clear difference between the groups would be found. It was one of the aims of this thesis to identify MRS markers of IRI. This was an early challenge to the hypothesis, that a bile marker might be found through ^{1}HNMR. Consequently, in subsequent experiments, the search for other metabolites was expanded, and conjugated bile acids were discarded as a candidate marker. The search for the best predictive marker, validating it through repeated experiments, comparing it with other published observations, and putting forward an explanation for these changes is a constant theme that runs through the following chapters.

In chapter five, BF in both the I/R and I/R+NAC groups fell sharply in response to ischaemia, and recovered after reperfusion. However, despite this consistent pattern of BF, ^{1}HNMR spectroscopy of bile revealed fluctuations in the concentration of some bile constituents.

Lactate in particular shows a large peak at 5hrs postreperfusion, this corresponds to a

large burst of PMN activity that constitutes the beginning of the late phase of ischaemia-reperfusion injury[532]. It has been observed that the injury produced during the initial part of the late phase is a more extensive hepatocellular injury in comparison to the early phase[546,547]. Interestingly, NAC administration abolished this peak in lactate, as it lowered the levels of ALT.

Acetate was observed to drop continuously from baseline throughout the experiment; however, it correlated strongly to COX activity. The I/R-induced reduction in ATP may result in decreased β-oxidation causing acetate production to falter; this could also explain its strong association with the change in COX.

In chapter six, for the first time, bile constituents were quantified as explained in the appendix (section 10.1). They are expressed in micromolar concentrations.

The I/R+Glycine group was associated with increased synthetic functional markers (BF and bile acid synthesis), decreased injury markers (lactate and PC levels) and enhanced metabolic indicators (acetate, pyruvate, glucose and acetoacetate).

The recovery of BF and a rise in bile acid secretion following I/R in the I/R+glycine group suggests an early recovery of metabolic activity in the glycine-treated livers, which is supported by observations that total serum bile acids were found to be early markers of liver function in porcine[521,522] and canine[523] liver transplants.

Lactate levels were elevated with I/R and were higher than the sham and I/R+glycine groups. They were elevated at a time point similar to the previous two experiments that corresponds to a large burst of PMN activity at the beginning of the late phase of IRI[512,516]. PC was observed to be similar in sham and I/R+glycine groups, while it was raised in the I/R group during the 2nd and 4thhr of reperfusion. Increased bile PC levels has also been observed in association with poor graft function in liver transplants[369].

An increase in post-reperfusion levels of biliary glucose and pyruvate were found on

reperfusion in the I/R+glycine group compared to I/R, this suggesting an increased metabolic activity in the glycolytic/gluconeogenic pathway, which may be due to conserved cellular energetics. Glycine-treated livers possessed a greater ability to produce acetate than I/R group, suggesting less injury to their metabolic energetics.

After a reduction in hepatic blood flow, the mitochondrial redox potential is reduced. Consequently, there is accelerated production of ketone bodies, to compensate for inhibited glucose utilization. Ketone body production is an alternative pathway to supply ATP when there is inhibition of glucose oxidation and the Krebs cycle. Recently, higher acetoacetate perfusate levels have been demonstrated in isolated-perfused rat livers preserved in University of Wisconsin versus Euro-Collins solution[549] which has been shown to correlate with NAD^+/NADH ratio in the hepatocyte mitochondria[550]. The elevated levels of acetoacetate observed in this study, during ischaemia and reperfusion, suggest that glycine-treated livers can utilize this alternative source of ATP, again suggesting conserved cellular energetics in this group.

In chapter seven, NAC administration was seen to reduce IRI mainly in the late phase in steatotic livers. Liver steatosis reduces flow in the hepatic microcirculation and mitochondrial ATP generation[244]. Fat accumulation in the cytoplasm of the hepatocytes causes compression or even complete occlusion of the sinusoidal spaces with shunting of a proportion of total hepatic blood flow[396,402]. In moderate steatosis, the THBF was reduced by 30% and flow in hepatic microcirculation was 50% of normal I/R group[159,168].

Recent work has also shown beneficial effects of NAC in normal liver following one hour of lobar ischaemia[396,560,561]. The dose of NAC administered, in chapter seven, is that used in clinical practice to treat patients with acute liver failure[532]. The beneficial effect of NAC was demonstrated by improvement in liver microcirculation, bile

production, associated with reduced hepatocellular injury.

In the I/R+NAC group hepatic microcirculation returned to baseline values at the end of reperfusion suggesting that NAC has reversed the perfusion failure of the late phase of IRI. This correlates well with the return of portal blood flow rates towards baseline at the end of the reperfusion period in the NAC group. Spectroscopy showed NAC administration enhanced the biliary excretion of acetate and pyruvate and reduced the excretion of PC.

The I/R–induced reduction or depletion of ATP may result in a decreased ability to utilize β-oxidation causing acetate production to falter. The higher bile acetate levels in the I/R+NAC group would suggest improved ATP production and energetics. The increased excretion of pyruvate in the bile of I/R+NAC group is difficult to interpret. Steatotic livers have lower ATP levels after stress compared to normal livers and mitochondrial injury has been proposed as one of the causes of reduced hepatocellular ATP stores in steatosis[394]. The main source of PC in the hepatocytes is the cell membrane. The increase following ischaemia and again at 5hr post-reperfusion correlates well with the theory of cellular breakdown and membrane lipid peroxidation. PC levels were reduced in the I/R+NAC group.

The administration of NAC, prior to and during reperfusion, reduced the extent of IRI in the steatotic liver. This was apparent during the late phase of reperfusion and was demonstrated by increased portal blood flow and liver parenchymal perfusion. Bile excretion was increased and acute liver injury was reduced.

In chapter eight, several strands of previous experiments started to converge. The experiment demonstrated that IPC protects fatty liver from IRI and maintains hepatic oxygenation, tissue perfusion and mitochondrial redox state. Most importantly it suggested that COX activity is compromised by IRI in the fatty liver, but can be protected by IPC.

NIRS *in vivo* measurements show extracellular tissue oxygenation was improved in the IPC+I/R group compared with the I/R group during reperfusion, this has been shown in normal livers[34,267,268]. However, this experiment suggests that IPC also protects fatty liver against microcirculatory dysfunction, this is supported by other findings[266,581]. This is of importance to fatty liver as it has diminished sinusoidal spaces due to fatty infiltration[239].

There is a fundamental difference between normal and fatty livers, making them more susceptible to IRI. Selzner et al noted the mechanism of cell death in fatty liver was significantly different to cell death in normal liver[256,257]. In fatty liver cell death occurs predominantly by necrosis, whilst apoptosis was dominant in normal liver after IRI. Necrosis is more damaging because it is accompanied by the breakdown of organelles, membranes and the release of cytotoxic cell contents, which induce inflammation, whereas, apoptosis does not. This may contribute to making fatty liver less tolerant to IRI injury[256]. Fatty liver has diminished sinusoidal spaces due to fatty infiltration[239] and inflammatory mediators such as TNF-α and leukocytes cause a further decrease in sinusoidal space and impairs microcirculation which reduces blood flow to certain areas resulting in prolonged periods of ischaemia to certain areas of the liver. This causing activation of KC and other mechanisms of IRI[569].

Glanemann et al have shown that IPC protects normal liver from IRI by maintaining hepatic microcirculation and reducing inflammatory response by preventing activation of KC and maintaining mitochondrial redox state which is dependent upon oxygen availability[34].

In chapter eight, a deeper understanding of the use of ^{1}HNMR in emerged through the use of bile redox ratios instead of measuring separate constituents. The energetic balance and redox status of hepatic tissue are intimately connected by substrate oxidation/reduction reactions *via* oxidized nicotinamide adenine dinucleotide

(phosphate) (NAD(P)) at several key points, such as pyruvate/lactate interconversion in the cytosol or βHb/AcAc interconversion in the mitochondria also known as the ketone body ratio.

βHb and AcAc are a redox pair coupled by interconversion from AcAc (with oxidation of NADH) to βHb and the βHb/AcAc ratio is an indicator of mitochondrial redox status[570]. βHb/AcAc equilibrates with hepatic mitochondrial NADH/NAD^+ because the enzyme, β-hydroxybutyrate dehydrogenase, resides in mitochondrial cristae[571] (figure 3b). In the IPC+I/R group more of the "oxidized" half of the couplet (AcAc) could be detected in bile, this suggests a shift toward more aerobic conditions in the mitochondria. This could lead to more aerobic conditions within the cytosol and, thus, the reconversion of lactate to pyruvate during reperfusion, lactate and pyruvate being a redox pair that is an indicator of the cytosolic redox state. This is supported by our findings of decreased lactate/pyruvate ratio in the IPC+I/R group during reperfusion.

Hirakawa et al have shown in normal rat liver cytochrome *c* is released into the cytosol by mitochondria during IRI[574]. It is a mediator of apoptosis inducing caspase 3 and 9 activation, which mediate apoptosis. The release of cytochrome *c* and caspases occurred during ischaemia, yet, apoptosis occurred during reperfusion in normal liver[575]. The release of cytochrome *c* is mediated by the mPTP, a voltage-dependent high-conductance channel of the inner mitochondrial membrane[576]. The pore is normally closed, but is opened at the onset of reperfusion. When cytochrome *c* is released there is no substrate for COX resulting in a decrease in ATP synthesis and mitochondrial function. COX directly binds to oxygen and its activity results in ATP synthesis. The rate of ATP synthesis is directly dependent on redox state of mitochondria. There is only a shortage in cytochrome *c* if the mPTP in the membrane remains open. The mPTP may remain open in the fatty liver leading to necrosis. IPC of the heart prevents the mPTP opening; it is possible that a similar situation occurs in

fatty liver[577].

The presence of non-esterified fatty acids in fatty liver is associated with the decrease in ATP as compared to a normal liver under normal conditions. It has been proposed that the reason fatty liver chooses to undergo necrosis rather than apoptosis is due to a decrease in ATP[256,265]. ATP is essential for apoptosis. Selzner et al have proved that IPC protects fatty liver against necrosis[265]. This may be because IPC maintains ATP levels in fatty liver. This is supported by the results of this experiment that suggest that the IPC+I/R group was in a more “oxidized” state than the I/R group.

Chandel et al studied whether hypoxia leads to suppression of electron transport chain and whether COX was involved in this process[578]. They showed that oxygen availability determines COX activity. Chandel et al support the reversible two transition state COX model proposed by Wilson et al[579]. Wilson et al proposed that COX switches reversibly between two states of activity, suggesting that COX may possess two different binding sites for oxygen[579]. One binding site decreased whereas the other increased ATP production. The switch between the two states of activity is said to be faster from low activity, in low oxygen states, to high activity when oxygen levels return to normal. This phenomenon is seen during the transition from baseline to end of ischaemia in the results, it takes time for activity to drop along with a decrease in oxygen. The faster change is seen in figure 47 because on reperfusion after extended ischaemia the IPC+I/R group shows a surge in COX activity, which is higher than the initial baseline value. This is also seen in the IPC+I/R group after a brief period of 5 minutes of ischaemia, on reperfusion there is a much higher COX activity than baseline. Suggesting oxygen supply is sufficient for Complex IV of the electron transport chain, ATP generation and COX function is normal. Improved extracellular oxygenation in IPC+I/R compared to I/R may be the main way in which IPC works to preserve mitochondrial function and blood flow preventing inflammation.

This experiment shows there is *in vivo* and *in vitro* preservation of COX activity in fatty livers, which are preconditioned in comparison to those that are not. This suggests that the mPTP may close after opening briefly on reperfusion and cytochrome *c* and oxygen are available as substrates for COX, as in normal liver. It is likely that ATP synthesis continues and if cell death were to occur, apoptosis may be more likely to be triggered than necrosis, i.e. there is a switch to the apoptotic pathway. A switch away from necrosis in fatty liver means there is less necrosis-induced inflammation, release of inflammatory mediators, activation of KCs and leukocytes and leukocyte and platelet adhesion to sinusoidal epithelial cells. The hepatic microcirculation and tissue perfusion would be maintained. This would lead to sustained oxygen delivery to mitochondria and would therefore maintain COX activity. Continued oxygen supply means that COX would probably be in a high active transition state with high ATP turnover, whereas a low active state may be related to necrotic pathway. A high active COX state may induce the mPTP to close[580]. A higher COX activity state is less likely to follow the necrotic pathway due to increased ATP production.

In conclusion, these experiments set out to discover if bile composition changed during IRI and its modulation, through 1HNMR analysis, and find a biomarker through that could effectively indicate IRI, particularly in steatotic livers, as well as exploring methods of modulating IRI in steatotic livers, that are increasingly being used in transplantation. The results have shown a consistent set of changes in composition, throughout several experiments, and use of redox ratios more closely mirrors liver energetic than any one particular marker.

10 Appendix

10.1 Quantification of biliary constituents in micromolar concentrations

10.1.1 Introduction

In chapters four and five, one of the limitations that were faced was the lack of quantification of bile constituents. Bile composition was expressed as a percentage of baseline values, in accordance with previously published reports[18]. Through a valid technique, we sought to quantify the constituents to gain a more accurate insight into the changes that developed during I/R.

10.1.2 Materials and Methods

A series of ascending known concentrations of taurocholic acid (TCA; Sigma-Aldrich, St Louis, Missouri, USA) in distilled water were analysed from 0.1-100 mMols. A methyl peak at 0.665 ppm was identified and the area under the curve integrated for each concentration. ^{1}HNMR analysis was performed on an 11.7 T (500 MHz for protons) spectrometer (Varian Unity+; Varian, Palo Alto, CA, USA) at 25°C. For a field/frequency lock a coaxial capillary insert was used (Wilmad, Buena, NJ, USA). This capillary insert was filled with a deuterium oxide solution of sodium TSP that acted as a chemical shift reference. One dimensional NMR spectra were obtained at 500MHz with a sweep width of 6kHz. The spectra were analysed using software from MestRe-C version 3.1.1 (Universidade de Santiage de Compostela, Spain).

10.1.3 Results

A taurocholic acid spectrum is shown in figure 52. The results of integration of the area under the curve of a C-18 methyl proton peak[12] at 0.7 ppm are shown in figure 53. This standard curve was then used to calculate concentrations of other peaks.

Figure 52: [1]HNMR spectra of taurocholic acid

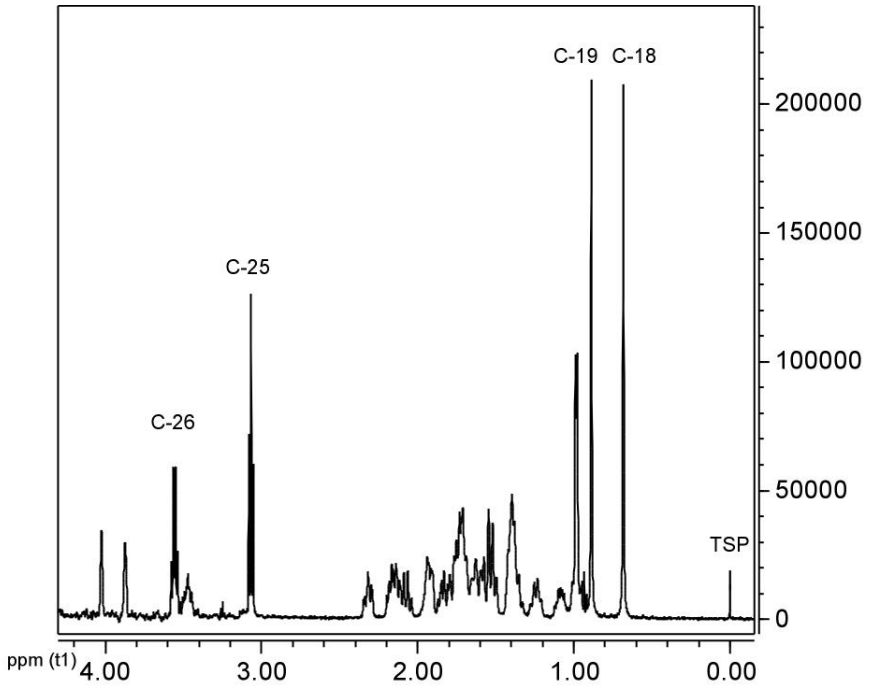

Figure 53: Standard curve for quantification

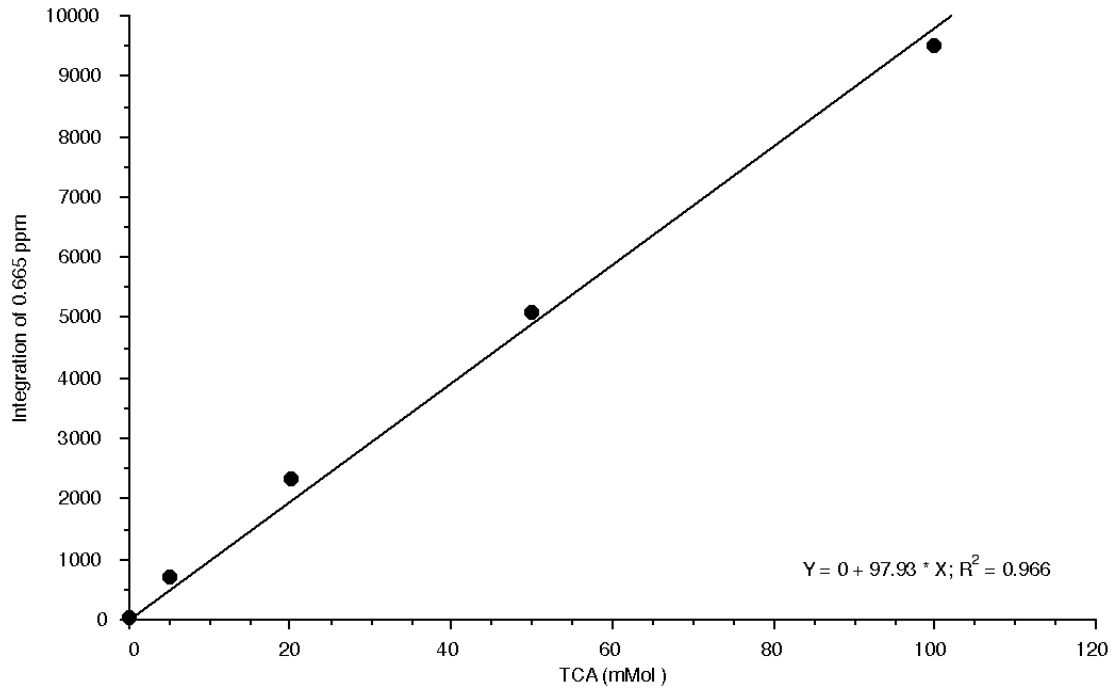

10.2 Localization of overlapping peaks acetoacetate and pyruvate

10.2.1 Introduction

In chapters eight, one of the limitations that were faced was overlapping peaks of pyruvate (2.38 ppm, CH_3 singlet) and acetoacetate (2.29 ppm, CH_3 singlet) that made it difficult to identify acetoacetate. At this region in the bile spectra, there were multiple small peaks, and it was not entirely clear, which could be attributed to which (figure 55a).

10.2.2 Materials and Methods

A 300μL sample of control bile was analysed initially as below, then augmented with 100μL of molar pyruvic acid (Sigma-Aldrich, St Louis, Missouri, USA). This sample was analysed as below, then a further 100μL of molar acetoacetic acid ethyl ester (Sigma-Aldrich, St Louis, Missouri, USA) was added and then reanalysed. ^{1}HNMR analysis was performed on an 11.7T (500 MHz for protons) spectrometer (Varian Unity+; Varian, Palo Alto, CA, USA) at 25°C. For a field/frequency lock a coaxial capillary insert was used (Wilmad, Buena, NJ, USA). This capillary insert was filled with a deuterium oxide solution of sodium TSP that acted as a chemical shift reference. One dimensional NMR spectra were obtained at 500MHz with a sweep width of 6kHz. The spectra were analysed using software from MestRe-C (Universidade de Santiage de Compostela, Santiage de Compostela, Spain).

10.2.3 Results

A normal bile sample is shown in figure 54a, and when it was augmented with pyruvate, there was a clear increase in one of the peaks shown in figure 54b. A pyruvate-augmented sample is shown in figure 55a. While the pyruvate and acetoacetate-augmented sample is shown in figure 55b. A clearer difference was discernable after augmentation, and peak assignments for pyruvate (2.38 ppm) and acetoacetate (3.45 ppm) were used.

Figure 54: [1]HNMR spectra of normal and pyruvate-augmented bile

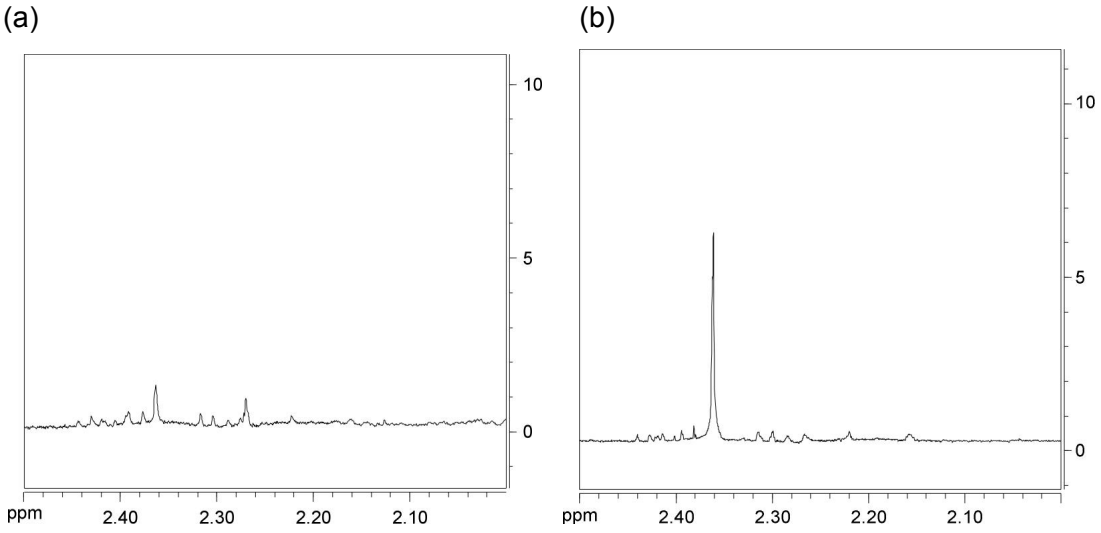

[1]HNMR spectra scaled to TSP of (a) a normal bile sample and (b) augmented with pyruvate (scale in ppm).

Figure 55: [1]HNMR spectra of pyruvate- and acetoacetate-augmented bile

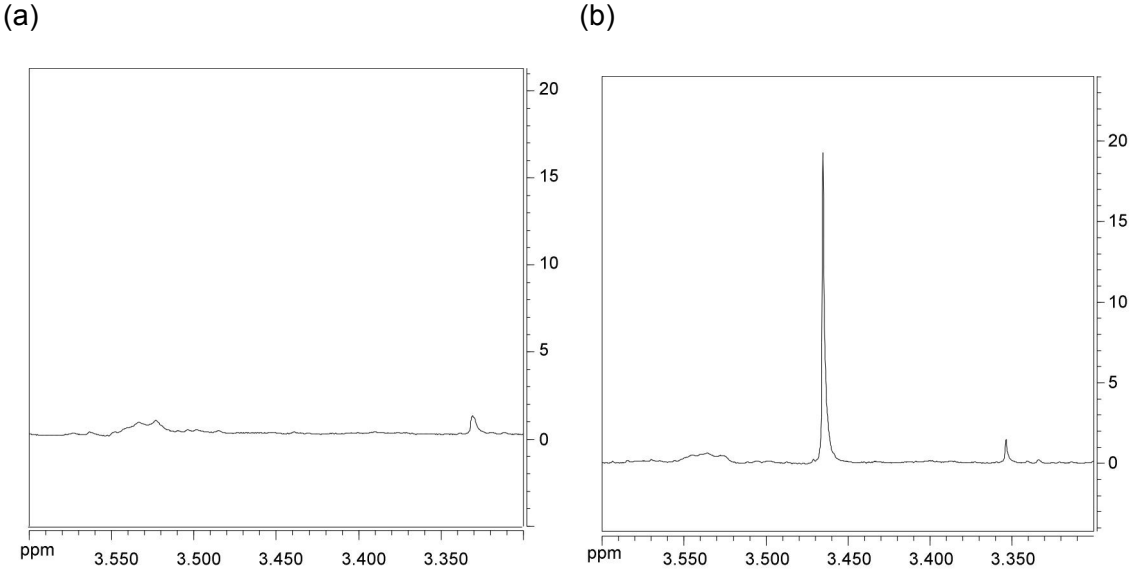

[1]HNMR spectra scaled to TSP of (a) a pyruvate-augmented bile sample and (b) a bile sample augmented with pyruvate and acetoacetate (scale in ppm).

10.3 Presentations and publications arising from this thesis

10.3.1 Conference presentations

1. Sheth H, **Hafez T**, Glantzounis G, Parkes HG, Seifalian A, Fuller B, Davidson BR: Intravenous glycine improves bile flow and modulates bile composition in a in-vivo warm liver ischaemia reperfusion injury model. Annual Meeting of the Society of Academic and Research Surgery **(SARS), Edinburgh**, UK, 11-13/1/2006
2. **Hafez T**, Sheth H, Glantzounis G, Yang W, Parkes HG, Seifalian A, Fuller B, Davidson BR: Bile flow and composition are modulated by intravenous glycine in an in-vivo warm ischaemia-reperfusion injury model. Annual Meeting of the British Society of Gastroentrology **(BSG), Glasgow**, Scotland, 21-24/3/2004
3. Sheth H, **Hafez T**, Glantzounis G, Sales KM, Seifalian A, Fuller B, Davidson BR: Glycine ameliorates the early phase of liver warm ischaemia reperfusion injury in a rabbit model. Annual Meeting of the British Society of Gastroentrology, **(BSG), Glasgow**, Scotland, 21-24/3/2004
4. **Hafez T**, Fusai G, Glantzounis G, Yang W, Sheth H, Kanoria S, Parks HG, Seifalian AM, Davidson BR: N-Acetylcysteine modulates bile composition following liver ischaemia-reperfusion injury in an experimental model with fatty liver. Society of Academic and Research Surgery **(SARS), Belfast**, UK, 14-16/1/2004
5. Glantzounis GK, **Hafez TS,** Cox IJ, Sheth H, Yang W, Seifalian AM, Fuller BJ, Davidson BR: The use of magnetic spectroscopy bile analysis as a tool for the assessment of antioxidant therapy in liver ischaemia-reperfusion injury. 13th Pan-Hellenic Congress of Transplantation, **Athens,** Greece, 11-13/12/2003
6. **Hafez T**, Glantzounis GK, Cox IJ, Sheth H, Yang W, Seifalian AM, Fuller B, Davidson BR: N-acetylcysteine (NAC) and liver warm ischaemia reperfusion injury: alterations to bile composition demonstrated by proton nuclear magnetic

resonance spectroscopy (MRS). 38th Annual Meeting of the European Association for the Study of the Liver **(EASL), Geneva**, Switzerland 2-6/7/2003

7. **Hafez T**, Glantzounis GK, Cox IJ, Yang W, Seifalian AM, Fuller B, Davidson BR: N-acetylcysteine and liver warm ischaemia reperfusion injury: alterations to bile composition demonstrated by proton nuclear magnetic resonance spectroscopy. Society of Academic and Research Surgery **(SARS), Leeds**, UK, 9-10/1/2003

10.3.2 Abstracts

1. Sheth H, Glantzounis G, **Hafez T,** Quaglia A, Duncan J, Davidson BR. Does perioperative N-acetylcysteine prevents ischaemia-reperfusion injury during liver resection? A prospective randomised double blind clinical trial. **Gut** 2005;54(Suppl 2):148.
2. **Hafez T**, Sheth H, Glantzounis G, Yang W, Parkes HG, Seifalian A, Fuller B, Davidson BR: Bile flow and composition are modulated by intravenous glycine in an in-vivo warm ischaemia-reperfusion injury model. ***Gut*** 2004;53 (Suppl 3):A36
3. Sheth H, **Hafez T**, Glantzounis G, Sales KM, Seifalian A, Fuller B, Davidson BR: Glycine ameliorates the early phase of liver warm ischaemia reperfusion injury in a rabbit model. ***Gut*** 2004;53 (Suppl 3):A92
4. **Hafez TS**, Glantzounis GK, Cox IJ, Sheth H, Yang W, Seifalian AM, Fuller B, Davidson BR: N-acetylcysteine and liver warm ischaemia reperfusion injury: alterations to bile composition demonstrated by proton nuclear magnetic resonance spectroscopy. ***Journal of Hepatology*** 2003;38(Suppl 2):39
5. **Hafez T,** Glantzounis GK, Cox IJ, Yang W, Seifalian AM, Fuller B, Davidson BR: N-acetylcysteine and liver warm ischaemia reperfusion injury: alterations to bile composition demonstrated by proton nuclear magnetic resonance spectroscopy. ***British Journal of Surgery*** 2003;90:604

10.3.3 Original articles

1. **Tariq Hafez,** Georgios Glantzounis, I Jane Cox, Hemant Sheth, Alexander Seifalian, Barry Fuller, Brian Davidson: Bile composition is modified by ischaemia reperfusion injury and attenuated by N-acetylcysteine: a proton nuclear magnetic resonance study. ***Journal of Gastroenterology and Hepatology*** *(submitted)*

2. **Tariq S. Hafez,** George K. Glantzounis, Guiseppe Fusai, Jan-Willem Taanman, Primeera Wignarajah, Harry Parkes, Barry Fuller, Brian R. Davidson, Alexander M. Seifalian: Intracellular oxygenation and cytochrome oxidase C activity in ischemic preconditioning of steatotic rabbit liver. ***The American Journal of Surgery*** 2010;200(4):507–18

3. Glantzounis G, Sheth H, Thompson C, **Hafez T,** Kanoria S, Pamecha V, Davies S, Mikhailidis D, Seifalian A, Davidson B: Acute limb ischaemia caused by femoral arterial line induces remote liver injury in a rabbit model of liver ischaemia/reperfusion injury ***Angiology*** 2009;60(5):554-61

4. **Hafez T,** Sheth H, Glantzounis G, Parkes H, Seifalian A, Fuller B, Davidson B: Glycine protects bile physiology and biliary-specific liver cell metabolism from ischaemia-reperfusion injury: A ^{1}HNMR Study ***Cell Preservation Technology*** 2008;6:173–180

5. Fusai G, Glantzounis G, **Hafez T**, Yang W, Quaglia A, Sheth H, Kanoria S, Parkes H, Seifalian A, Davidson BR: N-acetylcysteine ameliorates the late phase of liver ischaemia-reperfusion injury in the rabbit with hepatic steatosis ***Clinical Science (London)*** 2005;109:465-73

6. **Hafez TS,** Habib M, Seifalian A, Fuller B, Davidson B: Near infrared spectroscopic assessment of mitochondrial oxygenation status: comparison during normothermic extracorporeal liver perfusion by buffer only or buffer fortified with red blood cells ***Transplantation Proceedings*** 2004;36:1265–1267

7. Habib MM, **Hafez TS**, Parkes HG, Seifalian AM, Fuller BJ, Davidson BR. A comparison of bile composition from heart-beating and non-heart-beating rabbit organ donors during normothermic extracorporeal liver perfusion: experimental evaluation using proton magnetic resonance spectroscopy. ***Transplantation Proceedings*** 2004;36(10):2914-6.

Book chapters:

1. **Hafez T**, Fuller B. Applications: Organ Preservation for Transplantation. In: Baust JG, Baust JM, (eds). ***Advances in biopreservation***. Boca Raton, Fla.: CRC; London: Taylor & Francis [distributor]; 2007 pp197-270. (ISBN 0-849-32772-5)

2. Yang W, **Hafez T**, Thompson C, Mikhailidis DP, Davidson BR, Winslet MC, Seifalian AM: The effect of graded systemic hypoxaemia on hepatic tissue oxygenation in Thorniley MS, Harrison DK and James PE (Eds): ***Oxygen transport to tissue XXV*** Advances in Experimental Medicine and Biology, Volume 540, Kluwer Academic/Plenum Publishers, New York, 2003 pp317-323 (ISBN 0-306-48035-2)

11 References

1. Harper AM, Edwards EB and Ellison MD. The OPTN waiting list, 1988-2000. Clin Transpl 2001:73-85.

2. Cameron A and Busuttil RW. AASLD/ILTS transplant course: is there an extended donor suitable for everyone? Liver Transpl 2005;11(11 Suppl 2):S2-5.

3. Ploeg RJ, D'Alessandro AM, Knechtle SJ, Stegall MD, Pirsch JD, Hoffmann RM, Sasaki T, Sollinger HW, Belzer FO and Kalayoglu M. Risk factors for primary dysfunction after liver transplantation--a multivariate analysis. Transplantation 1993;55(4):807-13.

4. Strasberg SM, Howard TK, Molmenti EP and Hertl M. Selecting the donor liver: risk factors for poor function after orthotopic liver transplantation. Hepatology 1994;20(4 Pt 1):829-38.

5. Beckmann N, Hof RP and Rudin M. The role of magnetic resonance imaging and spectroscopy in transplantation: from animal models to man. NMR Biomed 2000;13(6):329-48.

6. Directorate SaA. Transplant Activity in the UK. Bristol, UK: NHS Blood and Transplant; 2009.

7. Olsen TS. Pathology of allograft rejection In: Burdick JF, editor. Kidney transplant rejection : diagnosis and treatment. 2nd ed. New York: Dekker; 1992. p. 333.

8. Small DM, Penkett SA and Chapman D. Studies on simple and mixed bile salt micelles by nuclear magnetic resonance spectroscopy. Biochim Biophys Acta 1969;176(1):178-89.

9. Stark RE, Gosselin GJ, Donovan JM, Carey MC and Roberts MF. Influence of dilution on the physical state of model bile systems: NMR and quasi-elastic light-scattering investigations. Biochemistry 1985;24(20):5599-605.

10. Ellul JP, Murphy GM, Parkes HG, Slapa RZ and Dowling RH. Nuclear magnetic resonance spectroscopy to determine the micellar cholesterol in human bile. FEBS Lett 1992;300(1):30-2.

11. Sequeira SS, Parkes HG, Ellul JP and Murphy GM. In vitro determination by 1H-NMR studies that bile with shorter nucleation times contain cholesterol-enriched vesicles. Biochim Biophys Acta 1995;1256(3):360-66.

12. Ishikawa H, Nakashima T, Inaba K, Mitsuyoshi H, Nakajima Y, Sakamoto Y, Okanoue T, Kashima K and Seo Y. Proton magnetic resonance assay of total and taurine-conjugated bile acids in bile. J Lipid Res 1999;40(10):1920-24.

13. Pollesello P, Eriksson O, Kvam BJ, Paoletti S and Saris NE. 1H-NMR studies of lipid extracts of rat liver mitochondria. Biochem Biophys Res Commun 1991;179(2):904-11.

14. Vejchapipat P, Eaton S, Fukumoto K, Parkes HG, Spitz L and Pierro A. Hepatic glutamine metabolism during endotoxemia in neonatal rats. Nutrition 2002;18(4):293-7.

15. Scarpa M, Corazza A, Vianello F, Rigo A, Furian L, Baldan N and Rigotti P. Deuterium nuclear magnetic resonance for evaluating the metabolic status of livers subjected to warm ischemia. Transplantation 2001;71(11):1515-7.

16. Hayakawa Y, Yoshioka Y and Yasuda N. Effects of ligation and reperfusion of hepatic afferent vessels on the composition of liver cell membrane in the rat: 1H- and 31P-magnetic resonance spectroscopic analysis. NMR Biomed 1997;10(6):257-62.

17. Powell J, Gartland K, Lombard M, Sallie R, Nicholson J and Thompson R. Proton NMR spectroscopy of bile as a marker of liver function in liver transplant patients [abstract]. Clin Sci (Colch) 1990;78:13P.

18. Melendez HV, Ahmadi D, Parkes HG, Rela M, Murphy G and Heaton N. Proton nuclear magnetic resonance analysis of hepatic bile from donors and recipients in human liver transplantation. Transplantation 2001;72(5):855-60.

19. Prescot AP, Collins DJ, Leach MO and Dzik-Jurasz AS. Human gallbladder bile: noninvasive investigation in vivo with single-voxel 1H MR spectroscopy. Radiology 2003;229(2):587-92.

20. Kunnecke B, Bruns A and von Kienlin M. Non-invasive analysis of gallbladder bile composition in cynomolgus monkeys using in vivo 1H magnetic resonance spectroscopy. Biochim Biophys Acta 2007;1771(4):544-9.

21. Boyer JL. Bile duct epithelium: frontiers in transport physiology. Am J Physiol 1996;270(1 Pt 1):G1-5.

22. Trauner M and Boyer JL. Bile salt transporters: molecular characterization, function, and regulation. Physiol Rev 2003;83(2):633-71.

23. Smith IC and Blandford DE. Nuclear magnetic resonance spectroscopy. Anal Chem 1995;67(12):509R-18R.

24. Vilca Melendez H, Rela M, Murphy G and Heaton N. Liver transplantation and bile analysis: a parallel evolution. Transplantation 1998;65(10):1289-93.

25. Bowers BA, Branum GD, Rotolo FS, Watters CR and Meyers WC. Bile flow--an index of ischemic injury. J Surg Res 1987;42(5):565-9.

26. Prandi D. Canalicular bile production in man. Eur J Clin Invest 1975;5(1):1-6.

27. Hofmann AF. Bile acid secretion, bile flow and biliary lipid secretion in humans. Hepatology 1990;12(3 Pt 2):17S-22S; discussion 22S-25S.

28. McCashland TM, Donovan JP, Amelsberg A, Rossi SS, Hofmann AF, Shaw BW, Jr. and Quigley EM. Bile acid metabolism and biliary secretion in patients receiving orthotopic liver transplants: differing effects of cyclosporine and FK 506. Hepatology 1994;19(6):1381-9.

29. Murphy GM. Serum bile acids. In: Setchell KDR, Kritchevsky D and Nair PP, editors. The bile acids; chemistry, physiology, and metabolism. New York: Plenum Press; 1988. p. 379.

30. Sherlock S and Dooley J. Diseases of the liver and biliary system. 9 ed. Oxford: Blackwell Scientific Publications; 1993.

31. Meier PJ. The bile salt secretory polarity of hepatocytes. J Hepatol 1989;9(1):124-9.

32. Nathanson MH and Boyer JL. Mechanisms and regulation of bile secretion. Hepatology 1991;14(3):551-66.

33. Erlinger S and Dhumeaux D. Mechanisms and control of secretion of bile water and electrolytes. Gastroenterology 1974;66(2):281-304.

34. Glanemann M, Vollmar B, Nussler AK, Schaefer T, Neuhaus P and Menger MD. Ischemic preconditioning protects from hepatic ischemia/reperfusion-injury by preservation of microcirculation and mitochondrial redox-state. J Hepatol 2003;38(1):59-66.

35. Hellinger A, Fiegen R, Lange R, Rauen U, Schmidt U, Hirche H, Kaiser S, de Groot H, Erhard J and Eigler FW. Preservation of pig liver allografts after warm ischemia:

normothermic perfusion versus cold storage. Langenbecks Arch Chir 1997;382(4):175-84.

36. McEnroe CS, Pearce FJ, Ricotta JJ and Drucker WR. Failure of oxygen-free radical scavengers to improve postischemic liver function. J Trauma 1986;26(10):892-6.

37. Nakano H, Nagasaki H, Barama A, Boudjema K, Jaeck D, Kumada K, Tatsuno M, Baek Y, Kitamura N, Suzuki T and Yamaguchi M. The effects of N-acetylcysteine and anti-intercellular adhesion molecule-1 monoclonal antibody against ischemia-reperfusion injury of the rat steatotic liver produced by a choline-methionine-deficient diet. Hepatology 1997;26(3):670-8.

38. Sundberg R, Lindell S, Jamieson NV, Southard JH and Belzer FO. Effects of chlorpromazine and methylprednisolone on perfusion preservation of rabbit livers. Cryobiology 1988;25(5):417-24.

39. Terajima H, Enders G, Thiaener A, Hammer C, Kondo T, Thiery J, Yamamoto Y, Yamaoka Y and Messmer K. Impact of hyperthermic preconditioning on postischemic hepatic microcirculatory disturbances in an isolated perfusion model of the rat liver. Hepatology 2000;31(2):407-15.

40. Jamieson NV, Sundberg R, Lindell S, Southard JH and Belzer FO. A comparison of cold storage solutions for hepatic preservation using the isolated perfused rabbit liver. Cryobiology 1988;25(4):300-10.

41. Sumimoto K, Inagaki K, Yamada K, Kawasaki T and Dohi K. Reliable indices for the determination of viability of grafted liver immediately after orthotopic transplantation. Bile flow rate and cellular adenosine triphosphate level. Transplantation 1988;46(4):506-9.

42. Adam R, Bismuth H, Diamond T, Ducot B, Morino M, Astarcioglu I, Johann M, Azoulay D, Chiche L, Bao YM and et al. Effect of extended cold ischaemia with UW solution on graft function after liver transplantation. Lancet 1992;340(8832):1373-6.

43. Anthuber M, Farkas S, Rihl M, Menger MD, Jauch KW, Schildberg FW and Messmer K. Conditioning of liver grafts by donor bolus pretreatment with epoprostenol. Transplantation 1996;62(1):13-7.

44. Fisher RA, Posner MP, Shiffman ML, Mills AS, Contos MJ, Beeston J, Bowman T, Wolfe L and Lee HM. Adenosine rinse in human orthotopic liver transplantation: results of a randomized, double-blind trial. Int J Surg Investig 1999;1(1):55-66.

45. Koeppel TA, Lehmann TG, Thies JC, Gehrcke R, Gebhard MM, Herfarth C, Otto G and Post S. Impact of N-acetylcysteine on the hepatic microcirculation after orthotopic liver

transplantation. Transplantation 1996;61(9):1397-402.

46. Rentsch M, Post S, Palma P, Gonzalez AP, Menger MD and Messmer K. Intravital studies on beneficial effects of warm Ringer's lactate rinse in liver transplantation. Transpl Int 1996;9(5):461-7.

47. Javitt NB, Fortner JG and Shiu MH. Bile salt synthesis in transplanted human liver. Gastroenterology 1971;60(3):405-8.

48. Waldram R, Kemp A, Williams R and Calne RY. Bile secretion following liver transplantation in man [Abstract]. Gut 1973;14(10):819-20.

49. Waldram R, Williams R and Calne RY. Bile composition and bile cast formation after transplantation of the liver in man. Transplantation 1975;19(5):382-7.

50. Starzl TE, Putnam CW, Hansbrough JF, Porter KA and Reid HA. Biliary complications after liver transplantation: with special reference to the biliary cast syndrome and techniques of secondary duct repair. Surgery 1977;81(2):212-21.

51. Calne RY. A new technique for biliary drainage in orthotopic liver transplantation utilizing the gall bladder as a pedicle graft conduit between the donor and recipient common bile ducts. Ann Surg 1976;184(5):605-9.

52. McMaster P, Herbertson BM, Cusick C, Calne RY, Syrakos T and Marni A. The development of biliary "sludge" following liver transplantation. Transplant Proc 1979;11(1):262-6.

53. McMaster P, Herbertson B, Cusick C, Calne RY and Williams R. Biliary sludging following liver transplantation in man. Transplantation 1978;25(2):56-62.

54. McMaster P. Bile studies after liver transplantation. Ann R Coll Surg Engl 1979;61(6):435-40.

55. Haagsma EB, Huizenga JR, Vonk RJ, Albers CJ, Grond J, Krom RA and Gips CH. Composition of bile after orthotopic liver transplantation. Scand J Gastroenterol 1987;22(9):1049-55.

56. Shiffman ML, Carithers RLJ, Mendez-Picon G, Posner M and Moore EW. Bile secretion following orthotopic liver transplantation (OLT): effects of rejection on bile flow and bile acid secretion [Abstract]. Hepatology 1988;8:1292.

57. Bowers BA, Rotolo FS, Watters CR, Cucchiaro G, Branum GD and Meyers WC. Regulation of biliary secretion following liver transplantation. Transplant Proc 1989;21(3):3554.

58. Farouk M, Branum GD, Watters CR, Cucchiaro G, Helms M, McCann R, Bollinger R and Meyers WC. Bile compositional changes and cholesterol stone formation following orthotopic liver transplantation. Transplantation 1991;52(4):727-30.

59. Tisone G, Angelico M, Baiocchi L, Nistri A, Pisani F, Gandin C, Romagnoli J, Anselmo A and Umberto Casciani C. Patterns of bile salts and biliary lipids early after liver transplantation differentiate patients with unfavourable graft outcome. Transplant Proc 1996;28(3):1655-6.

60. Shiffman ML, Carithers RL, Jr., Posner MP and Moore EW. Recovery of bile secretion following orthotopic liver transplantation. J Hepatol 1991;12(3):351-61.

61. Theilmann L, Otto G, Arnold J, Gmelin K and Stiehl A. Biliary secretion of bile acids, lipids, and bilirubin by the transplanted liver. A quantitative study in patients on cyclosporine. Transplantation 1991;52(6):1020-3.

62. Friman S, Persson H, Karlberg I and Svanvik J. The bile-acid-independent flow is reduced in the transplanted liver. Transplant Proc 1992;24(1):396-7.

63. Le Thai B, Dumont M, Michel A, Erlinger S and Houssin D. Cholestatic effect of cyclosporine in the rat. An inhibition of bile acid secretion. Transplantation 1988;46(4):510-2.

64. Dahlback-Sjoberg H, Bjorkhem I and Princen HM. Selective inhibition of mitochondrial 27-hydroxylation of bile acid intermediates and 25-hydroxylation of vitamin D3 by cyclosporin A. Biochem J 1993;293 (Pt 1):203-6.

65. Ericzon BG, Wijnen RM, Tiebosch A, Kubota K, Kootstra G and Groth CG. The effect of FK506 treatment on pancreaticoduodenal allotransplantation in the primate. Transplantation 1992;53(6):1184-9.

66. Ericzon BG, Angelin B and Einarsoon K. Changes in bile secretion after liver transplantation. In: Fromm H and Leuchner U, editors. Falk symposium 84. Bile acids-cholestasis-gallstones: advances in basic and clinical bile acid research. Dordrecht: Kluwer Academic Publishers; 1995. p. 53.

67. Ericzon BG. Early graft function in liver transplantation patients. Transplant Proc 1994;26(6):3276-8.

68. Sauer P, Stiehl A, Otto G and Theilmann L. In patients with orthotopic liver transplantation, serum markers of cholestasis are unreliable indicators of biliary secretion. J Hepatol 1995;22(5):561-4.

69. Sauer P, Rudolph G, Endele R, Senn M, Theilmann L, Otto G, Stremmel W and Stiehl A.

Kinetics of primary bile acids in patients after orthotopic liver transplantation. Eur J Clin Invest 1996;26(11):979-82.

70. Ericzon BG, Eusufzai S, Soderdahl G, Duraj F, Einarsson K and Angelin B. Secretion and composition of bile after human liver transplantation: studies on the effects of cyclosporine and tacrolimus. Transplantation 1997;63(1):74-80.

71. Codoceo R, Jara P, Diaz MC, Magallon M, Camarena C, Hierro L, De LaVega A, Pardo F and Cienfuegos JA. Changes of bile acid profile and coagulation during orthotopic liver transplantation. Transplant Proc 1989;21(1 Pt 2):2351-2.

72. Herrera J, Codoceo R, Mora NP, Pereira F, Jara P, Pardo F, Cienfuegos JA and Castillo-Olivares JL. Bile acid profile as an early indicator of allograft function during orthotopic liver transplantation. Transplant Proc 1989;21(1 Pt 2):2313-4.

73. Mora NP, Cienfuegos JA, Codoceo R, Jara P, Tendillo FJ, Menchaca C, Berisa F, Navidad R and Castillo-Olivares JL. Monitoring of serum total bile acids as an early indicator of graft function in clinical and experimental liver transplantation. Transplant Proc 1987;19(5):3840-1.

74. Kohlhaw K, Canello R, Ringe B, Hauss J, Schumann G, Oellerich M and Pichlmayr R. Evaluation of hepatic excretory system function by determination of serum bile acid clearance early after liver transplantation. Transplant Proc 1992;24(6):2699-700.

75. Muraca M, Kohlhaw K, Vilei MT, Ringe B, Bunzendahl H, Gubernatis G, Wonigeit K, Brunner G and Pichlmayr R. Serum bile acids and esterified bilirubin in early detection and differential diagnosis of hepatic dysfunction following orthotopic liver transplantation. J Hepatol 1993;17(2):141-5.

76. Azer SA, McCaughan GW and Stacey NH. Daily determination of individual serum bile acids allows early detection of hepatic allograft dysfunction. Hepatology 1994;20(6):1458-64.

77. Baumgartner U, Scholmerich J, Kremer B, Streckfuss G, Henne-Bruns D, Mergard BL, Kraemer-Hansen H and Farthmann EH. Early detection of graft dysfunction after orthotopic liver transplantation in man by serum and biliary bile acid analysis. Hepatogastroenterology 1995;42(6):950-60.

78. Baiocchi L, Tisone G, Nistri A, Pisani F, Anselmo A, Gandin C, Angelico M and Casciani C. Sequential changes in serum and biliary bile acids after liver transplantation. Transplant Proc 1995;27(6):3503-4.

79. Halliwell B and Gutteridge JMC. Free radicals in biology and medicine. 4th ed. ed.

Oxford: Oxford University Press; 2007.

80. Ames BN, Shigenaga MK and Hagen TM. Oxidants, antioxidants, and the degenerative diseases of aging. Proc Natl Acad Sci U S A 1993;90(17):7915-22.

81. Yu BP. Cellular defenses against damage from reactive oxygen species. Physiol Rev 1994;74(1):139-62.

82. Beckman KB and Ames BN. Oxidative decay of DNA. J Biol Chem 1997;272(32):19633-6.

83. Frank J, Pompella A and Biesalski HK. Histochemical visualization of oxidant stress. Free Radic Biol Med 2000;29(11):1096-105.

84. Sutton HC and Winterbourn CC. On the participation of higher oxidation states of iron and copper in Fenton reactions. Free Radic Biol Med 1989;6(1):53-60.

85. Lander HM. An essential role for free radicals and derived species in signal transduction. Faseb J 1997;11(2):118-24.

86. Adler V, Yin Z, Tew KD and Ronai Z. Role of redox potential and reactive oxygen species in stress signaling. Oncogene 1999;18(45):6104-11.

87. Pahl HL and Baeuerle PA. Oxygen and the control of gene expression. Bioessays 1994;16(7):497-502.

88. Arrigo AP. Gene expression and the thiol redox state. Free Radic Biol Med 1999;27(9-10):936-44.

89. Glantzounis GK, Salacinski HJ, Yang W, Davidson BR and Seifalian AM. The contemporary role of antioxidant therapy in attenuating liver ischemia-reperfusion injury: a review. Liver Transpl 2005;11(9):1031-47.

90. Gutteridge JM. Lipid peroxidation and antioxidants as biomarkers of tissue damage. Clin Chem 1995;41(12 Pt 2):1819-28.

91. Sies H. Oxidative stress : oxidants and antioxidants: Academic Press; 1991.

92. Marczin N, El-Habashi N, Hoare GS, Bundy RE and Yacoub M. Antioxidants in myocardial ischemia-reperfusion injury: therapeutic potential and basic mechanisms. Arch Biochem Biophys 2003;420(2):222-36.

93. Vertuani S, Angusti A and Manfredini S. The antioxidants and pro-antioxidants network: an overview. Curr Pharm Des 2004;10(14):1677-94.

94. Davis W, Jr., Ronai Z and Tew KD. Cellular thiols and reactive oxygen species in drug-induced apoptosis. J Pharmacol Exp Ther 2001;296(1):1-6.

95. Dufaure JP, Lareyre JJ, Schwaab V, Mattei MG and Drevet JR. Structural organization, chromosomal localization, expression and phylogenetic evaluation of mouse glutathione peroxidase encoding genes. C R Acad Sci III 1996;319(7):559-68.

96. Meister A. Glutathione metabolism and its selective modification. J Biol Chem 1988;263(33):17205-8.

97. Hanna PM and Mason RP. Direct evidence for inhibition of free radical formation from Cu(I) and hydrogen peroxide by glutathione and other potential ligands using the EPR spin-trapping technique. Arch Biochem Biophys 1992;295(1):205-13.

98. Moran LK, Gutteridge JM and Quinlan GJ. Thiols in cellular redox signalling and control. Curr Med Chem 2001;8(7):763-72.

99. Bilzer M and Lauterburg BH. Effects of hypochlorous acid and chloramines on vascular resistance, cell integrity, and biliary glutathione disulfide in the perfused rat liver: modulation by glutathione. J Hepatol 1991;13(1):84-9.

100. Winterbourn CC and Metodiewa D. The reaction of superoxide with reduced glutathione. Arch Biochem Biophys 1994;314(2):284-90.

101. Jaeschke H. Reactive oxygen and ischemia/reperfusion injury of the liver. Chem Biol Interact 1991;79(2):115-36.

102. Jones AL. Mechanism of action and value of N-acetylcysteine in the treatment of early and late acetaminophen poisoning: a critical review. J Toxicol Clin Toxicol 1998;36(4):277-85.

103. Broughan TA and Soloway RD. Acetaminophen hepatoxicity. Dig Dis Sci 2000;45(8):1553-58.

104. Cotgreave I. N-acetylcysteine: pharmacological considerations and experimental and clinical applications. Adv Pharmacol 1996;38:205-27.

105. Cho WH, Kim DG, Murase N, Mischinger HJ, Todo S and Starzl TE. Comparison of superoxide dismutase, allopurinol, coenzyme Q10, and glutathione for the prevention of warm ischemic injury. Transplantation 1990;50(2):353-5.

106. Schauer RJ, Kalmuk S, Gerbes AL, Leiderer R, Meissner H, Schildberg FW, Messmer K and Bilzer M. Intravenous administration of glutathione protects parenchymal and non-parenchymal liver cells against reperfusion injury following rat liver transplantation. World

J Gastroenterol 2004;10(6):864-70.

107. Schauer RJ, Gerbes AL, Vonier D, Meissner H, Michl P, Leiderer R, Schildberg FW, Messmer K and Bilzer M. Glutathione protects the rat liver against reperfusion injury after prolonged warm ischemia. Ann Surg 2004;239(2):220-31.

108. Winniford MD, Kennedy PL, Wells PJ and Hillis LD. Potentiation of nitroglycerin-induced coronary dilatation by N-acetylcysteine. Circulation 1986;73(1):138-42.

109. Moldeus P, Cotgreave IA and Berggren M. Lung protection by a thiol-containing antioxidant: N-acetylcysteine. Respiration 1986;50 Suppl 1:31-42.

110. Borgstrom L, Kagedal B and Paulsen O. Pharmacokinetics of N-acetylcysteine in man. Eur J Clin Pharmacol 1986;31(2):217-22.

111. Safirstein R, Andrade L and Vieira JM. Acetylcysteine and nephrotoxic effects of radiographic contrast agents--a new use for an old drug. N Engl J Med 2000;343(3):210-2.

112. Tepel M, van der Giet M, Schwarzfeld C, Laufer U, Liermann D and Zidek W. Prevention of radiographic-contrast-agent-induced reductions in renal function by acetylcysteine. N Engl J Med 2000;343(3):180-4.

113. Holt S, Goodier D, Marley R, Patch D, Burroughs A, Fernando B, Harry D and Moore K. Improvement in renal function in hepatorenal syndrome with N-acetylcysteine. Lancet 1999;353(9149):294-5.

114. Horowitz JD, Henry CA, Syrjanen ML, Louis WJ, Fish RD, Smith TW and Antman EM. Combined use of nitroglycerin and N-acetylcysteine in the management of unstable angina pectoris. Circulation 1988;77(4):787-94.

115. Sochman J. N-acetylcysteine in acute cardiology: 10 years later: what do we know and what would we like to know?! J Am Coll Cardiol 2002;39(9):1422-8.

116. Czernichow S and Hercberg S. Interventional studies concerning the role of antioxidant vitamins in cardiovascular diseases: a review. J Nutr Health Aging 2001;5(3):188-95.

117. Zafarullah M, Li WQ, Sylvester J and Ahmad M. Molecular mechanisms of N-acetylcysteine actions. Cell Mol Life Sci 2003;60(1):6-20.

118. Marui N, Offermann MK, Swerlick R, Kunsch C, Rosen CA, Ahmad M, Alexander RW and Medford RM. Vascular cell adhesion molecule-1 (VCAM-1) gene transcription and expression are regulated through an antioxidant-sensitive mechanism in human vascular endothelial cells. J Clin Invest 1993;92(4):1866-74.

119. Weber C, Erl W, Pietsch A, Strobel M, Ziegler-Heitbrock HW and Weber PC. Antioxidants inhibit monocyte adhesion by suppressing nuclear factor-kappa B mobilization and induction of vascular cell adhesion molecule-1 in endothelial cells stimulated to generate radicals. Arterioscler Thromb 1994;14(10):1665-73.

120. Faruqi RM, Poptic EJ, Faruqi TR, De La Motte C and DiCorleto PE. Distinct mechanisms for N-acetylcysteine inhibition of cytokine-induced E-selectin and VCAM-1 expression. Am J Physiol 1997;273(2 Pt 2):H817-26.

121. Rahman A, Bando M, Kefer J, Anwar KN and Malik AB. Protein kinase C-activated oxidant generation in endothelial cells signals intercellular adhesion molecule-1 gene transcription. Mol Pharmacol 1999;55(3):575-83.

122. Rahman A, Kefer J, Bando M, Niles WD and Malik AB. E-selectin expression in human endothelial cells by TNF-alpha-induced oxidant generation and NF-kappaB activation. Am J Physiol 1998;275(3 Pt 1):L533-44.

123. Friedrichs B, Muller C and Brigelius-Flohe R. Inhibition of tumor necrosis factor-alpha- and interleukin-1-induced endothelial E-selectin expression by thiol-modifying agents. Arterioscler Thromb Vasc Biol 1998;18(12):1829-37.

124. Schmidt AM, Hori O, Chen JX, Li JF, Crandall J, Zhang J, Cao R, Yan SD, Brett J and Stern D. Advanced glycation endproducts interacting with their endothelial receptor induce expression of vascular cell adhesion molecule-1 (VCAM-1) in cultured human endothelial cells and in mice. A potential mechanism for the accelerated vasculopathy of diabetes. J Clin Invest 1995;96(3):1395-403.

125. Spiecker M, Darius H and Liao JK. A functional role of I kappa B-epsilon in endothelial cell activation. J Immunol 2000;164(6):3316-22.

126. Zahler S, Kupatt C and Becker BF. Endothelial preconditioning by transient oxidative stress reduces inflammatory responses of cultured endothelial cells to TNF-alpha. Faseb J 2000;14(3):555-64.

127. Chappell DC, Varner SE, Nerem RM, Medford RM and Alexander RW. Oscillatory shear stress stimulates adhesion molecule expression in cultured human endothelium. Circ Res 1998;82(5):532-9.

128. Wung BS, Cheng JJ, Chao YJ, Hsieh HJ and Wang DL. Modulation of Ras/Raf/extracellular signal-regulated kinase pathway by reactive oxygen species is involved in cyclic strain-induced early growth response-1 gene expression in endothelial cells. Circ Res 1999;84(7):804-12.

129. Lee YW, Kuhn H, Hennig B and Toborek M. IL-4 induces apoptosis of endothelial cells through the caspase-3-dependent pathway. FEBS Lett 2000;485(2-3):122-6.

130. Toborek M, Barger SW, Mattson MP, McClain CJ and Hennig B. Role of glutathione redox cycle in TNF-alpha-mediated endothelial cell dysfunction. Atherosclerosis 1995;117(2):179-88.

131. Moldovan L, Irani K, Moldovan NI, Finkel T and Goldschmidt-Clermont PJ. The actin cytoskeleton reorganization induced by Rac1 requires the production of superoxide. Antioxid Redox Signal 1999;1(1):29-43.

132. Walther M, Kaffenberger W and Van Beuningen D. Influence of clinically used antioxidants on radiation-induced expression of intercellular cell adhesion molecule-1 on HUVEC. Int J Radiat Biol 1999;75(10):1317-25.

133. Mohan S, Mohan N, Valente AJ and Sprague EA. Regulation of low shear flow-induced HAEC VCAM-1 expression and monocyte adhesion. Am J Physiol 1999;276(5 Pt 1):C1100-7.

134. Wagener FA, da Silva JL, Farley T, de Witte T, Kappas A and Abraham NG. Differential effects of heme oxygenase isoforms on heme mediation of endothelial intracellular adhesion molecule 1 expression. J Pharmacol Exp Ther 1999;291(1):416-23.

135. Bouloumie A, Marumo T, Lafontan M and Busse R. Leptin induces oxidative stress in human endothelial cells. Faseb J 1999;13(10):1231-8.

136. Chua CC, Hamdy RC and Chua BH. Upregulation of vascular endothelial growth factor by H2O2 in rat heart endothelial cells. Free Radic Biol Med 1998;25(8):891-7.

137. Ramasamy S, Drummond GR, Ahn J, Storek M, Pohl J, Parthasarathy S and Harrison DG. Modulation of expression of endothelial nitric oxide synthase by nordihydroguaiaretic acid, a phenolic antioxidant in cultured endothelial cells. Mol Pharmacol 1999;56(1):116-23.

138. Chen G, Wang SH and Warner TD. Regulation of iNOS mRNA levels in endothelial cells by glutathione, a double-edged sword. Free Radic Res 2000;32(3):223-34.

139. Hashimoto S, Gon Y, Matsumoto K, Takeshita I and Horie T. N-acetylcysteine attenuates TNF-alpha-induced p38 MAP kinase activation and p38 MAP kinase-mediated IL-8 production by human pulmonary vascular endothelial cells. Br J Pharmacol 2001;132(1):270-6.

140. Liu W, Schoenkerman A and Lowe WL, Jr. Activation of members of the mitogen-activated protein kinase family by glucose in endothelial cells. Am J Physiol Endocrinol

Metab 2000;279(4):E782-90.

141. Terry CM, Clikeman JA, Hoidal JR and Callahan KS. TNF-alpha and IL-1alpha induce heme oxygenase-1 via protein kinase C, Ca2+, and phospholipase A2 in endothelial cells. Am J Physiol 1999;276(5 Pt 2):H1493-501.

142. Foresti R, Sarathchandra P, Clark JE, Green CJ and Motterlini R. Peroxynitrite induces haem oxygenase-1 in vascular endothelial cells: a link to apoptosis. Biochem J 1999;339 (Pt 3):729-36.

143. Hsieh HJ, Cheng CC, Wu ST, Chiu JJ, Wung BS and Wang DL. Increase of reactive oxygen species (ROS) in endothelial cells by shear flow and involvement of ROS in shear-induced c-fos expression. J Cell Physiol 1998;175(2):156-62.

144. Vendemiale G, Grattagliano I, Caruso ML, Serviddio G, Valentini AM, Pirrelli M and Altomare E. Increased oxidative stress in dimethylnitrosamine-induced liver fibrosis in the rat: effect of N-acetylcysteine and interferon-alpha. Toxicol Appl Pharmacol 2001;175(2):130-9.

145. Kim KY, Rhim T, Choi I and Kim SS. N-acetylcysteine induces cell cycle arrest in hepatic stellate cells through its reducing activity. J Biol Chem 2001;276(44):40591-8.

146. Shaikh ZA, Vu TT and Zaman K. Oxidative stress as a mechanism of chronic cadmium-induced hepatotoxicity and renal toxicity and protection by antioxidants. Toxicol Appl Pharmacol 1999;154(3):256-63.

147. Kozer E and Koren G. Management of paracetamol overdose: current controversies. Drug Saf 2001;24(7):503-12.

148. Schmidt LE, Dalhoff K and Poulsen HE. Acute versus chronic alcohol consumption in acetaminophen-induced hepatotoxicity. Hepatology 2002;35(4):876-82.

149. Jones AL. Mechanism of action and value of N-acetylcysteine in the treatment of early and late acetaminophen poisoning: a critical review. J Toxicol Clin Toxicol 1998;36(4):277-85.

150. Zaragoza A, Diez-Fernandez C, Alvarez AM, Andres D and Cascales M. Mitochondrial involvement in cocaine-treated rat hepatocytes: effect of N-acetylcysteine and deferoxamine. Br J Pharmacol 2001;132(5):1063-70.

151. Weigand MA, Plachky J, Thies JC, Spies-Martin D, Otto G, Martin E and Bardenheuer HJ. N-acetylcysteine attenuates the increase in alpha-glutathione S-transferase and circulating ICAM-1 and VCAM-1 after reperfusion in humans undergoing liver transplantation. Transplantation 2001;72(4):694-8.

152. Hur GM, Ryu YS, Yun HY, Jeon BH, Kim YM, Seok JH and Lee JH. Hepatic ischemia/reperfusion in rats induces iNOS gene transcription by activation of NF-kappaB. Biochem Biophys Res Commun 1999;261(3):917-22.

153. Vairetti M, Griffini P, Pietrocola G, Richelmi P and Freitas I. Cold-induced apoptosis in isolated rat hepatocytes: protective role of glutathione. Free Radic Biol Med 2001;31(8):954-61.

154. Gong G, Waris G, Tanveer R and Siddiqui A. Human hepatitis C virus NS5A protein alters intracellular calcium levels, induces oxidative stress, and activates STAT-3 and NF-kappa B. Proc Natl Acad Sci U S A 2001;98(17):9599-604.

155. Waris G, Huh KW and Siddiqui A. Mitochondrially associated hepatitis B virus X protein constitutively activates transcription factors STAT-3 and NF-kappa B via oxidative stress. Mol Cell Biol 2001;21(22):7721-30.

156. Vivot C, Stump DD, Schwartz ME, Theise ND and Miller CM. N-acetylcysteine attenuates cold ischemia/reperfusion injury in the isolated perfused rat liver. Transplant Proc 1993;25(2):1983-4.

157. Dunne JB, Davenport M, Williams R and Tredger JM. Evidence that S-adenosylmethionine and N-acetylcysteine reduce injury from sequential cold and warm ischemia in the isolated perfused rat liver. Transplantation 1994;57(8):1161-8.

158. Fukuzawa K, Emre S, Senyuz O, Acarli K, Schwartz ME and Miller CM. N-acetylcysteine ameliorates reperfusion injury after warm hepatic ischemia. Transplantation 1995;59(1):6-9.

159. Nakano H, Boudjema K, Alexandre E, Imbs P, Chenard MP, Wolf P, Cinqualbre J and Jaeck D. Protective effects of N-acetylcysteine on hypothermic ischemia-reperfusion injury of rat liver. Hepatology 1995;22(2):539-45.

160. Koeppel TA, Thies JC, Lehmann T, Gebhard MM, Herfarth C, Otto G and Post S. Improvement of hepatic microhemodynamics by N-acetylcysteine after warm ischemia. Eur Surg Res 1996;28(4):270-7.

161. Thies JC, Koeppel TA, Lehmann T, Schemmer P, Otto G and Post S. Efficacy of N-acetylcysteine as a hepatoprotective agent in liver transplantation: an experimental study. Transplant Proc 1997;29(1-2):1326-7.

162. Nakano H, Boudjema K, Jaeck D, Alexandre E, Imbs P, Chenard MP, Nagasaki H, Kumada K, Wolf P and Cinqualbre J. Amelioration of hepatocellular integrity and inhibition of sinusoidal oxidative stress by N-acetylcysteine pretreatment in cold

ischemia-reperfusion injury of rat liver. Eur Surg Res 1996;28(4):245-55.

163. Regueira FM, Hernandez JL, Sola I, Cienfuegos JA, Pardo F, Diez-Caballero A, Sierra A, Nwose E, Espi A, Baixauli J and Rotellar F. Ischemic damage prevention by N-acetylcysteine treatment of the donor before orthotopic liver transplantation. Transplant Proc 1997;29(8):3347-9.

164. Manika A, Trinh T, Lagace G, Dugas MA, Proulx F, Lepage G, Champagne J, Lavoie JC, Cousineau J, Russo P, Chartrand C and Yandza T. N-acetylcysteine in pig liver transplantation from non-heart-beating donors. Transplantation 1999;68(3):327-30.

165. Weinbroum AA, Rudick V, Ben-Abraham R and Karchevski E. N-acetyl-L-cysteine for preventing lung reperfusion injury after liver ischemia-reperfusion: a possible dual protective mechanism in a dose-response study. Transplantation 2000;69(5):853-9.

166. Weinbroum AA, Kluger Y, Ben Abraham R, Shapira I, Karchevski E and Rudick V. Lung preconditioning with N-acetyl-L-cysteine prevents reperfusion injury after liver no flow-reflow: a dose-response study. Transplantation 2001;71(2):300-6.

167. Le Moine O, Louis H, Stordeur P, Collet JM, Goldman M and Deviere J. Role of reactive oxygen intermediates in interleukin 10 release after cold liver ischemia and reperfusion in mice. Gastroenterology 1997;113(5):1701-6.

168. Demir S and Inal-Erden M. Pentoxifylline and N-acetylcysteine in hepatic ischemia/reperfusion injury. Clin Chim Acta 1998;275(2):127-35.

169. Sener G, Tosun O, Sehirli AO, Kacmaz A, Arbak S, Ersoy Y and Ayanoglu-Dulger G. Melatonin and N-acetylcysteine have beneficial effects during hepatic ischemia and reperfusion. Life Sci 2003;72(24):2707-18.

170. Crenesse D, Schmid-Alliana A, Hornoy J, Rossi B and Gugenheim J. Hypoxia-reoxygenation differentially stimulates stress-activated protein kinases in primary-cultured rat hepatocytes. Transpl Int 2000;13 Suppl 1:S597-9.

171. Steib A, Freys G, Collin F, Launoy A, Mark G and Boudjema K. Does N-acetylcysteine improve hemodynamics and graft function in liver transplantation? Liver Transpl Surg 1998;4(2):152-7.

172. Thies JC, Teklote J, Clauer U, Tox U, Klar E, Hofmann WJ, Herfarth C and Otto G. The efficacy of N-acetylcysteine as a hepatoprotective agent in liver transplantation. Transpl Int 1998;11 (Suppl 1):S390-2.

173. Taut FJ, Schmidt H, Zapletal CM, Thies JC, Grube C, Motsch J, Klar E and Martin E. N-acetylcysteine induces shedding of selectins from liver and intestine during orthotopic

liver transplantation. Clin Exp Immunol 2001;124(2):337-41.

174. Taut FJ, Breitkreutz R, Zapletal CM, Thies JC, Babylon A, Martin E and Droge W. Influence of N-acetylcysteine on hepatic amino acid metabolism in patients undergoing orthotopic liver transplantation. Transpl Int 2001;14(5):329-33.

175. Lemasters JJ, Bond JM, Chacon E, Harper IS, Kaplan SH, Ohata H, Trollinger DR, Herman B and Cascio WE. The pH paradox in ischemia-reperfusion injury to cardiac myocytes. Exs 1996;76:99-114.

176. Jaeschke H. Molecular mechanisms of hepatic ischemia-reperfusion injury and preconditioning. Am J Physiol Gastrointest Liver Physiol 2003;284(1):G15-26.

177. Cutrn JC, Perrelli MG, Cavalieri B, Peralta C, Rosell Catafau J and Poli G. Microvascular dysfunction induced by reperfusion injury and protective effect of ischemic preconditioning. Free Radic Biol Med 2002;33(9):1200-8.

178. Menger MD, Richter S, Yamauchi J and Vollmar B. Role of microcirculation in hepatic ischemia/reperfusion injury. Hepatogastroenterology 1999;46 Suppl 2:1452-7.

179. Jaeschke H. Mechanisms of reperfusion injury after warm ischemia of the liver. J Hepatobiliary Pancreat Surg 1998;5(4):402-8.

180. Fondevila C, Busuttil RW and Kupiec-Weglinski JW. Hepatic ischemia/reperfusion injury--a fresh look. Exp Mol Pathol 2003;74(2):86-93.

181. Jaeschke H, Smith CW, Clemens MG, Ganey PE and Roth RA. Mechanisms of inflammatory liver injury: adhesion molecules and cytotoxicity of neutrophils. Toxicol Appl Pharmacol 1996;139(2):213-26.

182. Jaeschke H and Smith CW. Mechanisms of neutrophil-induced parenchymal cell injury. J Leukoc Biol 1997;61(6):647-53.

183. Rymsa B, Wang JF and de Groot H. O2-. release by activated Kupffer cells upon hypoxia-reoxygenation. Am J Physiol 1991;261(4 Pt 1):G602-7.

184. Shibuya H, Ohkohchi N, Seya K and Satomi S. Kupffer cells generate superoxide anions and modulate reperfusion injury in rat livers after cold preservation. Hepatology 1997;25(2):356-60.

185. Jaeschke H and Farhood A. Neutrophil and Kupffer cell-induced oxidant stress and ischemia-reperfusion injury in rat liver. Am J Physiol 1991;260(3 Pt 1):G355-62.

186. Liu P, McGuire GM, Fisher MA, Farhood A, Smith CW and Jaeschke H. Activation of

Kupffer cells and neutrophils for reactive oxygen formation is responsible for endotoxin-enhanced liver injury after hepatic ischemia. Shock 1995;3(1):56-62.

187. Cutrin JC, Boveris A, Zingaro B, Corvetti G and Poli G. In situ determination by surface chemiluminescence of temporal relationships between evolving warm ischemia-reperfusion injury in rat liver and phagocyte activation and recruitment. Hepatology 2000;31(3):622-32.

188. Terashima T, Ohkohchi N, Kanno M, Seya K, Orii T, Satomi S, Taguchi Y and Mori S. Role of neutrophils in lipid peroxidation at reperfusion in liver transplantation. Transplant Proc 1996;28(1):324-6.

189. Mavier P, Preaux AM, Guigui B, Lescs MC, Zafrani ES and Dhumeaux D. In vitro toxicity of polymorphonuclear neutrophils to rat hepatocytes: evidence for a proteinase-mediated mechanism. Hepatology 1988;8(2):254-8.

190. Habib MM, Hodgson HJ and Davidson BR. The role of glycine in hepatic ischemia-reperfusion injury. Curr Pharm Des 2006;12(23):2953-67.

191. Rajendra S, Lynch JW and Schofield PR. The glycine receptor. Pharmacol Ther 1997;73(2):121-46.

192. Weinberg JM, Davis JA, Abarzua M and Rajan T. Cytoprotective effects of glycine and glutathione against hypoxic injury to renal tubules. J Clin Invest 1987;80(5):1446-54.

193. Marsh DC, Hjelmhaug JA, Vreugdenhil PK, Belzer FO and Southard JH. Glycine prevention of cold ischemic injury in isolated hepatocytes. Cryobiology 1991;28(1):105-9.

194. Marsh DC, Vreugdenhil PK, Mack VE, Belzer FO and Southard JH. Glycine protects hepatocytes from injury caused by anoxia, cold ischemia and mitochondrial inhibitors, but not injury caused by calcium ionophores or oxidative stress. Hepatology 1993;17(1):91-8.

195. Nichols JC, Bronk SF, Mellgren RL and Gores GJ. Inhibition of nonlysosomal calcium-dependent proteolysis by glycine during anoxic injury of rat hepatocytes. Gastroenterology 1994;106(1):168-76.

196. Ferri KF and Kroemer G. Organelle-specific initiation of cell death pathways. Nat Cell Biol 2001;3(11):E255-63.

197. TranVan Nhieu G, Clair C, Grompone G and Sansonetti P. Calcium signalling during cell interactions with bacterial pathogens. Biol Cell 2004;96(1):93-101.

198. Ueda N and Shah SV. Role of intracellular calcium in hydrogen peroxide-induced renal

tubular cell injury. Am J Physiol 1992;263(2 Pt 2):F214-21.

199. Wheeler MD, Ikejema K, Enomoto N, Stacklewitz RF, Seabra V, Zhong Z, Yin M, Schemmer P, Rose ML, Rusyn I, Bradford B and Thurman RG. Glycine: a new anti-inflammatory immunonutrient. Cell Mol Life Sci 1999;56(9-10):843-56.

200. Ikejima K, Qu W, Stachlewitz RF and Thurman RG. Kupffer cells contain a glycine-gated chloride channel. Am J Physiol 1997;272(6 Pt 1):G1581-6.

201. Takei Y, Marzi I, Kauffman FC, Cowper K, Lemasters JJ and Thurman RG. Prevention of early graft failure by the calcium channel blocker nisoldipine: involvement of Kupffer cells. Transplant Proc 1990;22(5):2202-3.

202. Li X, Bradford BU, Wheeler MD, Stimpson SA, Pink HM, Brodie TA, Schwab JH and Thurman RG. Dietary glycine prevents peptidoglycan polysaccharide-induced reactive arthritis in the rat: role for glycine-gated chloride channel. Infect Immun 2001;69(9):5883-91.

203. Wheeler M, Stachlewitz RF, Yamashina S, Ikejima K, Morrow AL and Thurman RG. Glycine-gated chloride channels in neutrophils attenuate calcium influx and superoxide production. Faseb J 2000;14(3):476-84.

204. Wheeler MD and Thurman RG. Production of superoxide and TNF-alpha from alveolar macrophages is blunted by glycine. Am J Physiol 1999;277(5 Pt 1):L952-9.

205. Weinberg JM, Venkatachalam MA, Garzo-Quintero R, Roeser NF and Davis JA. Structural requirements for protection by small amino acids against hypoxic injury in kidney proximal tubules. Faseb J 1990;4(15):3347-54.

206. Lynch JW. Molecular structure and function of the glycine receptor chloride channel. Physiol Rev 2004;84(4):1051-95.

207. Zafra F, Aragon C, Olivares L, Danbolt NC, Gimenez C and Storm-Mathisen J. Glycine transporters are differentially expressed among CNS cells. J Neurosci 1995;15(5 Pt 2):3952-69.

208. Rajendra S and Schofield PR. Molecular mechanisms of inherited startle syndromes. Trends Neurosci 1995;18(2):80-2.

209. Cascio M. Structure and function of the glycine receptor and related nicotinicoid receptors. J Biol Chem 2004;279(19):19383-6.

210. Breitinger HG and Becker CM. The inhibitory glycine receptor-simple views of a complicated channel. Chembiochem 2002;3(11):1042-52.

211. Froh M, Thurman RG and Wheeler MD. Molecular evidence for a glycine-gated chloride channel in macrophages and leukocytes. Am J Physiol Gastrointest Liver Physiol 2002;283(4):G856-63.

212. Spittler A, Reissner CM, Oehler R, Gornikiewicz A, Gruenberger T, Manhart N, Brodowicz T, Mittlboeck M, Boltz-Nitulescu G and Roth E. Immunomodulatory effects of glycine on LPS-treated monocytes: reduced TNF-alpha production and accelerated IL-10 expression. Faseb J 1999;13(3):563-71.

213. Stachlewitz RF, Li X, Smith S, Bunzendahl H, Graves LM and Thurman RG. Glycine inhibits growth of T lymphocytes by an IL-2-independent mechanism. J Immunol 2000;164(1):176-82.

214. Qu W, Ikejima K, Zhong Z, Waalkes MP and Thurman RG. Glycine blocks the increase in intracellular free Ca2+ due to vasoactive mediators in hepatic parenchymal cells. Am J Physiol Gastrointest Liver Physiol 2002;283(6):G1249-56.

215. Yamashina S, Konno A, Wheeler MD, Rusyn I, Rusyn EV, Cox AD and Thurman RG. Endothelial cells contain a glycine-gated chloride channel. Nutr Cancer 2001;40(2):197-204.

216. Wang YS, Yan YH and Zou XF. Protective effect of glycine on liver injury during liver transplantation. Chin Med J (Engl) 2010;123(14):1931-8.

217. Schanne FA, Kane AB, Young EE and Farber JL. Calcium dependence of toxic cell death: a final common pathway. Science 1979;206(4419):700-2.

218. Barros LF, Kanaseki T, Sabirov R, Morishima S, Castro J, Bittner CX, Maeno E, Ando-Akatsuka Y and Okada Y. Apoptotic and necrotic blebs in epithelial cells display similar neck diameters but different kinase dependency. Cell Death Differ 2003;10(6):687-97.

219. Estacion M, Weinberg JS, Sinkins WG and Schilling WP. Blockade of maitotoxin-induced endothelial cell lysis by glycine and L-alanine. Am J Physiol Cell Physiol 2003;284(4):C1006-20.

220. Frederiks WM, Myagkaya GL, van Veen HA and Vogels IM. Biochemical and ultrastructural changes in rat liver plasma membranes after temporary ischemia. Virchows Arch B Cell Pathol Incl Mol Pathol 1984;46(4):269-82.

221. Lemasters JJ, Stemkowski CJ, Ji S and Thurman RG. Cell surface changes and enzyme release during hypoxia and reoxygenation in the isolated, perfused rat liver. J Cell Biol 1983;97(3):778-86.

222. Caldwell-Kenkel JC, Currin RT, Tanaka Y, Thurman RG and Lemasters JJ. Reperfusion

injury to endothelial cells following cold ischemic storage of rat livers. Hepatology 1989;10(3):292-9.

223. Hilden M, Christoffersen P, Juhl E and Dalgaard JB. Liver histology in a 'normal' population--examinations of 503 consecutive fatal traffic casualties. Scand J Gastroenterol 1977;12(5):593-7.

224. Underwood Ground KE. Prevalence of fatty liver in healthy male adults accidentally killed. Aviat Space Environ Med 1984;55(1):59-61.

225. Hornboll P and Olsen TS. Fatty changes in the liver: the relation to age, overweight and diabetes mellitus. Acta Pathol Microbiol Immunol Scand [A] 1982;90(3):199-205.

226. D'Alessandro AM, Kalayoglu M, Sollinger HW, Hoffmann RM, Reed A, Knechtle SJ, Pirsch JD, Hafez GR, Lorentzen D and Belzer FO. The predictive value of donor liver biopsies on the development of primary nonfunction after orthotopic liver transplantation. Transplant Proc 1991;23(1 Pt 2):1536-7.

227. Miki C, Iriyama K, Mirza DF, Mayer AD, Buckels JA, Suzuki H and McMaster P. Postperfusion energy metabolism of steatotic graft and its relation to early graft viability following liver transplantation. Dig Dis Sci 1998;43(1):74-9.

228. Clavien PA, Harvey PR and Strasberg SM. Preservation and reperfusion injuries in liver allografts. An overview and synthesis of current studies. Transplantation 1992;53(5):957-78.

229. Selzner M and Clavien PA. Fatty liver in liver transplantation and surgery. Semin Liver Dis 2001;21(1):105-13.

230. Portmann B and Wight D. Pathology of liver transplantation. In: Calne RY, editor. Liver transplantation. 2nd ed. ed. London: Grune & Stratton; 1987. p. 437.

231. Busuttil RW and Tanaka K. The utility of marginal donors in liver transplantation. Liver Transpl 2003;9(7):651-63.

232. Yoong KF, Gunson BK, Neil DA, Mirza DF, Mayer AD, Buckels JA and McMaster P. Impact of donor liver microvesicular steatosis on the outcome of liver retransplantation. Transplant Proc 1999;31(1-2):550-1.

233. Canelo R, Braun F, Sattler B, Klinge B, Lorf T, Ramadori G and Ringe B. Is a fatty liver dangerous for transplantation? Transplant Proc 1999;31(1-2):414-5.

234. Hayashi M, Fujii K, Kiuchi T, Uryuhara K, Kasahara M, Takatsuki M, Takeichi T, Kitade H, Sugimoto T, Uemoto S, Asonuma K, Egawa H, Fujita S, Inomata Y and Tanaka K.

Effects of fatty infiltration of the graft on the outcome of living-related liver transplantation. Transplant Proc 1999;31(1-2):403.

235. Adam R, Reynes M, Johann M, Morino M, Astarcioglu I, Kafetzis I, Castaing D and Bismuth H. The outcome of steatotic grafts in liver transplantation. Transplant Proc 1991;23(1 Pt 2):1538-40.

236. Chui AK, Haghighi K, Painter D, Jayasundera M, Hall G, Rao AR, Verran DJ, McCaughan GW and Sheil AG. Donor fatty (steatotic) liver allografts in orthotopic liver transplantation. Transplant Proc 1998;30(7):3286-7.

237. Bengmark S. Liver steatosis and liver resection. Digestion 1969;2(5):304-11.

238. Behrns KE, Tsiotos GG, DeSouza NF, Krishna MK, Ludwig J and Nagorney DM. Hepatic steatosis as a potential risk factor for major hepatic resection. J Gastrointest Surg 1998;2(3):292-8.

239. Hakamada K, Sasaki M, Takahashi K, Umehara Y and Konn M. Sinusoidal flow block after warm ischemia in rats with diet-induced fatty liver. J Surg Res 1997;70(1):12-20.

240. Teramoto K, Bowers JL, Kruskal JB and Clouse ME. Hepatic microcirculatory changes after reperfusion in fatty and normal liver transplantation in the rat. Transplantation 1993;56(5):1076-82.

241. Teramoto K, Bowers JL, Kruskal JB, Hara J, Iwai T, Endo M and Clouse ME. In vivo microscopic observation of fatty liver grafts after reperfusion. Transplant Proc 1994;26(4):2391.

242. Sindram D, Porte RJ, Hoffman MR, Bentley RC and Clavien PA. Platelets induce sinusoidal endothelial cell apoptosis upon reperfusion of the cold ischemic rat liver. Gastroenterology 2000;118(1):183-91.

243. Yadav SS, Howell DN, Steeber DA, Harland RC, Tedder TF and Clavien PA. P-Selectin mediates reperfusion injury through neutrophil and platelet sequestration in the warm ischemic mouse liver. Hepatology 1999;29(5):1494-502.

244. Seifalian AM, Piasecki C, Agarwal A and Davidson BR. The effect of graded steatosis on flow in the hepatic parenchymal microcirculation. Transplantation 1999;68(6):780-4.

245. Ijaz S, Yang W, Winslet MC and Seifalian AM. Impairment of hepatic microcirculation in fatty liver. Microcirculation 2003;10(6):447.

246. Fromenty B, Berson A and Pessayre D. Microvesicular steatosis and steatohepatitis: role of mitochondrial dysfunction and lipid peroxidation. J Hepatol 1997;26 Suppl 1:13-22.

247. Fromenty B and Pessayre D. Impaired mitochondrial function in microvesicular steatosis. Effects of drugs, ethanol, hormones and cytokines. J Hepatol 1997;26 Suppl 2:43-53.

248. Berson A, De Beco V, Letteron P, Robin MA, Moreau C, El Kahwaji J, Verthier N, Feldmann G, Fromenty B and Pessayre D. Steatohepatitis-inducing drugs cause mitochondrial dysfunction and lipid peroxidation in rat hepatocytes. Gastroenterology 1998;114(4):764-74.

249. Letteron P, Fromenty B, Terris B, Degott C and Pessayre D. Acute and chronic hepatic steatosis lead to in vivo lipid peroxidation in mice. J Hepatol 1996;24(2):200-8.

250. Zhong Z, Connor H, Stachlewitz RF, Frankenberg M, Mason RP, Lemasters JJ and Thurman RG. Role of free radicals in primary nonfunction of marginal fatty grafts from rats treated acutely with ethanol. Mol Pharmacol 1997;52(5):912-9.

251. Kohli V, Selzner M, Madden JF, Bentley RC and Clavien PA. Endothelial cell and hepatocyte deaths occur by apoptosis after ischemia-reperfusion injury in the rat liver. Transplantation 1999;67(8):1099-105.

252. Gao W, Bentley RC, Madden JF and Clavien PA. Apoptosis of sinusoidal endothelial cells is a critical mechanism of preservation injury in rat liver transplantation. Hepatology 1998;27(6):1652-60.

253. Natori S, Selzner M, Valentino KL, Fritz LC, Srinivasan A, Clavien PA and Gores GJ. Apoptosis of sinusoidal endothelial cells occurs during liver preservation injury by a caspase-dependent mechanism. Transplantation 1999;68(1):89-96.

254. Kohli V, Madden JF, Bentley RC and Clavien PA. Calpain mediates ischemic injury of the liver through modulation of apoptosis and necrosis. Gastroenterology 1999;116(1):168-78.

255. Cursio R, Gugenheim J, Ricci JE, Crenesse D, Rostagno P, Maulon L, Saint-Paul MC, Ferrua B and Auberger AP. A caspase inhibitor fully protects rats against lethal normothermic liver ischemia by inhibition of liver apoptosis. Faseb J 1999;13(2):253-61.

256. Selzner M, Rudiger HA, Sindram D, Madden J and Clavien PA. Mechanisms of ischemic injury are different in the steatotic and normal rat liver. Hepatology 2000;32(6):1280-8.

257. Selzner M and Clavien PA. Failure of regeneration of the steatotic rat liver: disruption at two different levels in the regeneration pathway. Hepatology 2000;31(1):35-42.

258. Murry CE, Jennings RB and Reimer KA. Preconditioning with ischemia: a delay of lethal cell injury in ischemic myocardium. Circulation 1986;74(5):1124-36.

259. Clavien PA, Yadav S, Sindram D and Bentley RC. Protective effects of ischemic preconditioning for liver resection performed under inflow occlusion in humans. Ann Surg 2000;232(2):155-62.

260. Clavien PA, Selzner M, Rudiger HA, Graf R, Kadry Z, Rousson V and Jochum W. A prospective randomized study in 100 consecutive patients undergoing major liver resection with versus without ischemic preconditioning. Ann Surg 2003;238(6):843-50; discussion 51-2.

261. Yadav SS, Sindram D, Perry DK and Clavien PA. Ischemic preconditioning protects the mouse liver by inhibition of apoptosis through a caspase-dependent pathway. Hepatology 1999;30(5):1223-31.

262. Fernandez L, Heredia N, Grande L, Gomez G, Rimola A, Marco A, Gelpi E, Rosello-Catafau J and Peralta C. Preconditioning protects liver and lung damage in rat liver transplantation: role of xanthine/xanthine oxidase. Hepatology 2002;36(3):562-72.

263. Sindram D, Rudiger HA, Upadhya AG, Strasberg SM and Clavien PA. Ischemic preconditioning protects against cold ischemic injury through an oxidative stress dependent mechanism. J Hepatol 2002;36(1):78-84.

264. Ricciardi R, Schaffer BK, Kim RD, Shah SA, Donohue SE, Wheeler SM, Quarfordt SH, Callery MP, Meyers WC and Chari RS. Protective effects of ischemic preconditioning on the cold-preserved liver are tyrosine kinase dependent. Transplantation 2001;72(3):406-12.

265. Selzner N, Selzner M, Jochum W and Clavien PA. Ischemic preconditioning protects the steatotic mouse liver against reperfusion injury: an ATP dependent mechanism. J Hepatol 2003;39(1):55-61.

266. Koti RS, Yang W, Glantzounis G, Quaglia A, Davidson BR and Seifalian AM. Effect of ischaemic preconditioning on hepatic oxygenation, microcirculation and function in a rat model of moderate hepatic steatosis. Clin Sci (Lond) 2005;108(1):55-63.

267. Koti RS, Yang W, Dashwood MR, Davidson BR and Seifalian AM. Effect of ischemic preconditioning on hepatic microcirculation and function in a rat model of ischemia reperfusion injury. Liver Transpl 2002;8(12):1182-91.

268. Koti RS, Seifalian AM, McBride AG, Yang W and Davidson BR. The relationship of hepatic tissue oxygenation with nitric oxide metabolism in ischemic preconditioning of the liver. Faseb J 2002;16(12):1654-6.

269. Nishimura Y, Romer LH and Lemasters JJ. Mitochondrial dysfunction and cytoskeletal

disruption during chemical hypoxia to cultured rat hepatic sinusoidal endothelial cells: the pH paradox and cytoprotection by glucose, acidotic pH, and glycine. Hepatology 1998;27(4):1039-49.

270. Macedo FI and Miranda LE. Role of ischemic preconditioning in liver transplant: a review of literature. Exp Clin Transplant 2010;8(1):1-3.

271. Cavalieri B, Perrelli MG, Aragno M, Mastrocola R, Corvetti G, Durazzo M, Poli G and Cutrin JC. Ischemic preconditioning attenuates the oxidant-dependent mechanisms of reperfusion cell damage and death in rat liver. Liver Transpl 2002;8(11):990-9.

272. Sawaya DE, Jr., Brown M, Minardi A, Bilton B, Burney D, Granger DN, McDonald JC and Zibari GB. The role of ischemic preconditioning in the recruitment of rolling and adherent leukocytes in hepatic venules after ischemia/reperfusion. J Surg Res 1999;85(1):163-70.

273. Peralta C, Hotter G, Closa D, Prats N, Xaus C, Gelpi E and Rosello-Catafau J. The protective role of adenosine in inducing nitric oxide synthesis in rat liver ischemia preconditioning is mediated by activation of adenosine A2 receptors. Hepatology 1999;29(1):126-32.

274. Arai M, Thurman RG and Lemasters JJ. Contribution of adenosine A(2) receptors and cyclic adenosine monophosphate to protective ischemic preconditioning of sinusoidal endothelial cells against Storage/Reperfusion injury in rat livers. Hepatology 2000;32(2):297-302.

275. Peralta C, Rull R, Rimola A, Deulofeu R, Rosello-Catafau J, Gelpi E and Rodes J. Endogenous nitric oxide and exogenous nitric oxide supplementation in hepatic ischemia-reperfusion injury in the rat. Transplantation 2001;71(4):529-36.

276. Shah V and Kamath PS. Nitric oxide in liver transplantation: pathobiology and clinical implications. Liver Transpl 2003;9(1):1-11.

277. Carini R, De Cesaris MG, Splendore R, Vay D, Domenicotti C, Nitti MP, Paola D, Pronzato MA and Albano E. Signal pathway involved in the development of hypoxic preconditioning in rat hepatocytes. Hepatology 2001;33(1):131-9.

278. Carini R and Albano E. Recent insights on the mechanisms of liver preconditioning. Gastroenterology 2003;125(5):1480-91.

279. Przyklenk K, Bauer B, Ovize M, Kloner RA and Whittaker P. Regional ischemic 'preconditioning' protects remote virgin myocardium from subsequent sustained coronary occlusion. Circulation 1993;87(3):893-9.

280. Kanoria S, Jalan R, Davies NA, Seifalian AM, Williams R and Davidson BR. Remote

ischaemic preconditioning of the hind limb reduces experimental liver warm ischaemia-reperfusion injury. Br J Surg 2006;93(6):762-8.

281. Kume M, Yamamoto Y, Saad S, Gomi T, Kimoto S, Shimabukuro T, Yagi T, Nakagami M, Takada Y, Morimoto T and Yamaoka Y. Ischemic preconditioning of the liver in rats: implications of heat shock protein induction to increase tolerance of ischemia-reperfusion injury. J Lab Clin Med 1996;128(3):251-8.

282. Boesch C. Molecular aspects of magnetic resonance imaging and spectroscopy. Mol Aspects Med 1999;20(4-5):185-318.

283. Andrew ER. A historical review of NMR and its clinical applications. Br Med Bull 1984;40(2):115-9.

284. Becker ED, Fisk C and Khetrapal CL. The development of NMR. In: Grant DM and Harris RK, editors. Encyclopedia of Nuclear Magnetic Resonance. Chichester Sussex, UK: Wiley; 1996. p. 1-160.

285. Gerlach W and Stern O. Der experimentelle Nachweis des magnetischen Moments des Silberatoms. Zeitschrift für Physik 1921;8:110-11.

286. Estermann I and Stern O. Über die magnetische Ablenkung von Wasserstoffmolek ülen und das magnetische Moment des Protons. II. Zeitschrift für Physik 1933;85:17-24.

287. Rabi II, Zacharias JR, Millman S and Kusch P. A new method of measuring nuclear magnetic moment. Physical Review 1938;53:318-18.

288. Gorter CJ. Negative results of an attempt to detect nuclear magnetic spins. Physica (The Hague) 1936;3:995-98.

289. Gorter CJ and Broer LFJ. Negative result of an attempt to observe nuclear magnetic in solids. Physica (The Hague) 1942;9:591-96.

290. Purcell EM, Torrey HC and Pound RV. Resonance absorption by nuclear magnetic moments in solids. Physical Review 1946;69:37-38.

291. Bloch F, Hansen WW and Packard M. Nuclear induction. Physical Review 1946;69:127-27.

292. Bloch F. Nuclear induction. Physical Review 1946;70:460-74.

293. Bloembergen N, Purcell EM and Pound RV. Relaxation effects in nuclear magnetic

resonance absorption. Physical Review 1948;73:679-712.

294. Arnold JT, Dharmatti SS and Packard ME. Chemical effects on nuclear induction signals from organic compounds. Journal of Chemical Physics 1951;19:507-07.

295. Liddel U and Ramsey NF. Temperature dependent magnetic shielding in ethyl alcohol. Journal of Chemical Physics 1951;19:1608.

296. Proctor WG and Yu FC. The dependence of a nuclear magnetic resonance frequency upon chemical compound. Physical Review 1950;77:717-17.

297. Torrey HC. Transient nutations in nuclear magnetic resonance. Physical Review 1949;76:1059-68.

298. Hahn EL. An accurate nuclear magnetic resonance method for measuring spin-lattice relaxation times. Physical Review 1949;76:145-46.

299. Carr HY and Purcell EM. Effects of diffusion on free precession in nuclear magnetic resonance experiments. Physical Review 1954;94(3):630-38.

300. Meiboom S and Gill D. Modified spin-echo method for measuring nuclear relaxation times. Review of Scientific Instruments 1958;29:688-91.

301. Ernst RR and Anderson WA. Application of fourier transform spectroscopy to magnetic resonance. Review of Scientific Instruments 1966;37:93-102.

302. Ernst RR, Bodenhausen G and Wokaun A. Principles of nuclear magnetic resonance in one and two dimensions. Oxford: Clarendon; 1987.

303. Mueller L, Kumar A and Ernst RR. Two dimensional carbon-13 NMR spectroscopy. Journal of Chemical Physics 1975;63:5490-91.

304. Aue WP, Bartholdi B and Ernst RR. Two-dimensional spectroscopy application to nuclear magnetic resonance. Journal of Chemical Physics 1976;64:2229-46.

305. Kumar A, Welti D and Ernst RR. NMR fourier zeugmatography. Journal of Magnetic Resonance 1975;18:69-83.

306. Lauterbur PC. Image formation by induced local interactions: examples employing nuclear magnetic resonance. Nature 1973;242:190-91.

307. Hounsfield GN. Computerized transverse axial scanning (tomography). 1. Description of system. Br J Radiol 1973;46(552):1016-22.

308. Edelstein WA, Hutchison JM, Johnson G and Redpath T. Spin warp NMR imaging and

applications to human whole-body imaging. Phys Med Biol 1980;25(4):751-6.

309. Becker ED. High Resolution NMR. New York: Academic Press; 1980.

310. Freeman R. A Handbook of Nuclear Magnetic Resonance. . Harlow: Longman Scientific & Technical; 1987.

311. Derome AE. Modern NMR Techniques for Chemistry Research. Oxford: Pergamon Press; 1987.

312. Wider G and Wuthrich K. NMR spectroscopy of large molecules and multimolecular assemblies in solution. Curr Opin Struct Biol 1999;9(5):594-601.

313. Jardetzky O and Lefevre JF. Protein dynamics. FEBS Lett 1994;338(3):246-50.

314. Wuthrich K. Protein structure determination in solution by nuclear magnetic resonance spectroscopy. Science 1989;243(4887):45-50.

315. Wuthrich K. NMR of Proteins and Nucleic Acids. New York: Wiley; 1986.

316. Damadian R. Tumor detection by nuclear magnetic resonance. Science 1971;171(976):1151-3.

317. Damadian R, Goldsmith M and Minkoff L. NMR in cancer: XVI. FONAR image of the live human body. Physiol Chem Phys 1977;9(1):97-100, 08.

318. Mansfield P, Pykett IL and Morris PG. Human whole body line-scan imaging by NMR. Br J Radiol 1978;51(611):921-2.

319. Doyle FH, Gore JC, Pennock JM, Bydder GM, Orr JS, Steiner RE, Young IR, Burl M, Clow H, Gilderdale DJ, Bailes DR and Walters PE. Imaging of the brain by nuclear magnetic resonance. Lancet 1981;2(8237):53-7.

320. Mansfield P. Spatial mapping of the chemical shift in NMR. Magn Reson Med 1984;1(3):370-86.

321. Maudsley AA, Hilal SK, Perman WH and Simon HE. Spatially resolved high resolution spectroscopy by 'four-dimensional' NMR. J. Magn. Reson. 1983;51:147-52.

322. Brown TR, Kincaid BM and Ugurbil K. NMR chemical shift imaging in three dimensions. Proc Natl Acad Sci U S A 1982;79(11):3523-6.

323. Hennig J, Nauerth A and Friedburg H. RARE imaging: a fast imaging method for clinical MR. Magn Reson Med 1986;3(6):823-33.

324. Frahm J, Merboldt KD, Haenicke W and Haase A. Stimulated Echo Imaging. J. Magn. Reson. 1985;64:81-93.

325. Mansfield P. Multi-planar image formation using NMR spin echoes. J. Phys. C: Solid State 1977;10:L55-L58.

326. Mansfield P and Chapman B. Active magnetic screening of gradient coils in NMR imaging. J. Magn. Reson. 1986;66: 573-76.

327. Kreis R and Boesch C. Liquid-crystal-like structures of human muscle demonstrated by in vivo observation of direct dipolar coupling in localized proton magnetic resonance spectroscopy. J Magn Reson B 1994;104(2):189-92.

328. Gunther H. NMR spectroscopy : basic principles, concepts, and applications in chemistry. 2nd ed. ed. Chichester: Wiley; 1995.

329. Wuthrich K. The second decade--into the third millenium. Nat Struct Biol 1998;5 Suppl:492-5.

330. Wagner G. An account of NMR in structural biology. Nat Struct Biol 1997;4 Suppl:841-4.

331. Kay LE. Protein dynamics from NMR. Nat Struct Biol 1998;5 Suppl:513-7.

332. Boesch C, Bundi A, Oppliger M and Wuthrich K. 1H nuclear-magnetic-resonance studies of the molecular conformation of monomeric glucagon in aqueous solution. Eur J Biochem 1978;91(1):209-14.

333. Schwartz RB, Hsu L, Wong TZ, Kacher DF, Zamani AA, Black PM, Alexander E, 3rd, Stieg PE, Moriarty TM, Martin CA, Kikinis R and Jolesz FA. Intraoperative MR imaging guidance for intracranial neurosurgery: experience with the first 200 cases. Radiology 1999;211(2):477-88.

334. Jolesz FA. 1996 RSNA Eugene P. Pendergrass New Horizons Lecture. Image-guided procedures and the operating room of the future. Radiology 1997;204(3):601-12.

335. Silverman SG, Collick BD, Figueira MR, Khorasani R, Adams DF, Newman RW, Topulos GP and Jolesz FA. Interactive MR-guided biopsy in an open-configuration MR imaging system. Radiology 1995;197(1):175-81.

336. Belliveau JW, Kennedy DN, Jr., McKinstry RC, Buchbinder BR, Weisskoff RM, Cohen MS, Vevea JM, Brady TJ and Rosen BR. Functional mapping of the human visual cortex by magnetic resonance imaging. Science 1991;254(5032):716-9.

337. Belliveau JW, Rosen BR, Kantor HL, Rzedzian RR, Kennedy DN, McKinstry RC, Vevea

JM, Cohen MS, Pykett IL and Brady TJ. Functional cerebral imaging by susceptibility-contrast NMR. Magn Reson Med 1990;14(3):538-46.

338. Ogawa S, Lee TM, Kay AR and Tank DW. Brain magnetic resonance imaging with contrast dependent on blood oxygenation. Proc Natl Acad Sci U S A 1990;87(24):9868-72.

339. Le Bihan D, Breton E, Lallemand D, Grenier P, Cabanis E and Laval-Jeantet M. MR imaging of intravoxel incoherent motions: application to diffusion and perfusion in neurologic disorders. Radiology 1986;161(2):401-7.

340. Merboldt KD, Haenicke W and Frahm J. Self-Diffusion NMR imaging using stimulated echoes. J. Magn. Reson. 1985;64:479-86.

341. Wolff SD, Eng J and Balaban RS. Magnetization transfer contrast: method for improving contrast in gradient-recalled-echo images. Radiology 1991;179(1):133-7.

342. Balaban RS and Ceckler TL. Magnetization transfer contrast in magnetic resonance imaging. Magn Reson Q 1992;8(2):116-37.

343. Albert MS, Cates GD, Driehuys B, Happer W, Saam B, Springer CS, Jr. and Wishnia A. Biological magnetic resonance imaging using laser-polarized 129Xe. Nature 1994;370(6486):199-201.

344. Middleton H, Black RD, Saam B, Cates GD, Cofer GP, Guenther R, Happer W, Hedlund LW, Johnson GA, Juvan K and et al. MR imaging with hyperpolarized 3He gas. Magn Reson Med 1995;33(2):271-5.

345. Eliav U and Navon G. A study of dipolar interactions and dynamic processes of water molecules in tendon by 1H and 2H homonuclear and heteronuclear multiple-quantum-filtered NMR spectroscopy. J Magn Reson 1999;137(2):295-310.

346. Sharf Y, Seo Y, Eliav U, Akselrod S and Navon G. Mapping strain exerted on blood vessel walls using deuterium double-quantum-filtered MRI. Proc Natl Acad Sci U S A 1998;95(8):4108-12.

347. De Graaf RA. In vivo NMR spectroscopy : principles and techniques. Chichester: Wiley; 1998.

348. Danielsen ER and Ross B. Magnetic resonance spectroscopy diagnosis of neurological diseases. New York: M. Dekker; 1999.

349. Bell JD and Bhakoo KK. Metabolic changes underlying 31P MR spectral alterations in human hepatic tumours. NMR Biomed 1998;11(7):354-9.

350. Hetherington HP, Pan JW, Chu WJ, Mason GF and Newcomer BR. Biological and clinical MRS at ultra-high field. NMR Biomed 1997;10(8):360-71.

351. Allen PS, Thompson RB and Wilman AH. Metabolite-specific NMR spectroscopy in vivo. NMR Biomed 1997;10(8):435-44.

352. Nelson SJ, Vigneron DB, Star-Lack J and Kurhanewicz J. High spatial resolution and speed in MRSI. NMR Biomed 1997;10(8):411-22.

353. Beckmann N. 13C magnetic resonance spectroscopy as a noninvasive tool for metabolic studies on humans. In: Beckmann N, editor. Carbon-13 NMR spectroscopy of biological systems. San Diego ; London: Academic Press; 1995. p. 269-322.

354. Kent-Braun JA, Miller RG and Weiner MW. Magnetic resonance spectroscopy studies of human muscle. Radiol Clin North Am 1994;32(2):313-35.

355. Kemp GJ and Radda GK. Quantitative interpretation of bioenergetic data from 31P and 1H magnetic resonance spectroscopic studies of skeletal muscle: an analytical review. Magn Reson Q 1994;10(1):43-63.

356. Vion-Dury J, Meyerhoff DJ, Cozzone PJ and Weiner MW. What might be the impact on neurology of the analysis of brain metabolism by in vivo magnetic resonance spectroscopy? J Neurol 1994;241(6):354-71.

357. Howe FA, Maxwell RJ, Saunders DE, Brown MM and Griffiths JR. Proton spectroscopy in vivo. Magn Reson Q 1993;9(1):31-59.

358. Connelly A, Jackson GD, Frackowiak RS, Belliveau JW, Vargha-Khadem F and Gadian DG. Functional mapping of activated human primary cortex with a clinical MR imaging system. Radiology 1993;188(1):125-30.

359. Kaibara T, Tyson RL and Sutherland GR. Human cerebral neoplasms studied using MR spectroscopy: a review. Biochem Cell Biol 1998;76(2-3):477-86.

360. Taylor JS, Ogg RJ and Langston JW. Proton MR spectroscopy of pediatric brain tumors. Neuroimaging Clin N Am 1998;8(4):753-79.

361. Castillo M and Kwock L. Proton MR spectroscopy of common brain tumors. Neuroimaging Clin N Am 1998;8(4):733-52.

362. Ross BD, Ernst T and Kreis R. Proton Magnetic Resonance Spectroscopy in Hypoxic-Ischemic Disorders. In: Faerber EN, editor. CNS magnetic resonance imaging in infants & children. London: Mac Keith Press ; [Cambridge] : Cambridge University Press [distributor]; 1995. p. xii,334p.

363. Wardlaw JM, Marshall I, Wild J, Dennis MS, Cannon J and Lewis SC. Studies of acute ischemic stroke with proton magnetic resonance spectroscopy: relation between time from onset, neurological deficit, metabolite abnormalities in the infarct, blood flow, and clinical outcome. Stroke 1998;29(8):1618-24.

364. Kaji Y, Kurhanewicz J, Hricak H, Sokolov DL, Huang LR, Nelson SJ and Vigneron DB. Localizing prostate cancer in the presence of postbiopsy changes on MR images: role of proton MR spectroscopic imaging. Radiology 1998;206(3):785-90.

365. Kurhanewicz J, Vigneron DB, Hricak H, Parivar F, Nelson SJ, Shinohara K and Carroll PR. Prostate cancer: metabolic response to cryosurgery as detected with 3D H-1 MR spectroscopic imaging. Radiology 1996;200(2):489-96.

366. Hetherington HP and Pohost GM. High yeld whole body systems. In: Grant DM and Harris RK, editors. Encyclopedia of Nuclear Magnetic Resonance. Chichester Sussex, UK: Wiley; 1996. p. 2354-60.

367. Gruetter R, Seaquist ER, Kim S and Ugurbil K. Localized in vivo 13C-NMR of glutamate metabolism in the human brain: initial results at 4 tesla. Dev Neurosci 1998;20(4-5):380-8.

368. Robitaille PM, Abduljalil AM, Kangarlu A, Zhang X, Yu Y, Burgess R, Bair S, Noa P, Yang L, Zhu H, Palmer B, Jiang Z, Chakeres DM and Spigos D. Human magnetic resonance imaging at 8 T. NMR Biomed 1998;11(6):263-5.

369. Gibelin H, Eugene M, Hebrard W, Henry C, Carretier M and Hauet T. A new approach to the evaluation of liver graft function by nuclear magnetic resonance spectroscopy. A comparative study between Euro- Collins and University of Wisconsin solutions. Clin Chem Lab Med 2000;38(11):1133-36.

370. Sequeira SS, Parkes HG, Ellul JP and Murphy GM. In vitro determination by 1H-NMR studies that bile with shorter nucleation times contain cholesterol-enriched vesicles. Biochim Biophys Acta 1995;1256(3):360-6.

371. Ishikawa H, Nakashima T, Inaba K, Mitsuyoshi H, Nakajima Y, Sakamoto Y, Okanoue T, Kashima K and Seo Y. Proton magnetic resonance assay of total and taurine-conjugated bile acids in bile. J Lipid Res 1999;40(10):1920-4.

372. Sparling ML. Analysis of mixed lipid extracts using 1H NMR spectra. Comput Appl Biosci 1990;6(1):29-42.

373. Dabos KJ, Newsome PN, Parkinson JA, Davidson JS, Sadler IH, Plevris JN and Hayes PC. A biochemical prognostic model of outcome in paracetamol-induced acute liver

injury. Transplantation 2005;80(12):1712-7.

374. Dabos KJ, Newsome PN, Parkinson JA, Mohammed HH, Sadler IH, Plevris JN and Hayes PC. Biochemical prognostic markers of outcome in non-paracetamol-induced fulminant hepatic failure. Transplantation 2004;77(2):200-5.

375. Cordoba J, Alonso J, Rovira A, Jacas C, Sanpedro F, Castells L, Vargas V, Margarit C, Kulisewsky J, Esteban R and Guardia J. The development of low-grade cerebral edema in cirrhosis is supported by the evolution of (1)H-magnetic resonance abnormalities after liver transplantation. J Hepatol 2001;35(5):598-604.

376. Alwayn IP, Andersson C, Zauscher B, Gura K, Nose V and Puder M. Omega-3 fatty acids improve hepatic steatosis in a murine model: potential implications for the marginal steatotic liver donor. Transplantation 2005;79(5):606-8.

377. Niemann CU, Hirose R, Liu T, Behrends M, Brown JL, Kominsky DF, Roberts JP and Serkova N. Ischemic preconditioning improves energy state and transplantation survival in obese Zucker rat livers. Anesth Analg 2005;101(6):1577-83.

378. Radda GK, Gadian DG and Ross BD. Energy metabolism and cellular pH in normal and pathological conditions. A new look through 31phosphorus nuclear magnetic resonance. Ciba Found Symp 1982;87:36-57.

379. Changani KK, Fuller BJ, Bryant DJ, Bell JD, Ala-Korpela M, Taylor-Robinson SD, Moore DP and Davidson BR. Non-invasive assessment of ATP regeneration potential of the preserved donor liver. A 31P MRS study in pig liver. J Hepatol 1997;26(2):336-42.

380. Chu WC, Lam WW, Lee KH, Yeung DK, Sihoe J and Yeung CK. Phosphorus-31 MR spectroscopy in pediatric liver transplant recipients: a noninvasive assessment of graft status with correlation with liver function tests and liver biopsy. AJR Am J Roentgenol 2005;184(5):1624-9.

381. Davidson BR, Barnard ML, Changani KK and Taylor-Robinson SD. Liver transplantation: current and potential applications of magnetic resonance spectroscopy. Liver Transpl Surg 1997;3(5):481-93.

382. Singh HK, Yachha SK, Saxena R, Gupta A, Nagana Gowda GA, Bhandari M and Khetrapal CL. A new dimension of 1H-NMR spectroscopy in assessment of liver graft dysfunction. NMR Biomed 2003;16(4):185-8.

383. Kuntz E and Kuntz H-Db. Hepatology Principles and Practice. Berlin ; London: Springer; 2002.

384. Waniewski RA. Physiological levels of ammonia regulate glutamine synthesis from

extracellular glutamate in astrocyte cultures. J Neurochem 1992;58(1):167-74.

385. Suarez I, Bodega G and Fernandez B. Glutamine synthetase in brain: effect of ammonia. Neurochem Int 2002;41(2-3):123-42.

386. Trehout D, Desille M, Doan BT, Mahler S, Fremond B, Malledant Y, Campion JP, Desbois J, Beloeil JC, de Certaines J and Clement B. Follow-up by one- and two-dimensional NMR of plasma from pigs with ischemia-induced acute liver failure treated with a bioartificial liver. NMR Biomed 2002;15(6):393-403.

387. Thomas EL, Taylor-Robinson SD, Barnard ML, Frost G, Sargentoni J, Davidson BR, Cunnane SC and Bell JD. Changes in adipose tissue composition in malnourished patients before and after liver transplantation: a carbon-13 magnetic resonance spectroscopy and gas-liquid chromatography study. Hepatology 1997;25(1):178-83.

388. Vilca Melendez H, Gilani SS, Cochrane BC, Rela M, Murphy GM and Heaton ND. A validated technique for the analysis of biliary bile acid secretion in donor livers prior to transplantation. Transpl Int 1998;11(3):216-22.

389. Wolf RF, Haagsma EB, Kamman RL, Mooyaart EL, Sluiter WJ and Sloof MJ. Noninvasive metabolic assessment of human donor livers: prognostic value of 31P-magnetic resonance spectroscopy for early graft function. Transplantation 1997;64(1):147-52.

390. Taylor-Robinson SD, Sargentoni J, Bell JD, Thomas EL, Marcus CD, Changani KK, Saeed N, Hodgson HJ, Davidson BR, Burroughs AK, Rolles K, Foster CS and Cox IJ. In vivo and in vitro hepatic phosphorus-31 magnetic resonance spectroscopy and electron microscopy in chronic ductopenic rejection of human liver allografts. Gut 1998;42(5):735-43.

391. Wyatt JS, Cope M, Delpy DT, Richardson CE, Edwards AD, Wray S and Reynolds EO. Quantitation of cerebral blood volume in human infants by near-infrared spectroscopy. J Appl Physiol 1990;68(3):1086-91.

392. Matcher SJ, Cope M and Delpy DT. Use of the water absorption spectrum to quantify tissue chromophore concentration changes in near-infrared spectroscopy. Phys Med Biol 1994;39(1):177-96.

393. El-Desoky A, Seifalian AM, Cope M, Delpy DT and Davidson BR. Experimental study of liver dysfunction evaluated by direct indocyanine green clearance using near infrared spectroscopy. Br J Surg 1999;86(8):1005-11.

394. El-Desoky AE, Seifalian AM and Davidson BR. Effect of graded hypoxia on hepatic

tissue oxygenation measured by near infrared spectroscopy. J Hepatol 1999;31(1):71-6.

395. Jiao LR, El-Desoky AA, Seifalian AM, Habib N and Davidson BR. Effect of liver blood flow and function on hepatic indocyanine green clearance measured directly in a cirrhotic animal model. Br J Surg 2000;87(5):568-74.

396. El-Desoky AE, Delpy DT, Davidson BR and Seifalian AM. Assessment of hepatic ischaemia reperfusion injury by measuring intracellular tissue oxygenation using near infrared spectroscopy. Liver 2001;21(1):37-44.

397. Seifalian AM, El-Desoky A and Davidson BR. Hepatic indocyanine green uptake and excretion in a rabbit model of steatosis. Eur Surg Res 2001;33(3):193-201.

398. Seifalian AM, El-Desoky H, Delpy DT and Davidson BR. Effect of graded hypoxia on the rat hepatic tissue oxygenation and energy metabolism monitored by near-infrared and 31P nuclear magnetic resonance spectroscopy. Faseb J 2001;15(14):2642-8.

399. Seifalian AM, El-Desoky H, Delpy DT and Davidson BR. Effects of hepatic ischaemia/reperfusion injury in a rabbit model of Indocyanine Green clearance. Clin Sci (Lond) 2002;102(5):579-86.

400. Kanoria S, Glantzounis G, Jalan R, Davies NA, Seifalian AM, Williams R and Davidson BR. A model to study total hepatic ischemia-reperfusion injury. Transplant Proc 2004;36(9):2586-9.

401. Glantzounis GK, Sheth H, Thompson C, Hafez TS, Kanoria S, Pamecha V, Davies S, Mikhailidis DP, Seifalian AM and Davidson BR. Acute limb ischemia caused by femoral arterial line induces remote liver injury in a rabbit model of liver ischemia/reperfusion injury. Angiology 2009;60(5):554-61.

402. Koo A, Komatsu H, Tao G, Inoue M, Guth PH and Kaplowitz N. Contribution of no-reflow phenomenon to hepatic injury after ischemia-reperfusion: evidence for a role for superoxide anion. Hepatology 1992;15(3):507-14.

403. Nishiyama T, Yokoyama T and Hanaoka K. Effects of sevoflurane and isoflurane anesthesia on arterial ketone body ratio and liver function. Acta Anaesthesiol Scand 1999;43(3):347-51.

404. Vollmar B, Menger MD, Glasz J, Leiderer R and Messmer K. Impact of leukocyte-endothelial cell interaction in hepatic ischemia-reperfusion injury. Am J Physiol 1994;267(5 Pt 1):G786-93.

405. Chouillard EK, Gumbs AA and Cherqui D. Vascular clamping in liver surgery: physiology, indications and techniques. Ann Surg Innov Res 2010;4:2.

406. Kleinman REWWA. Walker's pediatric gastrointestinal disease physiology, diagnosis, management. 2008 2008 [cited; Available from: http://www.r2library.com/public/ResourceDetail.aspx?authCheck=true&resId=2392

407. Rappaport AM. Hepatic blood flow: morphologic aspects and physiologic regulation. Int Rev Physiol 1980;21:1-63.

408. Lautt WW. Mechanism and role of intrinsic regulation of hepatic arterial blood flow: hepatic arterial buffer response. Am J Physiol 1985;249(5 Pt 1):G549-56.

409. Lautt WW, Legare DJ and Ezzat WR. Quantitation of the hepatic arterial buffer response to graded changes in portal blood flow. Gastroenterology 1990;98(4):1024-8.

410. Lautt WW. Multiple Mechanisms Maintaining a Constant Hepatic Blood Flow to Liver Mass Ratio. In: Lautt WW, editor. Hepatic Circulation: Physiology and Pathophysiology. San Rafael (CA, USA): Morgan & Claypool Life Sciences; 2009. p. 137-43.

411. Accatino L, Contreras A, Fernandez S and Quintana C. The effect of complete biliary obstruction on bile flow and bile acid excretion: postcholestatic choleresis in the rat. J Lab Clin Med 1979;93(5):706-17.

412. Kountouras J, Billing BH and Scheuer PJ. Prolonged bile duct obstruction: a new experimental model for cirrhosis in the rat. Br J Exp Pathol 1984;65(3):305-11.

413. Accatino L, Contreras A, Berdichevsky E and Quintana C. The effect of complete biliary obstruction on bile secretion. Studies on the mechanisms of postcholestatic choleresis in the rat. J Lab Clin Med 1981;97(4):525-34.

414. Beckonert O, Keun HC, Ebbels TM, Bundy J, Holmes E, Lindon JC and Nicholson JK. Metabolic profiling, metabolomic and metabonomic procedures for NMR spectroscopy of urine, plasma, serum and tissue extracts. Nat Protoc 2007;2(11):2692-703.

415. Munshi SU, Rewari BB, Bhavesh NS and Jameel S. Nuclear magnetic resonance based profiling of biofluids reveals metabolic dysregulation in HIV-infected persons and those on anti-retroviral therapy. PLoS One 2013;8(5):e64298.

416. Wang L, Tang Y, Liu S, Mao S, Ling Y, Liu D, He X and Wang X. Metabonomic profiling of serum and urine by (1)H NMR-based spectroscopy discriminates patients with chronic obstructive pulmonary disease and healthy individuals. PLoS One 2013;8(6):e65675.

417. Carrola J, Rocha CM, Barros AS, Gil AM, Goodfellow BJ, Carreira IM, Bernardo J, Gomes A, Sousa V, Carvalho L and Duarte IF. Metabolic signatures of lung cancer in biofluids: NMR-based metabonomics of urine. J Proteome Res 2010;10(1):221-30.

418. Zhang F, Jia Z, Gao P, Kong H, Li X, Chen J, Yang Q, Yin P, Wang J, Lu X, Li F, Wu Y and Xu G. Metabonomics study of atherosclerosis rats by ultra fast liquid chromatography coupled with ion trap-time of flight mass spectrometry. Talanta 2009;79(3):836-44.

419. Schicho R, Shaykhutdinov R, Ngo J, Nazyrova A, Schneider C, Panaccione R, Kaplan GG, Vogel HJ and Storr M. Quantitative Metabolomic Profiling of Serum, Plasma, and Urine by (1)H NMR Spectroscopy Discriminates between Patients with Inflammatory Bowel Disease and Healthy Individuals. J Proteome Res 2012.

420. Atherton HJ, Bailey NJ, Zhang W, Taylor J, Major H, Shockcor J, Clarke K and Griffin JL. A combined 1H-NMR spectroscopy- and mass spectrometry-based metabolomic study of the PPAR-alpha null mutant mouse defines profound systemic changes in metabolism linked to the metabolic syndrome. Physiol Genomics 2006;27(2):178-86.

421. Jiang CY, Yang KM, Yang L, Miao ZX, Wang YH and Zhu HB. A H NMR-Based Metabonomic Investigation of Time-Related Metabolic Trajectories of the Plasma, Urine and Liver Extracts of Hyperlipidemic Hamsters. PLoS One 2013;8(6):e66786.

422. Fukuhara K, Ohno A, Ando Y, Yamoto T and Okuda H. A 1H NMR-based metabolomics approach for mechanistic insight into acetaminophen-induced hepatotoxicity. Drug Metab Pharmacokinet 2011;26(4):399-406.

423. Bradford BU, O'Connell TM, Han J, Kosyk O, Shymonyak S, Ross PK, Winnike J, Kono H and Rusyn I. Metabolomic profiling of a modified alcohol liquid diet model for liver injury in the mouse uncovers new markers of disease. Toxicol Appl Pharmacol 2008;232(2):236-43.

424. Kang SM, Park JC, Shin MJ, Lee H, Oh J, Ryu do H, Hwang GS and Chung JH. (1)H nuclear magnetic resonance based metabolic urinary profiling of patients with ischemic heart failure. Clin Biochem;44(4):293-9.

425. Bajaj JS, Gillevet PM, Patel NR, Ahluwalia V, Ridlon JM, Kettenmann B, Schubert CM, Sikaroodi M, Heuman DM, Crossey MM, Bell DE, Hylemon PB, Fatouros PP and Taylor-Robinson SD. A longitudinal systems biology analysis of lactulose withdrawal in hepatic encephalopathy. Metab Brain Dis 2012;27(2):205-15.

426. Hui AM, Kawasaki S, Makuuchi M, Nakayama J, Ikegami T and Miyagawa S. Liver injury following normothermic ischemia in steatotic rat liver. Hepatology 1994;20(5):1287-93.

427. Neuschwander-Tetri BA and Caldwell SH. Nonalcoholic steatohepatitis: summary of an AASLD Single Topic Conference. Hepatology 2003;37(5):1202-19.

428. Almond NE and Wheatley AM. Measurement of hepatic perfusion in rats by laser Doppler flowmetry. Am J Physiol 1992;262(2 Pt 1):G203-9.

429. Shepherd AP, Riedel GL, Kiel JW, Haumschild DJ and Maxwell LC. Evaluation of an infrared laser-Doppler blood flowmeter. Am J Physiol 1987;252(6 Pt 1):G832-9.

430. Wheatley AM and Zhao D. Intraoperative assessment by laser Doppler flowmetry of hepatic perfusion during orthotopic liver transplantation in the rat. Transplantation 1993;56(6):1315-8.

431. Wheatley AM, Almond NE, Stuart ET and Zhao D. Interpretation of the laser Doppler flow signal from the liver of the rat. Microvasc Res 1993;45(3):290-301.

432. Seifalian AM, Mallet SV, Rolles K and Davidson BR. Hepatic microcirculation during human orthotopic liver transplantation. Br J Surg 1997;84(10):1391-5.

433. Nicholls DG and Ferguson SJ. Bioenergetics 2: Academic; 1992.

434. Erecinska M and Wilson DF. Regulation of cellular energy metabolism. J Membr Biol 1982;70(1):1-14.

435. Jobsis FF, editor. Principles of multiwavelength near infrared spectroscopy for assessing oxidative metabolism. Frankfurt: PMI Verlagsgruppe; 1992.

436. Capaldi RA. Structure and assembly of cytochrome c oxidase. Arch Biochem Biophys 1990;280(2):252-62.

437. Edwards AD, Brown GC, Cope M, Wyatt JS, McCormick DC, Roth SC, Delpy DT and Reynolds EO. Quantification of concentration changes in neonatal human cerebral oxidized cytochrome oxidase. J Appl Physiol 1991;71(5):1907-13.

438. Nicholls DG and Ferguson SJ. Respiratory Chains. In: Nicholls DG and Ferguson SJ, editors. Bioenergetics 2. 2nd ed. London ; San Diego: Academic Press; 1992. p. 107-54.

439. Cooper CE, Matcher SJ, Wyatt JS, Cope M, Brown GC, Nemoto EM and Delpy DT. Near-infrared spectroscopy of the brain: relevance to cytochrome oxidase bioenergetics. Biochem Soc Trans 1994;22(4):974-80.

440. Cleeter MW, Cooper JM, Darley-Usmar VM, Moncada S and Schapira AH. Reversible inhibition of cytochrome c oxidase, the terminal enzyme of the mitochondrial respiratory chain, by nitric oxide. Implications for neurodegenerative diseases. FEBS Lett 1994;345(1):50-4.

441. Cooper CE. Nitric oxide and cytochrome oxidase: substrate, inhibitor or effector? Trends

Biochem Sci 2002;27(1):33-9.

442. Shiva S and Darley-Usmar VM. Control of the nitric oxide-cytochrome c oxidase signaling pathway under pathological and physiological conditions. IUBMB Life 2003;55(10-11):585-90.

443. Shiva S, Oh JY, Landar AL, Ulasova E, Venkatraman A, Bailey SM and Darley-Usmar VM. Nitroxia: the pathological consequence of dysfunction in the nitric oxide-cytochrome c oxidase signaling pathway. Free Radic Biol Med 2005;38(3):297-306.

444. Marks DB, Marks AD and Smith CM. Basic medical biochemistry : a clinical approach. Baltimore ; London: Williams & Wilkins; 1996.

445. Jobsis FF. Noninvasive, infrared monitoring of cerebral and myocardial oxygen sufficiency and circulatory parameters. Science 1977;198(4323):1264-7.

446. Boelens R and Wever R. Redox reactions in mixed-valence cytochrome c oxidase. FEBS Lett 1980;116(2):223-6.

447. Takashima S, Hirano S, Kamei S, Hasegawa M and Kimoto H. Cerebral hemodynamics on near-infrared spectroscopy in hypoxia and ischemia in young animal studies. Brain Dev 1995;17(5):312-6.

448. Grainger SL, Keeling PW, Brown IM, Marigold JH and Thompson RP. Clearance and non-invasive determination of the hepatic extraction of indocyanine green in baboons and man. Clin Sci (Lond) 1983;64(2):207-12.

449. Shinohara H, Tanaka A, Kitai T, Yanabu N, Inomoto T, Satoh S, Hatano E, Yamaoka Y and Hirao K. Direct measurement of hepatic indocyanine green clearance with near-infrared spectroscopy: separate evaluation of uptake and removal. Hepatology 1996;23(1):137-44.

450. Sterpetti AV, Hunter WJ, Schultz RD, Sugimoto JT, Blair EA, Hacker K, Chasan P and Valentine J. Seeding with endothelial cells derived from the microvessels of the omentum and from the jugular vein: a comparative study. J Vasc Surg 1988;7(5):677-84.

451. Kitai T, Tanaka A, Tokuka A, Tanaka K, Yamaoka Y, Ozawa K and Hirao K. Quantitative detection of hemoglobin saturation in the liver with near-infrared spectroscopy. Hepatology 1993;18(4):926-36.

452. Kitai T, Tanaka A, Tokuka A, Tanaka K, Yamaoka Y, Ozawa K and Hirao K. Changes in the hepatic oxygenation state during hemorrhage and following epinephrine or dextran infusion as assessed by near-infrared spectroscopy. Circ Shock 1993;41(3):197-205.

453. Elwell CE, Cope M, Edwards AD, Wyatt JS, Delpy DT and Reynolds EO. Quantification of adult cerebral hemodynamics by near-infrared spectroscopy. J Appl Physiol 1994;77(6):2753-60.

454. Wray S, Cope M, Delpy DT, Wyatt JS and Reynolds EO. Characterization of the near infrared absorption spectra of cytochrome aa3 and haemoglobin for the non-invasive monitoring of cerebral oxygenation. Biochim Biophys Acta 1988;933(1):184-92.

455. Ojha M, Cobbold RS and Johnston KW. Hemodynamics of a side-to-end proximal arterial anastomosis model. J Vasc Surg 1993;17(4):646-55.

456. Cooke JP, Rossitch E, Jr., Andon NA, Loscalzo J and Dzau VJ. Flow activates an endothelial potassium channel to release an endogenous nitrovasodilator. J Clin Invest 1991;88(5):1663-71.

457. De Blasi RA, Almenrader N and Ferrari M. Brain oxygenation monitoring during cardiopulmonary bypass by near infrared spectroscopy. Adv Exp Med Biol 1997;413:97-104.

458. Cope M. The application of near infrared spectroscopy to non invasive monitoring of cerebral oxygenation in the newborn infant. London: University College London; 1991.

459. Essenpreis M, Cope M, Elwell CE, Arridge SR, van der Zee P and Delpy DT. Wavelength dependence of the differential pathlength factor and the log slope in time-resolved tissue spectroscopy. Adv Exp Med Biol 1993;333:9-20.

460. Lautt WW and Greenway CV. Conceptual review of the hepatic vascular bed. Hepatology 1987;7(5):952-63.

461. Takata M and Robotham JL. Effects of inspiratory diaphragmatic descent on inferior vena caval venous return. J Appl Physiol 1992;72(2):597-607.

462. Doi R, Inoue K, Kogire M, Sumi S, Takaori K, Suzuki T and Tobe T. Simultaneous measurement of hepatic arterial and portal venous flows by transit time ultrasonic volume flowmetry. Surg Gynecol Obstet 1988;167(1):65-9.

463. Jakab F, Rath Z, Schmal F, Nagy P and Faller J. The interaction between hepatic arterial and portal venous blood flows; simultaneous measurement by transit time ultrasonic volume flowmetry. Hepatogastroenterology 1995;42(1):18-21.

464. Ayuse T, Brienza N, O'Donnell CP and Robotham JL. Pressure-flow analysis of portal vein and hepatic artery interactions in porcine liver. Am J Physiol 1994;267(4 Pt 2):H1233-42.

465. Tsubono T, Todo S, Jabbour N, Mizoe A, Warty V, Demetris AJ and Starzl TE. Indocyanine green elimination test in orthotopic liver recipients. Hepatology 1996;24(5):1165-71.

466. Plevris JN, Jalan R, Bzeizi KI, Dollinger MM, Lee A, Garden OJ and Hayes PC. Indocyanine green clearance reflects reperfusion injury following liver transplantation and is an early predictor of graft function. J Hepatol 1999;30(1):142-8.

467. Igarashi H, Kamisaka K, Maezawa H and Uesugi T. Degradation and metabolism of indocyanine green: high-pressure liquid chromatographic analysis. Bull Tokyo Med Dent Univ 1990;37(4):59-69.

468. Rakich PM, Prasse KW and Bjorling DE. Clearance of indocyanine green in dogs with partial hepatectomy, hepatic duct ligation, and passive hepatic congestion. Am J Vet Res 1987;48(9):1353-7.

469. Swank RL and Davenport HA. Chlorate-osmic formalin method for degeneration myelin. Staining Technololgy 1935;10:87–90.

470. Sýkora S. One-Page MR Primer. [Web Page] 2006 [cited 2010; Available from: http://www.ebyte.it/library/educards/nmr/OnePageMrPrimer.html

471. Keeler J. Understanding NMR spectroscopy. Chichester: John Wiley; 2005.

472. Sequeira SS, Parkes HG, Ellul JP and Murphy GM. One dimensional high resolution 1H NMR spectroscopy of human bile: lipid-derived resonance shifts. Biochem Soc Trans 1994;22(2):114S.

473. Ting KC, Gill M and Garbin O. GC/MS screening method for phthalate esters in children's toys. J AOAC Int 2009;92(3):951-8.

474. Kubwabo C, Kosarac I, Stewart B, Gauthier BR, Lalonde K and Lalonde PJ. Migration of bisphenol A from plastic baby bottles, baby bottle liners and reusable polycarbonate drinking bottles. Food Addit Contam Part A Chem Anal Control Expo Risk Assess 2009;26(6):928-37.

475. McDonald GR, Hudson AL, Dunn SM, You H, Baker GB, Whittal RM, Martin JW, Jha A, Edmondson DE and Holt A. Bioactive contaminants leach from disposable laboratory plasticware. Science 2008;322(5903):917.

476. Watson J, Greenough EB, Leet JE, Ford MJ, Drexler DM, Belcastro JV, Herbst JJ, Chatterjee M and Banks M. Extraction, identification, and functional characterization of a bioactive substance from automated compound-handling plastic tips. J Biomol Screen 2009;14(5):566-72.

477. Olivieri A, Degenhardt OS, McDonald GR, Narang D, Paulsen IM, Kozuska JL and Holt A. On the disruption of biochemical and biological assays by chemicals leaching from disposable laboratory plasticware. Can J Physiol Pharmacol 2012;90(6):697-703.

478. Dumas ME, Maibaum EC, Teague C, Ueshima H, Zhou B, Lindon JC, Nicholson JK, Stamler J, Elliott P, Chan Q and Holmes E. Assessment of analytical reproducibility of 1H NMR spectroscopy based metabonomics for large-scale epidemiological research: the INTERMAP Study. Anal Chem 2006;78(7):2199-208.

479. Keun HC, Ebbels TM, Antti H, Bollard ME, Beckonert O, Schlotterbeck G, Senn H, Niederhauser U, Holmes E, Lindon JC and Nicholson JK. Analytical reproducibility in (1)H NMR-based metabonomic urinalysis. Chem Res Toxicol 2002;15(11):1380-6.

480. Van QN and Veenstra TD. How close is the bench to the bedside? Metabolic profiling in cancer research. Genome Med 2009;1(1):5.

481. Blekherman G, Laubenbacher R, Cortes DF, Mendes P, Torti FM, Akman S, Torti SV and Shulaev V. Bioinformatics tools for cancer metabolomics. Metabolomics 2011;7(3):329-43.

482. Kholodenko B, Yaffe MB and Kolch W. Computational approaches for analyzing information flow in biological networks. Sci Signal 2012;5(220):re1.

483. Anderson NL and Anderson NG. Proteome and proteomics: new technologies, new concepts, and new words. Electrophoresis 1998;19(11):1853-61.

484. Blackstock WP and Weir MP. Proteomics: quantitative and physical mapping of cellular proteins. Trends Biotechnol 1999;17(3):121-7.

485. Wilkins MR, Pasquali C, Appel RD, Ou K, Golaz O, Sanchez JC, Yan JX, Gooley AA, Hughes G, Humphery-Smith I, Williams KL and Hochstrasser DF. From proteins to proteomes: large scale protein identification by two-dimensional electrophoresis and amino acid analysis. Biotechnology (N Y) 1996;14(1):61-5.

486. Ceglarek U, Leichtle A, Brugel M, Kortz L, Brauer R, Bresler K, Thiery J and Fiedler GM. Challenges and developments in tandem mass spectrometry based clinical metabolomics. Mol Cell Endocrinol 2009;301(1-2):266-71.

487. van der Greef J and Smilde AK. Symbiosis of chemometrics and metabolomics: past, present, and future. Journal of Chemometrics 2005;19(5-7):376-86.

488. Nicholson JK and Lindon JC. Systems biology: Metabonomics. Nature 2008;455(7216):1054-6.

489. Hoult DI, Busby SJ, Gadian DG, Radda GK, Richards RE and Seeley PJ. Observation of tissue metabolites using 31P nuclear magnetic resonance. Nature 1974;252(5481):285-7.

490. Holmes E and Antti H. Chemometric contributions to the evolution of metabonomics: mathematical solutions to characterising and interpreting complex biological NMR spectra. Analyst 2002;127(12):1549-57.

491. Lenz EM and Wilson ID. Analytical strategies in metabonomics. J Proteome Res 2007;6(2):443-58.

492. Holmes E, Wilson ID and Nicholson JK. Metabolic phenotyping in health and disease. Cell 2008;134(5):714-7.

493. Nicholson JK, Connelly J, Lindon JC and Holmes E. Metabonomics: a platform for studying drug toxicity and gene function. Nat Rev Drug Discov 2002;1(2):153-61.

494. Nicholson JK, Lindon JC and Holmes E. 'Metabonomics': understanding the metabolic responses of living systems to pathophysiological stimuli via multivariate statistical analysis of biological NMR spectroscopic data. Xenobiotica 1999;29(11):1181-9.

495. Trygg J, Holmes E and Lundstedt T. Chemometrics in metabonomics. J Proteome Res 2007;6(2):469-79.

496. Mercier P, Lewis MJ, Chang D, Baker D and Wishart DS. Towards automatic metabolomic profiling of high-resolution one-dimensional proton NMR spectra. J Biomol NMR 2011;49(3-4):307-23.

497. Munck L, Jespersen BM, Rinnan Å, Seefeldt HF, Engelsen MM, Nørgaard L and Engelsen SB. A physiochemical theory on the applicability of soft mathematical models—experimentally interpreted. Journal of Chemometrics 2010;24(7-8):481-95.

498. Jamieson NV, Lindell S, Sundberg R, Southard JH and Belzer FO. An analysis of the components in UW solution using the isolated perfused rabbit liver. Transplantation 1988;46(4):512-6.

499. Glantzounis GK, Yang W, Koti RS, Mikhailidis DP, Seifalian AM and Davidson BR. Continuous infusion of N-acetylcysteine reduces liver warm ischaemia-reperfusion injury. Br J Surg 2004;91(10):1330-9.

500. Arrese M, Pizarro M, Solis N and Accatino L. Recent advances in hepatobiliary transport. Recent Res Devel Lipids 2001;5:15-35.

501. Boyer JL. Sperber I. Secretion of organic anions in the formation of urine and

bile[Pharmacol. Rev. 1959;11:109-134]. J Hepatol 2002;36(1):4-7.

502. Paczkowska A, Toczylowska B, Nyckowski P, Patkowski W, Kanski A, Krawczyk M and Oldakowska-Jedynak U. High-resolution 1H nuclear magnetic resonance spectroscopy analysis of bile samples obtained from a patient after orthotopic liver transplantation: new perspectives. Transplant Proc 2003;35(6):2278-80.

503. Vilca Melendez H, Rela M, Setchell KD, Murphy GM and Heaton ND. Bile acids analysis: a tool to assess graft function in human liver transplantation. Transpl Int 2004;17(6):286-92.

504. Burn PR, Haider MA, Alfuhaid T, Brown MP and Roberts TP. Proton magnetic resonance spectroscopy as a potential tool for differentiating between abdominal fluid collections. J Magn Reson Imaging 2003;18(6):740-4.

505. Wang ZJ, Haselgrove JC, Martin MB, Hubbard AM, Li S, Loomes K, Moore JR, Zhao H and Cohen AR. Evaluation of iron overload by single voxel MRS measurement of liver T2. J Magn Reson Imaging 2002;15(4):395-400.

506. Perman WH, Balci NC and Akduman I. Review of magnetic resonance spectroscopy in the liver and the pancreas. Top Magn Reson Imaging 2009;20(2):89-97.

507. d'Assignies G, Ruel M, Khiat A, Lepanto L, Chagnon M, Kauffmann C, Tang A, Gaboury L and Boulanger Y. Noninvasive quantitation of human liver steatosis using magnetic resonance and bioassay methods. Eur Radiol 2009;19(8):2033-40.

508. Guiu B, Loffroy R, Petit JM, Aho S, Ben Salem D, Masson D, Hillon P, Cercueil JP and Krause D. Mapping of liver fat with triple-echo gradient echo imaging: validation against 3.0-T proton MR spectroscopy. Eur Radiol 2009;19(7):1786-93.

509. Kim H, Taksali SE, Dufour S, Befroy D, Goodman TR, Petersen KF, Shulman GI, Caprio S and Constable RT. Comparative MR study of hepatic fat quantification using single-voxel proton spectroscopy, two-point dixon and three-point IDEAL. Magn Reson Med 2008;59(3):521-7.

510. Noworolski SM, Tien PC, Merriman R, Vigneron DB and Qayyum A. Respiratory motion-corrected proton magnetic resonance spectroscopy of the liver. Magn Reson Imaging 2009;27(4):570-6.

511. Hiraoka M, Firbank M, Essenpreis M, Cope M, Arridge SR, van der Zee P and Delpy DT. A Monte Carlo investigation of optical pathlength in inhomogeneous tissue and its application to near-infrared spectroscopy. Phys Med Biol 1993;38(12):1859-76.

512. Clavien PA. Sinusoidal endothelial cell injury during hepatic preservation and

reperfusion. Hepatology 1998;28(2):281-5.

513. Nakamitsu A, Hiyama E, Imamura Y, Matsuura Y and Yokoyama T. Kupffer cell function in ischemic and nonischemic livers after hepatic partial ischemia/reperfusion. Surg Today 2001;31(2):140-8.

514. Jaeschke H, Smith CV and Mitchell JR. Reactive oxygen species during ischemia-reflow injury in isolated perfused rat liver. J Clin Invest 1988;81(4):1240-6.

515. Hafez TS, Habib MM, Seifalian AM, Fuller BJ and Davidson BR. Near-infrared spectroscopic assessment of mitochondrial oxygenation status--comparison during normothermic extracorporeal liver perfusion by buffer only or buffer fortified with washed red blood cells: an experimental study. Transplant Proc 2004;36(5):1265-7.

516. Jaeschke H, Farhood A and Smith CW. Neutrophils contribute to ischemia/reperfusion injury in rat liver in vivo. Faseb J 1990;4(15):3355-9.

517. Menger MD, Pelikan S, Steiner D and Messmer K. Microvascular ischemia-reperfusion injury in striated muscle: significance of "reflow paradox". Am J Physiol 1992;263(6 Pt 2):H1901-6.

518. Hamamoto I, Maeba T and Tanaka S. Role of leukocytes during the early phase of reperfusion injury after cold preservation of rat liver. Ann N Y Acad Sci 1994;723:476-9.

519. Caban A, Oczkowicz G, Abdel-Samad O and Cierpka L. Influence of Kupffer cells on the early phase of liver reperfusion. Transplant Proc 2002;34(2):694-97.

520. Vollmar B, Richter S and Menger MD. Leukocyte stasis in hepatic sinusoids. Am J Physiol 1996;270(5 Pt 1):G798-803.

521. Rovetto MJ, Lamberton WF and Neely JR. Mechanisms of glycolytic inhibition in ischemic rat hearts. Circ Res 1975;37(6):742-51.

522. Woods HF and Krebs HA. Lactate production in the perfused rat liver. Biochem J 1971;125(1):129-39.

523. Peralta C, Bartrons R, Riera L, Manzano A, Xaus C, Gelpi E and Rosello-Catafau J. Hepatic preconditioning preserves energy metabolism during sustained ischemia. Am J Physiol Gastrointest Liver Physiol 2000;279(1):G163-71.

524. Suzuki M, Fukuhara K, Unno M, Htwe T, Takeuchi H, Kakita T and Matsuno S. Correlation between plasma and hepatic phosphatidylcholine hydroperoxide, energy charge, and total glutathione content in ischemia reperfusion injury of rat liver. Hepatogastroenterology 2000;47(34):1082-9.

525. Habib MM, Hafez TS, Parkes HG, Seifalian AM, Fuller BJ and Davidson BR. A comparison of bile composition from heart-beating and non-heart-beating rabbit organ donors during normothermic extracorporeal liver perfusion: experimental evaluation using proton magnetic resonance spectroscopy. Transplant Proc 2004;36(10):2914-6.

526. Ambrose EJ and Easty DM. Cell Biology. Second ed. Sunbury-on-Thames: Thomas Nelson Ltd.; 1977.

527. Kim YI, Song KE, Ryeon HK, Hwang YJ, Yun YK, Lee JW and Chun BY. Enhanced inflammatory cytokine production at ischemia/reperfusion in human liver resection. Hepatogastroenterology 2002;49(46):1077-82.

528. Fevery J. Liver transplantation: problems and perspectives. Hepatogastroenterology 1998;45(22):1039-44.

529. Grattagliano I, Vendemiale G and Lauterburg BH. Reperfusion injury of the liver: role of mitochondria and protection by glutathione ester. J Surg Res 1999;86(1):2-8.

530. Lang T, Sendl AF, Esquivel CO, Berquist WE and Cox KL. Cholic acid synthesis is reduced in pediatric liver recipients during graft dysfunction due to ischemic injury and allograft rejection. Transplantation 1997;64(11):1585-90.

531. Harbrecht BG, Billiar TR, Curran RD, Stadler J and Simmons RL. Hepatocyte injury by activated neutrophils in vitro is mediated by proteases. Ann Surg 1993;218(2):120-8.

532. Vollmar B, Glasz J, Leiderer R, Post S and Menger MD. Hepatic microcirculatory perfusion failure is a determinant of liver dysfunction in warm ischemia-reperfusion. Am J Pathol 1994;145(6):1421-31.

533. Herrera FJ, Codoceo R, Cienfuegos J, Pardo F, Mora NP, Pereira F and Castillo-Olivares JL. Bile acid profile as early indicator of allograft function during orthotopic liver transplantation. Eur Surg Res 1990;22(1):19-26.

534. Menger MD, Bonkhoff H and Vollmar B. Ischemia-reperfusion-induced pancreatic microvascular injury. An intravital fluorescence microscopic study in rats. Dig Dis Sci 1996;41(5):823-30.

535. Fujiwara S, Ku Y and Saitoh Y. Serum bile acid monitoring as an early indicator of allograft function in canine orthotopic liver transplantation. Kobe J Med Sci 1992;38(4):217-31.

536. Brancatisano R, Isla A and Habib N. Is radical hepatic surgery safe? Am J Surg 1998;175(2):161-3.

537. Henderson JM. Liver transplantation and rejection: an overview. Hepatogastroenterology 1999;46 Suppl 2:1482-4.

538. Cutrin JC, Llesuy S and Boveris A. Primary role of Kupffer cell-hepatocyte communication in the expression of oxidative stress in the post-ischaemic liver. Cell Biochem Funct 1998;16(1):65-72.

539. Zhong Z, Jones S and Thurman RG. Glycine minimizes reperfusion injury in a low-flow, reflow liver perfusion model in the rat. Am J Physiol 1996;270(2 Pt 1):G332-8.

540. Schemmer P, Bunzendahl H, Klar E and Thurman RG. Reperfusion injury is dramatically increased by gentle liver manipulation during harvest. Transpl Int 2000;13 Suppl 1:S525-7.

541. Schemmer P, Bradford BU, Rose ML, Bunzendahl H, Raleigh JA, Lemasters JJ and Thurman RG. Intravenous glycine improves survival in rat liver transplantation. Am J Physiol 1999;276(4 Pt 1):G924-32.

542. Zhong Z, Wheeler MD, Li X, Froh M, Schemmer P, Yin M, Bunzendaul H, Bradford B and Lemasters JJ. L-Glycine: a novel antiinflammatory, immunomodulatory, and cytoprotective agent. Curr Opin Clin Nutr Metab Care 2003;6(2):229-40.

543. Lindert KA, Caldwell-Kenkel JC, Nukina S, Lemasters JJ and Thurman RG. Activation of Kupffer cells on reperfusion following hypoxia: particle phagocytosis in a low-flow, reflow model. Am J Physiol 1992;262(2 Pt 1):G345-50.

544. Nishimura Y and Lemasters JJ. Glycine blocks opening of a death channel in cultured hepatic sinusoidal endothelial cells during chemical hypoxia. Cell Death Differ 2001;8(8):850-8.

545. Elferink RO. Cholestasis. Gut 2003;52 Suppl 2:ii42-8.

546. Nishijima T, Nishina M and Fujiwara K. Measurement of lactate levels in serum and bile using proton nuclear magnetic resonance in patients with hepatobiliary diseases: its utility in detection of malignancies. Jpn J Clin Oncol 1997;27(1):13-17.

547. Pannen BH, Al-Adili F, Bauer M, Clemens MG and Geiger KK. Role of endothelins and nitric oxide in hepatic reperfusion injury in the rat. Hepatology 1998;27(3):755-64.

548. Williamson DH, Lund P and Krebs HA. The redox state of free nicotinamide-adenine dinucleotide in the cytoplasm and mitochondria of rat liver. Biochem J 1967;103(2):514-27.

549. Serracino-Inglott F, Habib NA and Mathie RT. Hepatic ischemia-reperfusion injury. Am J

Surg 2001;181(2):160-6.

550. Uhlmann D, Uhlmann S and Spiegel HU. Endothelin/nitric oxide balance influences hepatic ischemia-reperfusion injury. J Cardiovasc Pharmacol 2000;36(5 Suppl 1):S212-4.

551. Jaeschke H. Reactive oxygen and mechanisms of inflammatory liver injury. J Gastroenterol Hepatol 2000;15(7):718-24.

552. Jaeschke H. Kupffer cell-induced oxidant stress during hepatic ischemia-reperfusion: does the controversy continue? Hepatology 1999;30(6):1527-8.

553. Lentsch AB, Kato A, Yoshidome H, McMasters KM and Edwards MJ. Inflammatory mechanisms and therapeutic strategies for warm hepatic ischemia/reperfusion injury. Hepatology 2000;32(2):169-73.

554. Huguet C, Gavelli A and Bona S. Hepatic resection with ischemia of the liver exceeding one hour. J Am Coll Surg 1994;178(5):454-8.

555. Ijaz S, Yang W, Winslet MC and Seifalian AM. Impairment of hepatic microcirculation in fatty liver. Microcirculation 2003;10(6):447-56.

556. Cotgreave IA. N-acetylcysteine: pharmacological considerations and experimental and clinical applications. Adv Pharmacol 1997;38:205-27.

557. Harrison PM, Wendon JA, Gimson AE, Alexander GJ and Williams R. Improvement by acetylcysteine of hemodynamics and oxygen transport in fulminant hepatic failure. N Engl J Med 1991;324(26):1852-7.

558. Suter PM, Domenighetti G, Schaller MD, Laverriere MC, Ritz R and Perret C. N-acetylcysteine enhances recovery from acute lung injury in man. A randomized, double-blind, placebo-controlled clinical study. Chest 1994;105(1):190-4.

559. Tossios P, Bloch W, Huebner A, Raji MR, Dodos F, Klass O, Suedkamp M, Kasper SM, Hellmich M and Mehlhorn U. N-acetylcysteine prevents reactive oxygen species-mediated myocardial stress in patients undergoing cardiac surgery: results of a randomized, double-blind, placebo-controlled clinical trial. J Thorac Cardiovasc Surg 2003;126(5):1513-20.

560. Chavez-Cartaya RE, Ramirez-Romero P, Calne RY and Jamieson NV. Laser-Doppler flowmetry in the study of in vivo liver ischemia and reperfusion in the rat. J Surg Res 1994;56(5):473-7.

561. Seifalian AM, Chidambaram V, Rolles K and Davidson BR. In vivo demonstration of

impaired microcirculation in steatotic human liver grafts. Liver Transpl Surg 1998;4(1):71-7.

562. Neuschwander-Tetri BA and Caldwell SH. Nonalcoholic steatohepatitis: summary of an AASLD Single Topic Conference 1. Hepatology 2003;37(5):1202.

563. Hubscher SG. Histological assessment of non-alcoholic fatty liver disease. Histopathology 2006;49(5):450-65.

564. Montalti R, Nardo B, Bertelli R, Beltempo P, Puviani L, Vivarelli M and Cavallari A. Donor pool expansion in liver transplantation. Transplant Proc 2004;36(3):520-2.

565. Fishbein TM, Fiel MI, Emre S, Cubukcu O, Guy SR, Schwartz ME, Miller CM and Sheiner PA. Use of livers with microvesicular fat safely expands the donor pool. Transplantation 1997;64(2):248-51.

566. Verran D, Kusyk T, Painter D, Fisher J, Koorey D, Strasser S, Stewart G and McCaughan G. Clinical experience gained from the use of 120 steatotic donor livers for orthotopic liver transplantation. Liver Transpl 2003;9(5):500-5.

567. Fusai G, Glantzounis GK, Hafez T, Yang W, Quaglia A, Sheth H, Kanoria S, Parkes H, Seifalian A and Davidson BR. N-Acetylcysteine ameliorates the late phase of liver ischaemia/reperfusion injury in the rabbit with hepatic steatosis. Clin Sci (Lond) 2005;109(5):465-73.

568. Yang W, Hafez T, Thompson CS, Mikhailidis DP, Davidson BR, Winslet MC and Seifalian AM. Direct measurement of hepatic tissue hypoxia by using a novel tcpO2/pCO2 monitoring system in comparison with near-infrared spectroscopy. Liver Int 2003;23(3):163-70.

569. Wanner GA, Ertel W, Muller P, Hofer Y, Leiderer R, Menger MD and Messmer K. Liver ischemia and reperfusion induces a systemic inflammatory response through Kupffer cell activation. Shock 1996;5(1):34-40.

570. So PW and Fuller BJ. A comparison of the metabolic effects of continuous hypothermic perfusion or oxygenated persufflation during hypothermic storage of rat liver. Cryobiology 2001;43(3):238-47.

571. Lehninger AL, Sudduth HC and Wise JB. D-beta-Hydroxybutyric dehydrogenase of muitochondria. J Biol Chem 1960;235:2450-5.

572. Coen M, Lenz EM, Nicholson JK, Wilson ID, Pognan F and Lindon JC. An integrated metabonomic investigation of acetaminophen toxicity in the mouse using NMR spectroscopy. Chem Res Toxicol 2003;16(3):295-303.

573. Beauvieux MC, Tissier P, Gin H, Canioni P and Gallis JL. Butyrate impairs energy metabolism in isolated perfused liver of fed rats. J Nutr 2001;131(7):1986-92.

574. Hirakawa A, Takeyama N, Nakatani T and Tanaka T. Mitochondrial permeability transition and cytochrome c release in ischemia-reperfusion injury of the rat liver. J Surg Res 2003;111(2):240-7.

575. Soeda J, Miyagawa S, Sano K, Masumoto J, Taniguchi S and Kawasaki S. Cytochrome c release into cytosol with subsequent caspase activation during warm ischemia in rat liver. Am J Physiol Gastrointest Liver Physiol 2001;281(4):G1115-23.

576. Bernardi P, Krauskopf A, Basso E, Petronilli V, Blachly-Dyson E, Di Lisa F and Forte MA. The mitochondrial permeability transition from in vitro artifact to disease target. Febs J 2006;273(10):2077-99.

577. Javadov SA, Clarke S, Das M, Griffiths EJ, Lim KH and Halestrap AP. Ischaemic preconditioning inhibits opening of mitochondrial permeability transition pores in the reperfused rat heart. J Physiol 2003;549(Pt 2):513-24.

578. Chandel N, Budinger GR, Kemp RA and Schumacker PT. Inhibition of cytochrome-c oxidase activity during prolonged hypoxia. Am J Physiol 1995;268(6 Pt 1):L918-25.

579. Wilson MT, Peterson J, Antonini E, Brunori M, Colosimo A and Wyman J. A plausible two-state model for cytochrome c oxidase. Proc Natl Acad Sci U S A 1981;78(11):7115-8.

580. Halestrap AP, Clarke SJ and Javadov SA. Mitochondrial permeability transition pore opening during myocardial reperfusion--a target for cardioprotection. Cardiovasc Res 2004;61(3):372-85.

581. Rolo AP, Teodoro JS, Peralta C, Rosello-Catafau J and Palmeira CM. Prevention of I/R injury in fatty livers by ischemic preconditioning is associated with increased mitochondrial tolerance: the key role of ATPsynthase and mitochondrial permeability transition. Transpl Int 2009;22(11):1081-90.